INVESTIGATING MECHANISMS OF NEURONAL MIGRATION IN THE ZEBRAFISH EMBRYO

ALIFIYA KAPASI

SUPERVISOR – DR ANDREW J GRIERSON

This thesis is in partial fulfilment of the requirements for the Philosophy of Doctorate degree at SITraN, University of Sheffield.

June 2014

ACKOWLEDGMENTS

This project has been an enlightening and challenging journey through which I have shaped professional attitudes and developed research techniques. This would not have been possible without the patience and encouragements of those with whom I have worked closely on this project.

I would like to take this opportunity to express my utmost respect and gratitude to my supervisor, Dr Andrew Grierson, who has provided continuous support and inspiration throughout my project. Without his guidance and help this thesis would not have been possible. I thank Dr Jon Wood, my co-supervisor, for his kind suggestions and help. I would also like to thank the Sheffield Institute of Translational Neuroscience and the MRC Centre for Developmental and Biomedical Genetics for the use of the facilities where this research was undertaken. I am indebted to my many colleagues who have guided me and provided support at times when it was needed.

Lastly, I would like to take the time to say thank you to my family who have constantly provided support and motivation throughout this project.

Alifiya Kapasi

ABSTRACT

The construction of the brain architecture and its complex neuronal circuitry are coordinated processes. Cortical development is dependent on timely production and correct migration of neurons from proliferative regions. Cortical development involves a set of complex events which includes cell proliferation, migration and differentiation. Disruption in any of these processes can lead to cortical malformations. This thesis investigated different aspects of neuronal migration during development using the zebrafish embryo as a model. We chose to investigate three models of neuronal migration.

In our first model we investigated the role of the basement membranes in neuronal development using the laminin β1 zebrafish mutant grumpy (*gup*). We demonstrate that laminin β1 mutants display a decrease in the width of the ventricular space, a marked reduction in size of the forebrain, and ectopic FBMNs, resembling features of cobblestone (COB) Lissencephaly. We also attempted to identify an uncharacterised *gup* mutation.

Previous studies has implicated the hydroxymethylglutaryl co-enzyme A reductase pathway in motor neuron and oligodendrocyte precursor cell migration. In our second model, we investigated the role of the HMGCoAR pathway in forebrain development of zebrafish embryos. Our data suggests the requirement of prenylation, in particular gernaylgeranylation, downstream to the HMGCoAR pathway, is required for correct neuronal positioning and ventricular space morphogenesis in the forebrain.

FE65 null mouse model has previously been shown to display defects in basement membrane assembly, neuronal migration, and patterning of the cortex, thus highlighting the importance of FE65 proteins in development. In our third model we hypothesised that FE65 maintains integrity of the basement membrane in the zebrafish, and a loss of function will disrupt neuronal development. Knockdown of *FE65* using antisense oligonucleotides morpholinos display defects in neuronal specification and axonal projections in the forebrain, which can be rescued by knocking down p53, suggesting that p53 may be a downstream target of FE65 signalling.

TABLE OF CONTENTS

List of Figures

List of Tables

List of Abbreviations

µg - Microgram

µl - Microlitre

AD – Alzheimers Disease

AICD – Amyloid Intracellular Domain

AIS – Anterior Intraencephalic Sulcus

AMPK – AMP Activated Protein Kinase

APP – Amyloid Precursor Protein

ARX – Aristaless-related Homeobox

AT - Atorvastatin

BCIP – 5-Bromo-4-Chloro-3-indolyl Phosphate

BM – Basement Membrane

BMP – Bone Morphogenetic Protein

Bp - Basepairs

cDNA – Complementary DNA

C.elegans – Caenorhabditis elegans

COB – Cobblestone

COMO – Control Morpholino

CGE – Caudal Ganglionic Eminence

CNS – Cental Nervous System

CNTNAP – Contactin-associateed Protein-like 2

DA - Dopaminergic

DCX – Doublecortin

DEPC – Diethylpyrocarbonate

DNA – Deoxyribonucleic Acid

DISC 1 – Disrupted in Schizophrenia 1

DMSO – Dimethyl Sulfoxide

ECM – Extracellular Matrix

EtOH - Ethanol

FBMN – Facial Branchiomotor Neuron

FE65 atg – FE65 Translational Blocking Morpholino

FE65 sp – FE65 Splice Blocking Morpholino

FPP – Farnesyl Pyrophosphate

GABA – gamma Aminobutyric Acid

Gabra1 – GABA receptor 1a

gDNA – Genomic DNA

GFP – Green Flourescent Protein

GG - Geranylgeraniol

GGPP – Geranylgeranyl Pyrophosphate

GGT I – Geranylgeranyl Transferase I

GnRH-1 – Gonadotrophin Releasing Hormone 1

GPR – G Protein Receptor

GUP - Grumpy

HMGCoA – Hydroxymethyl Glutaryl Co-enzyme A

HMGCoAR - Hydroxymethyl Glutaryl Co-enzyme A Reductase

Hpf – Hours Post Fertilisation

HSF – Heat-Shock Factor

IHH – Idiopathic Hypogonadotrophic Hypogonadism

IL – Interleukin

IPP – Isopentenyl Diphosphate

JEB – Junctional Epidemolysis Bullosa

KO - Knockout

LAMB1 – Laminin beta-1

LASAF – Leica Application Suite Advanced Flourescence

LDL – Low Density Lipoprotein

LGE – Lateral Ganglionic Eminence

LIS – Lissencephaly

LOVA – Lovastatin

MEL - Mevalonate

MGE – Medial Ganglionc Eminence

MHBC – Midbrain Hindbrain Constriction

mL - Millilitre

MN – Motor Neuron

MO – Morpholino

mM - Millimolar

mRNA – Messenger RNA

MVA - Mevalonate

NBT – Nitro Blue Tetrazolium

NICD – Notch Intracellular Domain

NFT – Neurofibillary Tangles

NMD – Neruonal Migration Disorder

NMDA – N-methyl-D-aspartate

NT – Neurotrophic Factor

OFN – Olfactory Nerve

PAL – Pallium

PBS – Phosphate Buffer Saline

PCP – Planar Cell Polarity

PCR – Polymerase Chain Reaction

PFA - Paraformaldehyde

PI3K – Phosphotidylinositol 3 Kinase

PMG – Polymicrogyria

PS1 – Presenilin 1

PS2 – Presenilin 2

PTB – Phosphotyrosin Binding

PTU - Phenythiourea

RELN – Reelin

RGC – Retinal Ganglionic Cells

RNA – Ribonucleic Acid

RT – Room Temperature

RT-PCR – Reverse Transcription PCR

SIM - Simvastatin

SHH – Sonice Hedghog

SUBPAL – Sub-pallium

TALEN – Transcription Activator-like Effector Nucleases

Tbr – T box Transcription Factor

Tg - Transgenic

TGF – Transforming Growth Factor

TILLING – Targetting Induced Local Lesions in Genomes

UTR – Untranslated Region

VS – Ventricular Space

VZ – Ventricular Zone

ZA – Zaragozic Acid

ZNP – Zebrafish Neurophenome Project

CHAPTER 1

INTRODUCTION

1.1 Neuronal Migration

The unique positioning of the neurons in the human brain is dependent on migration of post-mitotic neurons during development. The precise positioning of neurons is imperative as the neural system depends on the connections made between different classes of neurons and their targets. In the cerebral cortex, neuroblasts exit the ventricular zone to migrate substantial distances to their destined position. Migrating neurons adopt two modes of migration depending on their cell type; projection neurons migrate via radial migration, and interneurons enter the cortex via tangential migration. The construction of the brain's complex circuitry requires neurons to be interactive with their environment whilst migrating. A vast amount of scientific literature has been published exploring how different mechanisms influence the migratory process. Some of these mechanisms have been shown to involve cytoskeletal dynamics, extracellular matrix molecules, and guidance cues. Disruption of the mechanisms which influence neuronal migration underlies the pathogenesis of a number of neurological diseases, thus it is important to have a better understanding of the neuronal migratory process.

This thesis aims to discuss various mechanisms which regulate neuronal migration and contribute to the body of work already published.

1.2 Neuronal Migration in the Cortex

1.2.1 Cell Movements in Early Embryogenesis

The inductive interactions between the ectoderm and mesoderm form the vertebrate central nervous system (CNS) (Woo *et al.* 1995). This morphogenetic process requires elaborate patterns of cell movements to construct complex structures (Marin *et al.* 2003). The conversion of the neural plate into the neural tube is called neuralation. Primary neuralation divides the ectoderm into three cell types; the neural tube which forms the prospective CNS, the epidermis, and the neural crest cells. The neural crest cells undergo extensive migration during embryogenesis and contribute to building diverse structures such as, the peripheral nervous system, pigments cells of the epidermis, and facial cartilage and bone (Bronner 2012). Upon neural tube closure,

the neural tube becomes polarised into dorsal and ventral regions. An extensive number of studies show that the dorsoventral patterning of the neural tube is dependent on signals induced by the notochord. Morphogen gradients of sonic hedgehog (SHH) "ventralise" the neural tube to induce differentiation of floor plate cells. The floor plate cells act as a secondary signalling centre and cause a cascade of SHH signals to induce various other cell types such as, ventral neurons, motor neurons and interneurons (Mayer *et al.* 1993; Placzek *et al.* 1993) (Figure 1).

Members of the transforming growth factor beta (TGF-β) superfamily, in particular bone morphogenetic proteins (BMP) 4 and 7, dorsalin, and activin induce the neural tube to differentiate into dorsal cell fates. Similar to the ventral region, gradients of BMP 4 and 7 induce differentiation of the roof plate, which acts as a secondary signalling centre (Liem *et al.* 1995).

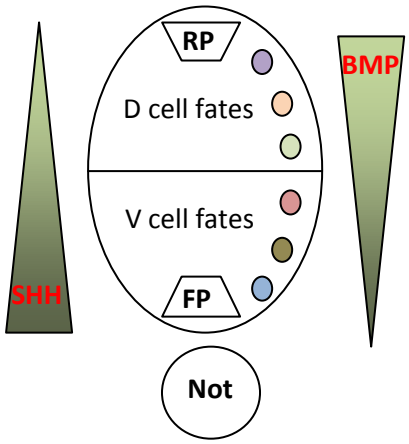

Figure 1 – A schematic representation of the different cell types induced after neural tube closure. Differing concentrations of SHH and BMP can induce ventral and dorsal cell fates, respectively. RP – roof plate, FP – floor plate, Not – notochord, V – ventral, D – dorsal.

The neural tube undergoes drastic changes to form three vesicles, the prosencephalon (forebrain), mesencephalon (midbrain), and rhombencephalon (hindbrain). The anterior prosencephalon further differentiates into the telencephalon, which gives rise to the cerebrum, olfactory lobes, and hippocampus. The posterior

prosencephalon forms the diencephalon, which gives rise to the retina, epithalamus, thalamus, and hypothalamus (Marin *et al.* 2003).

Differing concentrations of SHH and BMPs cause cells to express different transcription factors, which establishes boundaries between progentitor zones. This in turn activates genes whose protein products gives rise to distinct cell identities. BMPs have been shown to regulate expression boundaries of the homebox transcription factors Pax6, Dbx2, and Msx1 (Timmer *et al.* 2002), whilst SHH induces early expression of the ventral transcription factor Nkx2.2 (Barth *et al.* 1995). Once the patterning and specification of the cells in the forebrain has been set up, cells can migrate to their destined position in the cortex.

1.2.2 Radial Migration

The subdivision of the telencephalon into the dorsal ventricular zone (VZ) and ventral VZ gives rise to the neocrotex, and the striatum and pallidum, respectively (Rubenstein *et al.* 1994). In the CNS, neuronal progenitors and post-mitotic cells are generated in the dorsal VZ and migrate via two modes; radial migration and tangential migration. Early studies in the cerebellar cortex led to the discovery that post-mitotic neurons use radial glial fibers as scaffolding to migrate to their destined position (Rakic 1971). Radial glial cells are generated during neural tube development and provide scaffolding between the VZ and the pial surface of the brain (Marin *et al.* 2003). It was previously thought that subsequent separate populations of neuronal precursors generated radial glial cells and new born neurons, but studies showed that radial glial precursor cells residing in the VZ are mitotically active and have the ability to produce glial cells and neurons (Miyata *et al.* 2001; Noctor *et al.* 2002), suggesting they have additional roles as well as serving as a structural component.

The first waves of neurons from the VZ migrate radially to the pial surface to form the preplate. The preplate consists of the Cajal-Retzus cells and the first cohort of pyramidal cells. Subsequent waves of neurons split the preplate into the marginal zone and subplate, which establishes the cortical plate in between (Gupta *et al.* 2002). During embryogeneis, neurons exit the VZ to reside under the marginal zone to form

the sequential layers of the cortex. The layering pattern of the cortex occurs in an "inside out" fashion, where the older neurons are positioned in the deeper layers of the cortex compared to younger neurons which lie in the superficial layers (Angevine *et al.* 1961). After neurogenesis and migration is completed during cortical development, radial glial cells are transformed into astrocytes. Evidence suggests that this cell type transformation is mediated by the MAPK signalling pathway (Stipursky *et al.* 2012). By looking at specific radial glial markers, recent studies have showed radial glial-like cells can be identified in the forebrain and olfactory bulb of the adult mouse (Marko *et al.* 2011; Emsley *et al.* 2012) and the cerebellum of adult teolest fish (Zupanc *et al.* 2012).

Neurons taking the radial migratory route undergo two main modes of cell movement, somal translocation and glial-guided locomotion. Early born cortical neurons adopt somal translocation, to migrate radially from the VZ to their destined position, and display distinct morphological features. These neurons possess a long leading process which terminates at the pial surface. This process involves the soma of the cell moving toward the leading process and results in a continuous, smooth movement. Subsequently, as the soma reaches its desired position, the leading process becomes shorter. Pyramidal neurons, generated at later stages of corticogenesis, adopt the glial-guided locomotion. These cells maintain the length of their leading processes as they move forward and are dependent on radial glia cells. In contrast to somal translocation, glia-guided locomotion occurs in short bursts of forward movement with intermittent stationary pauses (Gupta *et al.* 2002; Nadarajah *et al.* 2003). Interestingly, multipolar cells passing through the transient subventricular zone have been shown to undergo a novel type of migration termed "multipolar migration". These cells possess very dynamic leading processes which extend and retract processes in multiple directions, unlike newly generated pyramidal cells. Their migratory route to the pial surface is not in a linear direction and they do no associate with radial glial fibers. Occasionally, these cells jump tangentially as they migrate via radial migration, suggesting multipolar cells may seek guidance from extracellular cues (Tabata *et al.* 2003). The morphological transformation of bipolar cells into multipolar cells whilst passing through the SVZ, and then back to bipolar cells has been shown to be associated with expression of connexin 43 (Liu *et al.* 2012).

1.2.3 Tangential Migration

Early retroviral lineage tracing experiments revealed that a large number of neurons are not confined to radial migratory routes, but alternatively follow another route called tangential migration (O'Rourke *et al.* 1995). Neural progenitors are born in the proliferative epithelium of the ventral ventricular zone (VZ), and give rise to the striatum and pallidum, which become components of the prospective basal ganglia. Neurons migrating tangentially are born in three areas of the ventral region, the medial (MGE), lateral (LGE), and caudal ganglionic eminence (CGE). In the mouse forebrain, neurons born in the LGE migrate ventrally and anteriorly to generate medium spiny neurons in the striatum, nucleus accumbens, and olfactory tubercule. These neural progenitors also give rise to granule and periglomerular cells in the olfactory bulb. Neurons born in the MGE migrate dorsally to find their position in the developing neocortex. These cells differentiate into populations of GABA-, parvalbumin-, or somatostatin-expressing interneurons (Wichterle *et al.* 2001; Kameda *et al.* 2012). Additionally, these cells express the LIM-homeobox gene, *Lhx6*, a marker of MGE (Lavdas *et al.* 1999). Neurons originating in the CGE express the 5-hydroxytryptamine (serotonin) 3A receptor, suggesting serotonergic activity may influence cortical sensory networks (Lee *et al.* 2010). Neurons generated in the ganglionic eminences enter the neocortex via several cortical zones, which include the subventricular zone, the intermediate zone, the subplate, and the marginal zone (Tanaka *et al.* 2012).

Further evidence that the ganglionic eminences were the major source of interneurons came from studies using mutant mice lacking the homeodomain transcription factors *Dlx1/2* and *Nkx2.1*. In *Dlx1/2* mutants migratory routes from the LGE to the neocrotex are absent and the number of GABA-expressing cells is reduced in the olfactory bulb (Anderson *et al.* 1997). Mice lacking *Nkx2.1* display an absence of ventral regions and a lack of cells expressing GABA (Sussel *et al.* 1999). These studies in mutant mice indicate the importance of *Dlx* and *Nkx* factors in the migration of interneurons from subcortical to cortical regions.

1.2.3.1 - Migration of Olfactory Interneurons

The rostral migratory stream (RMS) consists of the progenitor cells of olfactory interneurons formed from embryonic day 15-17 in the mouse (Pencea *et al.* 2003). During development progenitor cells are born in the dorsal regions of the LGE and migrate tangentially along the RMS to the olfactory bulb. Once they reach their destined position they undergo differentiation into olfactory interneurons (Sun *et al.* 2010). This migratory route is also persistent in the adult rodent, non-primate, and human brain. During adulthood, neuroblasts are generated in the anterior subventricular zone (SVZ) and migrate along the RMS to populate the olfactory bulb (Kornack *et al.* 2001; Bedard *et al.* 2004). In contrast to early development, where neural progenitors freely migrate through the extracellular space, in adults, SVZ neuroblasts aggregate together to form a chain-like morphology (Lois *et al.* 1996). Thus, mechanisms controlling migration of olfactory interneurons may differ in adults and embryos. Furthermore, these neuroblast chains are ensheathed by astrocytes, to form a glial tube structure (Lois *et al.* 1996; Peretto *et al.* 2005). Evidence suggests there is a high density of blood vessel networks orientated parallel to the RMS, extending from caudal to rostral regions. Neuroblasts and astrocytes have been shown to make direct contact with endothelial cells, suggesting astrocytes and blood vessel networks may provide scaffolding for migrating neuroblasts (Whitman *et al.* 2009). Gap junctions have also been identified to be involved in correct migration of neuroblasts in the RMS (Marins *et al.* 2009).

1.2.3.2 - Migratory route of Gonadotrophin Releasing Hormone 1 (GnRH-1) Neurons

Another population of cells which undergo tangential migration in the cortex are the GnRH-1 neurons. This hormone regulates the release of gonadotrophins from the anterior pituarity gland, thus essential in mammalian reproduction. GnRH-1 cells migrate from the nasal placode crossing the cribiform plate; a bone located behind the nose, and finally migrates caudally to the forebrain. GnRH-1 cells are associated with a subset of vomeronasal axons, olfactory sensory axons, and a large number of blood vessel during their migration, thus they are said to undergo axonphilic migration (Wray 2010).

Disruption of this migratory route can result in idiopathic hypogonadotropic hypogonadism (IHH) with anosmia (Kallmann syndrome). Patients with this disorder display a delay in puberty as well as infertility (Kim *et al.* 2008). Extracellular signals such as stromal derived growth factor SDF-1 and gamma- aminobutyric acid (GABA) have been shown to play a role in GnRH -1 migration, by accelerating it or slowing it down, respectively. This antagonistic effect on migrating cells has been suggested to be due to changes in chloride and potassium ions (Casoni *et al.* 2012). Similar to the pyramidal cortical cells, GnRH-1 cells extend their leading processes and display somal translocation in a salutatory movement (Wray 2010).

Tangential migratory mechanisms are highly dependent on a diverse range of extracellular signals and guidance cues, reviewed in later sections.

1.2.4 Granule Cell Migration

A unique feature of cerebellar granule cells is that they undergo both radial and tangential migration to reach their position in the internal granule layer (IGL). Granule cell precursors are generated in the rhombic lip (Wingate *et al.* 1999) and exit the external granule layer (EGL) to migrate tangentially in the cerebellum. They then turn vertically and migrate radially using the Bergmann glial fibers as scaffolding to reach the IGL. The leading processes of granule neurons migrating tangentially follow the axon trajectory of earlier born granule neurons, and differentiate into the prospective parallel fiber axons. In comparison, leading processes of neurons migrating radially are juxtaposed to the Bergmann radial glia and differentiate into future dendrites (Kawaji *et al.* 2004).

Patients with temporal lobe epilepsy display abnormal dendate granule cell migration (Frotscher *et al.* 2003). A study using adult rats showed prolonged seizures causes an increase in granule cell neurogenesis. Furthermore, the newly born neurons are ectopically located. Studies suggest that Disrupted in Schizophrenia 1 (DISC 1), a schizophrenia susceptibility gene, regulates granule cell migration in the hippocampus (Meyer *et al.* 2009).

1.3 Neuronal Migration in Non-Cortical Regions

1.3.1 Migration in the Retina

Migrating cells undergo two forms of migration, interkinetic nuclear migration and somal translocation, during retinal development. Interkinetic migration is the process where the nucleus of progenitor cells migrates in phase with the cell cycle. Cells at the apical surface of the retinal neuroepithelium migrate in M phase, whilst cells at the basal surface migrate in S phase to the apical surface to start the mitosis process again (Baye *et al.* 2007). This migratory process is thought to be driven by actomyosin networks (Norden *et al.* 2009). Neurogenesis during retinal development occurs in a wave-like manner from the central to peripheral neuroepithelium, under the influence of SHH and the basic helix-loop-helix transcription factor Atonal. Retinal cells migrate away from the apical surface to generate the different classes of cells found in the adult retina. Some post-mitotic cells attach themselves to the apical surface and differentiate into future photoreceptors and Muller glia (Malicki 2004). Charaterisation of three zebrafish mutants, *oko meduzy* (mutation in the crumbs gene), *glass onion* (mutation in the N-cadherin gene), and *nagie oko (*encoding the membrane-associated guanylate kinase family scaffolding protein), ahowed that each of these displayed disorganisation of retinal neurons and increased cell death (Malicki *et al.* 1996).

1.3.2 Migration in the Spinal Cord

Correct differentiation of distinct cell types is essential in establishing neural circuits in the spinal cord. Initial development of spinal cord progenitors occurs during dorso-ventral patterning in early embryogenesis. Morphogen gradients and the expression of transcription factors induce a variety of cell types including motor neurons and, ventral and dorsal spinal interneurons. Autonomic motor neurons exit the ventricular zone and migrate radially into the dorsal horn of the spinal cord. Here, they localise with somatic motor neurons to form a motor column (Markham *et al.* 1991). Specification of ventral interneurons relies on signals mediated by the floor plate,

whilst dorsal interneurons are induced by signals from the roof plate (Figure 1) (Chizhikov *et al.* 2005; Arber 2012). Studies in the *dreher* mutant mouse, harbouring a point mutation in the *LMX1a* gene, showed a loss of BMP expression, and an inability to generate dorsal interneurons (Millen *et al.* 2004). Dorsal interneurons are heterogeneous and can be characterised into six groups, D1 to D6. Dorsal interneurons in the D1 group exit the cell cycle and migrate ventrally to the dorsal horn of the spinal cord. These interneurons further split into two different neuronal subtypes which project ipsilaterally and contralaterally (Ding *et al.* 2012). A group of cells derived from the ventral (V1) progenitor domain termed Renshaw cells express the transcription factor *engrailed-1,* and project their axons ventrolaterally to terminate near motor neurons in the spinal cord (Saueressig *et al.* 1999; Benito-Gonzalez *et al.* 2012).

The first glial cells distinguishable in the developing rat spinal cord are radial glial cells, from E14 to 18 (McMahon *et al.* 2002). In the zebrafish, spinal cord precursors express radial glial markers under the influence of notch signalling (Kim *et al.* 2008).

1.4 Mechanisms Controlling Neuronal Migration

For neurons to migrate considerable distances, they require correct guidance from extracellular factors. These factors change the cells behaviour by regulating movement, speed, interaction with other cell types, or direction during migration. Table 1 lists some genes that regulate radial and tangential migration. These factors will be reviewed in the following sections.

Table 1 – List of factors which regulate neuronal migration

Gene	Function	Significance in migration	Reference
KLF4 (Kruppel-like factor)	Transcription factor	Regulate neurogenesis and radial migration of neurons	(Qin *et al.* 2012)
Brn-1/Brn- 2	Transcription factor	Controls inititation of neuronal migration	(McEvilly *et al.* 2002)
Pax6	Transcription factor	Induces differentiation of radial glia	(Marin *et al.* 2003)
BDNF	Neurotrophic factors	Regulates distribution of Cajal-Retzius cells	(Alcantara *et al.* 2006)
Neurotrophic factor 4 (NT4)	Neurotrophic factor	Promote migration of cortical neurons	(Behar *et al.* 1997)
Semaphorin 3A	Extracellular signal	Chemoattractive guidance cue for migrating neurons	(Chen *et al.* 2008)
Stromal-derived factor 1 (SDF1)	Chemoattractant	Required to maintain tangential migration	(Liapi *et al.* 2008)
Astroctactin (Astn1)	Glycoprotein	Implicated in neuron-glia interactions	(Wilson *et al.* 2010)
Neuregulin	Glial Growth factor	Expressed by migrating cortical neurons and promote maintenance of radial glial cells	(Anton *et al.* 1997)
Epidermal growth factor receptor (EGFR)	Growth factor	Modulates radial movement	(Puehringer *et al.* 2013)
Heat shock factor 2 (HSF2)	Heat shock protein	Maintains cellular populations, which influence radial migration	(Chang *et al.* 2006)
Lissencephaly 1 (Lis 1)	Microtubule-Associated Protein	Regulates cytoskeletal events during migration	(Liu *et al.* 2000)

Doublecortin (Dcx)	Microtubule-associated Protein	Stabalises microtubule network during migration	(Liu *et al.* 2011)
Reelin (Reln)	Extracellular glycoprotein	Important for radial glial migration	(Liu *et al*.2011)
p35/CDK5	Enzymatic signalling interaction	Important for neuronal/glia interaction	(Gupta *et al.* 2003)

1.5 Mechanisms Controlling Neuronal Migration – Cytoskeletal Dynamics

1.5.1 Leading Process Dynamics

In response to extracellular guidance cues, migrating neurons undergo three processes to direct their migratory route, namely, extension and retraction of the leading process, and translocation of the nucleus. The first sign of neuronal migration is the formation of the growth cone (GC) at the tip of the leading process (Ono *et al.* 1997; Schaar *et al.* 2005). The growth cone initially forms protrusive structures called filopodia and lamellipodia. The filopodia are thin spike-like structures consisting of parallel bundles of filamentous actin (F-actin), whilst the lamellipodia are flat thin sheets between the filopodia filled with actin meshwork. As these structures elongate they push the leading edge of the cell forward, thus initiating cell movement (Mattila *et al.* 2008). Myosin II motor proteins, important in co-ordination, and F-actin are important in the leading process of the granule cell. Inhibition of the Myosin II motor decreased the speed of granule cell migration, whilst activation of the motor protein increased co-ordination (Solecki *et al.* 2009). It has been suggested this actin-myosin dependent protrusion of the leading process consequently pulls the soma forward during neuronal migration (He *et al.* 2010). Another actin-binding protein, drerbin, has been shown to be involved in the formation and protrusion of the leading process of oculomotor neurons (Dun *et al.* 2012). The microtubule-associated proteins Lis1, and *doublecortin (DCX),* are involved in migrating interneurons. Loss of Lis 1 reduces the speed of tangentially migrating neurons from the MGE. Evidence suggests that this is due to instability of microtubules in the leading process (Gopal *et al.* 2010). Loss of *DCX* in a mouse model leads to defects in growth cone formation (Kappeler *et al.* 2006). These studies suggest a key role for cytoskeletal proteins in driving forward movement of the leading process.

Microtubules consist of plus and minus ends which are polarised in the leading process. The plus ends of microtubules uniformly face the tip of the leading process, whilst the minus ends face towards the nucleus (Rakic *et al.* 1996). The polarity of microtubules situated in the leading process has suggested that genes involved in

polarity plays an important part in leading process dynamics. Ablation of Cdc42, a regulator of polarity, has been shown to cause enlargement of the growth cone and inhibition of filopodia dynamics in neurons from a mutant mouse model (Garvalov *et al.* 2007). Furthermore, Cdc42 expression stimulates F-actin formation, suggesting this relationship may control actin re-modelling (Alberts *et al.* 2006). PAR-3, a protein part of the polarity complex, has been shown to be expressed in the growing tip of the growth cone. Evidence suggests localisation of PAR-3 to the distal tip is through its interaction with KIF3A, a microtubule motor protein (Nishimura *et al.* 2004).

Leading process dynamics in tangentially migrating neurons appears to be linked with chemoattractant cues from the environment. The leading processes of interneurons form two branches which are highly dynamic. As the cell moves forward it selects only one of the branches to follow, which results in extension of one branch and retraction of the other. Interestingly, the angles at which the branches are formed determine the direction of migration, thus geometry dictates cell trajectory. In alternative circumstances, intense chemoattractant cues cause branches to be formed at much larger angles, consequently allowing the migrating neurons to undergo rapid change of direction (Martini *et al.* 2009; Valiente *et al.* 2009).

1.5.2 Nucleokinesis

Nucleokinesis is the process where the nucleus translocates into the leading process and can be separated into two phases. The first phase involves cytoplasmic organelles such as the Golgi and centrosome, moving within a large swelling towards the leading process. The second phase involves the nucleus translocating towards these organelles (Bellion *et al.* 2005; Martini *et al.* 2009). Many studies that have investigated the mechanisms causing nucleokinesis favour the notion that the pulling forces drive nuclear movement. Evidence suggests that Myosin II motors are largely implicated in generating the force to cause nuclear translocation. It was suggested that Myosin II may modulate actin dynamics and pull the centrosome and soma forward during phase one of nucleokinesis (Solecki *et al.* 2009; Martini *et al.* 2010). Silencing Par6 inhibits Myosin II activity by decreasing phosphorylation of myosin light

chains, suggesting a relationship between the myosin II motor and polarity proteins (Solecki *et al.* 2009).

Dynein, another motor protein, may associate with myosin II to pull on the mitochondiral network, thus consequently driving a forward force (Tsai *et al.* 2007). *In vitro* studies show that inhibition of dynein results in an uncoupling between the centrosome and nucleus, resulting in migration defects (Tanaka *et al.* 2004). Lis1 interacts with microtubules and promotes stabilisation. Mutation in Lis 1 results in the human disorder, type I Lissencephaly, characterised by neuronal migration defects. Animal models lacking Lis1 activity display a range of neuronal migration, proliferation, and axonal transport defects (Liu *et al.* 2000; Youn *et al.* 2009). Lis1 interacts with dynein motors and NudE-like protein (Nudel) to form a complex. Nudel is localised at the centrosome and targets Lis1 and dynein to the centrosome. Loss of Lis1 activity in cerebellar granule cells resulted in a redistribution of Lis1 from the centrosome to the perinuclear region (Tanaka *et al.* 2004). Nudel facilitates microtubule anchoring in the centrosome (Shu *et al.* 2004; Guo *et al.* 2006) and functions in linking Lis1 and dynein together (Li *et al.* 2005). It has been proposed that Lis1 can bind to dynein by influencing the enzymatic activity of dynein in vitro, implicating a microtubule-independent role (Mesngon *et al.* 2006). In cortical slice assays, lack of Nudel or Lis1 activity resulted in an increase in the distance between the nucleus and centrosome and inhibition of nuclear movement (Youn *et al*. 2009).Initially, Lis1 and Nudel are localised in the centrosome of mitotically active neuroblasts, but as development continues their subcellular distribution became more widespread (Sasaki *et al.* 2000). Co-immunoprecipitation experiments show Lis1 can interact with *doublecortin* (DCX), a gene that when mutated also results in type I Lissencephaly. DCX interacts with microtubules and functions to enhance polymerisation. Interestingly, it has been suggested the coupling between the nucleus and centrosome is mediated by a DCX-Lis1-dynein complex in mouse cerebellar neurons (Tanaka *et al.* 2004). Neurons exiting the MGE display migratory defects in DCX-deficient mice. These neurons also exhibit aberrant neurite branching morphology and perturbed nuclear translocation, suggesting that DCX may also play a role in nucleokinesis (Kappeler *et al.* 2006). As well as nucleokinesis, dynein plays a role in other cellular processes such as mitosis and axonal transport. In axonal

transport, dynein motors are largely responsible for the retrograde movement of cargoes from the synapse to the cell body (Goldstein *et al.* 2000).

Other proteins are involved in nucleokinesis such as, members of the Rho GTPase superfamily. Inhibition of Rho in precerebellar neurons prevents nuclei migration (Causeret *et al.* 2004). Lis1 haploinsufficiency leads to defects in dentritic protrusions accompanied by an upregulation of RhoA and a downregulation of Rac1 and Cdc42, suggesting Lis1 promotes actin polymerisation through Rho GTPase activity (Kholmanskikh *et al*. 2003). Proteins containing a SUN domain, SUN1 and SUN2, have been shown to interact with the KASH domain of a protein called Syne-2. This SUN-KASH domain complex has been shown to have a role in mediating the interaction between the nucleus and centrosome in mice (Zhang *et al.* 2009).

1.6 Mechanims Controlling Neuronal Migration – Extracellular Matrix (ECM) Molecules

The basement membrane (BM) is a specialised form of the ECM, and is multifunctional and can influence a variety of cellular processes (Figure 2). Consequently, a loss of function in the proteins involved in ECM can result in abnormalities in multiple processes.

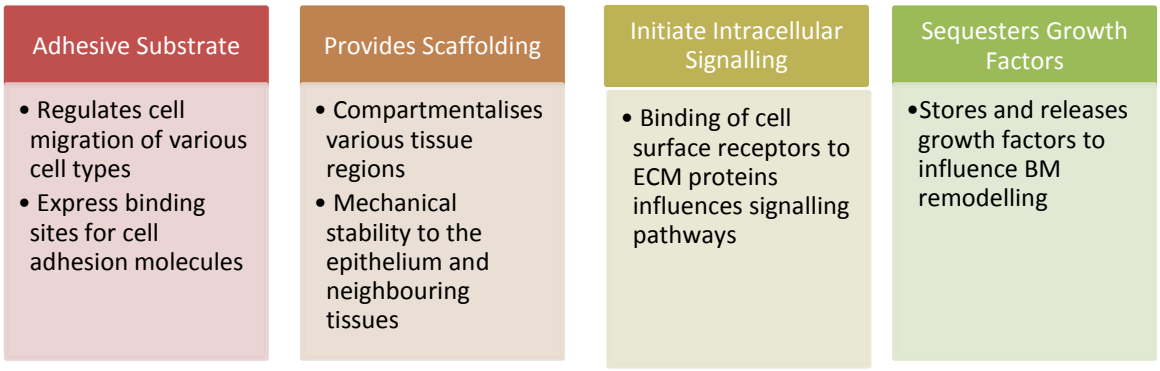

Figure 2 - A summary of the ECM functions during development. Adapted from (Frantz *et al.* 2010).

1.6.1 Laminins

The laminin family of heterotrimeric glycoproteins are major components of the basement membrane (BM). The BM also consists of other structural proteins such as collagen type IV, proteoglycans, nidogen (entactin), and BM-40 (osteonectin). The arrangement of the laminin α, β, and γ chains is cross-shaped (Figure 3). The four arms of laminin contain binding domains to mediate interaction with other components of the extracellular matrix to form the supramolecular architecture (Timpl 1989). The three chains are linked together by disulphide bonds in the long arm of the protein forming the coiled-coil helices. A single cysteine-rich repeat in the γ-chain binds to entactin (Nidogen) with high affinity (Mayer *et al.* 1993). The laminin-entactin complex can further bind to heparin proteoglycan and type IV collagen (Battaglia *et al.* 1992; Tryggvason 1993). To date there are 5 α chains, three β chains, and three γ chains which form 15 different laminin isoforms, all having differential expression during development (Table 2).

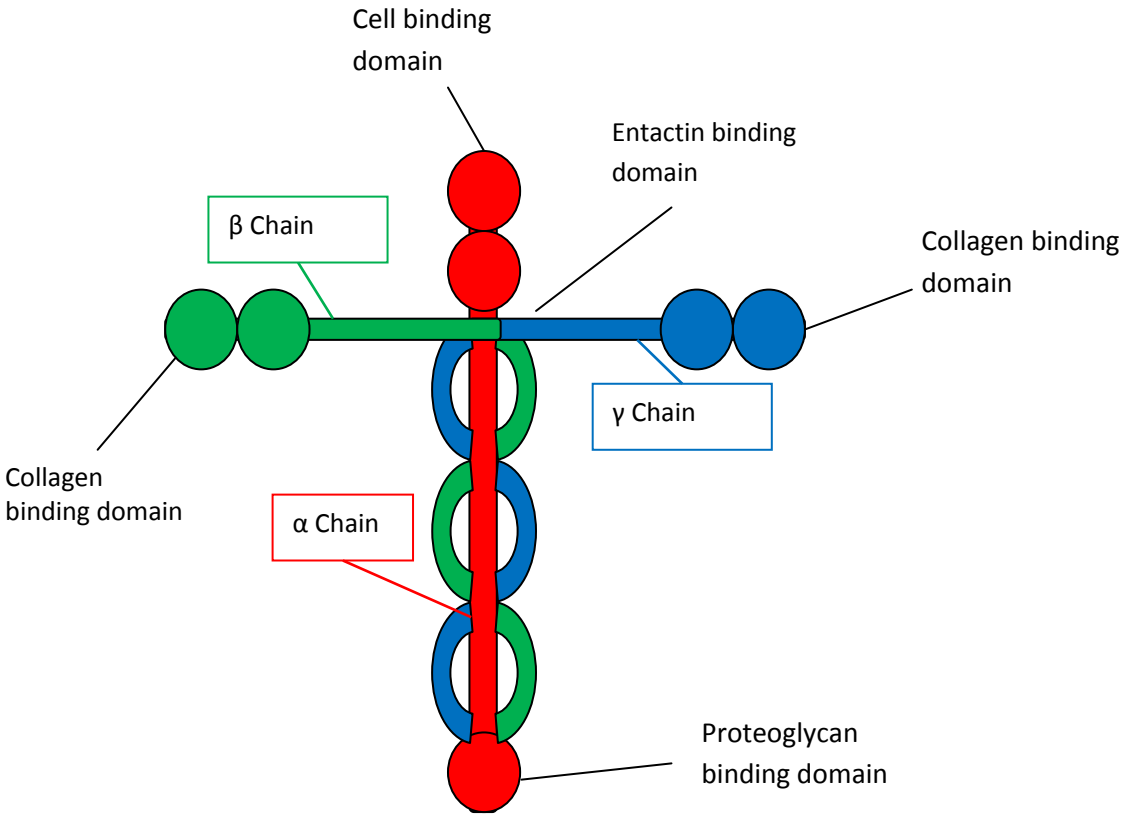

Figure 3 - A schematic representation of Laminin structure. Adapted from (Timpl 1989)

From the summary in Table 2, it is evident that laminins have significant roles in various cellular processes. In particular, an extensive amount of literature has been directed to the role of laminin in cell migration. In this section we will focus on the effects of laminin on neuronal migration

Many studies have demonstrated the ability of laminin to modulate neuronal migration and cortical development in vivo. During development, laminin is expressed by radial glial fibers (Liesi 1990). Mice deficient in laminin α2 and α4 display defects in the ability of radial glial cells to attach to the pial membrane, subsequently resulting in a decreased cortical size and radial glial cell death (Radakovits *et al.* 2009). In zebrafish laminin α1 mutants, the migration of facial branchiomotor neurons (FBMN) is disrupted (Paulus *et al.* 2006), resulting in ventral motor neuron ectopia (Grant *et al.* 2010). It has been suggested laminin α1 forms a genetic complex with proteins necessary for FBMN migration such as, Tag1 and stbm/vangl2 (Sittaramane *et al.* 2009). Furthermore, the zebrafish α1 mutant displays disrupted retinal ganglion, forebrain, and reticulospinal axonal projections (Paulus *et al.* 2006). Inhibition of the nidogen binding site in laminins stalled the tibial pioneer axons in the insect limb bud (Bonner *et al.* 2001), suggesting the role of laminins in directional decisions. In the mouse cerebellum, laminin α1 deficiency results in disorganised Bergmann glial fibers and granule cell migration defect (Ichikawa-Tomikawa *et al.* 2012). These studies suggest a global role for laminin α1 in the brain.

Complete knockout of laminin γ1 in mice results in embryonic lethality (Smyth *et al.* 1999), whereas mice with a specific deletion of the nidogen binding site in laminin γ1 are viable until birth (Willem *et al.* 2002), suggesting the importance of this domain for postnatal development. Furthermore, deletion in laminin γ1 resulted in detachment of radial glial cells from the pial membrane and ectopic localisation of cortial plate neurons (Willem *et al.* 2002). Laminin γ 1 is suggested to mediate correct neuronal migration in the cerebral cortex via integrin signalling, and through the downstream AKT/GSK3-β signalling pathway (Chen *et al.* 2009). Interestingly, laminin γ1 in migrating adult olfactory bulb stem cells has been reported to form a complex with netrin and integrin α6β1 to mediate proliferation and migration(Staquicini *et al.* 2009)

suggesting laminins can form various complexes in different neuronal cell types. *In vitro,* LAMA1, LAMB1, LAMC1, and LAMA2 are target genes for RE1 Silencing Transcription Factor (REST), which has been shown to have crucial roles in neuronal gene expression and development. During neurogenesis, REST deficiency impairs expression of laminin in neural stem cells (Sun *et al.* 2008). Additionally, laminin expression is disrupted in mouse models of cortical dysplasia, further suggesting its importance in correct neuronal migration and positioning (Costa *et al.* 2001; Chang *et al.* 2006; Guenette *et al*. 2006).

Table 2 – A summary of the expression and function of the laminin subunits.

Laminin Subunit	Tissue expression (Mammalian)	Tissue expression (Zebrafish)	Loss of function phenotype in animal models	Human Disease	References
α1	Early embryo, kidney, brain	Eye, SC, branchial arches	Impaired retinal differentiation, vascular development, membrane formation, and notochord formation	ND	(Biehlmaier *et al.* 2007; Edwards *et al.* 2010; Sztal *et al.* 2011); (Pollard *et al.* 2006)
α2	Skeletal and cardiac muscle,	Eye, brain, SC, trunk muscle	Growth abnormalities, defects in nerve and muscle formation	Muscular Dystrophy CNS defects	(Patton *et al.* 2008; Vigliano *et al.* 2009; Gupta *et al.* 2012)
α3	Skin	Eye, brain, SC, skin	Abnormal glomerular endothelial cells and skin blistering	JEB	(Ashton *et al.* 1997; Abrass *et al*. 2006; Rozario 2010)
α4	Kidney and developing muscle	Eye, brain, SC, trunk muscle	Chronic kidney disease, cardiac hypertrophy and impaired function	Cardiomyopathy	(Wang *et al.* 2006; (Knoll *et al.* 2007);(Abrass *et al*. 2010)
α	Widespread expression	Lens, pectoral fin	Defective glomerulogenesis, dilated airspaces in lungs	ND	(Miner *et al.* 2000; Nguyen *et al.* 2005; Webb *et al.* 2007)

β1	Most tissues	Eye, brain, SC, Otic vesicle, notochord, trunk muscle	Defects in gastrulation, notochord formation, and retinal differentiation	Cobblestone Lissencephaly	(Parsons *et al.* 2002; Pollard *et al*. 2006; Radmanesh *et al.* 2013)
β2	NMJ, glomerulus	Eye, brain, SC, trunk muscle	Dysplasia when subunit γ3 gene is disrupted as well, Neuromuscular and renal defects	Pierson Syndrome Congenital myasthenic syndrome	(Maselli *et al*. 2009; Rozario 2010; Radner *et al.* 2012)
β3	Skin and other epithelia	ND	Skin blistering	JEB	(Buchroithner *et al.* 2004; Rozario *et al.* 2010)
γ1	Most tissues	Eye, brain, SC, trunk muscle, notochord, fins	Embryonic lethality, eye, notochord, and neuronal migration defects	JEB	(Smyth *et al.* 1999; Pollard *et al.* 2006; Chen *et al.* 2009)
γ2	Skin and other epithelia	ND	Progeressive blistering and loss of bone mineralisation	JEB	(Castiglia *et al.* 2001; Bubier *et al.* 2010)
γ3	Brain	Eye, telencephalon, SC, gut, myosepta	Retinal dysplasia, disruption of cortical lamination	Autism, Occipital malformations	(Barak *et al.* 2011; O'Roak, *et al.* 2011)

1.6.2 Reelin

The most extensively studied ECM molecule is reelin, which has significant functions in embryonic and adult brain development. The 388kDa protein structure consisting of 3461 amino acids was identified by (D'Arcangelo *et al*. 1995) (Figure 4). Adjacent to the N-terminus is the hinge region which is necessary for cell signalling processes. Downstream to the hinge region are 8 reelin repeats, each being separated by an epidermal growth factor (EGF) motif. In vivo reelin is cleaved between repeat 2 and 3 and between repeat 6 and 7 generating a 330kDa central fragment, which is critical for the interaction between reelin and its receptors (Jossin *et al.* 2004).

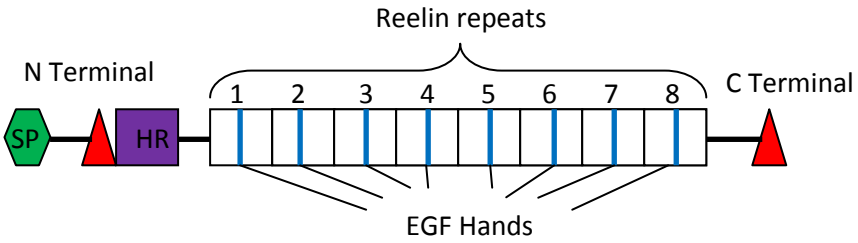

Figure 4 – A schematic representation of the reelin protein molecule. SP – signal peptide, HR – hinge region. Adapated from (Lakatosova 2012).

During embryogenesis reelin is expressed in the early-born Cajal-retzus cells in the cerebral cortex to promote correct cortical lamination and neuronal positioning, whereas in the adult, reelin transcripts disappear from the Cajal-retzus cells and become more prominent in GABAergic neurons in the cerebral cortex, cerebellar neurons, and hippocampal interneurons to mediate synaptic plasticity and memory formation (Alcantara *et al*. 1998; Costa *et al*. 2001; Liu *et al*. 2001).

The *reeler* mutant mouse model harbours a mutation in reelin and has been instrumental in understanding brain development. The developing neocortex has a six-layered structure of neurons which are organised in an “inside-out” alignment. The *reeler* mutant mice display incorrect positioning of neurons during brain development due to a disruption in the “inside-out” alignment in laminated structures. Homozygous

reeler mutants display decline in motor co-ordination, ataxia, and tremors (D'Arcangelo *et al*. 1995). In the developing forebrain of mutants, double labelling experiments show inhibitory interneurons exhibiting hypertrophic properties, resulting in abnormal positioning of forebrain interneurons (Yabut *et al.* 2007). Consequently, as the preplate fails to split correctly into the subplate in *reeler*, normal gene expression associated with the subplate is disrupted (Oeschger *et al*. 2012). Neurons which typically display neuronal polarity events such as the Lrp/Mig13a expressing neurons, are absent in the Reeler mutants (Schneider *et al*. 2011). Interestingly, a recent study showed the importance of the reelin signalling pathway in intestinal epithelium homeostasis. Microarray analysis in the reeler mice resulted in an upregulation of genes involved in intestinal metabolism (Garcia-Miranda *et al.* 2012). The reelin signalling pathway has also been found to be required in mammaray gland morphogenesis. Deletion of mouse reelin resulted in a disorganisation of the mammary epithelium and ductal patterning (Khialeeva *et al.* 2011). These studies demonstrate the widespread action of reelin in neural and non-neural tissue.

Selective knockdown of reelin in the medial prefrontal cortex of adult rats lead to behavioural and cognitive defect similar to these observed in neuropsychiatric diseases (Brosda *et al.* 2011). Unlike homozygous mutants, heterozygous mutant which express 50% of brain reelin display a normal hippocampal lamination structure, but they do exhibit impaired hippocampal plasticity (Qiu *et al.* 2006). Consistent with this reelin supplementation rescues impaired synaptic function associated with heterozygous reeler mutants (Rogers *et al*. 2013). Collectively, these studies suggest the importance of the reelin signalling pathway in behaviour and cognitive functions in adults. Loss of function of reelin in adult hippocampus resulted in aberrant migration and dendritic development of adult neuroprogentior cells, suggesting reelin may be a regulator of adult neurogenesis (Teixeira *et al*. 2012).

Reelin induces a complex downstream signalling pathway and is also involved in crosstalk with other signalling pathways. Reelin directly binds to two lipoprotein receptions, very low-density lipoprotein receptor (VLDLR) and the apoilioprotein E receptor 2 (ApoER2). Upon binding it induces tyrosine phosphorylation of adaptor protein Disabled1 (Dab1), which is believed to be the most critical downstream signal

to control correct neuronal positioning (D'Arcangelo *et al*. 1999; Howell *et al*. 1999; Fatemi 2005). A novel interaction between thrombospondin-1 with VLDLR and ApoER2 has been identified. Similarily to reelin, thrombospondin-1 induces Dab1 phosphorylation to mediate post-natal migration of neuronal precursors from the subventricular zone to the olfactory bulb, highlighting the importance of Dab1 phosphorylation in neuronal migration (Blake *et al*. 2008). Many loss-of-function studies which disrupt Dab1, VLDLR, or ApoER2 function result in pathological and behavioural phenotypes observed in the *reeler* mutants (Sheldon *et al.* 1997; Trommsdorff *et al.* 1999; Weeber *et al*. 2002; Trotter *et al*. 2011). Reelin-Dab1 interaction stimulates activation of phosphatidylinositol-3-kinase (PI3K), which can induce activation of cytoskeletal protein such as n-cofilin (Chai *et al.* 2009) and neuronal Wiskott-Aldrich syndrome protein (N-WASP) (Suetsugu *et al*. 2004), both of which are important in mediating actin polymerisation changes during migration, suggesting Dab1 influences cytoskeletal proteins to determine nuclear positioning. Interestingly, a recent study showed reelin interacts with the extracellular domain of Ephrin B and induces phosphorylation of Dab1. Consistent with this, triple Ephrin B1, B2, B3 knockouts recapitulated migration defects observed in the classic *reeler* mutant, identifying Ephrins to be important in the reelin signalling pathway during brain development (Senturk *et al.* 2011).

Many observations indicate cross-talk between reelin and notch signalling pathway. *Reeler* mutant mice have a decline in levels of the notch intracellular domain (NICD) and decreased expression of the notch target genes, Hes5 and brain lipid-binding protein, resulting in migration defects in the cortex (Hashimototorii *et a*l 2008). Overexpression of NICD alleviates the defects observed in the *reeler* mice. Indeed notch also co-localises with Dab1 in the hippocampal dendate gyrus (Sibber *et al*. 2009). A recent study indicates the potential of the reelin-notch signalling in cell fate determination and differentiation. Reelin-notch signalling was found to induce differentiation of human neural progenitor cells into radial glia cells (Keilani *et al*. 2012).

1.7 Mechanisms Controlling Neuronal Migration – Guidance Cues

1.7.1 Semaphorins

The semaphorin family encompasses five different classes of guidance cues which include secreted and membrane bound proteins. Sema3A-G are secreted, Sema7A is glycosiphosphatidylinositol (GPI)-anchored, and the remaining classes, Sema4A-G, Sema5A-B, and Sema6A-D, are transmembrane members (Yoshida 2012). The semaphorins display complex interactions with various members of the plexin and neuropilin receptor families (Figure 5).

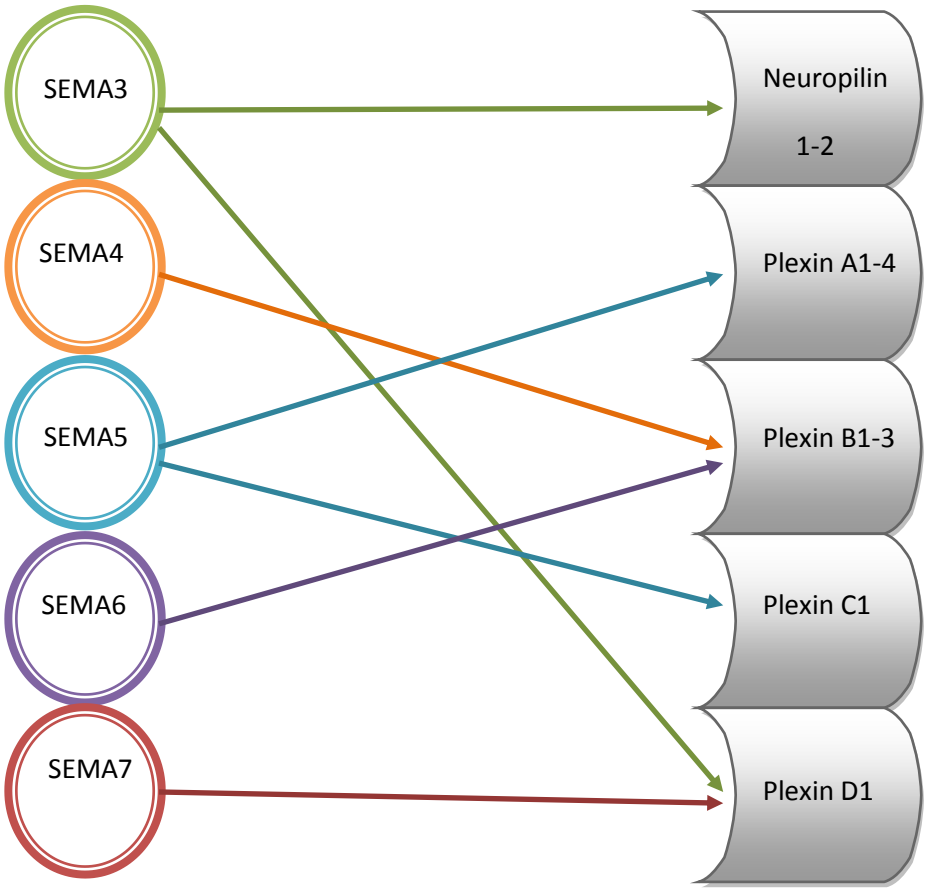

Figure 5 - A schematic to demonstrate interactions between members of the semaphorin family and, Neuropilin and Plexin. Adapted from (Yoshida 2012).

In mouse a population of neurons which align in the prospective lateral olfactory tract (LOT) have been identified to undergo “ventral tangential migration” These cells originate in the telencephalon and migrate ventrally and tangentially to the ganglionic eminence (Sato *et al*. 1998). This migratory stream is regulated by Sema3F and its interaction with Neuropilin 2. Mice lacking the guidance cue or its receptor result in ectopic localisation of “lot cells” (Ito *et al* 2008). Disrupting the interaction between neurpilin 1 and Sema3A leads to ectopic positioning of MGE neurons. Intrestingly, in vitro assays show Sema4A binds to membrane bound, chondroitin sulphate proteoglycans, to repel cortical interneurons (Zimmer *et al.* 2010).

During development semaphorins have been implicated in directing tangential migration of gonadotrophin-releasing hormone-1 (GnRH 1) expressing cells from the nasal placode to the hypothalamus. Sema4D and its receptor plexin B1 have been reported to be expressed by GnRH-1 migratory cells. Analysis of plexin B1 deficient mice show an altered migratory process of GnRH-1 cells, resulting in decreased proliferation. The correct directional migratory route of GnRH-1 cells may rely on activation of the Met tyrosinase kinase pathway downstream of Sema4D-plexin B1 interaction (Giacobini *et al.* 2008). Additionally, analysis of mice deficient in Sema7A also reveals disrupted GnRH-1 migration (Messina *et al.* 2011), suggesting that formation of proper neuronal networks is reliant on more than one family of guidance cues. Sema7A is expressed in various neuronal systems in the rat brain such as the, olfactory system, hippocampus, hypothalamus, and diencephalon, with transcript levels increasing towards adulthood (Pasterkamp *et al.* 2007).

Another member of the Sema4 subfamily, Sema4C, has been implicated in migration of granule cell precursors in the developing cerebellum and olfactory bulb by activating ErbB-2 and RhoA signalling (Deng *et al*. 2007). Sema4C mutant mice display exencephaly resulting in neonatal lethality. Sema4C and Sema4G double mutants showed enhanced cerebellar defects (Maier *et al.* 2011). A class 6 semaphorin is also important in guiding the migration of post-mitotic granule cells. Sema6A mutants display perturbed granule cell migration within the external granule layer (Kerjan *et al.* 2005), a phenotype similar to that seen when the receptor for sema6A, plexin A2, is mutated. It has been suggested the mechanism underlying the cerebellar phenotype

observed in plexin A2 and Sema6A deficient mice is due to a perturbed nucleus-centrosome coupling (Renaud *et al*. 2008).

1.7.2 Netrin

Interactions between netrin and its two receptors, deleted in colorectal cancer (DCC) and Unc5 have been implicated in neuronal migration and axonal elongation in various model systems. In vitro studies have shown that deletion of netrin or DCC results in abnormal distribution of LOT cells, thus disrupting the formation of the LOT (Kawasaki *et al.* 2006). In the cerebellum, netrin acts as a chemoattractant for migrating neurons from the lower rhombic lip (Alcantara *et al*. 2000). Interestingly, it has been suggested that the ability of netrin 1/DCC to act as a chemoattractant for migrating cerebellar neurons is coupled to exocytosis through SNARE proteins (Cotrufo *et al*. 2012). Netrin/DCC interaction has also been shown to exert influence on cytoskeletal dynamics through activation of Cdc42 and Rac1 (Shekarabi 2002). Loss of DCC function in mice disrupts dopaminergic (DA) progenitor cell migration and DA circuitry (Xu *et al.* 2010). Another member of the DCC family, neogenin, has been identified to interact with guidance cues. A high level of neurogenin is expressed on neural progenitors in the mouse forebrain, suggesting neurogenin may function to mediate migration of neurons in the forebrain (Fitzgerald *et al.* 2006). Mutations in the Unc5 family, member Unc5h3, cause a cerebellar malformation due to abnormal migration in mouse (Lane *et al*. 1992). Interestingly, Unc5h3 has been suggested to be a candidate gene underlying the cerebellar vermis defect (CVD) and the hobble (HB) rat mutants. Both mutants are characterised by lamination abnoramlities and ectopic localisation of cerebellar tissue (Kuramoto *et al.* 2004).

1.7.3 Neuregulin

The most extensively studied guidance cue is that of neuregulin (NRG) on interneurons derived from the MGE. In verterbrates there are 4 classes of neuregulins (NRG 1-4) which each possess an epidermal growth factor (EGF) motif and can bind to ErbB receptors, a class of tyrosine kinase receptors. NRG1 binds to ErbB4 and has been shown to play a directional role for interneurons derived from the ganglion eminences (Buonanno 2001). ErbB4 expression has been detected in the MGE during early development and in parvalbumins and GABA-positive interneurons, which

migrate tangentially from the ventral to dorsal telencephalon, suggesting the importance of neuregulin signalling in telencephalic interneurons (Yau *et al*. 2003). Disruption of this signalling causes a defective migratory pathway of telencephalic interneurons, resulting in a reduced interneuron population in the cortex. Three different isoforms of NRG1 reside in the developing telencephalon, type III and type I/II, of which type I/II acts as a chemoattractant for interneurons derived from the MGE (Flames *et al*. 2004). Interestingly, a recent study suggested a chemorepellant action of type III and type I on GABAergic interneurons migrating from the MGE (Li *et al.* 2012), suggesting NRG1 may undergo dual, attractive and repulsive roles in guiding interneurons. As well as guiding migrating GABAergic interneurons, NRG1/ErbB4 signalling is critical for wiring of GABA circuitry in the cortex (Fazzari *et al*. 2010). In the adult mouse forebrain, loss of ErbB4 display altered migratory routes of olfactory interneurons (Anton *et al*. 2004), suggesting the importance of guidance cues in adulthood as well as during development

Collectively, these studies imply that neurons seek guidance from chemoattractant or chemorepulsive cues in order for their correct migratory route. Disturbance of guidance cues and their receptor interactions can abolish this fine tuned molecular machinery, resulting in malformations during development.

1.8 Migration Defects in Disease

As discussed in the previous sections, many genes, signalling pathways, guidance cues, and protein-protein interactions regulate the complex phenomenon of neuronal migration. Mutations in genes involved in these cellular processes can result in neuronal migration defects; causing a variety of cortical malformations, see Table 3.

Table 3 – A summary of genes implicated in diseases associated with defects in neuronal migration.

Human Disease Associated with Migration Defects	Genes Involved	Gene Function	References
Isolated Lissencephaly sequence (ILS) (Classical Lissencephaly)	Tubulin alpha1 (TUBA1A) Doublecortin (DCX)	Microtubule Associated Protein Microtubule Associated Protein	(Liu 2011; Sohal *et al.* 2012)
Miller-Dieker Lissencephaly (Classical Lissencephaly)	Lissencephaly (LIS1)	Microtubule Associated Protein	(Liu *et a.l* 2011)
Lissencephaly with cerebellar hyperplasia	Very low density lipoprotein receptor (VLDLR) Reelin (RELN)	Receptor involved in signalling Involved in lamination	(Verrotti *et al*. 2010)
Fukuyama congenital muscular dystrophy (Cobblestone Lissencepahly)	FCMD	Modulates glycolsylation	(Kurahashi *et al.* 2005)
Walker-Warburg Syndrome (Cobblestone Lissencepahly)	Fukutin-related protein (FKRP) O-mannosyltransferase 1 (POMT1) O-mannosyltransferase 2 (POMT2) GTDC2 ISPD	Modulates gylcosylation Enzyme involved in glycosylation Enzyme involved in gylcosyation Predicted glycosyltransferase Encodes isoprenoid synthase domain	(Manzini *et al.* 2012; Roscioli *et al.* 2012)
Bilateral Periventricular Heterotropia	Filamin 1 Aristaless-related homeobox (ARX)	Actin binding protein Transcritption factor	(Kakita *et al.* 2002; Oegema *et al.* 2012)

	ARFGEF2	Involved in vesicle trafficking	
Polymicrogyria	GPR56	G-protein Coupled Receptor	(Oegema *et al.* 2012; Singer *et al.* 2012)
	TUBA1A	Cytoskeletal Protein	
	Tubulin beta2 (TUBB2B)	Cytoskeletal Protein	
	ARX	Transcription factor	
Baraiter-Winter Syndrome	Beta-actin (ACTB)	Actin genes	(Riviere *et al.* 2012)
	Actin gamma 1 (ACTG1)	Actin gene	
Schizophrenia	Disrupted-in-schizophrenia (DISC1)	Neurite outgrowth	(Saetre *et al.* 2008)
	MDGA1	Involved in adhesion	
Autism	Laminin γ3 (LAMC3)	Laminin hetrodimer	(O'Roak *et al.* 2011)
Epilepsy	Prickle	Component of planar cell polarity (PCP) pathway	(Tao *et al.* 2011)

1.8.1 Neuronal Migration Disorders

1.8.1.1 Lissencephaly

Lissencephaly, meaning "smooth brain", is characterised by a lack of cortical convolutions. Cortical malformations range in severity, from absence of gyria (agyria) to reduction of gyria (pachgyria), and occur approximately between the 12th to 16th weeks of gestation. Most classical (type I) Lissencephaly cases occur due to mutations in genes involved in axonal transport, thus these cases commonly lead to defects in axonal growth and guidance. Classical Lissencephaly can be further separated into two categories, isolated Lissencephaly sequence (ILS) and Miller-Dieker Syndrome (MDS). All cases of MDS and 40% of ILS cases are caused my mutation in Lis1, which encodes a subunit of platelet-activating factor acetylhydrolase (Hattori *et al*. 1994). Mutations in DCX and TUBA1A cause the other 60% of ILS cases. Unlike classical Lissencephaly, where neurons are unable to migrate due to mutations in cytoskeletal genes, cobblestone (type II) lissencephaly is associated with mutation in genes involved in the glycosylation pathway (Table 3). Classical and cobblestone lissencephaly have been

estimated to have an incidence of 1.2 in 100,000 births and 1 in 100,000 births, respectively (Dobyns *et al.* 1993; Gupta *et al.* 2002; Verrotti *et al.* 2010).

Neuronal migratory errors in classical Lissencephaly form 4 layers in the neocortex due to neuronal arrest, with each layer being highly disorganised (Reiner *et al.* 1995). Similar to humans, haploinsufficient Lis1 mice display neuronal migration defects (Hirotsune *et al.* 1998), disorganised neuronal positioning, lamination defects (Wang 2008), and seizure activity (Greenwood *et al.* 2009). Dose-dependent reduction of Lis1 in mice revealed an abnormal number of mitotically active cells and a progressive thinning of the ventricular zone, suggesting a role for Lis1 in maintaining neuroblast proliferation (Gambello *et al.* 2003). As discussed previously in section 1.4, Lis1 function is largely involved in regulating cytoskeletal dynamics by association with dynein motor proteins. Lis1 has multiple binding partners such as several nuclear distribution (NUD) genes, cytoplasmic dynein heavy chain, cAMP-specific phosphodiesterases, microtubule binding protein CLIP-170, and scaffold protein IQGAP1, and via these interactions is known to modulate cytoskeletal dynamics (Kholmanskikh *et al*. 2006; Murdoch *et al.* 2011).

Recently, studies have investigated the role of Lis1 in synaptic transmission questioning whether Lis1 contributes to an epileptic phenotype. Reduced Lis1 function In the hippocampus showed enhanced excitatory input to granule neurons, suggesting a direct effect between Lis1 disruption and synaptic transmission (Hunt *et al.* 2012). Patch clamp recordings in hippocampal slices revealed an increase in glutamate-mediated excitation and an increased number of vesicles at the presynaptic site, which may be associated with seizure activity (Greenwood *et al.* 2009). Calpains are a family of Ca^{2+}-dependent cysteine proteases. Administration of a specific protease inhibitor, ALLN, reverses the enhanced excitatory transmissions observed in Lis1 mutant mice, revealing a novel therapeutic to treat hyperexcitability (Sebe *et al*. 2013). Interestingly, depletion of Lis1 interacting proteins such as NDE1 and CDK in Caenorhabditis elegans (C.elegans) also leads to defective synaptic vesicle trafficking (Locke *et al.* 2006). Collectively, these studies implicate a direct influence of Lis1 on synaptic transmission.

Mutations manifested in the tubulin 1a (TUBA1A) gene are also reported to cause type I Lissencephaly. A mouse model which harbours an S140G mutation in TUBA1A showed an abnormal layering pattern in the hippocampus due to a decreased neuronal motility. Furthermore, the superior colliculus displayed a loss of postmitotic neurons due to apoptosis (Edwards *et al*. 2011). Analysis of the dendate gyrus in a TUBA1A deficient mouse model revealed ectopic neurogenesis in the granule layer due to defective migration of prospero-homeobox-1-positive neurons and T box-brain-2-positive progenitors (Keays *et al*. 2010), highlighting the importance of TUBA1A in neuronal migration. Polymycogyria, another NMD, has also been reported to be associated with mutations in TUBA1A, suggesting TUBA1A mutations display a phenotypic spectrum from Lissencephaly to polymycogyria (Jansen *et al.* 2011; Poirier *et al*. 2012). Interestingly, mutations in TUBB2B which also result in polymycrogyria show an overlap of neuropathological features with TUBA1A-related forms. These studies reinforce the importance of microtubule proteins in cortical development, and suggest microtubule proteins may share pathogenic mechanism to develop a phenotypic spectrum ranging from lissencephaly and polymycrogyria (Jaglin 2009; Cushion *et al*. 2013).

1.8.1.2 Polymycrogyria (PMG)

PMG is another neuronal migration disorder. The surface of the brain displays an excessive number of small convolutions (gyri). Whether the excessive folds manifested in the cortex are local or widespread, or which region of the brain is affected, contributes to the severity of the neurological symptoms. Patients can experience a range of symptoms from intellectual disability, epilepsy, encephalopathy, and motor and cognitive deficits (Schmidlin *et al.* 2009). A clinical study identified twelve patients with bilateral generalised PMG who displayed clinical features including cognitive and motor delays and seizures (Chang *et al.* 2004).

Different forms of this disorder have been described. In some cases of PMG, cortical layers are distorted into 2 or 4 layers from the normal 6 layers. The cortices of these forms of PMG are defined as being unorganised and unlaminated. Some cases of PMG

have been described to have normal cortical organisation, but there is a reduction of thickness of the cortex and decreased neuronal populations, suggesting PMG is a result of post-migration defects (Judkins *et al.* 2011). Examination of the brain of a macaque monkey exhibiting spontaneous PMG showed disorganisation of the cortex and reduced number of pyramidal neurons in layer III of the motor cortex (Schmidlin *et al.* 2009). Experiments have also shown that excitotoxic influences can mimic the pathology observed in microgyria pathology in animal models. An intracerebral injection of N-methyl-D-asparate (NMDA) receptor agonist induces brain lesions resembling microgyria pathology in hamsters (Takano *et al.* 2004; Marret *et al.* 1995). A mouse model injected with a glutamatergic agonist induced a neuronal depopulation in cortical layers five and six (Marret *et al.* 1995. Excitotoxic injury in rat pups results in the absence of early generated neurons (Rosen *et al.* 1996). In humans, PMG can arise during early to middle second trimester from fetal ischemia and maternal hydrocarbon exposure (Barkovich *et al.* 1995). One case study of a child with fetal alcohol syndrome has been reported with PMG (Reinhardt *et al.* 2010). These studies suggest that environmental toxins play an important role in causing PMG. It has been well documented that mutations in *GPR56*, a g-protein coupled receptor results in bilateral frontoparietal polymicrogyria (BFPP) (Piao *et al.* 2004; Jansen 2005; Chiang *et al.* 2011), suggesting its importance in brain development. In situ hybridisation experiments show strong expression of GPR56 in the ventricular and subventricular zones of the cortex, and in neuronal progenitor cells (Piao *et al.* 2004). It has been suggested that GPR56 mutations may exert a combination of different mechanisms to cause BFPP. These include reduced expression of receptors on the cell surface, an inabitlity of GPR56 to bind to its ligand to promote cell adhesion, and a loss of GPR56 proteolysis (Chiang *et al*. 2011). Cortical lamination defects and breaks in the pial basement membrane in a GPR56-deficient mouse causes overmigration of neurons, resembling BFPP pathology (Li *et al*. 2008). Recently, novel mutations in the genes of α and β tubulin, TUBA1A and TUBB2B, have been linked to case studies reported with PMG (Poirier *et al*. 2012; Romaniello *et al*. 2012), re-enforcing the importance of cytoskeletal genes during cortical development

1.8.2 Neuropsychiatric and Neurodevelopment Diseases

1.8.2.1 Schizophrenia

Schizophrenia is a complex psychiatric disorder and is thought to be caused by a combination of environmental and genetic factors. It is characterised by positive symptoms such as hallucinations and delusions, and negative symptoms such as deficits in thought and emotional processing, lack of motivation, and lack of speech (Rapoport *et al.* 2005).

Many studies have investigated neurodevelopmental models of schizophrenia, suggesting abnormal brain development occurs perinatally and leads to onset of symptoms in young adulthood. A large amount of evidence associates the onset of schizophrenia with prenatal insults and obstetric complications. Exposure to prenatal infections, such as rubella, influenza, and toxoplasmosis, has been suggested to contribute to the etiology (Brown 2006). Additionally, prenatal hypoxia, pre-eclapmsia, hemorrhages, ischemia, and asphyxia have been suggested to play a role in the pathophysiology (Rapoport *et al*. 2005; Sommer *et al.* 2010; Folsom 2012). A vast amount of research has shown linkage between structural brain abnormalities such as deficits in grey and white matter, and enlarged ventricles with schizophrenia (Davis *et al.* 2003; Tenyi 2011; Collin *et al*. 2012). Another hypothesis to support the neurodevelopmental model is the abnormal expression of genes involved in neuronal migration, intracellular signalling pathways, and proliferation in schizophrenia animal models (Akbarian *et al.* 1993; Folsom 2012).

DISC1 is a candidate risk gene for schizophrenia and other psychiatric disease. It was first identified in an association study of a large Scottish family with mental illnesses (St Clair *et al.* 1990). It has been shown to be involved in many neuronal processes such as migration, neurogenesis, neurite extension, and synapse formation (Hennah *et al.* 2006; Brandon *et al.* 2009). Although it is difficult to model some of the symptoms of schizophrenia, such as hallucinations and psychosis in experimental conditions, animal models can give further insight towards the neurobiology, genetics, and anatomical and cognitive characteristics underlying this disorder (Johnstone *et al.* 2011). In the mouse embryo, DISC1 transcripts are expressed in the MGE. Knockdown of DISC1 in the MGE-derived interneurons delayed interneuron migration by causing

deficits in the formation of leading processes (Steinecke *et al.* 2012). Additonally, suppression of DISC1 expression in the mouse hippocampus results in a migration defect of the CA1 pyramidal neurons (Tomita *et al*. 2011); suggesting the involvement of DISC1 in neuronal migration affects different cell types. Interestingly, administration of an NMDA receptor antagonist results in overmigration of neurons in the dendate gyrus of the hippocampus, and decreases expression of DISC1. The neuronal migration defect can be rescued by exogenous administration of DISC1. This suggests that NMDA signalling and DISC1 expression work together to control migration of neurons in the denate gyrus (Namba *et al.* 2011). Knockdown of a known DISC1 interacting protein, coiled-coiled protein associated with myosin II and DISC 1 (CAMDI), impairs radial migration by disrupting the centrosome (Fukuda *et al*. 2010). Schizophrenic risk factors, prenatal stress and maternal immune activation, result in disrupted GABAergic interneuron migration in murine models (Oskvig *et al.* 2012; Stevens *et al.* 2012). These studies implicate altered expression of genes involved in neuronal migration. Many studies have reported that reduced reelin expression is associated with schizophrenia. Brain white matter of schizophrenia subjects displays decreased reelin expression (Eastwood 2003). Significant associations were found between reelin polymorphisms and schizophrenia in the Han Chinese population (Li *et al*. 2011).

1.8.2.2 Autism

Autism spectrum disorders (ASD) are a family of neurodevelopment disorders which commonly occur during childhood. Patients display deficits in social interaction and language development, and repetitive behaviour (Geschwind 2009). Although cellular mechanisms which underlie autism are not clearly understood, many studies have suggested an involvement of aberrant neuronal migration. MRI studies of thirteen male subjects with autism display polymicrogyria, schizencephaly, and macrogyria, all of which are neuronal migration disorders that occur during gestation (Piven *et al*. 1990). Quantification of the boundary between the grey and white matter showed abnormal cell patterning between cortical layer VI and the white matter in ASD subjects. It was suggested this abnormal patterning might be a result of migration defects (Avino 2010). Postmortem studies on autistic brains showed cell patterning and gene expression abnormalities in the cerebellum (Bauman 1985; Fatemi *et al.*

2002; Fatemi *et al.* 2008). Immunohistochemistry studies on the cerebellum of autistic subjects showed a significant increase in interleukin 6 (IL-6) protein expression. Overexpression of IL-6 in cerebellar neurons causes defects in granule cell adhesion and migration, suggesting elevated levels of IL-6 may alter neuronal processes and play a role in the pathophysiology of autism (Wei *et al.* 2011). Other key regulators involved in the migration process are extracellular matrix molecules and may contribute to the pathophysiology of autism. Decreased protein and mRNA levels of reelin have been found in the frontal and cerebellar regions of autistic brains compared with controls (Fatemi *et al.* 2005). Postmortem tissue from brains of autistic tissue display defects in the components of the extracellular matrix such as N-sulfated heparin sulphate and laminin (Pearson *et al.* 2013). Interestingly, novel mutations in Laminin γ3 have been shown to be implicated in ASD (O'Roak *et al.* 2012).

Modelling mutations associated with disease in animals models provide us with a greater understanding of gene function and opportunites for therapeutic development. A mouse model deficient in the contactin-associated protein-like 2 gene (*cntnap2)* displays characteristics associated with ASD. These mice have symptoms that have been reported in humans with CNTNAP2 mutations, such as hyperactivity and epileptic seizures. (Penagarikano *et al*. 2011) Histological analysis showed abnormalities in neuronal migration, resulting in the presence of ectopic neurons in the corpus callosum. Additionally, mutant mice displayed a reduced number of GABAergic interneurons, and abnormal connectivity. Altered expression of the *met* gene, which encodes a tyrosine kinase receptor, has been implicated in autism. Morpholino knockdown of *met* in the zebrafish leads to a reduced number of granule cells in the cerebellum and a migration defect in hindbrain branchiomotor neurons (Elsen *et al.* 2009).

In conclusion these studies implicate the occurrence of early migration defects during development, before the onset of ASD symptoms. These defects may be associated with brain abnormalities and aberrant synaptic connectivity found in patients with schizophrenia and epilepsy.

1.8.3 Migration Defects in Neurodegenerative diseases

1.8.3.1 Alzheimer's Disease (AD)

The brain of patients diagnosed with AD are characterised by 2 hallmark pathologies; amyloid plaques and neurofibillary tangles (NFTs). The extrallular neuritic plaques are composed of deposits of amyloid-beta (Aβ) peptide, whereas the intracellular lesions of the NFTs are comprised of hyperphosphorylated tau (De Strooper 2000). Early onset of familial AD encompasses 10% of all AD cases and is a result of autosomal dominant mutations in APP (Korenberg *et al.* 1989), Presenilin 1 (PS1) (Cruts, Backhovens et al. 1995), and 2 (PS2) (Levy-Lahad *et al*. 1995). The APP protein is a type I transmemebrane protein comprising an intracellular C termina and an extracellular N terminal. The Aβ peptide is generated through sequential cleavage by β-secretase and γ-secretase (Figure 6). The γ-secretase can cleave the protein at two sites thus generating two isoforms of the Aβ protein, Aβ-42 and Aβ-40. Both isoforms are toxic, however the Aβ-42 peptide can aggregate to form plaques due to its insolubility (Slomnicki 2008; Pardossi-Piquard 2012). During this cleavage process, the APP intracellluar domain (AICD) is also generated. In recent studies the AICD has received much attention and been shown to have important biological functions which may contribute to the development or progression of AD in patients.

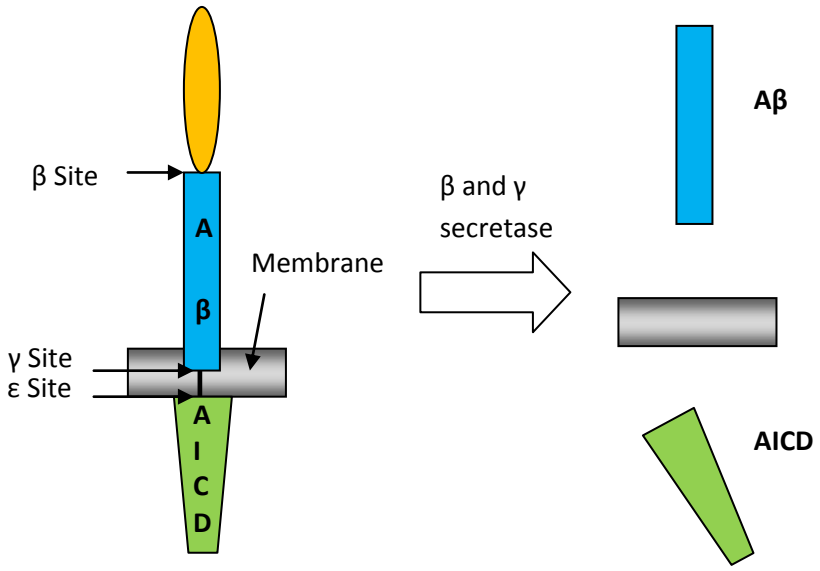

Figure 6 – A schematic representation of APP cleavage. Aβ and AICD fragments are generated through sequential cleavage by β and γ secretase. Cleavage via the γ-secretase occurs at 2 sites; γ site or ε site, thus can generate production of both Aβ40 and Aβ42.

The APP family comprises APP, APP-like protein 1 (APLP1), and APP-like protein 2 (APLP2). Many studies have suggested APP is an important facor in brain development by regulating neurogenesis and neuronal migraiton. Mice deficient in APP show a decreased neural progneitor cell proliferation and defective migration (Haughey *et al.* 2002). Using in utero electroporation to knock down APP, (Young-Pearse *et al.* 2007), identifies a role for both extra- and intracellular domains of APP to mediate correct migration of neuronal precursor cells into the cortical plate. Studies have revelaed APP can interact with downstream genes such as disabled 1 (DAB1) and disrupted-in-schizophrenia 1 (DISC1), both of which have been implicated in cortical development (Young-Pearse *et al.* 2007; Young-Pearse *et al.* 2010). Recently, APP has been shown to interact with pancortins, a family of secreted gylcoproteins expressed in the developing and mature cortex, giving further insight into the physiological mechanism of APP function (Rice *et al*. 2012). An insect orthologue of APP inteacts with heterotrimeric G protein mediating migration of epithelial cells in the entiric nervous system (Swanson *et al.* 2005), thus suggesting APP may have a role in mediating

migration outside the CNS. The most compelling evidence to suggest the role of APP in neuronal migration comes from the triple APP, APLP1, and APLP2 knockout mouse models. These mice display cortical dysplasia characterised by abnormal migration of neuroblasts through the pial membrane, mimicking pathology observed in human type II lissencephaly (Herms *et al.* 2004). A recent study implicates APLP2 in neuronal differentiation of cortical progenitor cells. Silencing APLP2 in vivo revealed a higher number of mitotically active progentitor cells due to cortical progenitors being able to remain in their undifferentiated state longer (Shariati *et al*. 2013).

The AICD domain generated from sequential cleavages harbours a –YENPTY- motif that is conserved in all species, suggesting it may have a functional importance (Slomnicki 2008). This motif is recognised by a number of adaptor proteins, which can form functional complexes and regulate different biological processes (Table 4). The most intensively studied AICD binding proteins are the FE65 family, consisting of FE65, FE65-like protein (FE65L1), and FE65-like protein 2 (FE65L2). These adaptor proteins all have 3 structural domains; one WW domain and two phosphotyrosine binding (PTB) domains (McLoughlin *et al.* 2008), and each domain can interact with a variety of partners to form functional complexes (Figure 7).

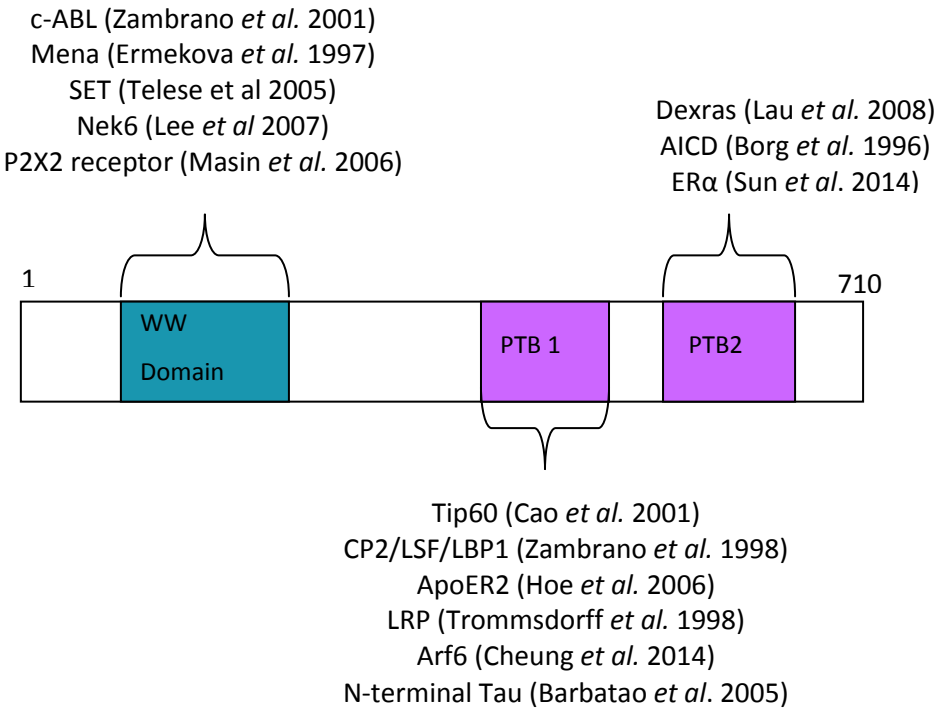

Figure 7 - A schematic representation of the structural domains and of the FE65 family and their binding partners.

All members of the FE65 family have been shown to bind to the AICD fragment (Borg *et al.* 1996; Guenette *et al.* 1996; Zambrano *et al.* 1997). This interaction is mediated by threonine-668 located near the YENPTY motif (Ando *et al.* 2001). FE65-APP has been shown to be involved in cell migration by regulating actin dynamics (Sabo *et al.* 2001). Co-localisation of FE65 and APP in neural stem cell niches in the ventricular zone indicates a role for FE65 in neurogenesis (Ma *et al*. 2008). Two knockout mouse models, one deficient in th 97kDa FE65 isoform and the other deficient in the 60kDa FE65 isoform show an increase of the gonadotrophin-releasing-hormone 1 (GnRH 1) neurons during embryonic development. These neurons are the first to be generated in the nasal placode and migrate into the forebrain. Although migration of GnRH 1 neurons appear normal in the knockout mice, birth tracing experiments revealed prolonged neurogenesis of the GnRH 1 neurons (Forni *et al*. 2011). Double FE65/FE65L1 knockout results in cortical dysplasia (Guenette *et al*. 2006), a similar phenotype observed in triple APP knockout mice (Herms *et al.* 2004). The mutant mice are also characterised by disrupted laminin organisation, and incorrect axonal projections and neuronal positioning (Guenette *et al*. 2006).

Table 4 – summary of APP intracellular domain (AICD) binding proteins

Protein	Interaction to AICD	Downstream interacting proteins	Implications in functional Processes	Selected References
Fe65 (Fe65L1 & Fe65L2)	-YENPTY-	Tip60 CPS/LSF/LBP1 N-terminal of tau Dexras 1 c-ABL Mena Nek6 ERα LRP Arf6 ERα SET APoER2 P2x2 receptor	• Transcriptional activation • Neuronal migration • Cytoskeletal dynamics • Cellular motility • Trafficking and Processing • Apoptosis	(Borg *et al* 1996; Sabo *et al* 2001; Muller *et al* 2013; King *et al* 2011; Guenette *et al* 2006; Ha *et al* 2011)

X11/MINT family (X11α,β,γ and MINT 1, 2, 3)	-YENPTY-	Munc 18 KIF17 PSEN1 CASK-veli CCS (copper chaperone for SOD1) Alcadeins (Alcs)	• Synaptic vesicle docking • Exocytosis • Modulate APP processing • Transcriptional activity	(Borg *et al* 1996; Rogelj *et al* 2006)
JIP (JNK interacting protein 1a, 1b, 2)	-YENPTY-	JNK Kinesin 1	• Scaffold protein • Modulate APP processing • Axonal transport	(Taru *et al.* 2002; Tamayev *et al.* 2009)
Dab1 & 2	-NPTY-	FE65 ApoER2 VLDLR	• Neuronal positioning and migration • Cell growth • Nuclear exporting signalling	(Pramatarova *et al.* 2008; Young-Pearse *et al.* 2010)
ARH	--	--	• Regulates cholesterol uptake • Component of endocytic machinery	(Noviello *et al.* 2003; Tamayev *et al.* 2009)

c-ABL	-YENPTY-	--	• Cell differentiation • Cell division • Cell adhesion • Stress response	(Vazquez *et al.* 2009; Ozaki *et al* 2006; McLoughlin *et al.* 2008)
PAT 1	-YTSI-	--	• Microtubule binding protein • Mediates transport of APP through secretory pathway	(Muller *et al.* 2008; Chang *et al* 2006)
GTPase G 0	Residues 657-676 in c-terminal	--	• Apoptosis	(King *et al.* 2004)
Shc	-YENP-	--	--	(Fiore *et al.* 1995; Tarr *et al.* 2002)
APP-BP1	Recognises last 31 amino acids	--	--	(Chen *et al.* 2003)
UV-DDB	-YENTPY-	--	--	(Muller *et al*. 2008)

During development PS1 is required for neurogenesis by maintaining the neural progenitor population. PS1 deficient mice reveal a thinner ventricular zone due to a reduction in neural progenitor cells, aberrant neuronal migration, and disorganised lamination in the cortex. Reduction of progenitor cells leads to premature differentiation of progenitor cells to post-mitotic neurons (Shen *et al.* 1997; Handler *et al.* 2000). Birthdate analysis in a conditional knock-out of PS1 in a mouse model revealed that late-born neurons failed to migrate past the younger born neurons and thus unable to arrive at their destined position in the superficial layers. PS1 deficient mice also display a reduction of radial glial cells, suggesting a role for PS1 in neuronal positioning and radial glial development (Wines-Samuelson *et al.* 2005). Abnormal migration defects observed in PS1 deficient mice may be due to unstable cytoskeleton architecture, thus leading to a collapse of growth cones (Shvartsman *et al.* 2008).

1.9 Zebrafish as a Model of Neuronal Migration

1.9.1 Zebrafish Model

The zebrafish has emerged as a sophisticated model to study neurobiology in development and in disease. Scientific investigations using this model can provide valuable information absent gene function in development and disease, and potential targets for therapeutics (Bradbury 2004). One of the most important assets in using the zebrafish as a model is that there is a high conservation of genetic pathways that regulate development between zebrafish and higher vertebrates. Due to the high homology of sequences between human and zebrafish genes, a genome database has been generated; Zebrafish Information Network (ZFIN) and more recently the Zebrafish Neurophenome Project (ZNP), which provides neurobiological and physiological phenotpyes of adult zebrafish (Santana *et al*. 2012). The zebrafish has many benefits for use in research; it is a small fish and has a short generation time, thus reducing husbandry costs and is less laborious to maintain than other higher vertebrate models. Being a vertebrate it is genetically closer to humans than other simple *in vivo* models such as, *Drosophila* and *C.elegans* (Flinn *et al.* 2008).

Importantly, with regard to development, the transparency of the zebrafish embryo is a key advantage. Fluorescent proteins can be inserted into the zebrafish genome which can then be visualised in specific cells or tissues. Many studies have used transgenic lines which label specific neurons to investigate the migratory route of these neurons and the development of the CNS (Higashijima *et al.* 2000; Park *et al.* 2000; Abraham et al. 2009). Recent advances in transgenic manipulation like the *Tol2* transposon system have increased the efficiency of introducing trangenes into the zebrafish germline (Kwan *et al.* 2007). Transgenic lines and injection of fluorescent dyes can also provide fate maps and facilitate cell lineage tracing (Kozlowski *et al.* 1997) phenythiourea (PTU) is used to maintain optical transparency, however is should be noted PTU exposure may affect thyroid function (Elsalini 2003). There are several possible ways to investigate gene function in development and disease. Firstly, one can induce a loss of function of a particular gene by injecting antisense morpholino oligonucleotides. Translation blocking morpholino are typically targeted to the 5' untranslated region (UTR) and are effective in blocking translation of a particular mRNA (Corey *et al* 2001). Splice blocking morpholinos interfere with the pre-mRNA splicing process and can create specific effects such as exon deletion or intron insertion (Figure 8).

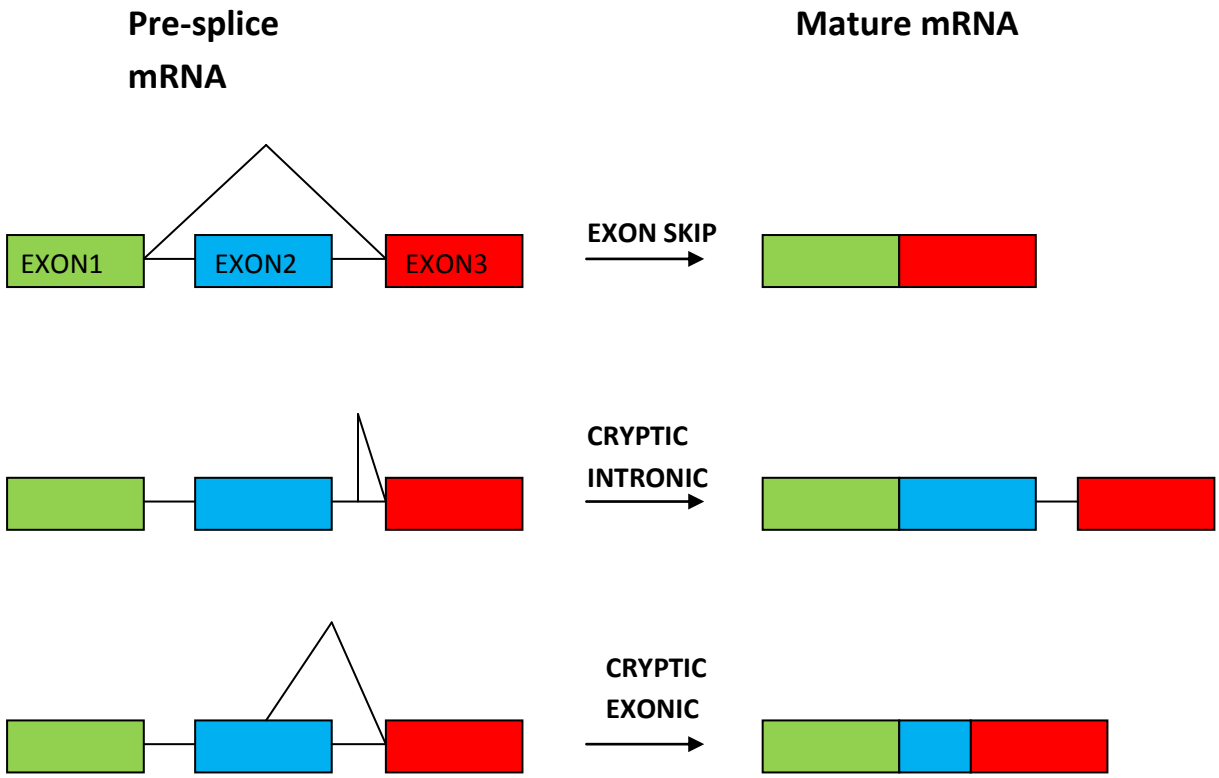

Figure 8 – Examples of mature mRNA products produced by using a splice donor site blocking morpholino

Although this is a rapid technique, morpholino efficacy is transient and is lost by day 5 of development (Flinn *et al.* 2008), and can occasionally induce off target effects such as activation of p53 (Robu *et al*. 2007). Secondly, one can knockout gene function via reverse genetics such as, TILLING, which uses a combination of chemical mutagenesis and DNA screening to identify mutations (Leong *et al.* 2011). Thirdly, one can knockout of gene function via targeted mutagenesis by using zinc finger nuclease, TALEN , and CRISPR methodologies, which create mutations at targeted sites (Sander *et al*. 2011).

1.9.2 Migration in the Zebrafish Forebrain

There are some differences in the way the zebrafish undergoes brain morphogenesis compared to higher vertebrates. The telencephalic hemispheres expand out laterally through an invagination process in higher vertebrates (Figure 9), whereas in the

zebrafish the hemispheres turn outward in a process eversion. Consequently, the ventricular surface lies on the outside covering the dorsal pallial structures in the zebrafish, rather than encompassed within the telecephalic hemispheres in higher vertebrates (Wullimann 2002). The first step in the morphogenesis of the telencephalon in the zebrafish is the formation of the anterior intraencephalic sulcus, responsible for the formation of the lumen between the telencephalon and diencephalon. The second step is the growth and proliferation of the telencephalon causing rearrangements to the olfactory bulb and telencephalon (Folgueira *et al.* 2012). In regards to morphology differences, the zebrafish telencephalon does not form into a layered cortex, and lacks primary and sensory telencephalic domains (Mione *et al*. 2008).

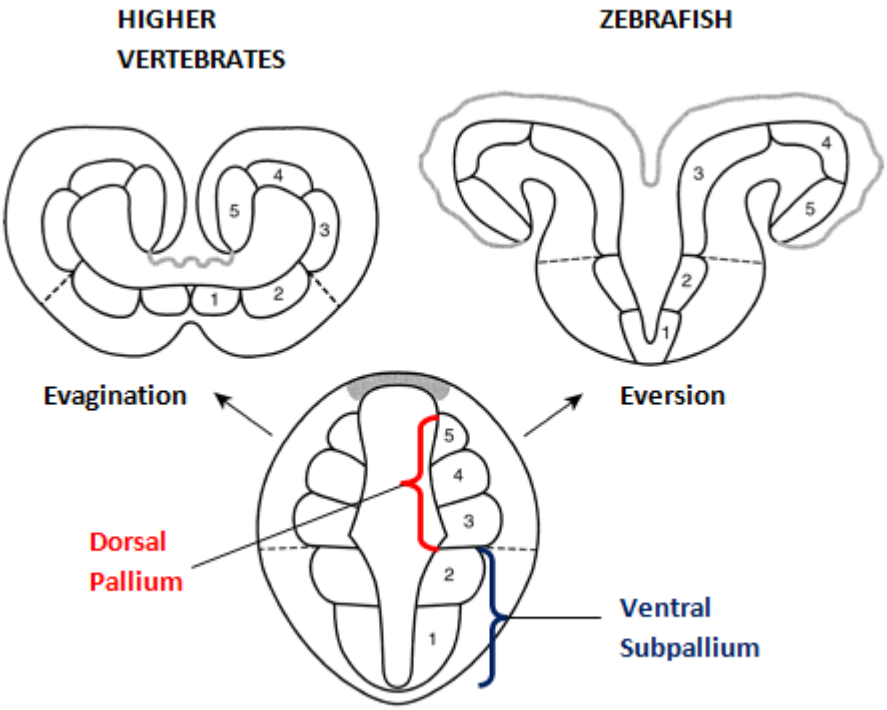

Figure 9 – Schematic representation of the development of the telencephalic hemispheres in zebrafish and higher vertebrates. The initial forebrain vesicle undergoes morphogenesis to form either evaginated cerebral hemispheres in higher vertebrates or everted cerebral hemispheres in zebrafish. Zebrafish display a reversed orientation of the dorsal pallium subgroups compared to higher vertebrates. Choroid plexus is highlighted in grey. Adapted from (Northcutt 2002).

Despite these morphological differences, the zebrafish posses all the sensory systems (visual, olfactory, taste, tactile, balance, and hearing) and the basic structures of the CNS are similar to higher vertebrates and humans (Becker 2012). The developmental mechanisms and assembly of neural circuits in the telencephalon are highly conserved in all vertebrates. Early expression patterns of pax, dlx, and wnt genes, expressed in the presumptive telencephalon, are remarkably well conserved between mouse and zebrafish (Macdonald *et al.* 1994; Quint *et al.* 2000; MacDonald *et al.* 2010). These conserved gene expression patterns are instrumental in specifying different cell types in the telencephalon, such as GABAergic interneurons (MacDonald *et al.* 2010), oligodendrocytes (Miyake *et al.* 2005) and mitral cells (Bundschuh *et al.* 2012). Other extracellular factors such as growth factors and guidance cues also play important roles in zebrafish telencephalon development (Gaudin *et al* 2012; Miyake *et al* 2005). Similar to higher vertebrates, alteration of gene expression or signalling mechanisms within boundaries disrupts neuronal differentiation, migration, and axogenesis (Macdonald *et al.* 1994; Onuma, Ding *et al.* 2011). During development, loss of function of specific genes has been shown to be important in forebrain development in both zebrafish and mice (Shimizu 2009). Table 5 lists zebrafish mutants with forebrain defects. Additionally, many of the genes implicated in human diseases affecting the forebrain development and migration such as Parkinson's disease, Rett Syndrome, and autism have been identified in the zebrafish (Tropepe 2003; Flinn, Bretaud *et al.* 2008; Danesin *et al.* 2012).

Table 5 – Selected zebrafish mutants display defects in forebrain development

Zebrafish Mutant	Gene	Phenotype of mutant	References
Masterblind (mbl)	Mutation in wnt scaffolding protein, axin1	Eyes, olfactory placode, and telencephalon structures are absent	(Heisenberg, Brand et al. 1996)
Silberblick (slb)	Encodes Wnt 11	Eyes are partially fused	Heisenburg et al 1996
Knollnase	NA	Formation of telencephalon ventricle is affected	Heisenburg et al 1996
You-too (yot)	Encode dominat repressor form of Gli2	Defects in ventral forebrain differentiation	Karlstrom et al 1999
Small eye (sye)	Pax6	Defects in forebrain regions, disturbed development of the hypothalamo-telencephalic boundary	Stoykova et al 1996
Foggy (fog)	Transcription elongation factor	Reduced dopaminergic neurons in telencephalon and hypothalamus	Guo et al 2000
Belladonna (Bel)	Lim-homeodomain transcription factor (lhx2)	Failed formation of the axonal tracts in the forebrain	Seth et al 2006
Disarrayed (drya64)	NA	Defects in neurogenesis, small forebrain	Baye et al 2007
Aussicht (aus)	Suggested encodes a locus which regulates fgf8 homolog (ace)	Defects in forebrain differentiation	Heisenberg et al 1999

The zebrafish forebrain undergoes two waves of neurogenesis. The first wave establishes simple clusters of neurons such as the dorsorostral cluster (drc) and ventrorostral cluster (vrc) at 16hpf. The second wave of neurogenesis replaces the early specified clusters by more complex neuronal clusters and axonal projections appear at 2-3dpf (Wullimann 2009). The most advantageous tool when investigating neuronal migration in the zebrafish is the use of transgenic lines. In one such study, three transgenic lines labelling three different populations of neuronal cells in the forebrain were used to investigate their migratory routes during zebrafish development (Figure 10). The first population of telencephalic interneurons investigated were the mitral cells (Mione *et al.* 2008). In higher vertebrates mitral cell precursors originate from the dorsal telencephalon and are the first to differentiate in the olfactory bulb to become the principal projection neuron (*Blanchart et al.* 2006). In the zebrafish, T-box transcription factor (tbr1), expressed by mitral cells, was observed in the dorsal and ventral telencephalon regions. Tbr1-expressing cells in the dorsal telencephalon are initially bipolar in shape gradually adopting a multipolar fate. These cells are observed migrating to a location just dorsal to the developing olfactory placode. Another group of telencephalic neurons investigated were the glutamatergic cells. These cells first appear in paired groups at the level of the olfactory placode, at the telencephalon/diencephalon boundary, and in the midbrain. The telencephalon glutamatergic cells were seen to undergo dorsal to ventral migration, with many of the cells extending axons to other brain regions. Expression of different cell markers such as, *vglut2* and *gad,* resembles the expression found in mammalian septal glutamatergic neuorns. The third class of neurons investigated were the GABAergic neurons which undergo a ventral to dorsal migration. The number of these cells found at the dorsal telencephalon increased from 5 cells at 3dpf to 700 cells at 30dpf (Mionei *et al.* 2008). Similar to mice, dlx5a and dlx6a cis-regulatory elements have been shown to be important in determining dlx expression during GABAergic interneuon development in the zebrafish, suggesting a conserved genetic pathway (Yu *et al*. 2011).

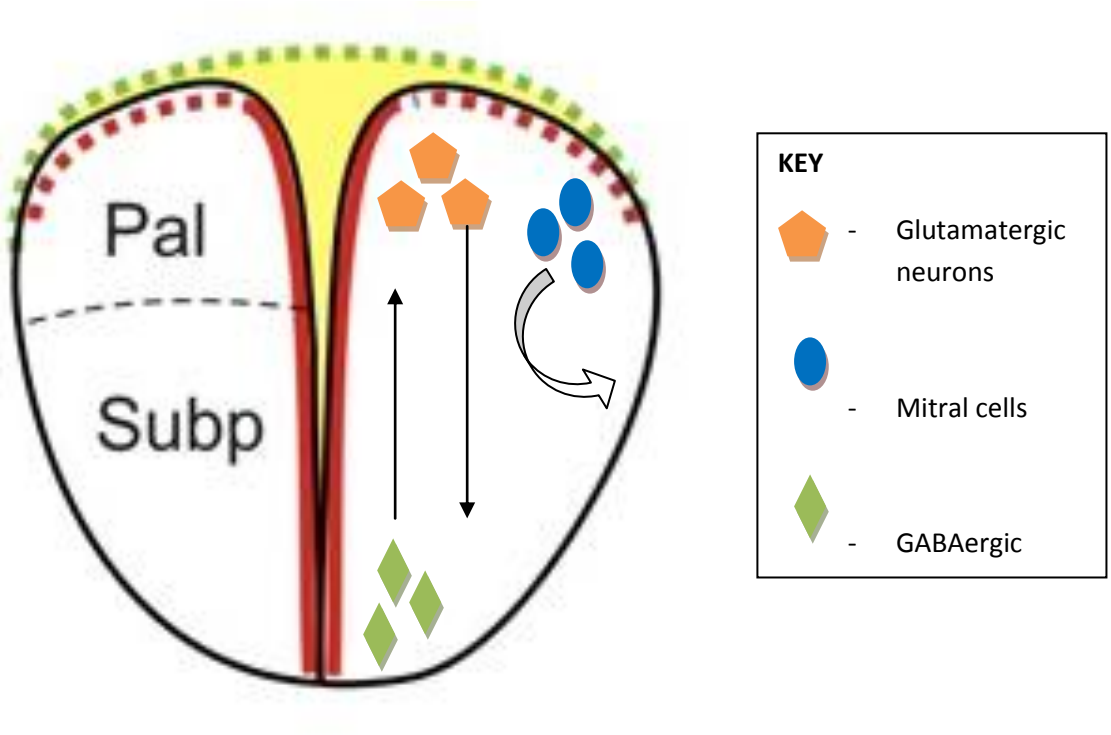

Figure 10 – A schematic representation of the migratory routes of telencephalic neuronal sub-populations. Glutamatergic cells (orange) migrate from dorsal (pallium) to ventral region (subpallium) GABAergic cells (green) migrate from ventral (subpallium) to dorsal (pallium) regions and mitral cells (blue) migrate towards the position of the olfactory bulb

1.9.3 Migration in the Zebrafish Hindbrain

Branchiomotor neurons (BMNs) are classified as cranial motor neurons located in the hindbrain and are extensively investigated in the zebrafish system to explore neuronal migration. In the zebrafish, the trigeminal BMNs innervate the pharyngeal arches which are involved in jaw movement, and originate in rhombomeres 2 (r2) and 3 (r3). Axons project from r2 and r3 dorsolaterally to reach their exit points. Facial BMNs (FBMN) (cranial nerve VII) are born in rhombomere 4 and migrate caudally to be located in rhombomere 6/7. Cell bodies of these neurons migrate in a perikayal translocation manner. The glossopharyngeal BMNs (cranial nerve IX) are generated in r6 and migrate caudally to r7. Vagal and accessory BMNs (cranial nerve X and XI, respectively) are generated in caudal hindbrain, r7 and r8 (Chandrasekhar *et al.* 1997;

Chandrasekhar 2004). Table 6 lists selected zebrafish mutants and morphants where motor neuron defects are observed.

Table 6 – A list of zebrafish mutants and morphants displaying motor neuron migration defects.

Zebrafish mutant/morphant	Funtion	Loss of function phenotype	Selected reference
Valentino (val) mutant	Bzip transcription factor encoding gene	Absence of hindbrain boundaries	(Cooke, Moens et al. 2001)
Trilobite (Tri) mutant	Interacts with the planar cell polarity (PCP) and Wnt signalling cascade	Gastrulation associated cell movement defects. nVII and nIX neurons migration defects	(Bingham, Higashijima et al. 2002)
Colgate (Col) mutant	Encodes Histone deacetylase 1 (hdac1)	Defective migration of FBMNs	(Nambiar *et al.* 2007)
Kto/med12 mutant	Affects mediator componenet med12	Loss of rhombomere boundary cells	(Hong 2011)
Acerebellar (Ace) mutant (mutation in FGF8)	Fibroblast growth factor	Lack midbrain-hindbrain organiser	(Reifers *et al.* 1998)
Prickle (Fh122) mutant	REST interacting LIM domain protein	Defective FBMN migration	(Mapp *et al.* 2011)
Hmgcrb mutants	Encodes an enzyme in the mevalonate pathway	Partial disruption of FBMN	(Mapp *et al* 2011)
Cadeherin 2(Cdh2) mutants	Involved in cell-cell adhesion	Ectopic migration of FBMN	(Stockinger *et al.* 2011)

Detour (Dtr) mutants	Encodes component of Hedgehog signalling pathway	Loss of cranial motor neurons	(Vanderlaan *et al.* 2005)
Met morphant	Encodes a tyrosine receptor kinase	Met knockdown results in disruption of FBMN migration	(Elsen *et al.* 2009)
Hox 1a morphant	Homeodomain transcription factors	Hox1a knockdown disrupts neuronal organisation in r4	(Cooper *et al.* 2003)

Many mechanisms have been documented to regulate motor neuron migration in the zebrafish hindbrain, one of which is the noncanonical Wnt/Planar Cell Polarity (PCP) signalling pathway. Strabismus (Stbm)/Van Gogh (Vang) is a transmembrane protein associated with the PCP signalling pathway and has been implicated in motor neuron migration. The zebrafish *trilobite* mutation disrupts the stbm/vang protein resulting in a failure of nVII and nIX tangential migration (Bingham *et al.* 2002; Jessen, Topczewski et al. 2002). Interestingly, a loss of *vangl2* function in mouse embryos also inhibits the caudal migration of motor neurons from r4 to r6 (Glasco *et al.* 2012), suggesting a conserved function of the vang protein in regulating the migratory mechanism of FBMN neurons. Furthermore, it has been suggested vangl2 may interact with ECM molecules, laminin α1 and transient axonal glycoprotein1, to participate in a common pathway which regulates FBMNs (Sittaramane *et al.* 2009). Another gene involved in the PCP pathway is prickle (pkb), which can interact with stbm/vang to regulate cell movements during gastrulation and migration of motor neurons (Carreira-Barbosa *et al.* 2003). Prickle1b disruption alters FBMN migratory speed, thus hindering the cells exploratory behaviour. Additionally, prickle1b may be important in correctly polarising FBMNs (Mapp *et al.* 2011). Disrupting the farnesylation motif in the zebrafish *prickle1b* mutant confirmed the involvement of the isoprenylation process in regulating FBMN migration. The isoprenylation pathway is critical in post-translational modification of proteins to facilitate their attachement to cell membranes. Disruption

of the hmgcrb gene, which is upstream to the isoprenylation pathway, and enzyme components of the prenylation pathway displayed partial disruption of FBMN migration (Mapp *et al.* 2011). A novel gene associated with the planar polarity complex, nhsl1b, has also been identified to be required for FBMN migration (Walsh *et al.* 2011). Migrating FBMNs explore their surrounding environment which influences the cells' migratory behaviour. Olig 2-expreessing cells are located near r5/r6 and have been shown to guide FBMNs to complete caudal migration (Zannino *et al*. 2012). Other guidance molecules such as chemokine receptors and ephrins are also important in correct FBMN migration in the zebrafish hindbrain (Cookes *et al.* 2001; Cubedo, Cerdan *et al*. 2009). Collectively, these studies indicate complex interactions between multiple factors and mechanisms to maintain caudal tangential migration of motor neurons in the hindbrain.

1.9.4 Migration in the Adult Zebrafish Brain

The regenerative process was initially investigated using the adult zebrafish fins (Johnson and Weston 1995). In recent years the zebrafish has been extensively used in investigating the regerative process in the brain. The adult zebrafish brain exhibits a remarkable capacity for regeneration unlike the mammalian brain. In contrast to the mammalian brain which consists of two regions of proliferative zones, the subventricular zone in the telencephalon and dendate gyrus of the hippocampus, the adult zebrafish brain consists of 16 proliferative zones (Zupanc *et al*. 2005; Grandel *et al*. 2006; Kizil 2011). Migrating neurons from the lateral telencephalic area, homologous to the mammalian dendate gyurs, display similar migratory patterns to mammals (Grandel *et al.* 2006). Consistent with this, neuronal precursors migrating from the ventricular zone to the olfactory bulb in the zebrafish display similarities with neural cells migrating in the mammalian rostral migratory stream (RMS) (Kishimoto *et al*. 2011).

In response to telencephalon injury there is an increase in the number of radial glial cells that express proliferation nuclear antigen in the ventricular zone (Marz *et al*. 2011). Various studies have documented that radial glial cells are mitotically active and generate neuroblasts that can migrate to lesion sites (Kroehne *et al*. 2011). These radial glial cells act as progenitors and express aromatase, an enzyme which converts

androgens to estrogens, suggesting an importance of estrogen in regeneration (Pellegrini *et al.* 2007; Diotel *et al.* 2013). Studies have investigated which regenerative programs are turned on post-injury to the adult zebrafish brain. One transcription factor, *gata3*, was identified to be expressed in the proliferating progenitors of the telencephalon after injury. This inducible gata3 expression was found to be dependent on FGF signalling (Kizil *et al*. 2012). In keeping with this, FGF signalling is required to maintain adult neural stem cell niches in the zebrafish telencephalon and cerebellum (Kaslin *et al*. 2009). Other factors identified in the regenerative response are the chemokine cxcr5 receptor (Kizil *et al.* 2012) and the secreted protein prokineticin 2 (Ayari *et al*. 2010), both thought to be important in ventricular cell proliferation and neurogenesis. Spinal cord injury in the adult zebrafish leads to an upregulation of anti-apoptotic factors Bcl-2 and phospho-Akt in motor neurons (Ogai *et al*. 2012). Spinal cord regeneration may also require the ability of microRNA miR-133b to regulate expression of RhoA, a GTPase found to be an inhibitor of axonal growth (Yu *et al.* 2011). These studies indicate that the zebrafish posses a variety of characteristics which make them a potent tool to investigate and discover therapeutics to stimulate CNS regeneration in human tissue.

1.10 Rationale

Correct migration of neuronal cells to their destined position is a key mechanim to build the CNS architecture during development. Neuronal migration disorders (NMD), neurodevelopmental and neurodegenerative diseases have all identified to have neuronal migratory defects as a pathogenetic mechanism. In recent years the zebrafish has become a sophisticated model to use in understanding CNS development and possesses many advantages compared to other vertebrate model systems. This thesis aims to further elucidate the mechanisms underlying brain development in the zebrafish embryo by investigating three different factors known to be implicated in neuronal migration. Our investigations are mainly focussed on the zebrafish forebrain, in particular the telencephalon, as this region is homologous to the mammalian cortex.

Model 1 – Investigating brain development in laminin 1 β (LAMB1) mutants

The laminin proteins are components of the basement membrane and have been widely implicated in neuronal migration and cortical development. Loss of function animal models has implicated laminin subunits in neural development. Recently, a study reported homozygous mutations in LAMB1 in two families with cobblestone lissencephaly, a NMD (Radmanesh *et al.* 2013). Brain development in an *in vivo* model harbouring mutation in LAMB1 is yet to be characterised, thus we chose zebrafish mutant defective in LAMB1, *grumpy (gup*^{tj229a}*)*, to investigate neuronal migration (Parsons *et al* 2002). In this study we attempted to identify an uncharacterised *gup* mutation and further characterised the forebrain and hindbrain in mutants.

Model 2 – Investigating the role of the hydroxmethylglutaryl Co-enzyme A reductase (HMGCoAR) in forebrain devlopment

Many studies have investigated the HMGCoAR pathway during develeopment. In the zebrafish, inhibition of the HMGCoAR pathway disrupts the migratory mechanism of a variety of cell types, such as germ cells motor neurons, and myocardial cells (Thorpe *et al.* 2004; D'Amico *et al.* 2007; Mapp *et al*. 2011). Downstream of HMGCoAR, the pathway splits to form the cholesterol biosynthesis pathway and isoprenylation pathway. Isoprenylation is a form of post-translational modification. Enzymes involved in the prenylation pathway facilitate the attachment of prenyl lipids to proteins, a post-translational modification, resulting in the attachment of proteins to membranes. Developmental studies have also implicated the importance of isoprenylation in migration. Additionally, many studies have focussed on the productions of isoprenoids in aging and neurodegeneration. We were interested at investigating this pathway in zebrafish forebrain development. We hypothesised that inhibition of HMGCoAR would result in a defective forebrain development. Furthermore we speculated that supplementation of metabolites downstream of HMGCoAR in the isoprenoid pathway would rescue the defect.

Model 3 – Investigating the role of FE65 proteins during development.

FE65 proteins are adaptor proteins which recognise the YENPTY motif in the AICD, which is generated through sequential cleavage of the APP protein. They have been shown to be involved in diverse cellular functions such as transcription, cytoskeletal arrangements, apoptosis, and brain development (Sabo *et al.* 2003; Guenette *et al.* 2006; *Stante et al.* 2009). FE65 and FE65L1 knockout mice have been shown to display cortical heterotopias, a phenotype observed in NMD's. These mice display aberrant neuronal migrations and improper cortical lamination (Guenette *et al*. 2006). We chose to investigate how the loss of FE65 function in the zebrafish affects forebrain development. We hypothesised loss of FE65 would result in defective brain development due to an over-migration of neuronal cell, thus leading to a morphology resembling cortical heterotopia.

CHAPTER 2

MATERIALS & METHODS

2.1 Materials

2.1.1 General Working Solutions

1%/1.5% Agarose – 1g or 1.5g agarose (Bioline) in 100ml TAE buffer (1X)

1-Phenyl 2-thiourea (PTU) – 0.3mM 100X stock

Diethylpyrocarobonate (DEPC) (Sigma) - treated H20 – 0.1% DEPC in dH2O, and autoclaved

Dimethyl sulfoxide (DMS0) (Sigma)

E3 buffer (10X) - 5Mm NaCl, 0.1Mm KCl, 0.33M CaCl2, 0.33Mm MgSO4

E3 buffer (1X) – 0.1% E3 buffer (10X) in dH2O with 3 drops of methylene blue

Glycerol Dilutions – A series of glycerol dilutions ranging from 10% to 80% were made with PBS

LB Agar – 10g/L triptone, 5g/L yeast extract, 5g/L NaCl, 20g/L agar

LB Broth – 10g/L triptone, 5g/L yeast extract, 5g/L NaCl

Mineral Oil (Sigma)

Paraformaldehyde (PFA) – 4% PFA in PBS (heated to 70°C and stored at -20°C)

Phenol red (Sigma)

Phosphate buffered saline (PBS) – 1 PBS tablet (Oxoid) in 100ml dH2O, and autoclaved

RNase free Water (Naglene)

Sheep serum (Sigma)

TAE buffer (50X) – 242g Tris HCL, 57.1ml Acetic Acid, 100ml EDTA (40mM Tris-acetate, 1mM EDTA)

TAE buffer (1X) – 0.02% TAE buffer (50X) in dH_2O

2.1.2 Whole Mount In-Situ Hybridisation

Tween 20 (Sigma)

PTW – 0.1% Tween 20 in PBS

Proteinase K (Sigma) 10mg/ml

Deionised Formamide (Sigma)

20X SSC – 3M NaCl, 0.3M Trisodium Citrate in dH_2O

Ribonucleic acid, transfer from Baker's yeast (*S.cerevisiae*) (tRNA) (Sigma) – 9-11mg/ml

Heparin (Sigma) – 50mg/ml

Complete Hybridisation Solution (c-Hyb) – dH_2O with 50% Formamide, 25% 20X SSC, tRNA (25mg/ml), Heparin (50mg/ml), 0.1% Tween 20, 1M citric acid

Reduced Hybridisation Solution (r-Hyb) - dH_2O with 50% formamide, 25% 20X SSC, 0.1% Tween 20, 1M citric acid

Bovine serum albumin (BSA) (Sigma)

PBT – PTW with 2% sheep serum, and 0.2% BSA

Anti-Digoxigenin-AP Fab Fragment (Roche)

Staining buffer – dH_2O with 1M Tris Ph 9.5, 1M $MgCl_2$, 5M NaCl, and 10% Tween 20

5-Bromo 4-Chloro 3 Indolyl Phosphate (BCIP) – 50mg/ml (Roche)

Nitro Blue Tetrazdium (NBT) – 50mg/ml (Roche)

Trypsin

2.1.3 Whole-mount Immunohistochemistry

PBS-Block – PBS with 0.1% Tween 20 + 1% DMSO + 10% sheep serum

Secondary Antibody – Mouse IgG was obtained from the Vestastain *Elite* (ABC) kit (Vector laboratories, Burlingame, CA, USA)

Preformed ABC complex – Avidin DH solution and Biotinylated Enzyme were supplied by the Vectastain *Elite* (ABC) kit (Vector laboratories, Burlingame, CA, USA)

2.1.4 – Flourescent Immunohistochemistry

PBT – 1% Triton-X-100 in PBS

Blocking Buffer – PBT with 10% sheep serum + 1% BSA (Sigma) + 1% DMSO

Antibody Dilution Buffer – PBS with 5% sheep serum +1% BSA + 1% DMSO

2.1.5 Pharmacological Treatments

Simvastatin (Calbiochem)

Lovastatin (Calbiochem)

Atorvastatin (Calbiochem)

Mevalonate (Calbiochem)

2.2 Molecular Biology Techniques

2.2.1 Agar plate preparation

LB agar was prepared as instructed by manufacturer. In a sterile environment, appropriate antibiotic was added to the agar and poured into plates under a lit bunsen burner. The lid of the plate was slightly ajar to avoid any condensation droplets falling on the agar, whilst the agar set. Once plates were set, they were placed upside down in the cold room.

2.2.2 Transformation of DNA in chemically competent cells

α-Select chemically competent cells (Bioline) were removed from -70°C and left to thaw on wet ice. Cells were mixed by gentle flicking of the tube and 50µl of cells were aliquoted into chilled eppendorf tubes. 1-5µl of DNA solution was added to the cells and mixed, by swirling a pipette tip in the solution. The solution was incubated on ice for 30 minutes. Bacterial cells were heat shocked at 42°C water bath for 30-45 seconds and then re-placed on ice for 2 minutes. In sterile conditions, 900µl of LB broth was added to the transformation mixture and incubated at 37°C for 60 minutes. 5-200µl of the cell transformation mixture was spread on LB agar plates containing appropriate antibiotic concentrations. Plates were incubated over night at 37°C.

2.2.3 Bacterial culture

Selected colonies of DNA were picked using a pipette tip and placed in 5ml of LB broth containing appropriate antibiotic, under aseptic conditions. Tubes were kept on their side and shaken at 37°C, overnight. To make a glycerol stock, 500µl of the bacterial culture was mixed with 500µl of 50% PBS/glycerol and kept at -80°C. The remaining bacterial culture was centrifuged for 12 minutes at maximum speed to harvest cells. The supernatant was discarded in bleach and tubes were placed upside down on paper to remove traces of LB broth.

2.2.4 Plasmid DNA purification (Mini Prep)

Plasmid DNA was prepared from 5ml of bacterial culture using the nucleospin kit (Machinery-Nagel) as recommended by the manufactures instructions.

2.2.5 Spectophotometric measurement of DNA/RNA

The concentration of DNA and RNA was measured using the nanodrop ND-1000. 1µl of DNA or RNA was pipetted on the lower measurement pedestal. The sampling arm was closed and the spectral measurement was initiated by operating the software on the PC.

2.2.6 Gel electrophoresis

Samples plus ladder were run on TAE agarose gels (1%-1.5%), supplemented with 0.2µg/ml ethidium bromide (sigma) and imaged using the GENi gel documentation system.

2.3 Reverse Transcription Polymerase Chain Reaction

All reactions were done at room temperature unless stated otherwise.

2.3.1 Preparation of RNA

Embryos were collected at the desired time points. 250µl of trizol (Invitrogen) was added to the embryos and they were homogenised by pipetting. Homogenised embryos in trizol were left for 5 minutes. 50µl of chloroforom was added to denature proteins, shaken for 15 seconds, and left for 3 minutes. Samples were centrifuged 13,000g for 15 minutes at 4°C. 100µl of the upper aqueous phase, which contains nucleic acids, was taken into a new eppendorf tube and 83µl of isopropanol was added. Tubes were inverted gently 6-8 times, to allow RNA precipitates to form.

Samples were further centrifuged at 13,000g for 15 minutes at 4°C. The supernatant was discarded, and 250µl of 75% EtOH was added. EtOH was quickly removed and an extra centrifugation step was carried out to remove any excess EtOH. RNA samples were left to air dry for 10 minutes and re-suspended in 15µl RNase free water (Naglene), and stored at -80°C.

2.3.2 cDNA preparation

2µg of RNA sample was made upto a total volume of 8µul using RNase free water. 1µl of 10X DNse buffer (Invitrogen) and 1µl of DNase (Invitrogen) was added to samples, mixed well and incubated for 15 minutes at room temperature (RT). 1µl of 25mM EDTA (Invitrogen) was added, and samples were incubated at 65° for 10 minutes, resulting in inactivation of DNase. 1µl of random hexamers (Invitorgen) and 1 µl dNTPs (Applied Biosystems) were added, and samples were heated at 65°C for 5 minutes. Samples were then chilled on ice. A mixture consisting of 4µl of 5X transcriptase buffer (Invitrogen), 2µl of 0.1M DTT (Invitorgen), and 1µl of RNase free water was added to samples. Samples were placed in the Peltier Thermal Cycler 200 PCR machine on programme SS2, which had the following incubation settings:

PCR SS2 SETTINGS
25°C for 10 minutes
42°C for 2 minutes
42°C for 50 minutes
72°C for 15 minutes
15°C for infinity

After samples had been incubated at 42°C for 2 minutes, the PCR programme was paused and 1µl of superscript III (Invitrogen) was added to samples. Once the reaction was complete, cDNA samples were stored at -4°C or -20°C.

2.3.3 Genomic DNA Preparation

Individual embryos were placed in 0.2ml eppendorfs. 30µl of QuickExtract solution (Epicentre) was added to samples and placed in the PCR machine (GSTORM) using the following incubation settings:

PCR SETTINGS for gDNA
65°C for 120 minutes 45°C for 5 minutes 15°C hold

Once the reaction was complete genomic DNA samples were kept at 2-4°C.

2.3.4 Primer Design

Forward and reverse primers were designed and ordered from Sigma-Aldrich. All FE65 and LAMB primers were made up to 100µM in d H_2O. Actin primers were made up to a concentration of 10µM.

Table 7 – A list of primer sequences

Primer	**Nucleotide Sequence (5'-3')**
FE65sp (7-8) Reverse (R1)	TGCTTGATGACTTCCTCTGAGCAG
FE65sp (7-8) Forward	TCAGACTGAGGAGGAAGAGGAACAGA

(F1)	
FE65sp (7-8) (R2)	TCCCTGGGATCCAGAATGCAG
FE65sp (7-8) (R3)	TCCCTCACTGGGTGGTCCTGA
Lamb1a_1F	TGTAAAACGACGGCCAGTTTTAGGGGCCTGGGCTCTGGC
Lamb1a_1R	CCAGTTCCATCGACAGGGGCG
Lamb1a_2F	TGTAAAACGACGGCCAGTACTGCACACTCTCGGCGACA
Lamb1a_2R	TGCCAAACATGTGCTCCCGAC
Lamb1a_3F	TGTAAAACGACGGCCAGTACGTCTGGTTACCGGAAGGAACT
Lamb1a_3R	CCCTGGTGCAGAAGAGCTGACA
Lamb1a_4F	TGTAAAACGACGGCCAGTGGCTCCGGAACAGAGGGTGGAAA
Lamb1a_4R	CCAGTGCGGGCATCACACGAC
Lamb1a_5F	TGTAAAACGACGGCCAGTTGGCGGAGAATGTCGGCCCT
Lamb1a_5R	TCGGCAAAGCACTGGTGGCA
Lamb1a_6F	TGTAAAACGACGGCCAGTTGTGACACGTGTGCTCGAGGT
Lamb1a_6R	AGCTGTCCAGCCAGGTTGTCC
Lamb1a_7F	TGTAAAACGACGGCCAGTAGGATGAGTTTTCGAAGAAACTGGACA
Lamb1a_7R	CTTCCTGGCCTTGCGGGCTT
Lamb1a_8F	TGTAAAACGACGGCCAGTCCTCAACCAGAGCGCCGCAG
Lamb1a_8R	CAGACATGTGCTGTAGACGGTCACT
Gup_Mutant R	ACGACCCACTGACCCACCAGT
Gup_Mutant F	GCCCTGGAAATGCCATGTCAAAAT

2.3.5 PCR Amplification

Recipes used for Actin, FE65, and LAMB reactions can be seen in table 8.

Table 8 – Recipes for Actin, FE65, and LAMB1 PCRs

	Actin 1x reaction	**FE65sp 1x reaction**	**LAMB 1x reaction**
H_2O	5µL	6.8µl	6.8µl
Solis biodyne 5x mastermix	2µl	2µl	2µl
Forward Primer	1µl	0.1µl	0.1µl
Reverse Primer	1µl	0.1µl	0.1µl
cDNA template	1µl	1µl	1µl
Total	10µl	10µl	10µl

PCR products were amplified using the GSTORM machine. Products were amplified on a programme which included touchdown setting of 65°C to 50°C (for 15 cycles) followed by 30 cycles of 94°C for 30 seconds, 58°C for 45 seconds, and 72°C for 1 minute and 30 seconds.

2.3.6 Sequencing of PCR products

For 5µl of PCR product, 1µl of shrimp alkaline phosphatise (SAP) and 0.05µl of Exonuclease I (Exo1) was added, and diluted with nuclease free water to make a final volume of 10µl. SAP inactivates dNTPs by removing phophate groups, and Exo1 degrades excess primers via exonuclease activity. Samples were mixed and incubated for 1 hour on the PCR machine (GSTORM). For sequencing, samples and the corresponding primers diluted 1:100 were sent to the Core Genomic Facility, Sheffield.

2.4 Zebrafish Husbandry

2.4.1 Zebrafish Stocks

The study utilised the following zebrafish strains, which were maintained at the MRC Centre for Development and Biomedical Genetics, University of Sheffield (Table 9).

Table 9 –Zebrafish strains used in this project

Zebrafish strain	**Type of strain**
AB/LWT/TL	Wild-type
Grumpy (*gup*^{tj229a})	Mutant line harbouring a mutation in the laminin 1β gene (Odenthal *et al.* 1996)
HuC/gfp	GFP under the control of the HuC promoter. Labels post-mitotic neurons with GFP
HuC/gfp:*Gup*	Transgenic line labelling post-mitotic neurons in the *gup* mutant line with GFP

2.4.2 Outcrossing the HuC/gfp transgenic line

The *gup* and HuC/gfp transgenic lines were available from the MRC centre for Development and Biomedical Genetics. We outcrossed adult zebrafish from the HuC/gfp line to adulta from the *gup* line, and selected embryos that were GFP positive. The embryos selected were set up into tanks in groups of 60, and were raised to adulthood.

2.4.3 Harvesting Embryos

The onset of the light cycle initiates the zebrafish breeding process. Zebrafish are exposed to light for 14 hours and then kept in the dark for 10 hours. Embryos from different strains were collected from 2 processes, marbling or pair mating.

The marbling process involves placing a plastic box lined with a mesh base with marbles on top of a clear plastic box, submerged in the aquarium tank. The impregnated females are attracted towards the marbles to lay their eggs. The embryos fall through the mesh lining into the clear box and can be transferred into a 30mm petri dish using a plastic strainer.

The pair mating technique involves separating the males from the females, and pairing up individual female fish with male fish in boxes. Plastic dividers can be specifically placed to separate the individual female from the male. They can then be removed from the boxes to ensure specific timings of when the embryos are laid.

Embryos were sorted depending on their development stage under the Leica L2 microscope at 3.2x to 4x magnification. Embryos were raised in E3 buffer, which replaced the aquarium water.

2.4.4 1-phenyl 2-thiourea (PTU) treatment

A major advantage of using the zebrafish embryo as a model system is its optical transparency. To maintain this transparency, embryos can be treated with 1-phenyl 2-thiourea (PTU). PTU inhibits tyrosinase, an enzyme which is essential in catalysing the production of melanin, thus inhibits melanogenesis. It is important to add this treatment before initial pigmentation occurs, and to optimise the concentration of PTU as high concentrations can result in toxicity (Karlsson *et al*. 2001). Embryos were treated with 0.003% PTU after 10hpf and raised at 28°C in the incubator.

2.5 Morpholino Design and Microinjecting Morpholinos

2.5.1 Morpholino Design

Morpholino antisense oligonucleotides were designed by GeneTools, LLC (Philomath, OR, USA). The translation blocking morpholino was designed to be targeted towards the 5' untranslated region to ATG translational start site of the post spliced *FE65* mRNA. The splicing blocking morpholinos were designed to target the splice donor site of zebrafish *FE65*. Standard control morpholinos (COMO) and p53 morpholinos were also provided by GeneTools (Table 10).

Table 10 – A list of morpholinos used in experiments.

NAME	**Morpholino Sequence**	**Target**
FE65 ATG	5' ATCTGATGGGCTCTTCACCGACATG 3'	Blocks translation of FE65
FE65 sp7-8	5' AATTATGCTCACAGACTCACCTGCC 3'	Interferes with splicing of FE65 exon 7- intron8
COMO	5'CCTCTTACCTCAGTTACAATTTATA 3'	Targets β-globulin in thallasemic humans
P53	5' GCGCCATTGCTTTGC 3'	Targets p53 mechanisms in apoptosis

All morpholinos were dissolved in sterile water to create a 2 millimolar stock concentration. Both FE65 translation and splice blocking morpholinos were 300 nanomoles, therefore 0.15ml was added to make a final concentration of 2mM. Further working concentrations of 0.3mM, 0.4mM, 0.5mM, 0.6mM, and 0.9mM were made from the 2mM stock concentration with sterile water and 1% phenol red. Required dilutions for COMO and p53 were also made up with sterile water and 1% phenol red.

2.5.2 Microinjecting Morpholinos

Borosilicate glass capillary needles (1mm OD x 0.5mm ID) were pulled using the micropipette puller (model p-97) on programme 90 which had the following parameters set up; heat - 410, pull - 100, vel - 150, and time - 200. A diamond etcher was used to break the end of the capillary needle, and was placed in an eppendorf containing morpholino solution. This allows uptake of the morpholino solution through the needle. To calibrate the needle, solution was injected onto a microscope graticule containing mineral oil. Prior to injections, 1 cell stage embryos were lined up onto the ridges of an agarose mould. A narishinge IM 300 microinjector was used to pressure inject 1-2nL of solution directly into the of fertilised 1-4 cell zebrafish embryos. Embryos were maintained in E3 buffer and raised at 28°C. Prior to fixation, embryos were dechorinated using fine forceps.

2.5.3 Fixation of Embryos

After dechorination, embryos underwent washes in 1.5ml Eppendorf tubes using E3 buffer (1 wash) and PBS (2 washes) at RT. 1ml of 4% PFA was added to embryos, which were placed on a rocking platform overnight at 4°C . The following morning embryos underwent a series of washes with PBS (x2), 50/50 PBS:MeOH (x1), and 100% MeOH (x1). Embryos were stored at -20°C in MeOH until further use.

Embryos used for confocal imaging were fixed with 4% PFA for 2 hours at room temperature, washed twice with PBS, and stored in 50% glycerol at 4°C.

2.6 Pharmacological Treatments

2.6.1 Statin Pharmacology

To inhibit HMGCoAR activity embryos were treated with statins, which are competitive inhibitors of HMGCoA reductase. Embryos were treated with Simvastatin, Lovastatin, or Atorvastatin in E3 buffer at 28°C. Final concentrations of 0.1µM, 0.01µM, and 0.001µM for Simvastatin and Lovastatin were used. Final concentrations of 10µM, 25µM, and 75µM for Atorvastatin were used.

2.6.2 Microinjecting Metabolites

Embryos were injected with the following metabolites, Mevalonate, Geranylgeraniol, Farnesol, Squalene, and GGTI-2147. The working concentrations of the metabolites were made up using sterile water and 1% phenol red. 50% DMSO was also made up with sterile water and phenol red. 1nL of 50% DMSO was injected into embryos at 1 cell stage. The working concentrations used and the volume of solution injected can be seen in the (Table 11).

Table 11 –Stock and working concentrations of injected metabolites

Metabolite	**Stock concentration**	**Working concentration**	**Volume of solution injected**
Mevalonate	1M	0.5M	1nL
Geranylgeraniol	2M	2M	2nL
Farnesol	1M	0.25M	1-2nL
Squalene	2M	2M	1-2nL
GGTI 2147	10M	3mM	1-2nL

The capillary needles were calibrated in the same way as described above for morpholino injections.

2.7 DIG-labelled probe synthesis

2.7.1 Probe Information

Probe	Vector	Resistance	Restriction Enzyme	RNA Polymerase
EMX3	PCS2+	Amp	BamHI	T7
GABAR1	PCS2+	Amp	EcoRI	T7
REELIN	PCS2+	Amp	Sal I	SP6
Dlx3	pbluescript	Amp	EcoRI	T7

2.7.2 Template Preparation

10-20µg of desired plasmid was cut with appropriate restriction enzyme to linearise plasmid DNA. After linearisation, equal volume of phenol/chloroform was added and centrifuged for 30 seconds at 13,000 rpm. The upper aqueous phase was taken into a new eppendorf. The DNA was precipitated with 0.1 x volume of 3M sodium Acetate pH 5.2, 1µl of glycogen, and 2 x volumes of 100% EtOH at -20°C for 1 hour. The precipitate was centrifuged at 13,000rpm for 10 minutes at 4°C. The pellet was washed with 70% ethanol made up with DEPC H_2O and left to air dry for 5-10 minutes. DNA was re-suspended in 20µl of RNase free H_2O.

2.7.3 In-vitro Transcription Reaction

The following in-vitro transcription reaction was set up and incubated at 37°C for 2 hours.

DNA	1µg
10X Transcription Buffer (Roche)	2µl

10X DIG Labelling Mix (Roche)	2µl
RNA Polymerase (Roche)	2µl
RNase Inhibitor (Biolabs)	1µl
DEPC-Treated Water	To 20µl

After 2 hours, 1µl of reaction was retained for an analytical gel

2.7.4 Probe Purification

2.5µl of 10X DNase buffer (Biolabs) and 2.5µl RNase-free DNaseI (Biolabs) was added to the transcription reaction and incubated for 30 minutes at 37°C. After the incubation, a 1ul was retained for an analytical gel. The probe was then precipitated by adding 2.5ul of 4M LiCl and 75ul of 100% EtOH and incubating the reaction at -80°C overnight. The precipitate was centrifuged for 20 minutes at 4°, 13,000rpm. The pellet was washed with 70% EtOH made with DEPC H_2O, and re-centrifuged for 15 minutes at 4°C. The pellet was left to air dry for 5 minutes at room temperature and re-suspended in 50µl of DEPC treated H_2O. The RNA probe diluted in H_2O was left to hydrate on ice for 10-15 minutes. 1µl of solution was retained for analytical gel. 50µl of deionised formamide was added and the probe was stored at -20°C.

An analytical agarose gel was run to confirm that synthesis of the RNA probe was successful.

2.8 RNA Labelling and Antibody Staining of Zebrafish Embryos

2.8.1 Whole Mount In Situ Hybridisation

DAY 1 – Embryos were washed in 50/50 PBS/MeOH (once) and in PTW (4 times), 5 minutes each at room temperature on a rocking platform. For embryos 48hpf or older,

acetone cracking was required, which is described in the next section 2.8.2. Embryos were incubated in proteinase K in PTW for varying times dependant on the age of the embryos.

Age of Embryo	Proteinase K incubation
24 hpf	5 minutes
36 hpf	15 minutes
48 hpf	20 minutes

Embryos were re-fixed in 4% PFA for 20 minutes, and underwent 5 PTW washed for 5 minutes. 200µl of c-Hyb solution was used to rinse embryos, another 200µl of c-Hyb solution was added to embryos and left to prehybridise at 70°C for 1-3 hours. 300µl of pre-heated DIG-labelled probe diluted in c-Hyb solution was added to the embryos, and were left to hybridise overnight at 65°C (Table 12).

Table 12 – DIG-labelled probes

DIG labelled probe	**Dilution in Hyb**	**Labelling**
Gabar1	1:200	GABA 1 receptor-expressing cells
Emx3	1:300	Dorsal telencephalon cells
Reelin	1:300	Post-mitotic neurons involved in migration
Dlx3	2:300	Olfactory cells and precursor cells

DAY 2 – Dilutions of 50/50 r-Hyb:2X SSC, 2X SSC, and 0.2X SSC were made up and pre-heated to 65°C. Embryos were washed at 65°C in 300ul of 50/50 r-Hyb/2X SSC for 20

minutes (x1), 300µl of 2X SSC for 20 minutes (x1), and 0.2X SSC for 45 minutes (x2). The next sets of washes were carried out at room temperature. Embryos were washed in 50/50 PTW/0.2X SSC for 10 minutes (x1) and PTW for 10 minutes (x1). Embryos were blocked in PBT for 2 hours. The anti-DIG antibody (Roche) was diluted in PBT at a dilution of 1:2000. Embryos were incubated in the antibody overnight at 4°C on a rocking platform.

Day 3 – The embryos underwent washes in PBT for 20 minute (x6) and were transferred to a 12 well plate after the final wash. Staining buffer (lacking BCIP and NBT) was prepared; embryos were equilibrated in 0.5ml buffer solution for 20 minutes (x3). Staining buffer with BCIP and NBT was prepared and added to the embryos, and left in the dark for staining to develop. Once sufficient staining had developed, embryos were washed in PTW for 5 minutes (x3) and fixed in 4% PFA overnight at 4°C.

2.8.2 Acetone Cracking

Acetone cracking facilitates further permeabalisation of the embryo to allow greater access for the antibody or probe. For antibody staining, pre-chilled acetone at -20°C was added to embryos for 7 minutes. For in situ hybridisation pre-chilled acetone was added to embryos 48 hpf or older. Eppendorfs were place on their side at -20°C. After cracking embryos were very carefully washed in dH2O.

2.8.3 Whole Mount Immunohistochemistry

DAY 1 – Embryos underwent a series of MeOH/H_2O washes (75%, 50%, and 25%) for 5 minutes each and rinsed with water (x1). Acetone maintained at -20°C was added to embryos for 7 minutes to allow partial permeabalisation of embryos. Embryos were rinsed with water (x3) and then incubated in 0.25% trypsin for the desired time. This facilitates the permeabalisation process further.

Age	Trypsin Incubation
24 hpf	2 minutes
30 hpf	3 minutes
48 hpf	6 minutes
72 hpf	12 minutes

Trypsin was replaced by PTW for 5 minutes to allow re-hydration of embryos, and then embryos were re-fixed in 4% PFA for 20 minutes. Embryos were incubated in blocking solution (PBS + 0.1% Tween 20 + 1% DMSO + 10% sheep serum) for 2-3 hrs at room temperature on the rocking platform. Primary antibodies diluted in the blocking solution added to embryos and left overnight on the rocking platform at 4°C. The primary antibody, HuC (Invitrogen), was diluted at a concentration of 1 in 500 in blocking solution.

DAY 2 – Embryos underwent 4 washes for 30 minutes each in blocking solution at RT. Mouse IgG, the secondary antibody, was provided in the Vectastain Elite ABC kit and was diluted at a concentration of 1 in 400 in blocking solution. Embryos were incubated with secondary antibody on a rocking platform overnight at 4°C.

DAY 3 – Embryos were washed four times with blocking solution for 30 minutes each. During the 4^{th} wash, avidin-biotin complex (ABC) was preformed in blocking solution at room temperature. Embryos were incubated with ABC for 1 hour. Embryos were washed three times with blocking solution for 30 minutes, and further washed three times with PTW for 10 minutes each. 3' diaminobenzidine (DAB) (Vector laboratories) staining enhanced with nickel staining solution was prepared as recommended by the manufacturer and added to the embryos. Once staining had sufficiently developed, embryos were rinsed twice in PBS and then re-fixed in 4% PFA.

2.8.4 Fluorescent Immunohistochemistry

DAY 1 – Embryos fixed at 36hpf were rehydrated in 75%, 50%, and 25% PBS/methanol and washed three times in PBT for 5 minutes each. Embryos were incubated in 0.25% Trypsin for 5 minutes to allow partial permeabalisation of 36hpf embryos. To stop the reaction PBT with 1% sheep serum was added to each tube. Embryos were further washed with three times with PBT for 5 minutes each, and left at room temperature for 1-3 hours in blocking buffer. The primary anti-Islet 1 antibody was diluted in PBT 1:400. Embryos were incubated with the primary antibody dilution on a rocking platform overnight at 4°C.

DAY 2 – Embryos were washed five times with PBT for 45 minutes at room temperature. The secondary anti-mouse 488 antibody (Molecular Probes) was diluted 1:1000. Embryos were incubated with 250µl of the secondary antibody on the rocking platform overnight at 4°C.

DAY 3 – Embryos were washed with PBT for 45 minutes at room temperature (x5). Embryos were transferred in a series of glycerol dilutions, 20%, 40%, 60%, and 80%, and stored at 4°C, ready for confocal imaging.

2.9 Microscopy

2.9.1 Mounting

Embryos undergone histological protocols were immersed in glycerol. Two layers of electrical tape were stuck to a microscope slide and a small well was cut out in the centre of the tape. Different anatomical regions of the zebrafish were dissected under a Leica L2 microscope using needles (BD microlane 0.5mm x 16mm). Dissected regions were placed in 80% glycerol in the well on the microscope slide. A coverslip was gently placed over the specimen and orientated to correctly position the specimen, ready for compound or confocal microscopy.

2.9.2 Compound Light Microscopy

All images were taken on a Olympus BX51 upright compound microscope with a 20X lens and DIC optics. Fixed embryos were deyolked and dissected in 80% glycerol solution. Dissected regions were placed in and mounted in wells cut in electrical tape and covered with a coverslip.

2.9.3 Confocal Microscopy

Images were captured on the confocal microscope Leica TCS SP5II. The Leica Application Suite Advanced Fluorescence (LASAF) programme was used to set up the settings of the confocal microscope. All images were taken with a HCX PL AP 20X dry objective. The confocal settings were set to take images in xyz dimensions, at a format of 1024 pixels by 1024 pixels. The pinhole dimensions were set to 60.8µm, and the laser power was at 30%. Upper and lower Z sections were set to allow scanning at Z-axis. Optical sections were taken at every 2 microns throughout the specimen to produce a Z-stack. All experiments were saved as a .lif files and individual were exported to .TIFF file.

2.9.4 Quantitative analysis of the ventricular surface between HuC-positive hemispheres

Confocal images of the frontal views of the forebrain were quantified using Image J. TIFF image files were converted to a maximum z projections stack. All images were processed using the despeckled tool. Scale in microns was set to all images, where distance in pixels corresponded to logical size on the confocal image and known distance corresponded to physical length dimension on the confocal image. Each maximum z projection image was converted to binary format (Figure 11). Each binary image was cropped to minimise the space around the forebrain image. The vertical length of the binary format was documented and formulas were set into Microsoft Excel to give the vertical position at 16.67%, 50%, and 83.33% of each image. The

ventricular surface length between the HuC-positive hemispheres was measured in microns at these positions and an average of three distances was plotted.

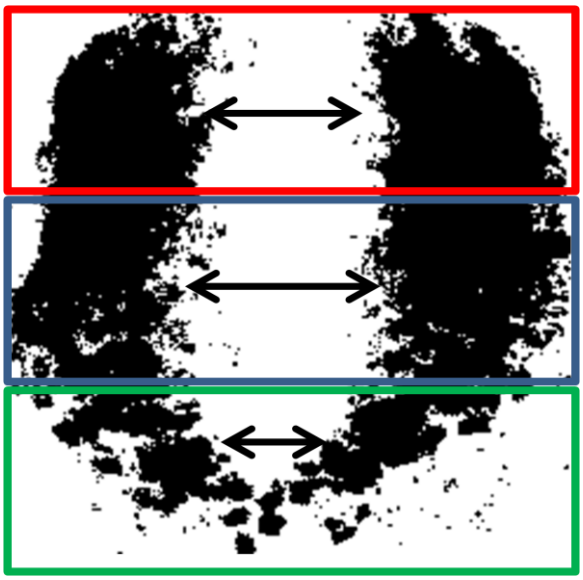

Figure 11 – A schematic representation to show the binary image of the forebrain. Converted binary image of the forebrain highlighting the ventricular surface distance between the HuC +ve hemispheres at middle of dorsal segment (16.67%, red box), middle of 2nd segment (50%, blue box), and middle of ventral segment (83.33%, green box).

2.9.5 Statistical Analysis

Statistical analysis was conducted using the software programme Graphpad Prism. Statistical analysis comparing two groups used t-test analysis, whereas analysis comparing three or more groups used a one-way anova analysis.

CHAPTER 3

ROLE OF LAMININ β1 IN BRAIN DEVELOPMENT

3.1 Abstract

The laminin family of glycoproteins are integral components of the basement membrane. Many laminin isoforms have been implicated in a variety of neuronal processes such as neurite extension, axonal pathfinding, and neuronal migration. Laminin β1 deficiency in zebrafish embryos has been shown to underlie defects in retinal development, axonal projections, notochord differentiation, and blood vessel development. The focus of this investigation was to determine whether laminin β1 (*lamb1*) deficiency altered neuronal patterning in the zebrafish embryo. We demonstrate that laminin β1 mutants display a decrease in the width of the ventricular space, a marked reduction in size of the forebrain, and ectopic FBMNs, resembling features of cobblestone (COB) Lissencephaly. Recently LAMB1 mutations have been associated with COB Lissencephaly in two families, strengthening our belief that LAMB1 is required for migratory processes in the zebrafish, and that zebrafish may be used as an animal model of COB Lissencephaly.

3.2 Introduction

3.2.1 Role of Laminins in Development and Disease

The laminin proteins belong to a family of glycoproteins which provide structural scaffolding to the basement membrane, an extracellular matrix which holds tissues and cells together. To date, there are 15 isoforms which all have different expression patterns in various tissues (Colognato *et al.* 2000). As previously discussed in section 1.6.1, an extensive amount of literature has focussed on how laminins regulate neuronal and brain development. Additionally, a number of studies have linked disrupted laminin signalling with neurodegenerative diseases. A mouse model of spinal muscular atrophy showed disruption in laminin signalling, which resulted in impaired axonal translation of β-actin (Rathod *et al.* 2012). Knocking down expression of α-laminin resulted in protein proteotoxicity and formation of protein aggregates, a pathological feature shared by Parkinson's and Alzheimer's disease, suggesting a role for laminin in protein toxicity (Jensen *et al.* 2012). Prion disease-associated mutations disrupt the interaction of prion proteins with laminin γ1 chain, thus impairing neural cell survival and outgrowth (Machado *et al.* 2012). Laminins have also been identified to have critical roles in cortical development. Homozygous mice null for lamb2 and lamc3 display cortical laminar disorganisation, and altered distribution and morphology of Cajal-Retzus and radial glial cells, producing cortical dysplasia (Radner *et al.* 2013). In the mouse cerebellum, lama1 deficiency resulted in defective cerebellar development (Ichikawa-Tomikawa *et al.* 2012). Other cortical dysplasia animal models produced by mutations in other genes important in development also display disrupted laminin expression (Costa *et al.* 2001; Guenette *et al.* 2006). Recessive mutations in LAMBC3 have been reported to be associated with complex occipital cortical abnormalities in subjects (Tsao *et al.* 1998). Additionally, mutations in LAMB1 have been reported to result in cobblestone lissencephaly.

3.2.2 Laminin β1 (LAMB1)

In two families, homozygous mutations in laminin β1 (LAMB1*)* resulted in cobblestone Lissencephaly, typically referred to type II Lissencephaly. Cobblestone Lissencephaly displays features of cortical dysplasia which is characterised by aberrant neuroglial migration, resulting in ectopic neurons. As well as cortical malformations, these patients displayed muscular and ocular abnormalities (Radmanesh *et al.* 2013). Additionally, linkage analysis has identified LAMB1 as a candidate gene for autism (Hutcheson *et al.* 2004), which has also been linked to neuronal migration defects.

The zebrafish lamb1 protein shares 61% identity with human LAMB1. It consists of a N terminal domain, laminin type EGF-like domain, laminin IV type A domain, and four coiled coil domains, spanning 34 exons (Figure 12).

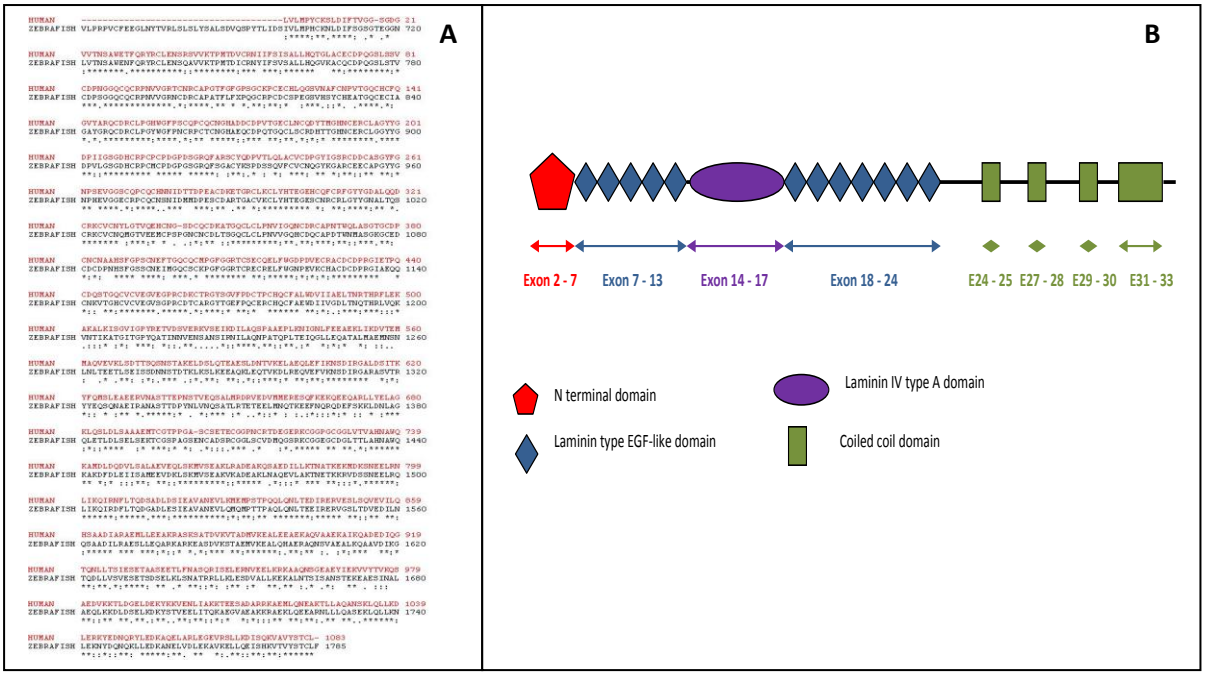

Figure 12 – The zebrafish Laminin β1 (*lamb1*) protein alignment and gene structure. Protein alignment between human LAMB1 and zebrafish lamb1 shows 61% sequence similarity (A). Functional domains and exon numbers are mapped out on a schematic representation of the zebrafish lamb1 gene (B).

In zebrafish a positional cloning study identified nonsense mutations that lead to premature stop codons associated with the *grumpy (gup)* allele, gup^{m189} (Parsons *et al.* 2002). This allele has been identified to be important in a range of zebrafish developmental processes. Morphologically these mutants have been characterised to have a shortened body axis and a smaller retina (Parsons *et al.* 2002). Many studies have focussed on investigating retinal developmental defects in these mutants. In wild-type embryos retinal ganglion cell (RGC) axons exit the eye and cross the midline. After crossing they turn dorsally and posteriorly to reach the contralateral tectum. RGC axons in the *lamb1* mutants display errors in this dorsal-posterior turn, and undergo anterior and ipsilateral projections (Karlstrom *et al.* 1996). A small lens and altered ganglion cell layer, optic nerve, and photoreceptor morphogenesis were consistently present in *lamb1* mutants (Biehlmaier *et al.* 2007). The gup^{m189} allele has also been a valuable model for eye disease and for usage in preclinical drug screening. Mutants display apoptosis dependent optic fissue closure defects, a pathology which resembles ocular coloboma, a congenital eye abnormality. Results demonstrated both aminoglycoside drugs, gentamicin and paramomycin, can suppress the nonsense mutation in *lamb1* by producing a full length, functional protein. Thus, these drugs increased survival of *gup* mutant embryos and reversed morphology and retinal defects. Furthermore, cell death was not observed at the optic fissure closure in embryos treated with the drugs (Moosajee *et al.* 2008). Laminin β1 has furthermore been identified to be important in notochord differentiation and blood vessel development (Pollard et al 2006). During brain development *gup* mutants display an abnormally shaped midbrain-hindbrain boundary (Lowery *et al.* 2009). In conclusion, these studies implicate the importance of laminin β1 in developmental processes, in particular retinal development.

With the extensive amount of literature linking the role of laminins to developmental processes and neuronal migration, we further investigated the role of LAMB1 in brain development. We chose to use the zebrafish *lamb1* mutant and focussed our attention on whether the neuronal architecture in the forebrain and hindbrain was affected. We demonstrate neuronal patterning and migration is affected in the mutants, suggestive of neuronal migration defect. The recent finding that LAMB1 mutations result in cobblestone Lissencephaly confirmed our results suggesting that

LAMB1is required for migratory processes in brain development. In this study we also sequenced the *gup* mutation and further characterised the forebrain and hindbrain in mutants.

3.3 Forebrain patterning is disrupted in laminin 1β (*lamb1*) mutants

The overall morphology of the *gup* mutant, and in particular retinal development, has been extensively studied, but as of yet neuronal architecture in the forebrain has not been characterised. We first addressed whether loss of laminin affects forebrain patterning by analysing post-mitotic neuronal expression in siblings compared to mutants. HuC is a neuron-specific RNA binding protein and is one of the earliest post-mitotic neuronal markers in the zebrafish, suggesting it has a role underlying cell fate determination (Kim *et al.* 1996). Using an antibody recognising HuC to carry out whole mount immunohistochemisty, we observe prominent HuC expression in defined regions of the olfactory placode and telencephalon (Figure 13A, C). In *gup* mutants HuC expression is disrupted, resulting in indistinguishable olfactory placode and telencephalon regions (Figure 13B, D). This disrupted neuronal expression was highly consistent in mutants with 98% of mutants displaying neuronal disorganisation (Table 1). Interestingly, normal HuC expression can be observed in the cranial ganglion cells, suggesting that lamb1 loss may affect the specification of neuronal cells in the forebrain (Figure 13A, B).

Availability of zebrafish transgenic lines expressing GFP in a subset of cells is a major advantage of using this model system, thus we raised a new transgenic line (Gup:HuC/GFP) by crossing the *gup* line with the transgenic HuC line (HuC/GFP). At 24hpf there appears to be minimal difference in HuC expression between sibling and mutants (Figure 14A, B). At 30hpf, mutants display some post-mitotic neurons localised amongst the ventricular space and olfactory regions start to become indistinguishable (Figure 14C, D). The most significant difference in post-mitotic neuronal expression between siblings and mutants can be observed at 36hpf. Mutants display a gross reduction in size of the forebrain, a smaller ventricular space, and discrete telencephalon and olfactory region are not observed (Figure 14E, F). An important process of neural tube development is the formation of the ventricles and the appearance of folds and bends. A previous study in zebrafish has indicated a role for laminin in the morphogenesis of the midbrain-hindbrain boundary (Gutzman *et al.* 2008), an important event that determines normal midbrain and hindbrain ventricles.

Upon observing a smaller forebrain ventricle in mutants, we identified a novel method to quantify the width of the ventricular space (VS) (discussed in section 2.9.4). Siblings displayed a mean ventricular surface width of 28.4 ± 1.8µm, whereas the width in mutants decreased to a mean distance of 20.0 ± 1.6µm (Figure 13G). We suggest that laminin 1β deficiency disrupts the organisation of post-mitotic neurons, consequently leading to a smaller forebrain ventricular space.

The forebrain of the zebrafish embryo is composed of a variety of cell types. We further investigated whether *gup* mutants displayed altered expression of different cellular markers. We initially looked at reelin expression in the forebrain. Reelin is an important molecule involved in mediating neuronal migration in the cortex. In a comparative study of other vertebrates, reelin mRNA expression is conserved in many regions of the vertebrate brain (Costagli *et al.* 2002). At 30hpf and 36hpf, siblings show prominent expression of reelin in pallial and subpallial domains of the telencephalon (Figure 15A, C). At 48hpf, reelin expression is restricted to the dorsal region of the telencephalon in siblings (Figure 14E). Mutants display a reduced expression of reelin in the forebrain during development (Figure 15B, D, F); suggesting a deficiency of laminin affects expression of important molecules which guide neuronal migration in the zebrafish forebrain.

We further investigated expression of markers of different cell types in the zebrafish forebrain (Figure 16 and 17). We first looked at the expression of *emx3*, one of the earliest transcription factors expressed in dorsal telencephalic neurons in the zebrafish. In the siblings, emx3 is highly expressed in the telencephalon and the ventricular zone (Figure 16A). In comparison, mutants show a dispersed expression of *emx3* within the ventricular space and also an increased expression in the ventricular zone (Figure 16B), suggesting a displacement of dorsal telencephalon neurons in the laminin 1β deficient embryos. During zebrafish forebrain development a population of ventral telencephalic neurons migrate dorsally to provide the dorsal telencephalon with GABAergic neurons (Mione *et al.* 2008). We chose to look at the expression of GABA receptor subunit gene, *gabra1*. Siblings display a circular population of *gabra1* expressing cells in the forebrain, implying the existence of inhibitory GABA receptor subunits at 30hppf (Figure 16C). In mutants this population is less organised, with some *gabra1* expressing cells being located more ventrally (Figure 16D, red arrow).

The frontal view of the forebrain of laminin β1 deficient embryos stained with HuC antibody showed a co-localisation of cells normally found in the telencephalon and olfactory placode, disrupting boundary formations (Figure 13). Additionally, the forebrain of mutants of *Gup*:HuC/GFP appeared much smaller at 36hpf (Figure 14E and F). We questioned whether laminin β1 had a role in specification of olfactory placode cells. To identify whether localisation of cells of the olfactory placode was disrupted we carried out *in situ* hybridisation using *dlx3*, a member of the *distal-less* family (Figure 17). In the zebrafish, *dlx3* has been shown to be expressed in the olfactory placode and precursor cells from as early as 16hrs post-fertilisation (Akimenko *et al.* 1994). Gup mutants displayed a markedly reduced dlx3 staining in the forebrain compared with siblings at 24hpf (Figure 17A and B). Interestingly, at 36hpf dlx3 expression appears to be absent from the forebrain in mutants compared to siblings (Figure 17C and D). This suggests laminin β1 function is required for the correct specification and development of olfactory placode cells. These results also suggest correct olfactory placode specification may play a role in telencephalon development in mutants.

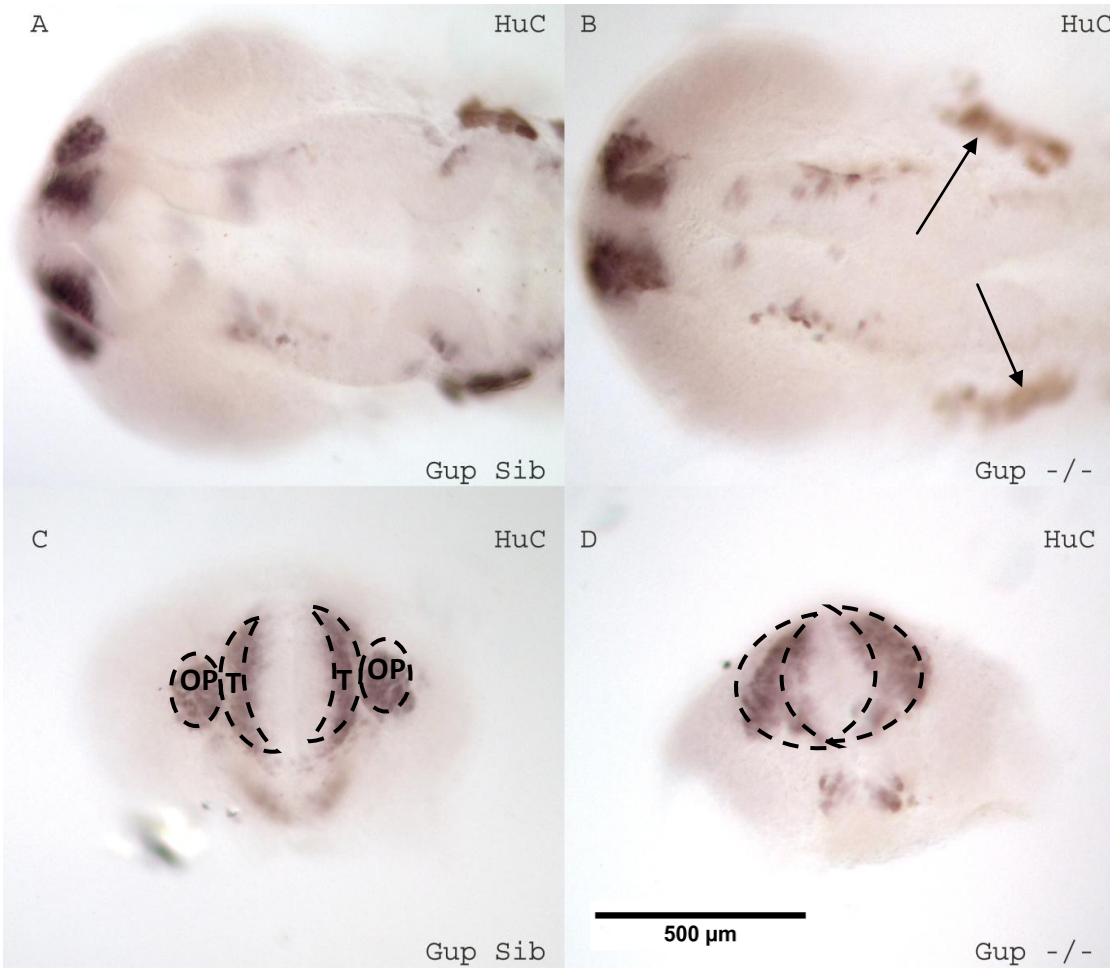

Table 1	Normal HuC Patterning	Defective HuC Patterning
Gup Sib	81/81	0/81
Gup -/-	2/41	39/41

Figure 13 - Post-mitotic neuron patterning is disrupted in the forebrain of laminin 1β mutants.

Images show whole-mount immunohistochemisty using HuC in *gup* siblings (A and C) and mutants (B and D) at 30hpf. Panels A and B show dorsal views with anterior to the left. Panels C and D show frontal views of the forebrain with anterior uppermost. Siblings display prominent HuC expression in the olfactory placode and telencephalon (A and C). Mutants appear to lose the regional boundaries between the olfactory placode and telencephalon, resulting in disrupted expression of HuC (B and D, black dashed line). Prominent expression is evident in cranial ganglion neurons in mutants (black arrows). Table 1 quantifies the number of mutants and siblings displaying defective HuC patterning at 30hpf. Telencephalon (T), olfactory placode (OP).

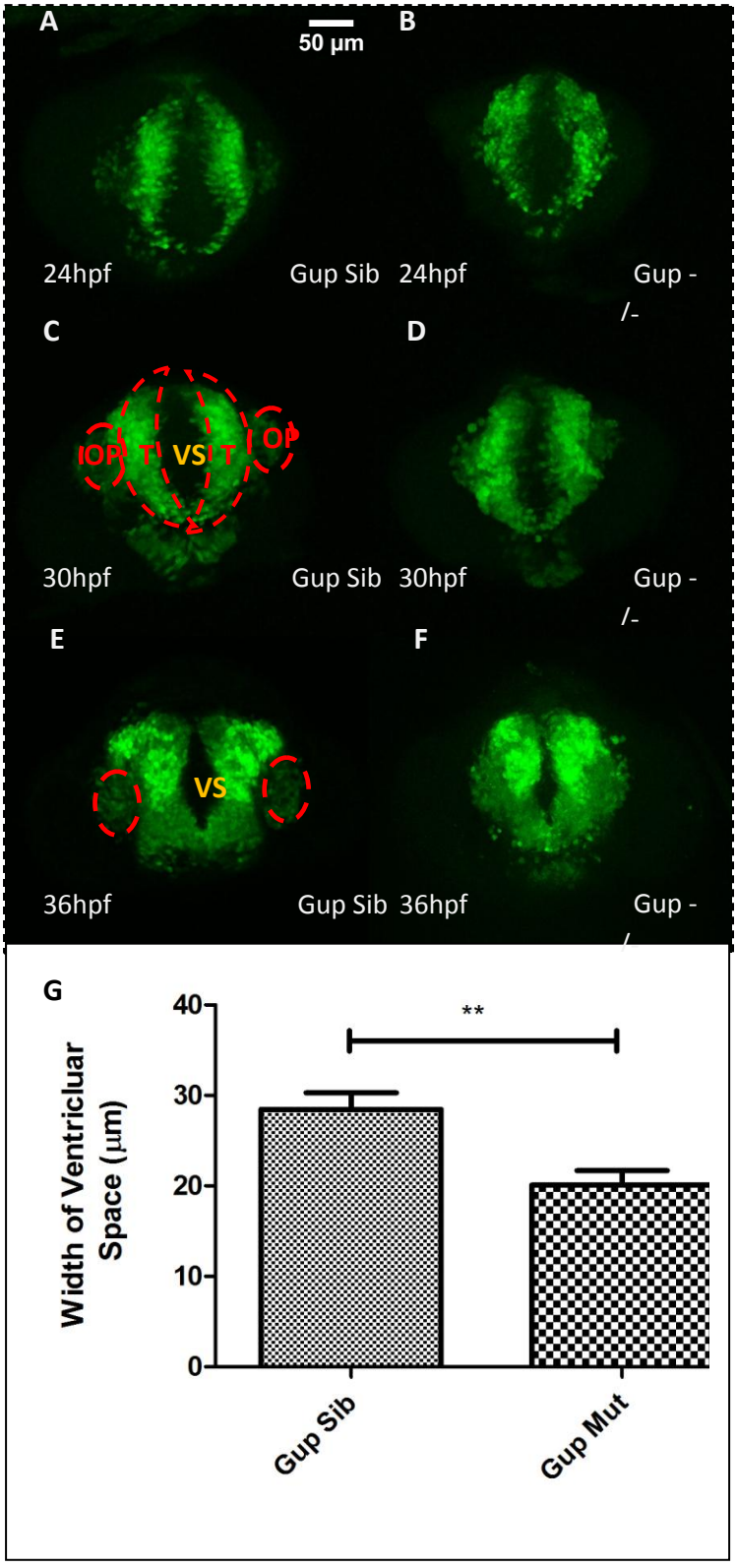

Figure 14 – Post-mitotic neuronal patterning is disrupted in the forebrain of laminin 1β mutants, using the Tg:Gup/HuC line

Confocal images of the frontal views of the forebrain of Tg:gup/HuC siblings (A, C, E) and mutants (B, D, F) during development. HuC expression in the forebrain of mutants appears to be disrupted at 30hpf (D) Forebrain appears much smaller and neurons appear to be ectopically positioned in the ventricular zone region, reducing lumen size. Disruption in post-mitotic patterning in mutants is most evident at 36hpf (E). Red dashed circles outline the telencephalon (T) and olfactory placode (OP), VS marks the ventricular surface

Data represents quantitative analysis of the ventricular surface between HuC-positive hemispheres of the forebrain at 36hpf ± SEM (G). *Gup* mutants show a smaller ventricular surface in the forebrain. Results were statistically analysed using a t test, n=10, $p > 0.05$

.

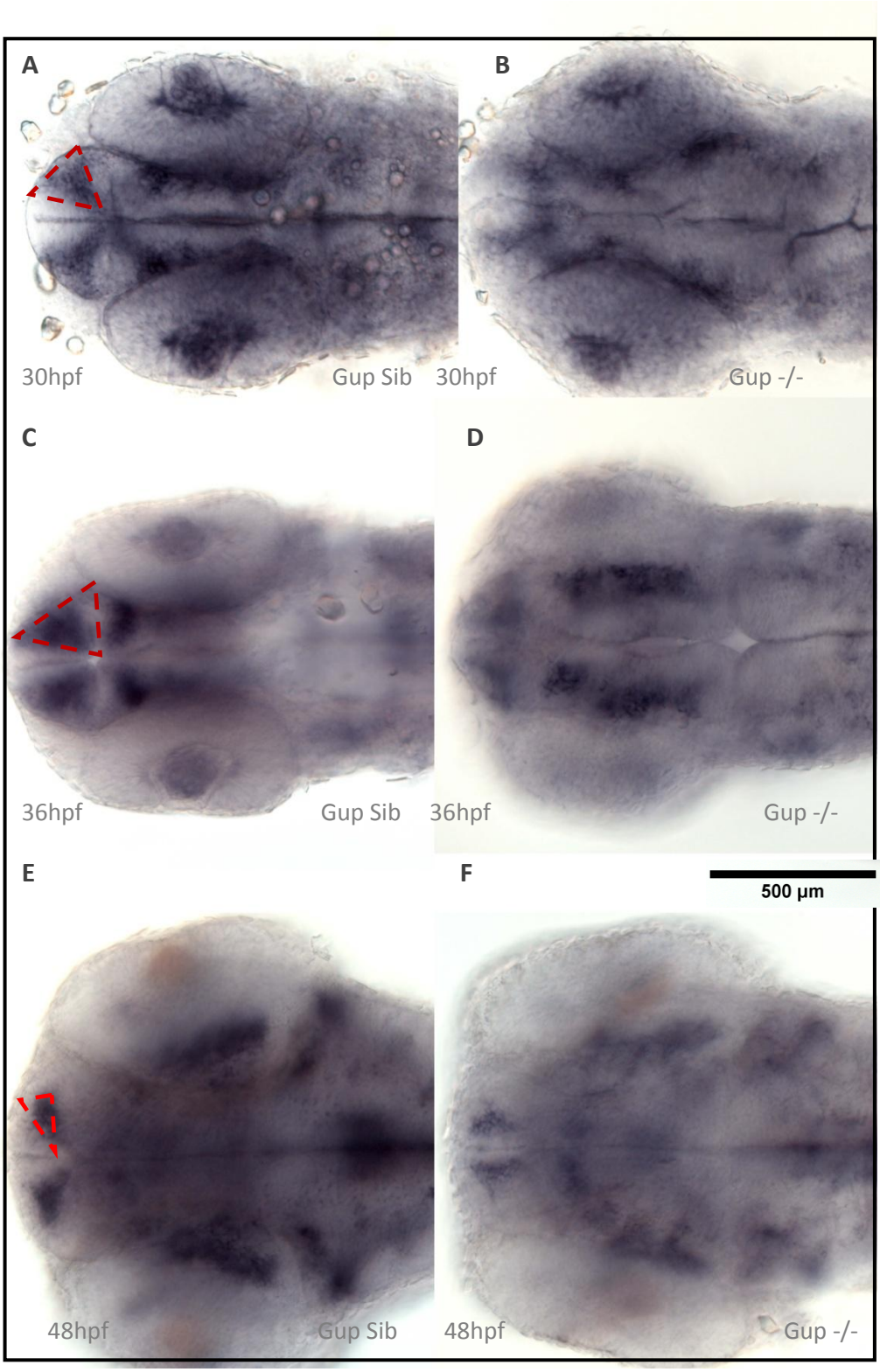

Figure 15 - Laminin β1 mutants display decreased *reelin* expression in the forebrain during development.

Whole mount in situ hybridisation using reelin in siblings (A, C, E) and mutants (B, D, F) at 30hpf, 36hpf, and 48hpf. All images show dorsal views of embryos with anterior to the left. Mutants display a reduced expression of reelin, particularly in the forebrain region. Red dashed line outlines prominent reelin expression in the forebrain of siblings.

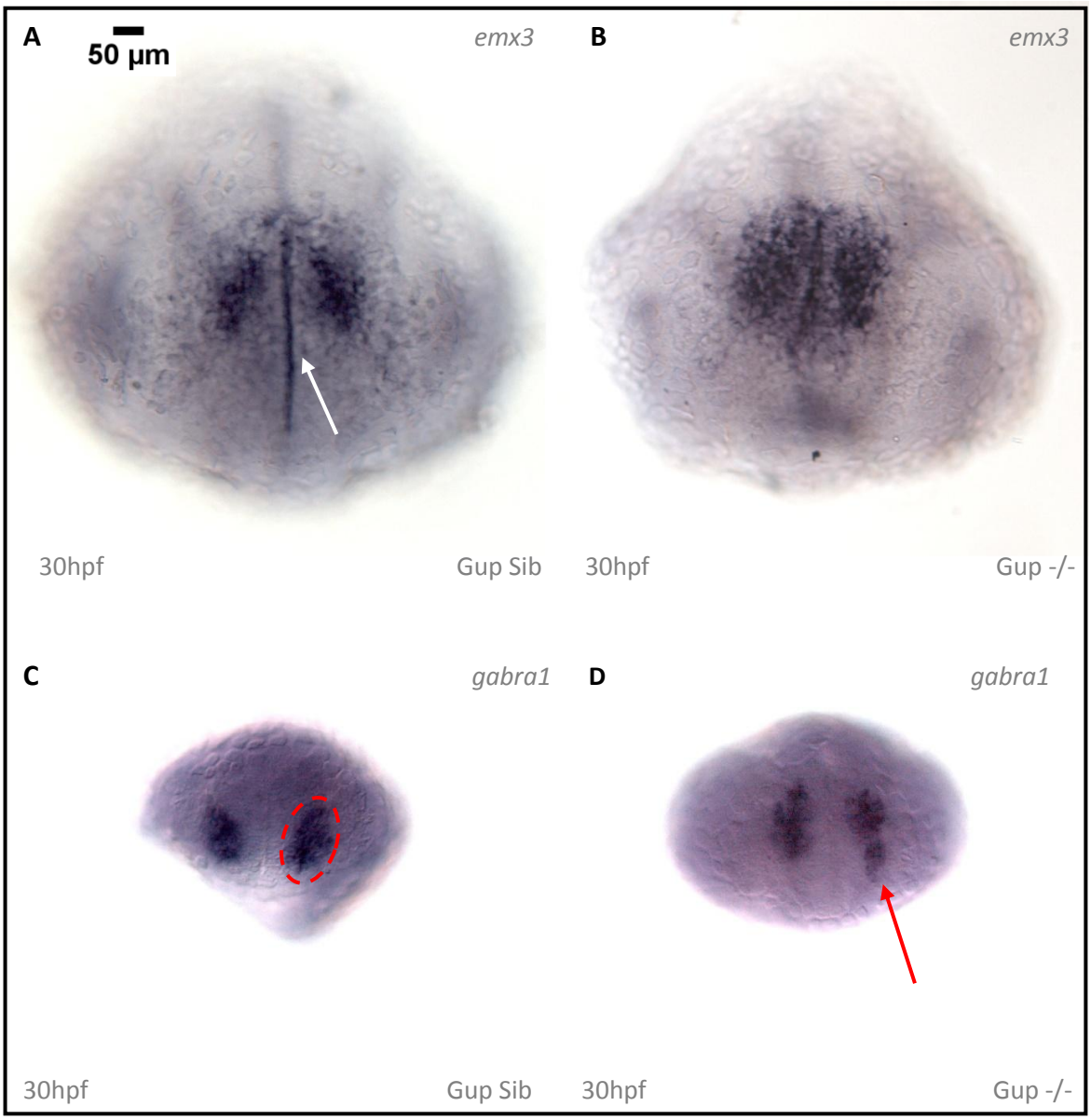

Figure 16 - Expression patterns of emx3 and gabra1 expressing cells are altered in the forebrain of mutants

Whole mount in situ hybridisation in siblings and mutants using emx3 (A and B), and GABA1 (B and D). All images show frontal views of the forebrain with anterior uppermost. *Emx3* expression is prominent in dorsal telencephalon cells and ventricular zone (A, white arrow). Mutants display a disruption in *emx3* expression in the ventricular space (B). Siblings display strong expression of GABA receptor component gene, *gabra1* in the forebrain. In mutants it appears there is a disruption in the localisation of *gabra1* expressing cells (C and D).

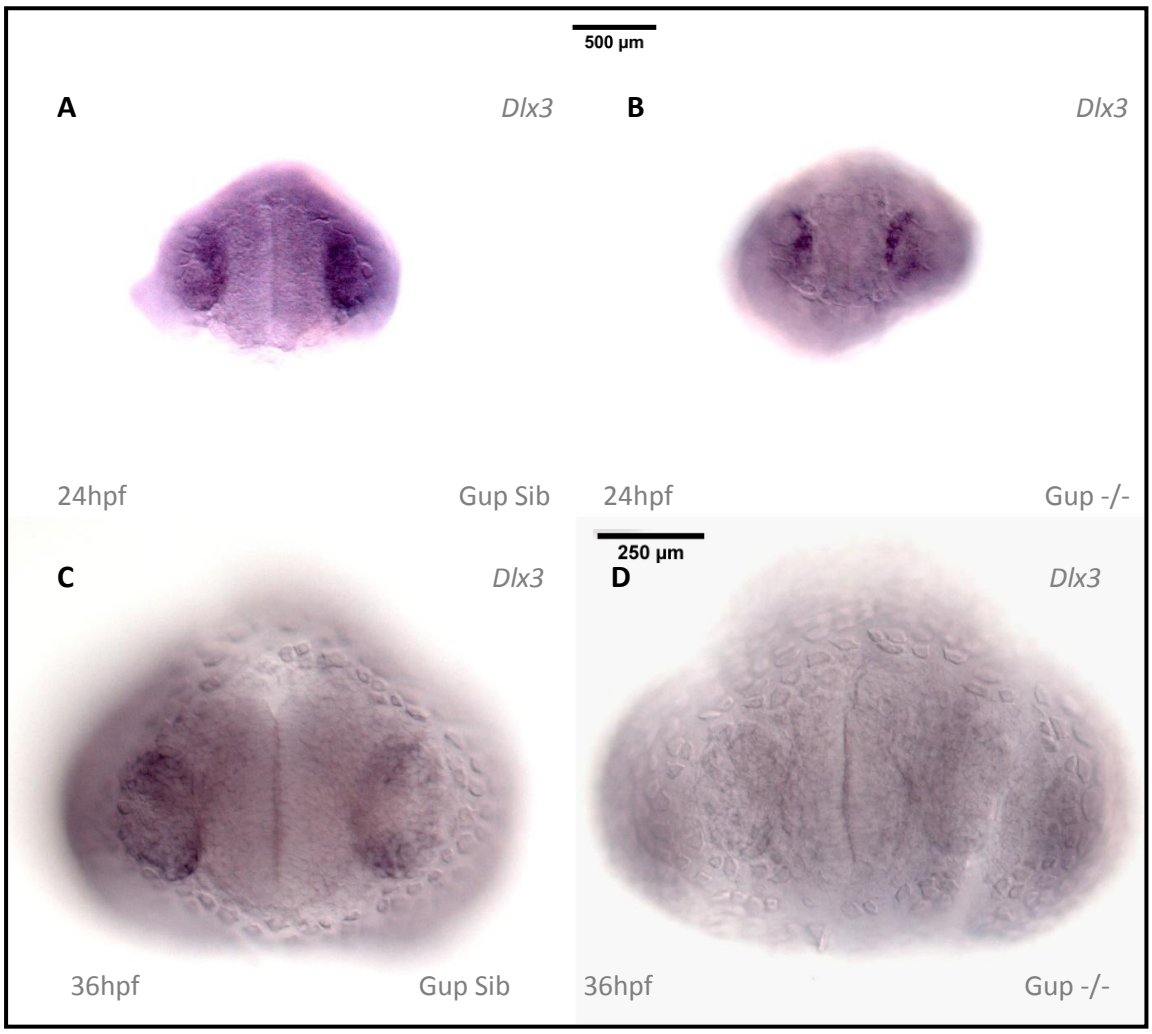

Figure 17 – Expression patterns of *dlx3* is altered in the olfactory placode of laminin β1 mutants.

Whole mount in situ hybridisation using a *dlx3* marker. Images show frontal views of the forebrain with anterior uppermost. At 24hpf, siblings display a clear dlx3 expression in the olfactory placode (A) whereas in the mutants this expression is decreased (B). Again at 36hpf, *dlx3* expression can be identified in the olfactory placode (C) whereas this expression appears to be lost in the mutants (D).

3.4 Laminin β1 is required for correct neuronal patterning in the hindbrain

We extended our characterisation by looking at the development of the hindbrain in laminin β1 mutants. We observed the patterning of post-mitotic neurons in the hindbrain by using the Tg:HuC line. At 36hpf, HuC expression is observed in the trigeminal ganglion and rhombomeres margins of the hindbrain in siblings (Figure 17A, red bar). In the mutant we observe a striking difference in the neuronal patterning in the hindbrain in mutants (Figure 18B), resulting in a disruption of the organised patterning.

Since laminin β1 deficient embryos display defective post-mitotic neuronal patterning in the hindbrain, we questioned whether migration of specific cells types within the hindbrain was disrupted. For this we employed an antibody against *islet 1,* which is a member of the LIM/homeobox gene family and a marker for post-mitotic motor neurons (Higashijima et al 2000). In the hindbrain, facial branchiomotor neurons (FBMNs) have been characterised to undergo a caudal migration from rhombomere 4 (r4) to 6 (r6) (Chandrasekhar *et al.* 1997). Using fluorescence immunohistochemistry, we can identify cell bodies of the branchiomotor neuron groups in the hindbrain of embryos from *gup* line. At 36hpf siblings display a clustering of FMBNs at r6, suggesting that the FBMNs have undergone a caudal migration from r4 to be located in r6 (Figure 18C). In mutants, this caudal migration appears disrupted, resulting in ectopic neurons (Figure 18D, red arrows). nVII nerve cell bodies are not found in a discrete cluster in r6, and appear to be diminished in number, suggesting that posterior migration is partially disrupted. Additionally, we identify laterally positioned ectopic islet-1 positive cells in the hindbrain of mutants. Failure of NVII cell migration from r4 to r6 is also observed in laminin α1 mutant (Sittaramane *et al.* 2009). Overall we suggest laminin 1β is a substrate required for correct localisation of motor neurons in the hindbrain, and may play a role, like laminin α1, in caudal migration of FBMNs.

Previous studies have shown a link between localisation of motor neurons and the reelin signalling pathway (Palmesino *et al.* 2010). Upon identifying decreased *reelin* expression in the forebrain during development (Figure 15) and disrupted motor neuron migration in the hindbrain of laminin 1β mutants (Figure 18), we were

confident to hypothesise that the mutant would display reduced expression of *reelin* in the hindbrain. At 36hpf, siblings express reelin in the central domains of the rhombomeres 2 to 7(r2-r7) but expression is excluded between the rhombomere boundaries (Figure 18A, numbered). Mutants display a massive reduction in reelin in the rhombomeres, resulting in an undistinguishable rhombomere patterning (Figure 19B, white arrowheads). Additionally, transverse sections between r4 and r6 show a loss of reelin expression in mutants (Figure 19D). We suggest the reelin signalling pathway may be one of the mechanisms which regulates FBMNs migration in the zebrafish hindbrain and that this process is impaired in laminin 1β mutants.

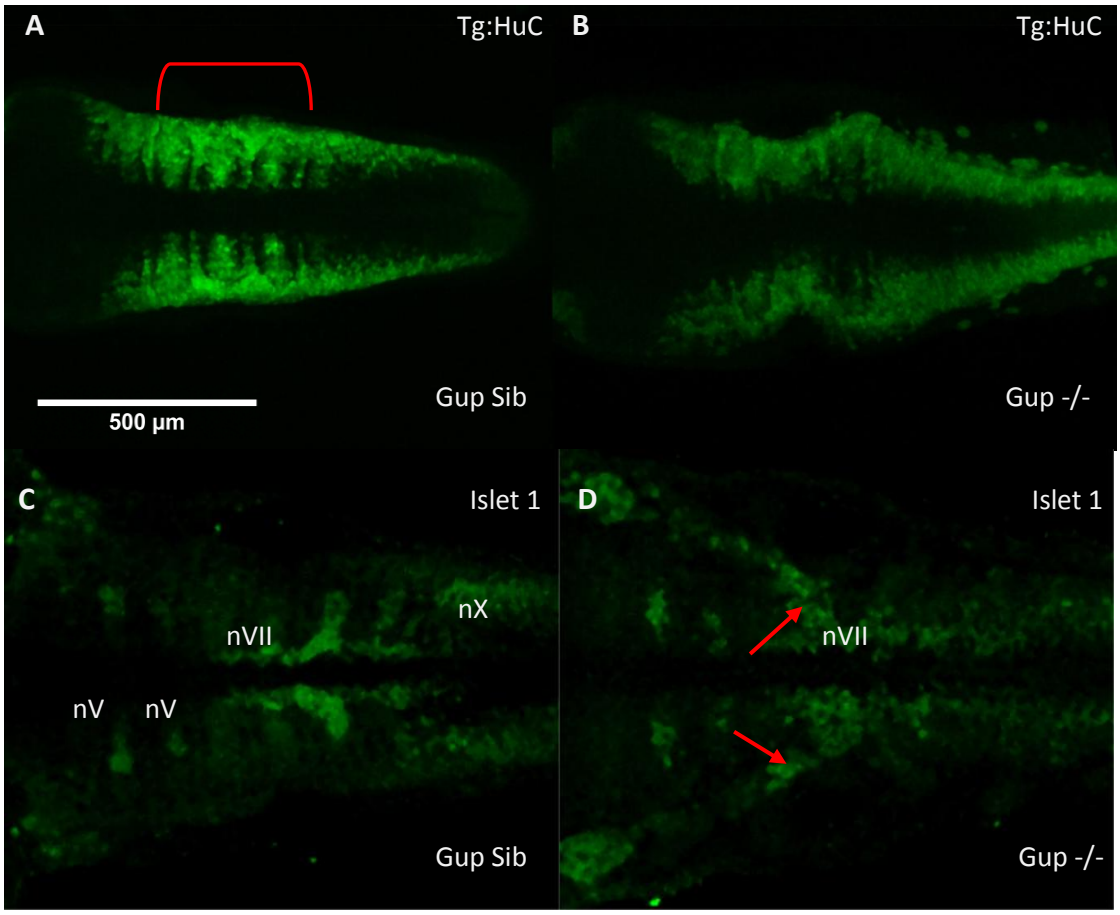

Figure 18 – Post-mitotic and facial branchiomotor neuronal patterning is altered in the hindbrain in mutants at 36hpf

All panels display dorsal views of the embryo with anterior to the left. Images show hindbrain of siblings and mutants expressing GFP (A and B) and fluorescent Immunohistochemistry using Islet 1 antibody (C and D). HuC expression is disrupted in the hindbrain of mutants (B). In siblings the hindbrain consists of the trigeminal branchiomotor neurons (nV), facial branchiomotor neurons (nVII), and the Vagal nuclei (nX). Caudal migration of facial branchiomotor neurons which occurs from rhombomere 4 to 6 in siblings is disrupted in mutants (D), resulting in the appearance of laterally ectopic islet-1 positive neurons in the hindbrain (red arrows). Images are displayed as maximum Z projections.

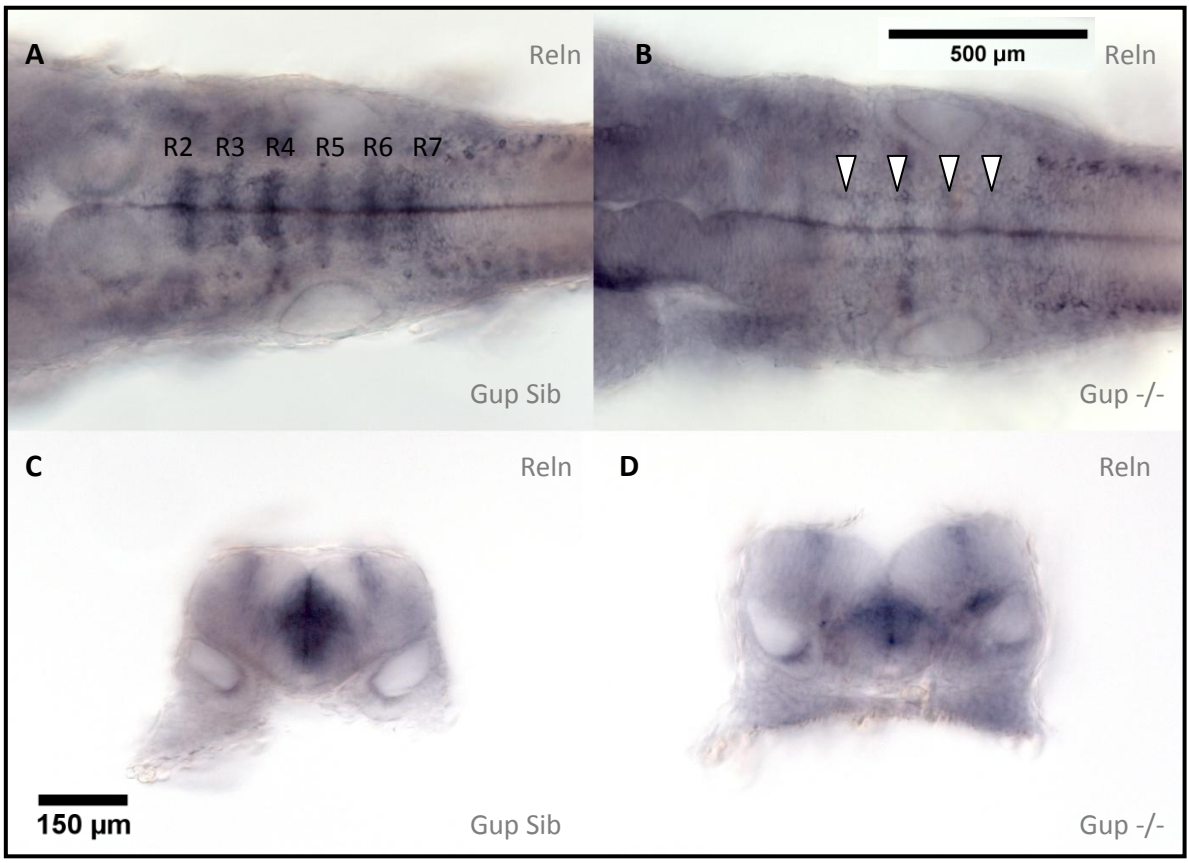

Figure 19 - Laminin mutants display decreased expression of reelin in the hindbrain at 36hpf.

Panels A and B show dorsal views of the embryo with anterior to the left. Panels C and D show transverse sections of the hindbrain at the level of rhombomere 5, with dorsal uppermost. Reelin expression is prominent in the central domains of rhombomeres 2 to 7 in the hindbrain (A), whereas this expression appears to be lost in the mutants (B, white arrowheads). In the transverse sections, there is a strong expression of reelin in the ventricular zone of siblings (C), which appears to be reduced in the mutants (D).

3.5 Sequencing of laminin β1 mutants

In Sheffield, we maintain the tj229a allele of the grumpy line, first described in 1996 by Tubigen screen (Odenthal *et a.l* 1996; Stemple *et al.* 1996). The only published mutatnt LAMB1 *gup* allele that has been verified by sequencing is *gup*^{m189} which is a C>T transition that results in a Q544 to stop codon change at the protein level [Parsons *et al.* 2002].

In order to screen for mutations we set up crosses between *gup* heterozygote fish, and collected embryos at 1-3 days post fertilisation. We then used RT-PCR to sequence cDNA obtained from pools of phenotypically homozygous *gup* mutants, pools of unaffected siblings, and pools of wild type AB and LWT zebrafish strains. Our prediction was that pooled siblings would carry both wild type and mutant *gup* alleles, while phenotypic fish would only carry mutant alleles. AB and LWT cDNA sequences should help to clarify whether any new variants were likely to be unrelated polymorphisms or pathogenic mutations.

Gel electrophoresis showed a higher band product in the cDNA of laminin β1 mutant embryos compared with siblings (Figure 20A). We sequenced the complete coding region of the LAMB1A cDNA and found only a single candidate missense pathogenic mutation. This was formed by the inclusion of 34 base pairs of intronic sequence between exons 21 and 22 (Figure 20A). The effect of this mutation at the protein level is addition of 18 novel amino acids followed by a premature stop codon in exon 22 (Figure 20B).

The inclusion of intronic sequence in mRNA is most commonly associated with splice site mutations. To investigate this we sequenced splice donor and acceptor regions of the genomic DNA of pooled mutant and sibling embryos. The splice acceptor region showed several differences (Figure 20C). There was no mutation at the acceptor site, but there were changes in the poly-pyrimidine tract region upstream of the splice acceptor. The changes included an interrupted (GT)n microsatellite repeat, which is polymorphic between mutants and siblings, and wild type fish. The sequence differences found only in the gup mutant allele are highlighted (Figure 20C). Based on our analysis it is unclear which mutation actually disrupts splicing of the LAMB1A mRNA. The G>C at the -4 position replaces a purine with a pyrimidine. Since

pyrimidines at this position are associated with increased splicing it is possibly unlikely that this is the pathogenic mutation. The TC>AA mutation at -11 and -12 positions replaces two pyrimidines with purines, thus disrupting a tract of 7 contiguous pyrimidines. This is the most likely causative mutation. From the cDNA sequence we are able to identify the cryptic splice acceptor site 34bp upstream. This cryptic splice acceptor site has no polypyrimidine tract, and lies immediately adjacent to an upstream pure (GT)n microsatellite.

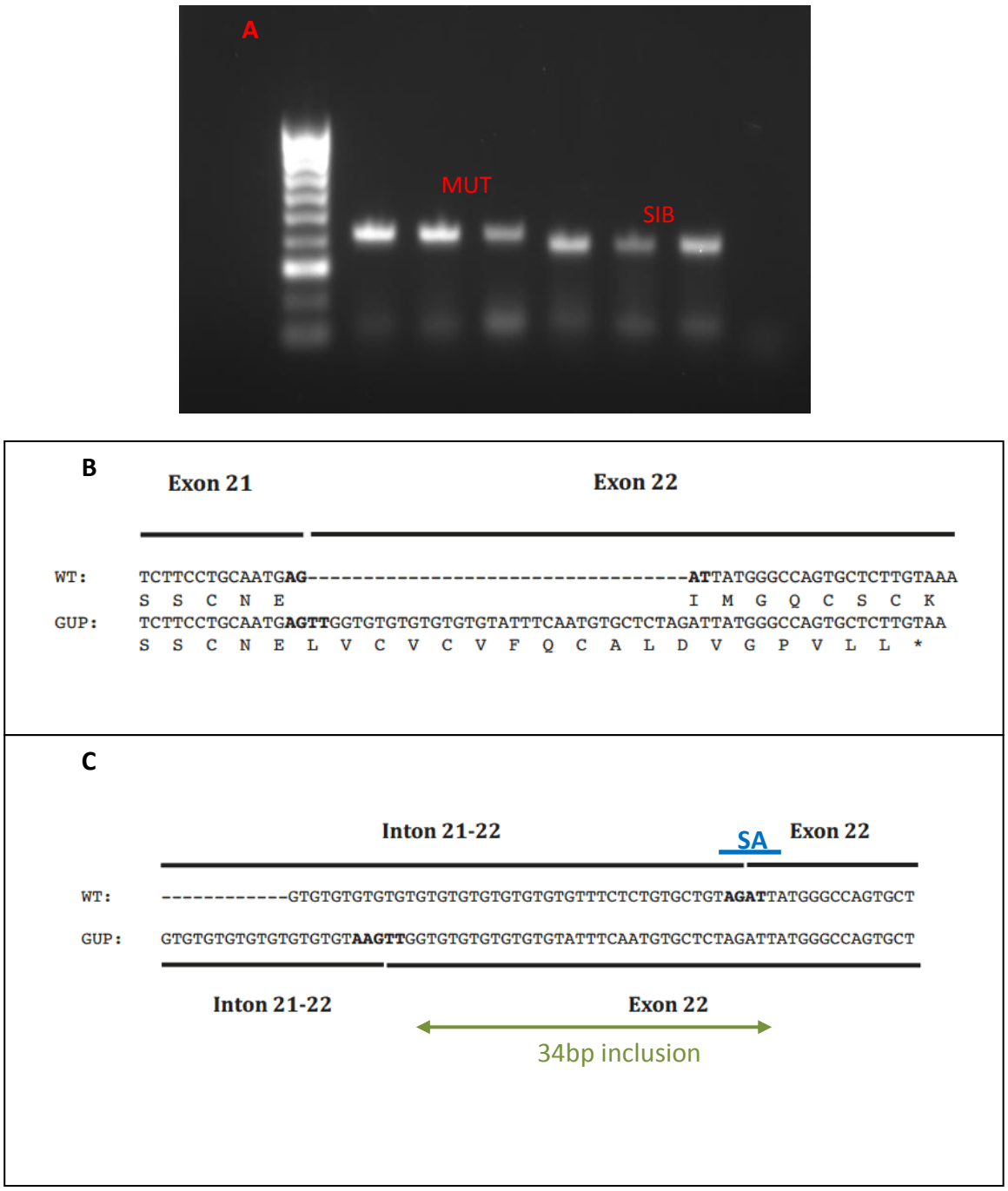

Figure 20 - cDNA alignment of laminin β1 mutants and siblings

A gel electrophoresis image shows 3 cDNA samples of laminin β1 mutants and 3 cDNA samples of laminin β1 siblings. Zebrafish mutants display a higher band product than their siblings (A). cDNA alignment between zebrafish laminin β1 mutants and siblings shows mutants have a 34 basepair (bp) inclusion of intronic sequence between exon 21 and exon 22 and results in an addition of 18 novel amino acids (B). Genomic DNA alignment show the 34bp is upstream to the splice acceptor (SA) site. The inclusion includes an interrupted TG polymorphic repeat (C)

3. 6 Discussion

Laminins consist of 3 subunits, α, β, and γ chains (Timpl 1989) and have significant roles in neuronal processes.

We demonstrate that laminin β1 zebrafish mutants express show a defective post-mitotic neuronal patterning in the forebrain (Figure 13 and 14). We observed alterations in the telencephalon and olfactory placode, to the extent that the developing olfactory placode became indistinguishable, suggesting there is a defect in migration resulting in dysplasia. Consistent with this studies have shown ablation of other laminin genes (LAMB2 and LAMC3) also produced cortical dysplasia (Radner *et al.* 2013). The zebrafish telencephalon lobes are separated by a T-shaped ventricle. The ventricular system appears at 18hpf and becomes inflated to form the anterior intraencephalic sulcus (AIS) (Folgueira *et al.* 2012). We hypothesise that the basement membrane outlining the AIS may play a role in the formation of the ventricle and consequently have an effect on the organisation of cells in the telencephalon and olfactory placode. In later stages of development the laminin β1 mutants displayed a marked reduction of ventricular space width in the forebrain, as well as a distinguished difference in the neuronal patterning of the forebrain. A study using a laminin β1 mutants harbouring a viral insertion in the first intron revealed the requirement for laminin β1 in the mid-brain hindbrain constriction (MHBC) formation, a fold in the brain which is formed after neural tube closure (Gutzman *et al.* 2008).

As the sensory placode morphology appeared disrupted in mutants we questioned whether the olfactory placode cells were affected in the mutants (Figure 17). At 24hpf, we observed a markedly reduced expression of *dlx3*, a marker of olfactory placode cells, in mutants. In particular, lateral *dlx3* expressing cells appear absent whereas the medial *dlx3*-expressing cells are present. As development occurs we see a progressive loss of dlx3 positive neurons in the mutants. We suggest that the disrupted HuC patterning observed may be a result of a loss of olfactory placode cells. Interestingly, studies have suggested telencephalon development is influenced by the olfactory placode, suggesting there is a direct link between these two regions(Graziadei *et al.* 1992). Additionally, we show that expression of *gabra1*, a GABA receptor subunit gene, is disturbed with some ectopic cells being identified in ventral regions of the

forebrain, suggesting mutants may have an altered GABA neurotransmission (Figure 16 C and D). Interestingly, interferences with GABA signalling have been associated with cortical dysplasias (Xiang *et al.* 2006). Epilepsy is clinically presented in patients of the neuronal migration disorder, COB Lissencephaly. In a mouse model of epilepsy cortical expression of GABA receptor 1α (garbra1) is altered (Seo *et al.* 2014). In keeping with this, mutations in GABA receptor 1A (GABRA1) are associated with idiopathic epilepsy syndrome (Macdonald *et al.* 2012).

The zebrafish hindbrain is an ideal system to examine the tangential migration of facial branchiomotor neurons (FBMNs), and identify how migrating neurons interact with their environment. FBMNs extend axons to the CNS and innervate the pharyngeal muscles. They are born in rhombomere 4 (r4) and migrate caudally to r6 and r7 (Chandrasekhar *et al.* 1997). Many genes have been identified to regulate this migratory process, of which laminin isoforms have been implicated in the development and migration of FBMNs. We first investigated motor neuron development in the hindbrain of laminin 1β mutants by looking at expression of an early post-mitotic marker, HuC. We observed a disruption in post-mitotic neuron organisation in the hindbrain compared with wild-type embryos (Figure 18 A and B). This disruption in neuronal organisation may be partially due to laminin β1 deficient embryos displaying reduced hindbrain ventricle size and an abnormally shaped midbrain-hindbrain constriction. One of the key mechanism which influences brain ventricle morphogenesis is cell proliferation (Lowery *et al.* 2009). Correct neuronal organisation is dependent on the successful differentiation of neuroepithelial daughter cells, migrating from the ventricular zone, into neurons and consequently influences shaping of the brain. This neuronal differentiation process is also closely linked to cell proliferation (Lumsden 1990). We may speculate that the defective patterning of HuC cells in the hindbrain of *gup* mutants may be attributed to defects in cell proliferation.

We identified a disruption in the posterior migration of FBMNs in *gup* mutants (Figure 18 C and D). In *gup* mutant embryos some FBMNs have failed to migrate and are still located in r4. Rather than a normal accumulation of FBMNs at r6 and r7, *gup* mutants display a spread of neurons from r4 to r6. NvII cell bodies mutants fail to migrate correctly, resulting in the appearance of ectopic motor neurons, a defect phenocopied

by laminin α1 depletion (Paulus *et al.* 2006; Sittaramane *et al.* 2009). The fact that laminin β1 and laminin α1 mutants share this phenotype suggests a functional link between these two genes. Laminin α1 mutants also display a ventral mis-migration of FBMNs, which has been suggested to be a cause of the failure of posterior migration. It has been suggested laminin α1 can influence the velocity and orientation of centrosomes, influencing the posterior migration of FBMNs (Grant *et al.* 2010). Additionally, laminin α1 genetically interacts with the adhesion molecule transient axonal glycoprotein 1 (TAG1), and the polarity molecule strabismus, have been shown to control directional migration of FBMN (Sittaramane *et al.* 2009). Upon gene co-expression analysis, laminin β1 has been identified to be highly correlated with expression of zinc transcription factors 1 (zic1) and 2 (zic2), suggesting there may be a direct link between these genes (Radmanesh *et al.* 2013). In keeping with this, zebrafish *zic1*has been shown to be important for progenitor cell proliferation (Elsen *et al.* 2008). Zic1 knockdown in the zebrafish results in defects in midline and forebrain formation, features which resemble holoprosencephaly, a disorder of forebrain development (Maurus *et al.* 2009). It is tempting to postulate that laminin β1 may function with transcription factors to regulate neurogenesis and control migration of neuronal cells in the forebrain and hindbrain.

Two consanguineous families with homozygous mutations in LAMB1 have been reported to display CNS defects resembling cobblestone lissencephaly, a neuronal migration disorder. Cobblestone lissencephaly can be identified in several clinical syndromes, including fukuyama congenital muscular dystrophy, Walker-Warburg syndrome, and muscle-brain eye disease (Radmanesh *et al.* 2013). The disorder is characterised by an over-migration of neurons through a defective basement membrane/glia limitans, which lies below the pia matter and serves as a barrier to migrating neurons (Siegenthaler *et al.* 2011; Devisme *et al.* 2012). Mouse models deficient in laminin β2 and γ3 chains exhibit cortical laminar disorganisation, a hallmark of cobblestone Lissencephaly (Radner *et al.* 2013). Here we demonstrate laminin β1 deficient zebrafish embryos display a decrease in the ventricular surface width, a marked reduction in size of the forebrain, and ectopic FBMNs, resembling features of cobblestone Lissencephaly. Interestingly, we observe a disrupted reelin patterning in the forebrain and hindbrain of laminin β1 mutants, also a pathology seen

in mice models of cobblestone lissencephaly (Hartmann *et al.* 1999; Li *et al.* 2008). Additionally, reelin has been described to play a role in migration of FBMNs in the developing mouse brainstem (Terashima *et al.* 1993; Ohshima *et al.* 2002). This strengthens our belief that laminin β1 mutant embryos display features typical of cobblestone Lissencephaly.

We investigated the gup^{tj229a} mutation by sequencing cDNA from phenotypic embryos, and comparing with data from unaffected siblings and wild type controls (Figure 20). We identify a pathogenic mutation which occurs in the region of a splice acceptor site, and results in the use of a cryptic splice site. This in turn leads to inclusion of 34bp of intronic sequence, resulting in a frameshift and the creation of a premature stop codon. This would result in a non-functional allele that is either subject to nonsense mediated decay or generates a truncated protein that lacks part of the Laminin LE domain and the C-terminal region of the protein. We report a frameshift/truncation allele in exon 22 of the gup^{tj229a} (Figure 21). In human patients with COB Lissencephaly, this same exon has also been identified to harbour a mutation which leads to a frameshift and premature stop codon in a consanguineous Eygyptian family (Radmanesh *et al*. 2013), supporting the idea that this is the pathogenic mutation. In comparison, other zebrafish lamb1 mutations have been mapped to exon 13 and exon 24 (Parsons *et al.* 2002; Hochgreb-Hagele *et al.* 2013) (Figure 21).

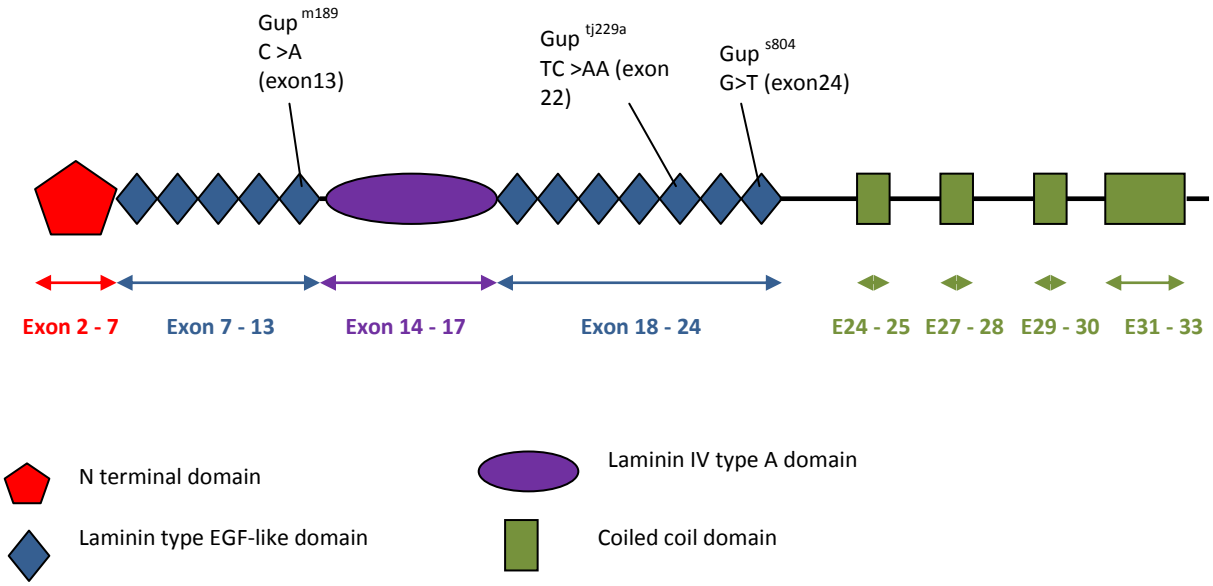

Figure 21 - A schematic representation of the zebrafish lamb1 structure and mapping different *gup* alleles. Zebrafish *lamb1* alleles and causative mutations are mapped out.

One of the DNA changes in this intronic region includes a polymorphic (GT)n microsatellite repeat. On the basis of our analysis we predict that the TC>AA mutation at -11 and -12 positions relative to the splice acceptor site is most likely to be pathogenic. This disrupts the only polypyrimidine tract in the region, a sequence known to regulate splicing (Reed *et al.* 1985). The reason for the use of the alternative, cryptic, splice site is more puzzling. In the mutant allele the (GT)n tract is interrupted by the insertion of AAGTTG, and AG/TT becomes the novel splice acceptor site.

3.7 Future Work

We believe the zebrafish laminin β1 mutants (allele ^{tj229a}) can be utilised as a model for cobblestone lissencephaly. In patients with COB lissencphaly, clinical aspects show that generalised epilepsy begins at an early age (Verotti *et al.* 2010). Previous studies have indicated an altered expression of GABA receptor subunits in animal models of epilepsy. We show an altered pattern of gabra1 subunit in the forebrain of zebrafish mutant embryos. It would be interesting to further this study by investigating whether laminin β1 mutants display alterations in other neurotransmitter receptors or proteins which are important for neurotransmission. Furthermore COB patients with LAMB1 mutations have pronounced cerebellar hypoplasia (Suarez-Vega *et al.* 2013). This could be explored in zebrafish using fgf8 in situ hybridisation. Gene co-expression analysis using the human brain transcriptome suggested a correlation between LAMB1 and Zinc-finger transcription factors, ZIC1 and ZIC2 (Radmanesh *et al.* 2013). In the zebrafish, *Zic1* has been shown to control forebrain patterning by regulating Nodal, Hedgehog and Retinoi acid signalling pathways (Maurus *et al.* 2009). Further studies could investigate which signalling pathways lead to the defects observed in the forebrain and hindbrain of zebrafish laminin 1β mutants. Another avenue to investigate is to create an artificial splice cassette in a reporter gene construct to understand the effects of the (GT)n and various mutations within the intron upon splicing.

CHAPTER 4

THE ROLE OF HYDROXYMETHYL-GLUTARYL CO-ENZYME A REDUCTASE (HMGCoAR) IN FOREBRAIN DEVELOPMENT

4.1 Abstract

The hydroxymethylglutary co-enzyme A reductase (HMGCoAR) catalyses the rate-limiting step in the mevalonate (MVA) pathway which produces cholesterol and isoprenoid. *In vivo* studies have implicated this pathway in various developmental processes. A previous study has implicated this pathway in motor neuron and oligodendrocyte precursor cell migration, but it is not known whether this pathway plays a role in cortical development. We investigated how this pathway infuences cortical development by using the zebrafish forebrain as a model, in particular observing the telencephalon and olfactory placode. In our study we used the the zebrafish HuC transgenic (Tg:HuC) line which labels post-mitotic neurons. We used three structurally different statin molecules to inhibit HMGCoAR protein function, all of which resulted in a disruption of telencephalon morphology. Ectopic post-mitotic neurons were present amongst the forebrain ventricular space, suggesting a disruption in migratory movement of post-mitotic neurons. We also demonstrate that prior supplementation of mevalonate and precursors for isoprenoid intermediates, farnesyl and geranygeraniol (GG), rescues the statin-induced forebrain defects. Further analysis on the downstream isoprenoid pathway suggested geranylgeranly transferase I, an enzyme involved in prenylation, is involved in forebrain development. Taken together, our data suggests the requirement of protein gernaylgeranylation, which acts downstream to the HMGCoAR pathway, for correct neuronal positioning and ventricular space morphogenesis in the forebrain.

4.2 Introduction

4.2.1 The Hydroxy-methyl-glutaryl Co-enzyme A (HMGCoAR) Pathway

The mevalonate (MVA) pathway is critical in producing cholesterol and isoprenoids, both of which are vital components in celluar functions in most eukaryotic cells (Figure 19). The pathway initially starts with the condensation of Acetyl CoA to Hydroxymethylglutaryl – Co-enzyme A (HMGCoA) by HMGCoA synthase. This is followed by a reduction to mevalonate by the rate-limiting enzyme, HMGCoA reductase (HMGCoAR). This rate-limiting step occurs as a two-step reaction as the ester linkage of HMGCoA is reduced to an aldehyde, and then finally to an alcohol (Miziorko 2011). Biosynthesis of mevalonate occurs mainly in the endoplasmic reticulum (ER) as the HMGCoAR is located in the membrane of the ER (Hooff *et al.* 2012). (Hooff *et al.* 2012)Downstream of HMGCoAR are the cholesterol biosynthesis and isopentenyl diphosphate (IPP) production, a precursor important in producing isprenoid intermediates involved in prenylation. Intrestingly, plant cells display two alternative routes for isoprenoid biosynthesis. Isoprenoids produced in the mitochondria and endoplasmic reticulum occur via the MVA pathway, whereas isoprenoids are produced in choloroplasts via the 2-C-methyl-D-erythritol 4-phosphate (MEP) pathway. The isoprenoid precursor, IPP, is formed from glyceraldehyde phosphate and pyruvate in the MEP pathway (Lichtenthaler *et al.* 1997; Vranova *et al.* 2012).

Statins are competititve inhibitors of HMGCoAR and can inhibit the enzymatic activity by occupying a part of the HMGCoA-binding site (Istvan *et al.* 2001). Thereby, statins are highly efficient in reducing cholesterol levels and are widely prescribed for treatment of hypercholesterolemia. As well as inhibiting cholesterol biosynthesis, statins also inhibit the isoprenoid pathway, which results in the pleiotropic effects of statins (reviewed by (Liao *et al.* 2005).

4.2.2 Prenylation

The isoprenoid intermediates, farnesyl pyrophosphate (FPP) and geranylgeranly pyrophosphate (GGPP) serve as lipid donors in the post-translational modification of certain families of proteins which possess a CAAX motif, a four amino acid CAAX sequence at the C-terminal. The attatchment of these isoprenoid lipids occus via specific enzymes inovolved in the prenylation process, geranylgeranyl (GG) transferase and farnesyl transferase. These enzymes facilitate geranylgeranylation and farnesylation, where a 20 carbon isoprenoid or a 15 carbon isoprenoid is attached, respectively. This prenylation process enhances lipophilicity and facilitates attachment of proteins to their target membranes (Nguyen *et al.* 2010). The largest group of proteins which undergo this type of post-translational modification are GTPases that belong to the ras superfamily. These GTPases are involved in a variety of cellular processes such as proliferation, mitosis, migration, actin formation, adhesion, apoptosis, and intracellular vesicular transport (Figure 22). Other proteins which undergo prenylation include the γ subunit of G proteins, as well as lamins and centromic proteins (Hooff *et al.* 2012).

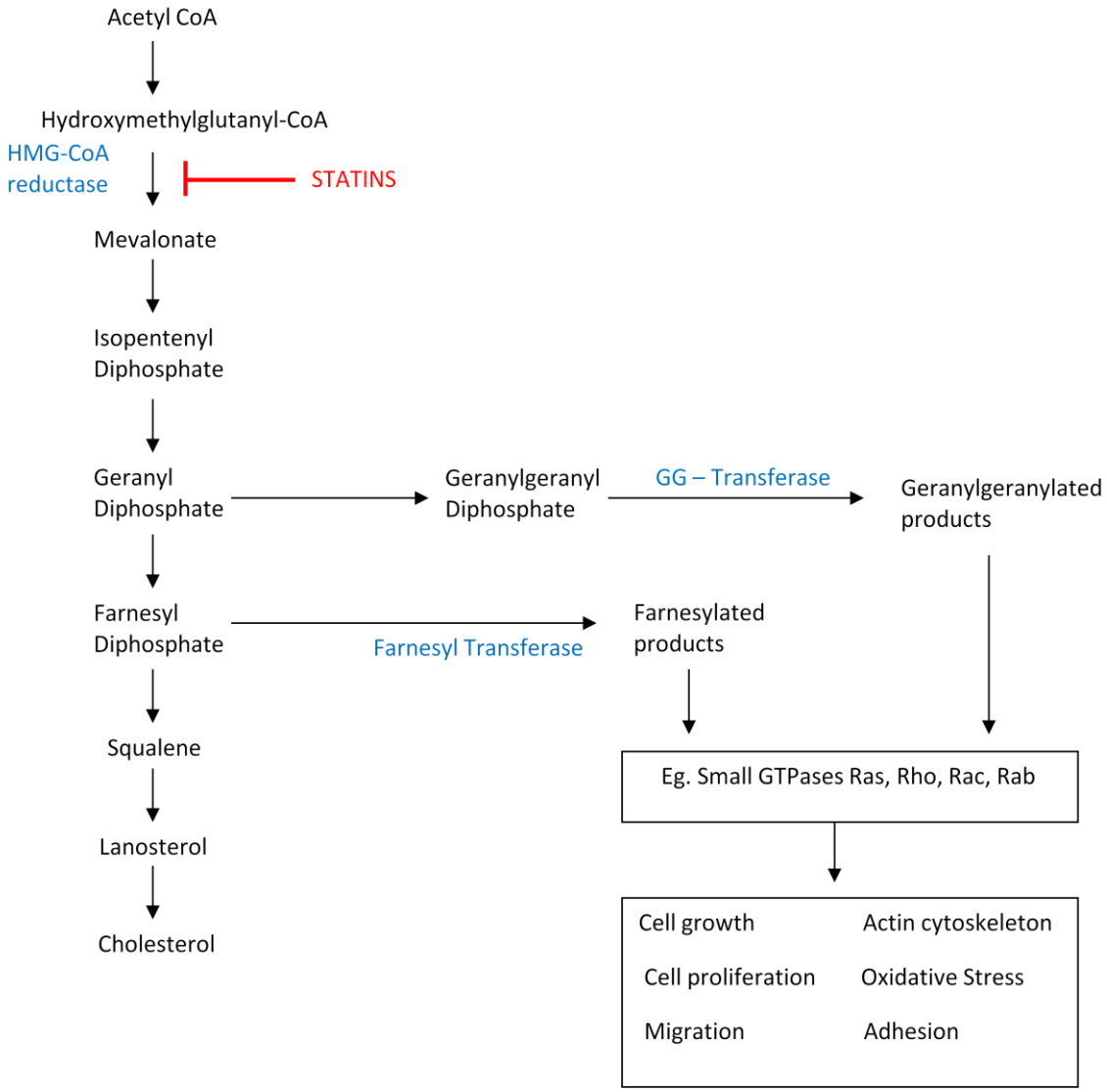

Figure 22 – A schematic representation of the HMGCoAR pathway.

Downstream of HMGCoAR are two branches, the prenylation pathway and cholesterol biosynthesis. Stains can inhibit the production of both these pathways. The ras superfamily of GTPases, which are involved in a variety of cellular processes, are dependent on the prenylation process. Thus, statin treatment can affect these cellular processes.

4.2.3 Importance of prenylation in neurodegenration

Investigation of the prenylation process and production of isoprenoid intermediates in the brain, in particular in aging and neurodegeneration is an expanding field of research. The blood brain barrier serves to protects the brain from foreign molecules entering, thus the MVA pathway provides brain cells with de novo biosynthesis of isoprenoid intermediates. In aging mice, farnesyl pyrophosphate (FPP) and geranylgeranly pyrophosphate (GGPP) levels were significantly higher than younger mice. Consistent with this higher levels of HMGCoA reductase were also observed (Hooff *et al.* 2012). Isoprenoid synthesis is also affected in a drosophila model of neurodegeneration, the *loechrig* mutant, caused by a loss of the AMP-activated protein kinase (AMPK) gamma-subunit. The mutant displays increased prenylation of RhoA, which aggravates the degenerative phenotypes (Cook *et al.* 2012). Disruption of the prenylation process of rab proteins induces retinal degeneration. Mutations in the rab GG transferase, an enzyme involved in attaching 20 carbon isoprenoids to rab proteins, has been shown to be linked to choroidermia, an X-linked form of retinal degeneration (Cook *et al.* 2012). Mutations in the rab escort 1 protein (REP1), also involved in prenylation of rab, results in a decreased number of hair cells and partial retinal degeneration (Starr *et al.* 2004). Increasing evidence from experimental studies implicate prenylated proteins and elevated levels of isoprenoid intermediates in the pathogenesis of Alzheimers Disease (AD). The grey and white brain matter of patients with AD display elevated levels of FPP and GGPP, suggesting disrupted isoprenoid homeostasis in AD (Eckert *et al.* 2009). Additionally, the study shows inhibiton of HMGCoA reductase decreases isoprenoid intermediate levels in mouse brains. Inhibition of HMGCoA reductase decreases the formation of γ-secretase within lipid rafts. This effect was partially rescued by addition of prenyl metabolite, geranylgerniol (Urano *et al.* 2005). Collectively, these studies suggest an altered isoprenoid metabolism in aging and neurodegenerative pathologies. They also suggest the use of HMGCoAR inhibitiors may be beneficial in different brain pathologies.

4.2.4 Importance of prenylation in development

Inhibition of HMGCoAR activity in utero has been associated with cases of severe midline CNS defects and limb deficiences, suggesting the importance of the enzyme in prenatal development (Edison *et al.* 2004). Many studies have elucidated HMGCoAR gene function by exploiting statins. One of the underlying mechanisms which may contribute to CNS defects may be apoptosis. In vitro studies show administration of HMGCoAR inhibitors induced apoptosis in cortical neurons and increased p53 levels (Tanaka *et al.* 2000). Administration of Lovastatin, a HMGCoAR inhibitor resulted in neuroblast apoptosis in the rat brain and activation of the p38 mitogen-activated protein kinase pathway (Cerezo-Guisado *et al.* 2007), suggesting multiple apoptic pathways may be induced by statins. In the zebrafish, the HMGCoAR pathway has been implicated in many developmental processes (summarised in Table 13) . Inhibition of HMGCoAR and the enzyme geranylgeranyltransferase results in germ cell, myocardial cell, facial branchiomotor neuron, and oligodendrocyte progentitor cell migration defects, and disrupts the cerebral vasculature. These studies suggest HMGCoAR activity and post-translational protein modification is essential for the devlopment of the zebrafish. The isoprenoid pathway has also been investigated in drosophila development, where geranylation of the G protein γ subunit of G protein is required to release the signalling molecule hedgehog (Hh) for correct germ cell migration (Deshpande *et al.* 2009).

To further investigate how this pathway infuences brain development, we observed the effect of HMGCoAR inhibitors on forebrain morphology. We present data which shows inhibition of HMGCoAR results in presence of ectopic post-mitotic neurons, suggesting an altered migratory movement of post-mitotic neurons. We also demonstrate the requirement of the downstream pathway, protein geranylgeranylation, in forebrain development.

Table 13 – A summary of the role of HMGCoAR activity in the zebrafish

	Defects due to inhibition of HMGCoAR	Defects rescued by supplementation of isoprenoid intermediates	Mechanism	Selected references
Germ Cells	Abnormal migration. 90% embryos have ectopic gem cells.	Yes	Disrupted prenylation of Gγ subunit of GPCRs reduces Ca^{2+} accumulation.	(Thorpe *et al.* 2004; Mulligan *et al.* 2010; Mulligan *et al.* 2011)
Myocardial Cell	Migration of myocardial cell to the midline during heart morphogenesis is disrupted.	Yes	Ras and Rho A proteins mislocalised away from plasma membrane.	(D'Amico *et al.* 2007)
Facial Branchiomotor Neurons (FBMN)	Migration of FBMN disrupted from rhombomere 4 to 6.	Not done	Farnesylation and nuclear localisation of Pkb1 required for FBMN migration.	(Mapp *et al.* 2011)
Cerebral Vasculature	Cerebral haemorrhages due to blood vessel dilation and rupture.	Yes	Reduced expression of cdc42, a GTPase involved in vascular permeability.	(Eisa-Beygi *et al.* 2012)
Muscle cells	Induces muscle fiber damage	Yes	Induces expression of Atrogin-1, a gene involved in the muscle atrophy porcess	(Cao *et al.* 2009)
Oligodendrocyte Progenitor cells	Cells migrate past their target axons	Yes	Decreaded expression of myelin genes	(Mathews *et al.* 2014)

4.3 Pharmacological inhibition of the HMGCoAR pathway results in defective forebrain development

The zebrafish HMGCoA reductase (HMGCoAR) homologs have conserved catalytic binding sites, the region where statins occupy the HMGCoAR, suggesting a functional conservation (Eisa-Beygi *et al.* 2012). We used the Huc:GFP stable transgenic line to visualise post-mitotic neurons in the forebrain region of the zebrafish during development. We initially observed the effect of three structurally different HMGCoAR inhibitors, Simvastatin (SIM), Lovastatin (LOVA) , and Atorvastatin (AT) on the phenotype of the embryos (Figure 23). We exposed embryos to various doses of SIM and AT at 5hpf for 25hrs, and found that the statins induced a variety of phenotypes (Figure 23A). We catergorised the phenotypes into 4 groups and quantified the percentage of embryos in each group upon SIM or AT treatment at 30hpf. A mild phenotype manifested in a slight kink in tail or a slight bend in tail, where as moderate and severe phenotypes displayed an increasing body axis defect and necrosis (Figure 21B). Both SIM and AT displayed an increase in severity of phenotype in a dose-dependent manner. Embryos treated with 0.1µM SIM or LOVA caused severe and moderate soamtic defects, whereas much higher doses of AT (25-50µM) are required to generate similar phenotypic defects (Figure 23C, D).

Our interest was to look at how inhibition of this pathway affected forebrain development, thus we looked at confocal images of frontal views of the forebrain which showed the telencephalon and olfactory placode regions. Treatment with high doses of SIM and AT disturbed the gross morpholgy of both the telencephalon and olfactory placode regions (Figure 23 and 24). An increased number of ectopic HuC-positive cells were observed as statin concentrations increased, suggesting pharamacological inhibtion of HMGCoAR inteferes with the migratory route of HuC-positive cells. Additionally, ectopic HuC-positive cells appear to be localised in the area forming the ventricular space (VS), consequently resulting in a smaller midline lumen (Figure 23B, 23C, 24B, 24C).

The zebrafish ventricular space undergoes initial inflation from 20hpf. This morphogenesis requires correct cell movements and causes a lateral movement of caudal telencephalic cells. The forebrain VS is important in formation of the anterior

intraencephalic sulcus (AIS) (Lowery *et al.* 2009; Folgueira *et al.* 2012), thus we developed a novel method to quantify the width of the forebrain ventriclar space (refer to section 2.9.4). Upon quantification of the VS, we observed a dose-dependent decrease in the width when embryos were treated with statins at 5hpf for 25hrs (Figure 25). Much lower concentrations of SIM compared with AT are required to result in drastic width reductions in the lumen. To observed whether inhibition of HMGCoAR was important after the zebrafish gastrulation period, we exposed embryos to varying concentration of SIM just after gastrulation events occur, at 12hpf for 18hrs. Simlar to previous experiements we saw a decrease in the ventricular space in a dose-dependent manner (supplementary data, Figure 35) Treatment with 10µM AT resulted in a slight decrease in width but was not significant, where as 15µM and higher concentrations led to significant reduction of width (Figure 23B). Treatment with 15µM AT resulted in 80% of embryos displaying a mild phenotype, and none with either moderate or sever phenotypes, (Figure 23D) whilst still significantly disrupting the localisation of HuC-positive cells in the forebrain (Figure 25) and VS formation (Figure 26). Treatment of embryos with AT results in defective forebrain patterning which is not due to the overt morphology defect only observed with higher AT doses, suggesting the statin-induced forebrain defect is specific to HMGCoAR inhibition.

As well as looking at the distribution of HuC-positive cells, we carried out in situ hybridisation using *emx3*, a marker for dorsal telencephalon cells, on embryos treated with 15µM AT (Figure 27). In vehicle treated embryos we observed prominent expression in the telencephalon regions and forebrain ventricular zone (VZ) (Figure 27A and C), suggesting a proportion of proliferative cells near the VZ are of dorsal telencephalon fate. Upon AT treatment, *emx3* staining appeared to be more dispersed in the telencephalon and much more prominent in the ventricular zone, which may indicate that pharmacological HMGCoAR inhibition may affect the positioning and/or differentiation of dorsal telencephalon cells. We chose to use 0.01µM SIM and 15µM AT in our further investigations.

To confirm the specificity of HMGCoAR inhibition in these experiments we injected embryos with mevalonate (MEL), a direct downstream product of HMGCoAR which acts as a precursor to both isoprenoids and cholesterol, followed by statin treatment at 5hpf (Figure 28A). We injected various doses of MEL alone, and prior to SIM

treatment to assess which dose gave a phenotypic rescue (Table 14). Higher doses of MEL led to a higher ratio of embryos displaying more severe phenotypes. Lower doses of MEL resulted in a normal phenotype, but at these concentrations no phenotypic rescue was observed. We chose to inject 1nL of 0.5M MEL in our future experiments. Upon Mevalonate treatment we observed a partial rescue of statin-induced somatic defects (Figure 28B-D). Injections of 1nl 0.5M MEL resulted in 50% of embryos displaying a mild phenotypic defect, suggesting this compound may be slightly toxic. As a control, embryos were injected with 50% DMSO, which failed to rescue the somatic defects upon statin treatment (Figure 28 D). Brightfield images of populations of embryos treated with vehicle and mevalonate prior to SIM treatment shows a partial morphology rescue across the entire population of embryos (Figure 29). Mevalonate injections in the presence of statin treatment reversed the forebrain morphology defects (Fig 30A-F). Ectopic neurons were not observed in embryos co-treated with mevalonate and AT (Fig 30F) Mevalonate injections results in a small, yet insignificant, decrease in the width of the VS, suggesting accumulation of mevalonate may be slightly toxic to the development of the ventricular space. SIM treatment induces a mean average distance of 16µm across the ventricular surface, which is partially rescued to a distance of 25µm when mevalonate is injected (Figure 30G). In comparison, mevalonate treatment rescues the ventricular width from 22µm to 28µm, in AT treated embryos.

These data suggest HMGCoAR activity and its downstream product, mevalonate is required for correct neuronal positioning to form the VS. Additionally, forebrain disruption is a primary defect due to pharmacological disruption to the HMGCoAR activity, thus validating the specificity of our approach.

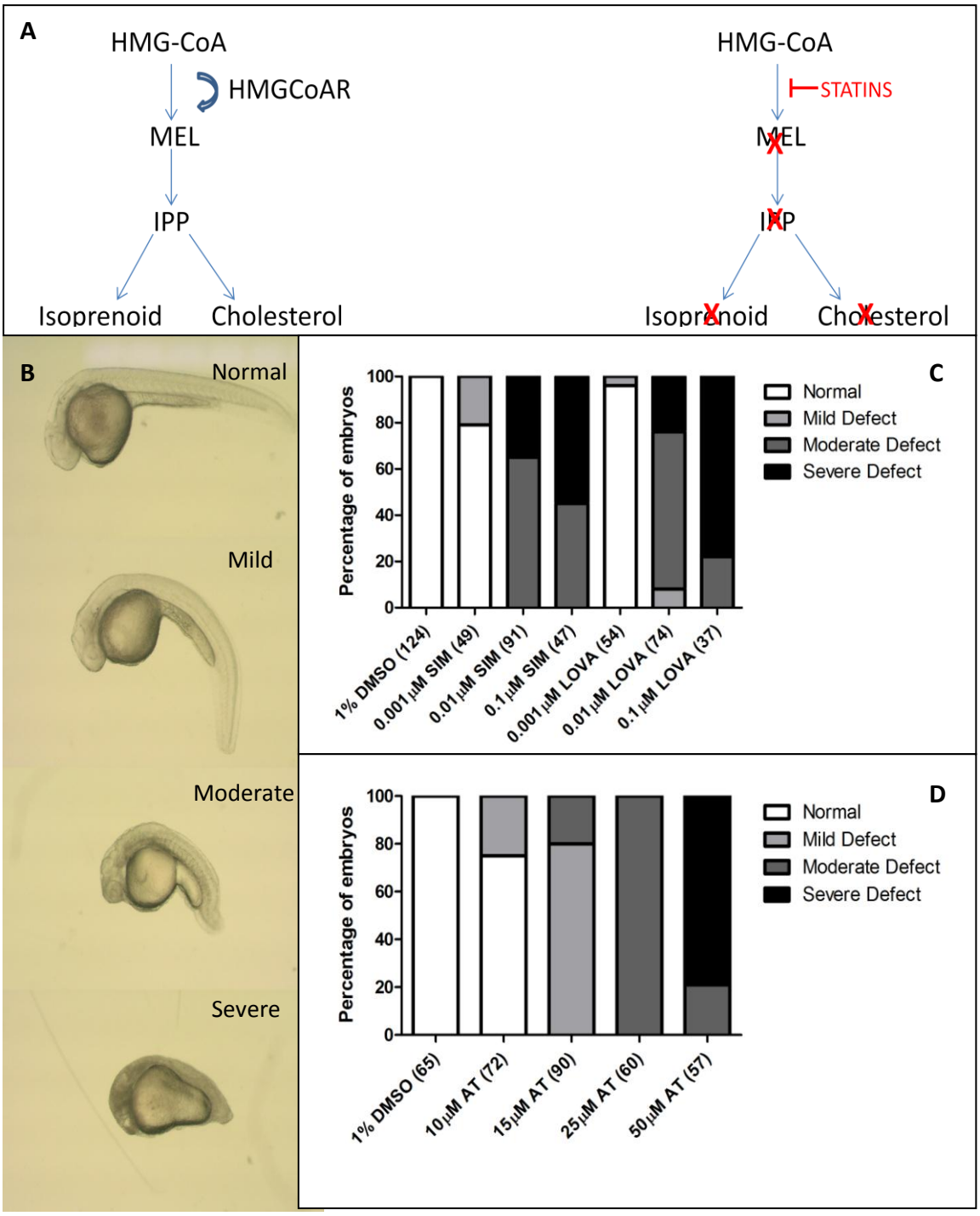

Figure 23 – Statin treatment induces a morphological defect in a dose-dependent manner.

A schematic representation of the HMGCoAR pathway and where statins inhibit the pathway (A). Representative brightfield images classifying different morphological phenotypes when embryos are treated with statins from 5hpf to 30hpf (B). Quantification of embryos displaying different morpholgy phenotypes when treated with varying concentration of Simvastatin (SIM), Lovastatin (LOVA) (C) and Atorvastatin (AT) (D) at 5hpf for 25hrs.

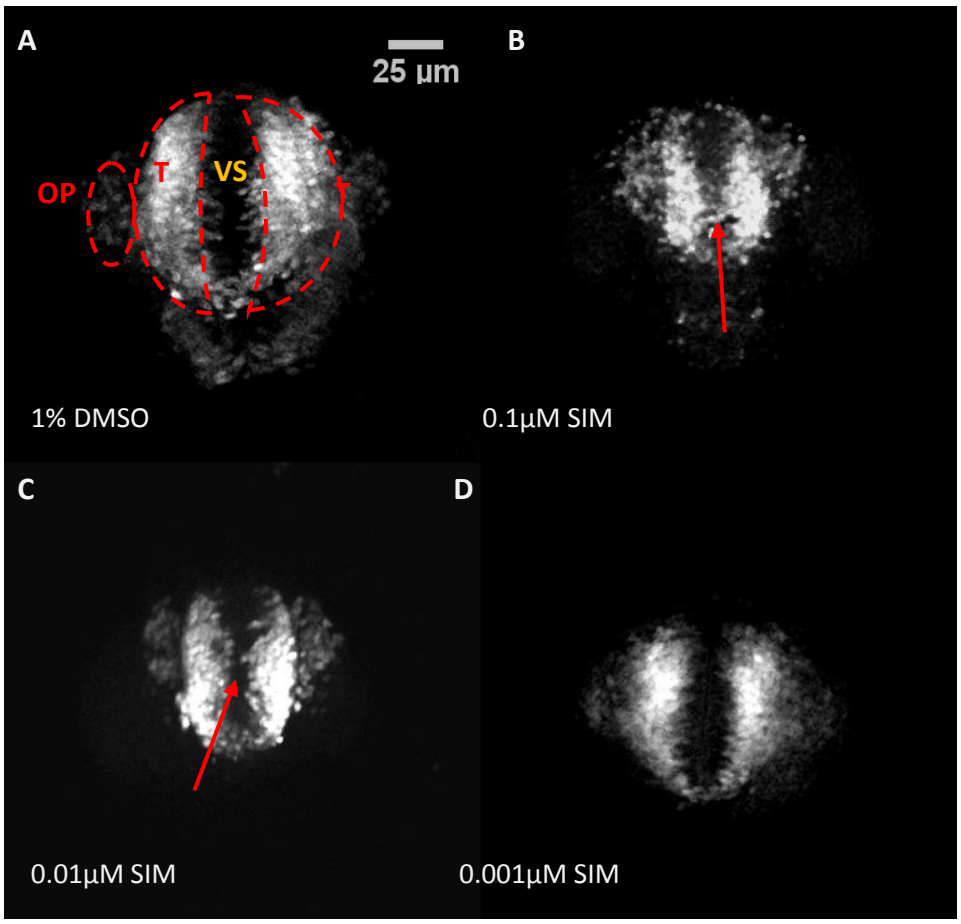

Figure 24 – SIM treatment results in a disruption of forebrain morphology.

Confocal images of the frontal view of the forebrain of Tg:HuC embryos upon vehicle and SIM treatments (A-D). Embyros were immersed in varying doses of Simvastatin (SIM) from 5hpf to 30hpf. Forebrain regions, telencephalon and olfactory placode appear disrupted in upon 0.1µM (B) and 0.01µM SIM (C) treatment. Ectopic cells were observed within the ventricular space (VS) disrupting the ventricular region (red arrows). All images are maximum Z projection stacks. Red dashed outline identifies the olfactory placode (OP) and the telencpehalon (T).

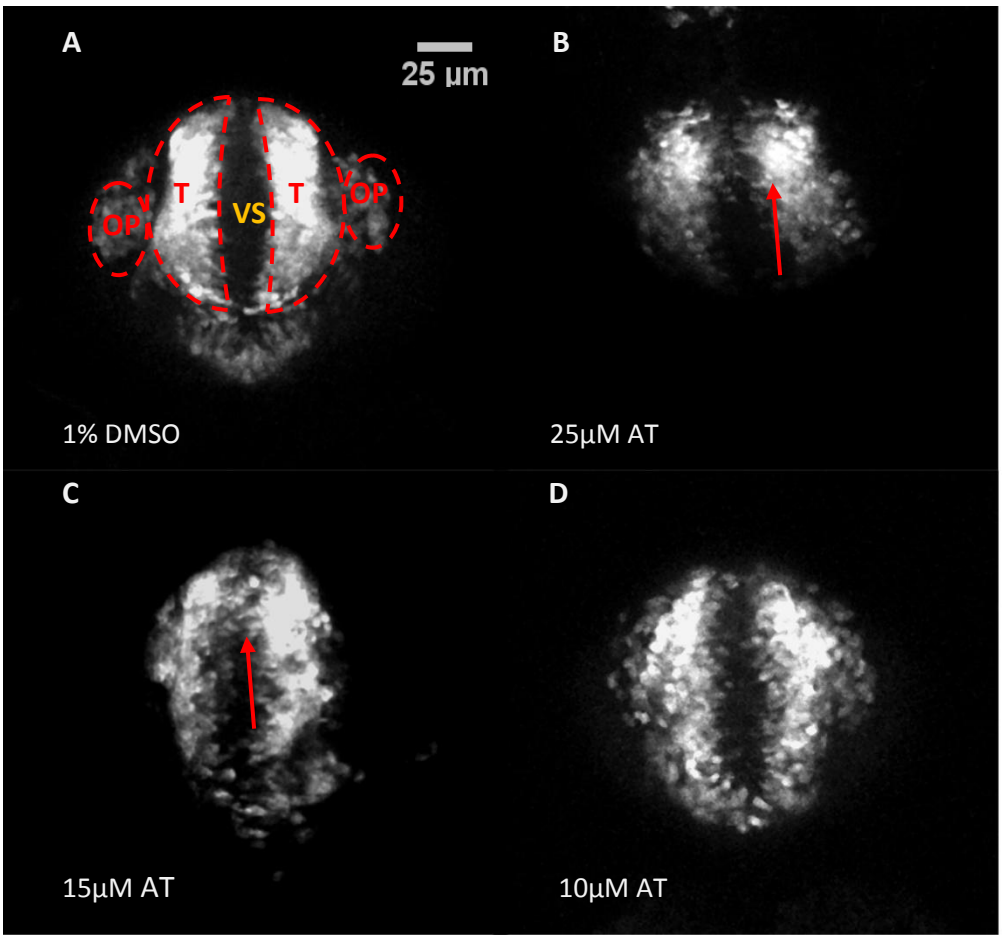

Figure 25 – AT treatment results in disruption of forebrain morphology.

Confocal images of the frontal view of the forebrain of Tg:HuC embryos upon vehicle and AT treatments (A-D). Embryos were immersed in varying doses of Atorvastatin (AT) from 5hpf to 30hpf. Ectopic neurons are present amongst the ventricular sapce (VS), disupting the development of the lumen at 25µM (B) and 15µM AT (C). Embroys immersed in 10µM AT show a forbrain morphology similar to that of vehicle treated embyros. All images are maximum Z projection stacks. Red dashed ouline identifies the olfactory placode (OP) and telencephalon (T).

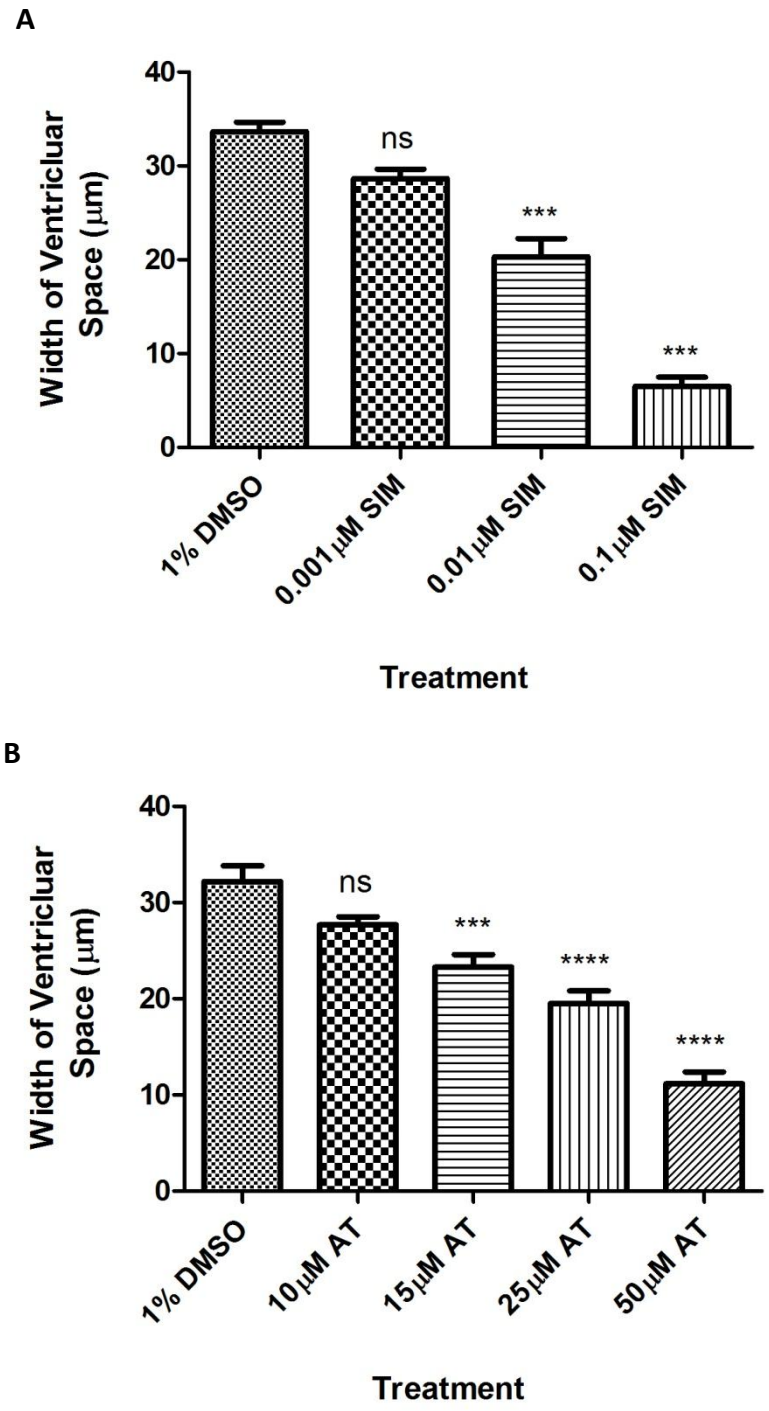

Figure 26 – Statin treatment induces a disruption in forebrain ventricle formation.

Data represents the distance between the forebrain ventricular lumen upon treatment of varying SIM and AT concentrations at 5hpf for 24hrs (A, B). SIM and AT treatment both result in a smaller ventricular space, which is dose-dependent. Much lower concentrations of SIM compared to AT are required to cause a drastic width reduction in the ventricular space. Data represents the mean distance ± SEM , n = 10 in each treatment group, one-way ANOVA Bonferroni's multiple comparison tests used for analysis, $p > 0.05$.

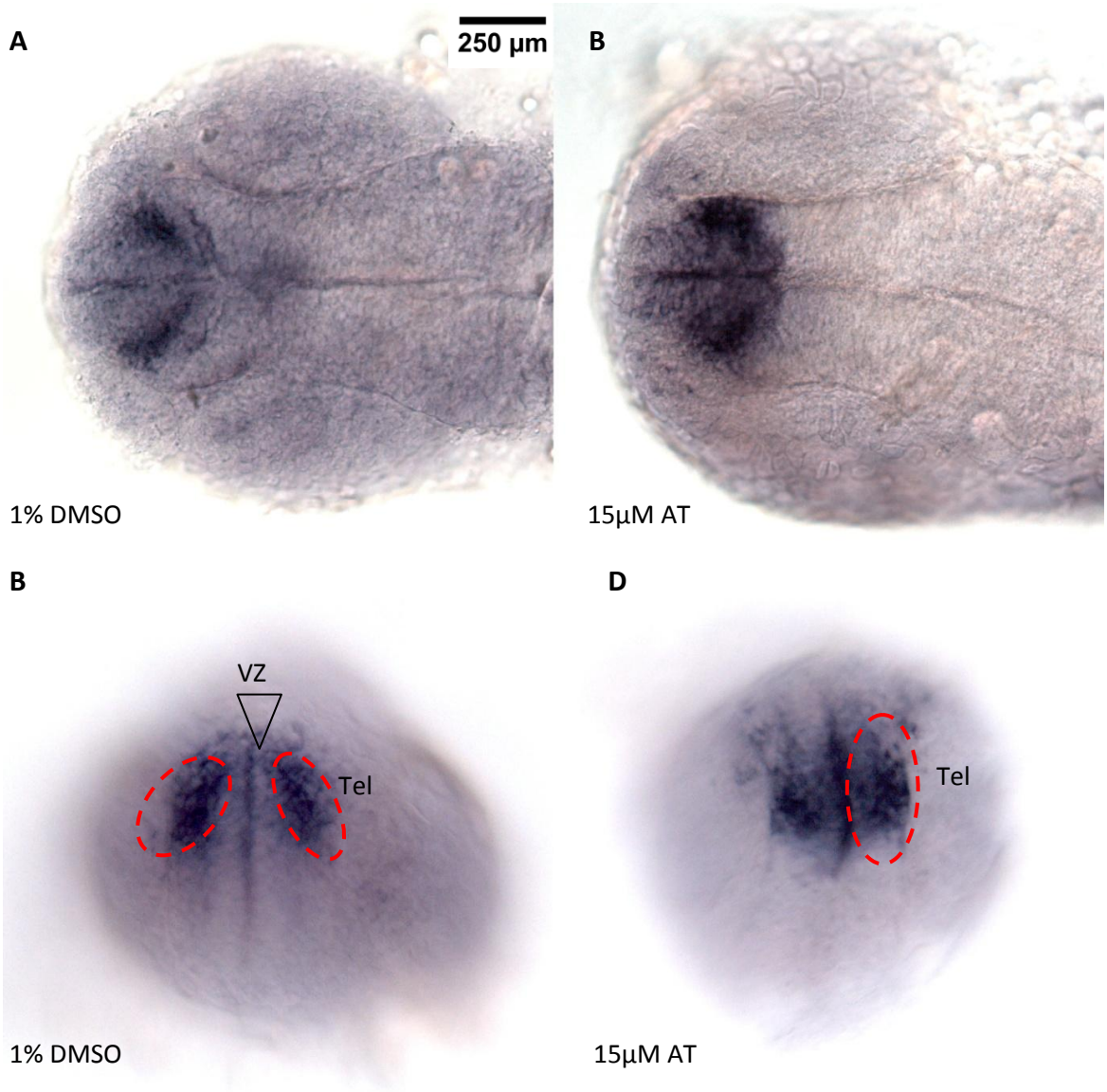

Figure 27 – Atorvastatin treatment alters emx3 expression in embryos at 30hpf.

Whole mount in situ hybridisation of emx3 expression in vehicle treated embryos (A and B), and embryos treated with 15µM AT (C and D) at 30hpf. Panels A and C show dorsal views with anterior to the left. Panels B and D are frontal views of the forebrain with anterior being uppermost. Vehicle treatment results in prominent expression in the telencephalon (Tel) and ventricular zone (VZ). 15µM AT treatment appears to result in more widespread distribution of emx3-positive cells, disturbing telencephalon morphology, and increased expression in the VZ. Red dashed line outlines the telencephalon region, black arrowhead identifies the VZ.

Table 14 - Dose response for mevalonate injections by assessing phenotype rescue

Treatment	**Phenotype**
50% DMSO 50% DMSO + SIM	Normal phenotype (18) Moderate phenotype (11)
2nl 1M MEL 2nl 1M MEL + SIM	Mild – moderate phenotype (21) Mild phenotype (15)
1nl 1M MEL 1nl 1M MEL +SIM	Mild phenotype (18) Normal (4) to mild phenotype(13)
1nl 0.5M MEL **1nl 0.5M MEL + SIM**	**Normal (16) to mild phenotype (6)** **Normal (11) to mild phenotype (7)**
1nl 0.25M MEL 1nl 0.25M MEL + SIM	Normal (25) phenotype Mild (8) to moderate (11) phenotype

Phenotype rescue was assessed by injecting different doses of mevalonate at the 1 cell stage prior to SIM treatment. Injecting doses higher than 1nL of 0.5M MEL alone led to mild to moderate phenotype, where as injecting less than 1nL of 0.5M MEL prior to SIM treatment did not result in a phenotype rescue. We chose to inject 1nL of 0.5M MEL in our experiments.

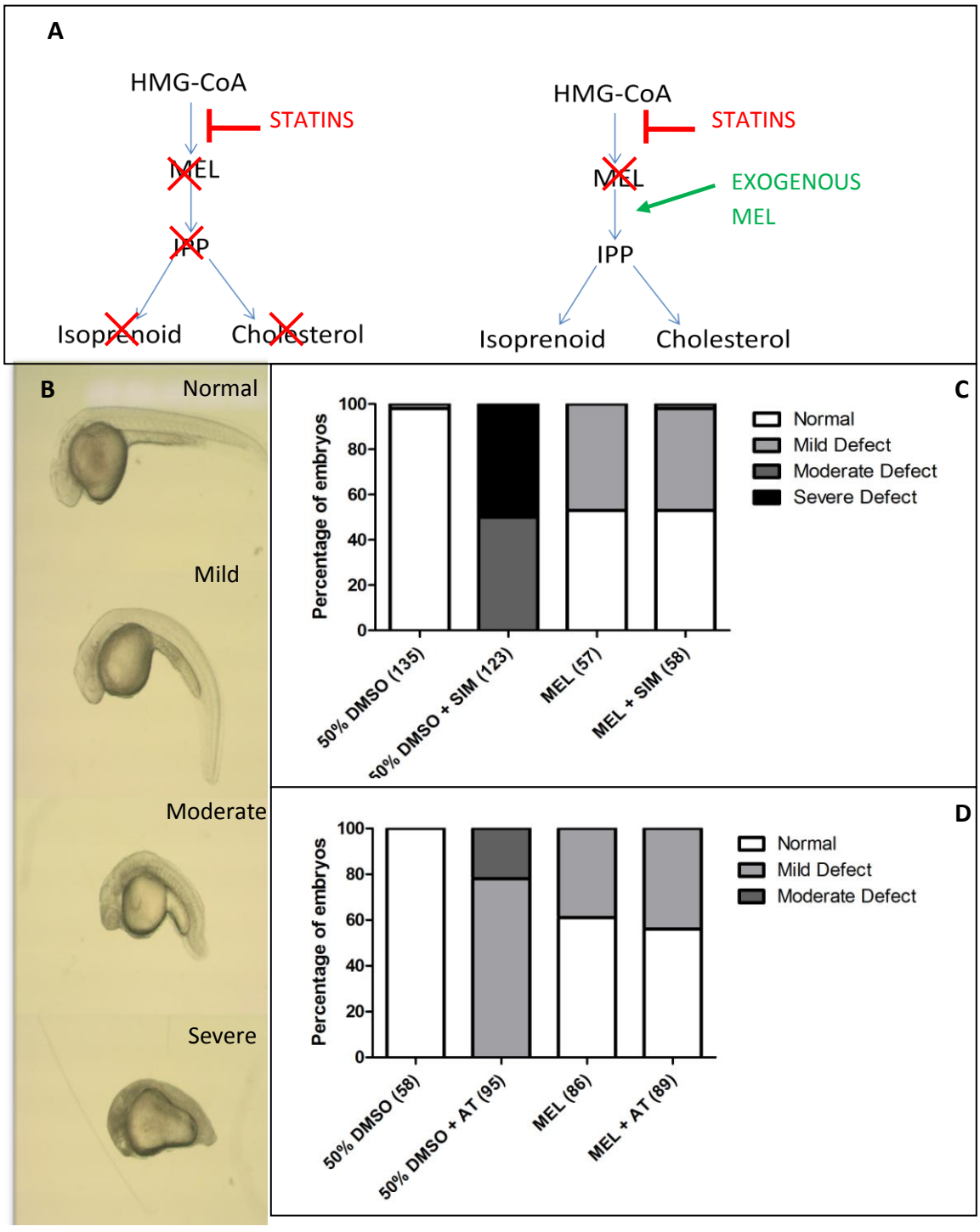

Figure 28 – Mevalonate supplementation partially rescues statin-induced morphology defects.

A schematic representation of how exogenous mevalonate acts on the HMGCoAR pathway to allow normal isoprenoid and cholesterol biosynthesis (A). Brightfield images grouping different phenotypes upon statin treatment (B). Quantification of percentage of embryos displaying a phenotype rescue upon mevalonate supplementation prior 0.01uM SIM (C) and 15uM AT (D) treatment.

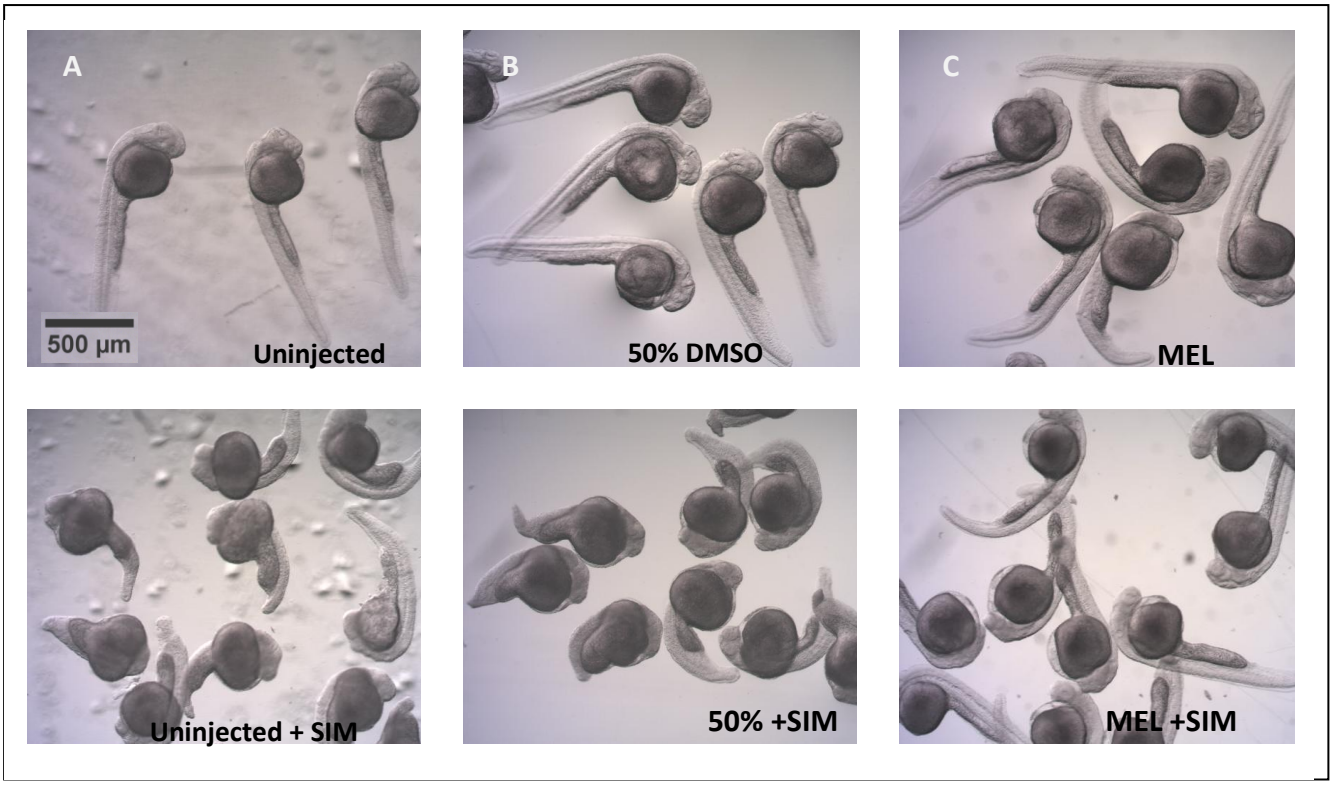

Figure 29 – Mevalonate supplementation partially rescues Simvastatin-induced morphology defects.

Brightfield images displaying morphology of populations of embryos under different treatment groups. Control treatments uninjected (A), 50% DMSO (B), and mevalonate (C) display normal to mild phenotypes. Simvastatin treatment results in moderate to severe morphology defects (D and E). Mevalonate injections partially rescues the statin-induced somatic defects (F)

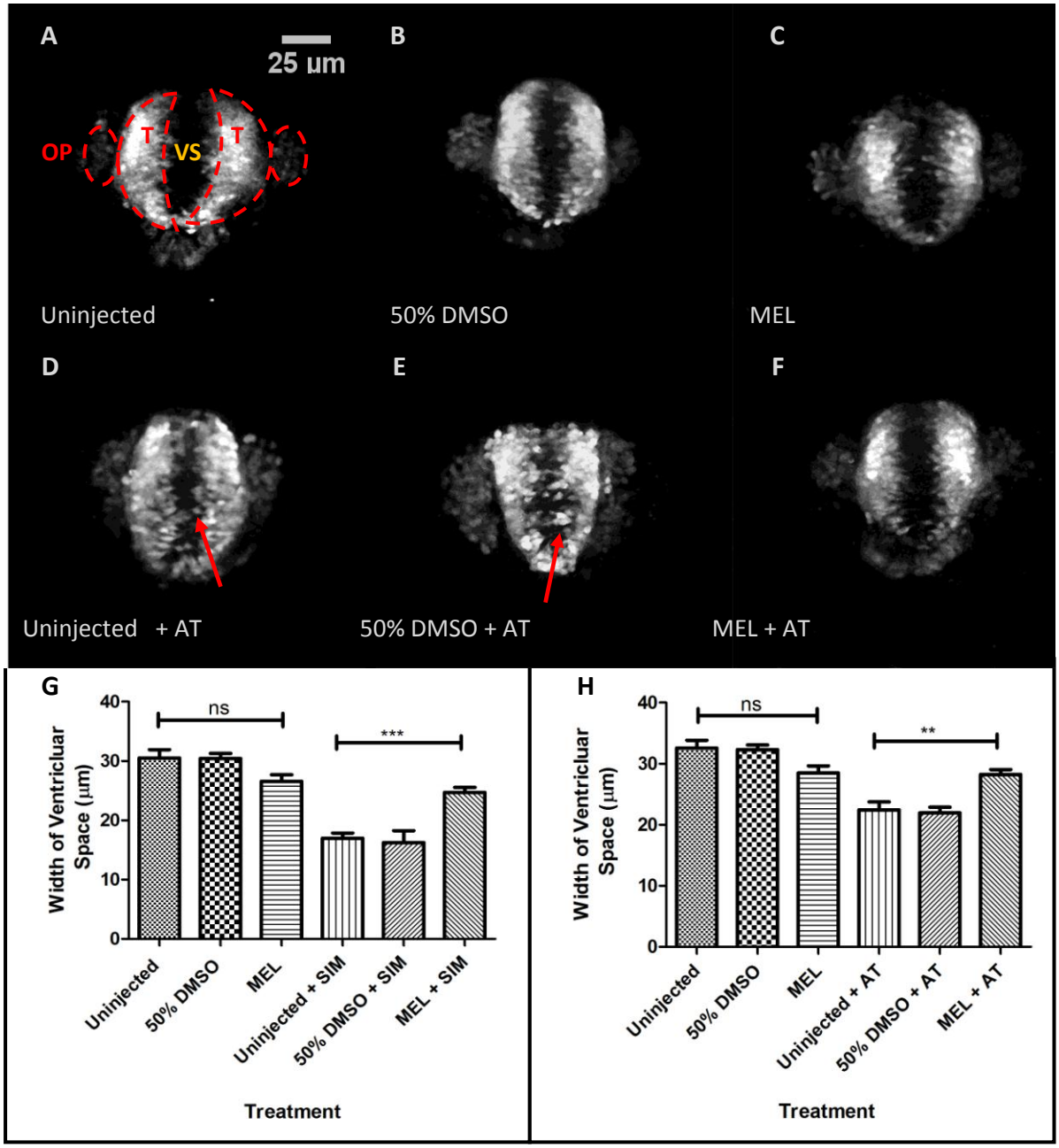

Figure 30 – Mevalonate supplementation rescues statin-induced forebrain defects.

Confocal images of the frontal view of the forebrain of Tg:HuC embryos (A-F). Uninjected, 50% DMSO, and mevalonate (A-C) embryos display normal forebrain morphology. Atorvastatin treatment disrupts the HuC-positive cells in the olfactory placode and results in ectopic cells in the ventricular space (VS) (D, E) (red arrows). Mevalonate treatment prior to 15µM AT treatment rescues morphology defects (F). Graphs display the mean quantification ± SEM of the ventricular space upon mevalonate injections prior to SIM (G) and AT (H) treatment. Mevalonate treatment reverses the statin-induced forebrain ventricle defect. n = 10 in each treatment group, one way ANOVA Bonferroni's multiple comparison test used for analysis, $p > 0.05$. Abbreviations: Telencephalon (T) and olfactory placode (OP).

4.4 The isoprenoid pathway plays a role in forebrain development

Studies in zebrafish show prenylation is required for heart morphogenesis, motor neuron and germ cell migration (Thorpe *et al.* 2004; D'Amico *et al.* 2007; Mapp *et al.* 2011). Following our observation of mevalonate rescuing statin-induced forebrain defects, we investigated whether other metabolites downstream of HMGCoA played a role. We modulated the isoprenoid pathway by injecting embryos with farnesol and geranylgernaiol (GG), two alcohols which readily increase substrate levels of farnesyl diphosphate (FPP) and geranygeranyl diphosphate (GGPP), respectively. FPP acts as a precursor for the isoprenoid enzyme farnesyl transferase, where as GGPP is required by geranylgeranyl transferase (Crick *et al.* 1994). 1 cell stage embryos were injected with the metabolites (2M GG, 0.25M farnesol) and control (50% DMSO) prior to 15µM AT treatment at 5hpf for 24 hrs (Figure 29). Somite defects and forebrain defects were assessed at 30hpf. Statin treated embryos injected with prenylation precursors GG and farnesol should result in normal isoprenoid production, whilst the cholesterol biosynthesis pathway is inhibited (Figure 31A). Embryos injected with GG and farnesol not only rescued somatic defects induced by statin treatment (data not shown), but also the morphology of the telencephalon and olfactory placode (Figure 31B-E). Ectopic HuC-positive cells were not apparent within the ventricular space when embryos were injected with farnesol and GG, followed by AT treatment (Figure 29D and E), suggesting the involvement of farnesol and GG in the migratory behaviour of HuC-positive cells. There was no significant difference in the size of the forebrain ventricle between embryos which were injected with vehicle, GG or farnesol alone, and embryos which were uninjected or injected with 50% DMSO (Figure 31F). Upon injecting embryos with GG and farnesol prior to AT treatment reversed the ventricle defect induced by statins from a mean width of 22µm to 29µm and 31µm, respectively (Figure 31G). This rescue by isoprenoid precursors was also observed when AT was substituted for SIM (supplementary data, Figure 36). The rescue observed by adding substrates required by isoprenoid intermediates suggest a requirement for

prenylation in ventricle lumen formations, thus resulting in correct localisation of neuronal cells in the forebrain.

To further investigate the role of the isoprenoid pathway in telencephalon development, we used a cell permeable compound which acts as a potent and selective inhibitor of the geranylgeranyl transferase I (GGTase I), GGTI 2147 (Figure 30A). GGTase I is critical for adding 20-carbon gernayl groups to various GTPases such as, rab (Farnsworth *et al.* 1994) rac1, rhoA, and cdc42 (Roberts *et al.* 2008). Injection of 2nl of 3mM GGTI 2147 resulted in a disruption of post-mitotic neuronal organisation in the forebrain. Ectopic HuC-positive cells were localised within the ventricular space (Figure 32C), thus phenocopying the effect of HMGCoAR inhibition. GGTI 2147 injections also mimicked the statin-induced decrease in the ventricular space (Figure 32D). GGTI 2147 injections resulted in an 8µm decrease in the width of the between the ventricular width, a result similar to that seen when uninjected embryos are treated with AT. Together, these results suggest the importance of geranylgeranylation in telencephalon development.

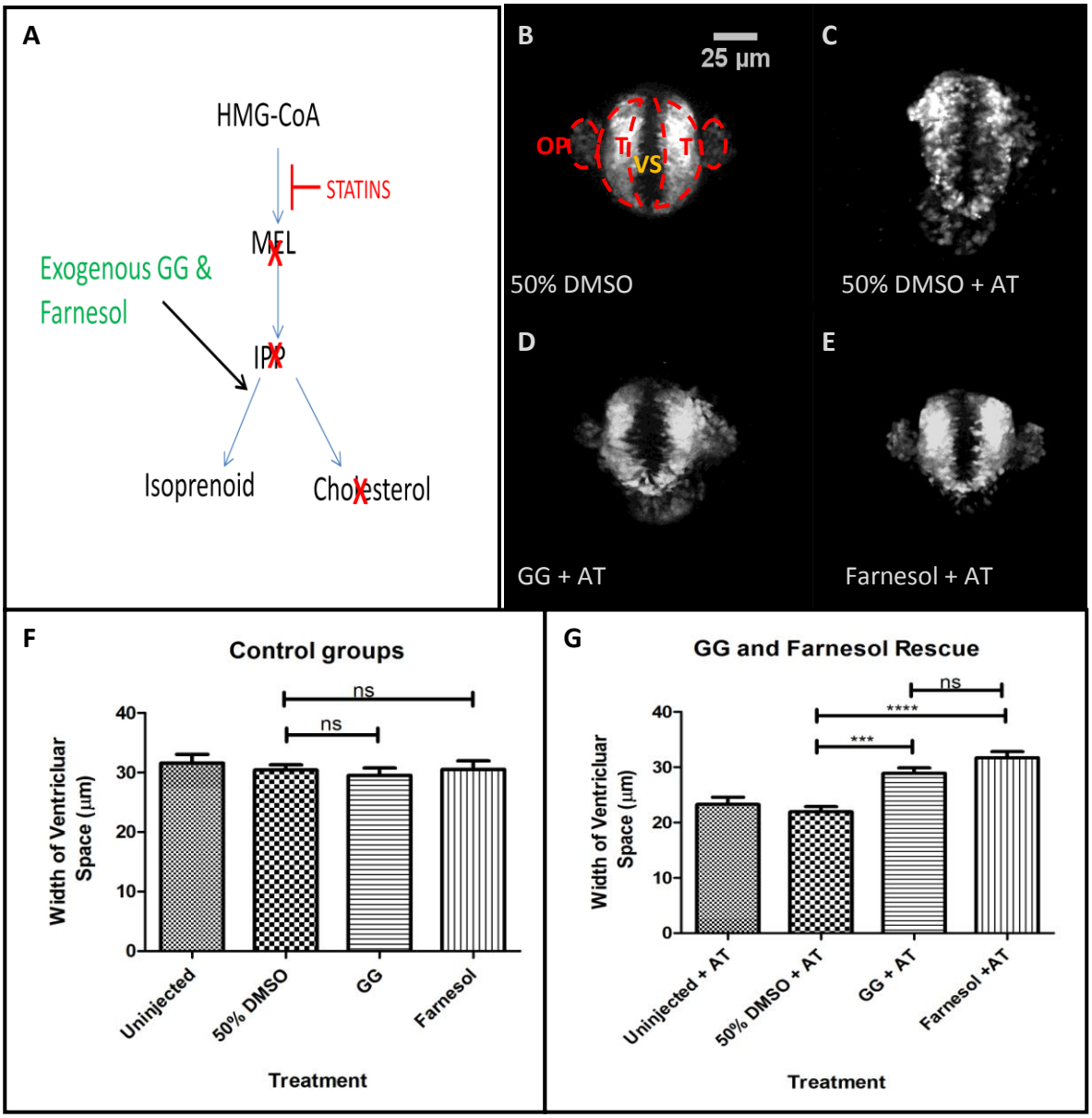

Figure 31 – Supplementation with GG or farnesol, rescues statin-induced forebrain defects.

A schematic representation to show supplementation of GG and farnesol prior to statin treatment allows for isoprenoid, but not cholesterol, production (A). Confocal images of the frontal view of the forebrain of Tg:HuC embryos upon injections of prenylation precursors prior to statin treatment (B-E). Data represents the width of the ventricular space under control conditions (F). No significant differences were observed between embryos injected with GG and farnesol, and embryos injected with 50% DMSO. 15µM AT treatment disrupts the forebrain architecture (C). Prior injection of GG and farnesol reverses morphology defects (D and E) and the width of the ventricular space (F and G).Images represent maximum Z projection stack. Data represents the mean ± SEM, n = 10 in each treatment group. One way ANOVA Bonferroni's multiple comparison test used, $p > 0.05$. Abbreviations: telencephalon (T), olfactory placode (OP).

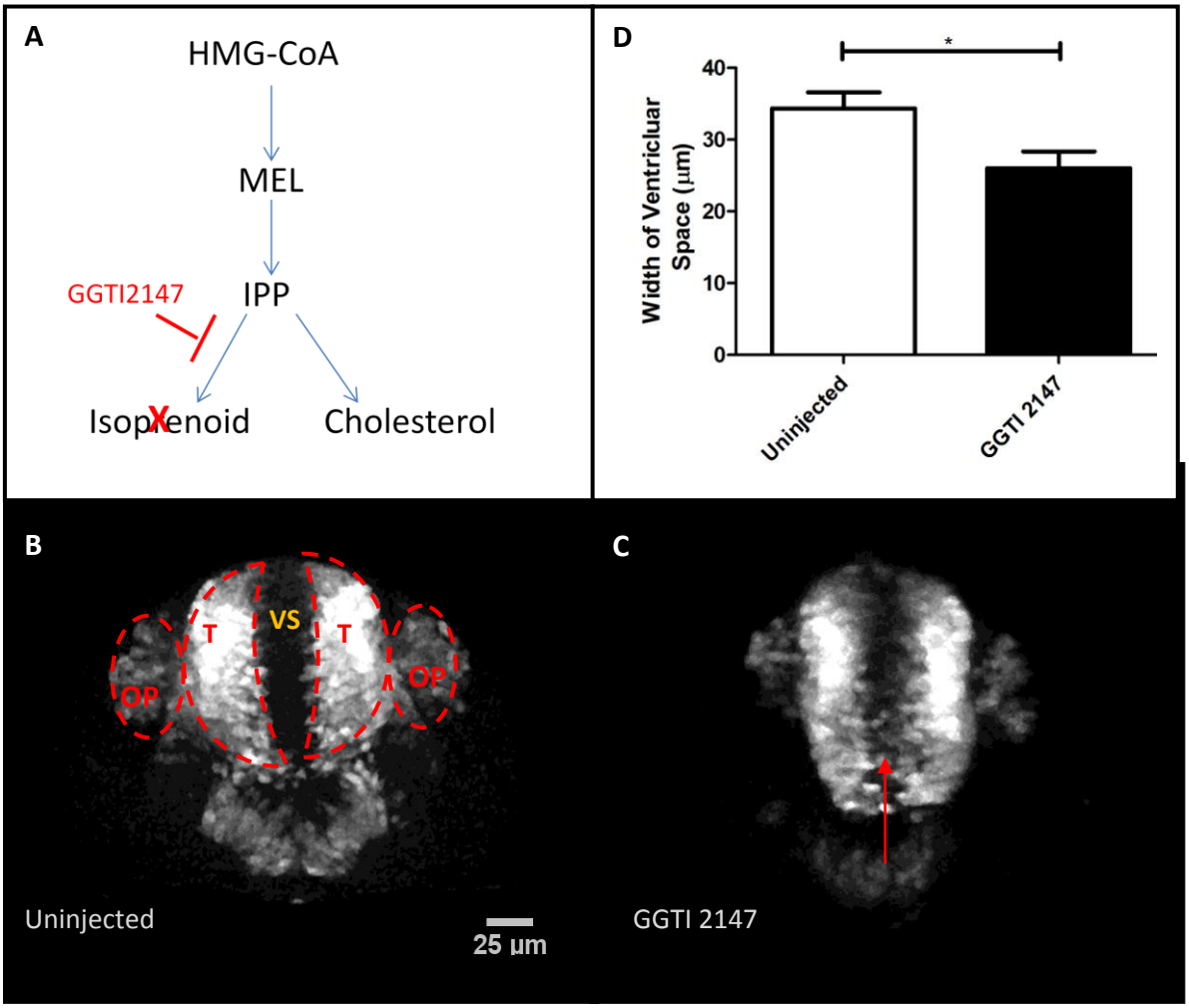

Figure 32– Inhibition of geranylgeranyl transferase disrupts forebrain development.

A schematic representation of how GGT12147, an inhibitor of geranylgeranyl transferase, inhibits isoprenoid production (A). Maximum Z projections of the frontal view of the forebrain of Tg:HuC embryos which were uninjected (B) and injected with GGTI2147 (C). Injection of 2nL of 3mM GGTI2147 disrupted post-mitotic neuron organisation, thus leading to ectopic neurons in the forebrain ventricular region (red arrow). Data represents mean distance ± SEM of the ventricular space (VS) upon vehicle (C) and GGTI2147 treatment (D), n=10 in each treatment group. A significant decrease within the ventricle was observed when embryos were injected with the inhibitor compared with uninjected controls, $p > 0.05$. Images represent maximum Z projection stack Red dash outlines the telencephalon (T) and olfactory placode (OP). One way ANOVA Bonferroni's multiple test used for statistical analysis.

4.5 Investigation of the Cholesterol Biosynthesis pathway

HMGCoAR plays an important role in the cholesterol biosynthesis pathway. Some studies have indicated that cholesterol biosynthesis is not involved cell migration, in particular of germ cells and myocardial cells (Thorpe *et al.* 2004; D'Amico *et al.* 2007). In contrast, inhibition of cholesterol productions has been shown to affect motor neurons migration during development (Mapp *et al.* 2011). We questioned whether the cholesterol pathway was involved in post-mitotic neuron migration or ventricle formation in the forebrain (Figure 33A). We used zaragozic acid (ZA), an inhibitor of squalene synthase, to inhibit cholesterol production. Embryos were immersed in 40µM ZA from the 1 cell stage and analysed at 30hpf (D'Amico *et al.* 2007). We observed no neuronal positioning defects in the forebrain upon ZA treatment (data not shown). Additionally, we observed no significant differences in the width of the ventricular space between embryos that were treated with 1% DMSO and ZA (Figure 33B). We injected squalene, an intermediate which is required by squalene synthase to form cholesterol (Thorpe *et al.* 2004). We injected embryos with 2nl of 2M squalene prior to treating them with 0.01µM SIM. Unlike mevalonate, GG, and farnesol we observed no rescue of neuronal or ventricle defects when embryos were co-treated with squalene and SIM (Figure 33C). Unfortunately, we did not have a positive control to identify whether our ZA or squalene treatments were decreasing or increasing cellular cholesterol levels, respectively.

We identified AY9944 as an additional compound which inhibits 7-dehydrocholesterol reductase, and thus prevents cholesterol biosynthesis. Zebrafish embryos exposed to 7.5µM AY9944 at the dome stage (4hpf) for 6hrs have been reported to display developmental malformations such as partial cyclopia, thus presenting a phenotypic assay to observe whether cholesterol synthesis was blocked (Li et al 2007). We exposed embryos to a range of concentrations of AY9944 (5µM, 7.5µM, 9.5µM, and 20µM) for 6 hrs, and analysed phenotype at 30hpf (data not shown). Unfortunately in our assay we could not replicate previous published results of (Li et al 2007). Furthermore we exposed embryos to the same concentrations as previously tested but for, 24hrs. Again, we did not observe any developmental malformations (data not

shown). Confocal images of embryos treated with 5µM 7µM, and 9.5µM for 24hrs displayed no evidence of a telencephalon defect (Figure 34A-C). However, the forebrain of embryos treated with 20µM for 24hrs appears smaller (Figure 34D).

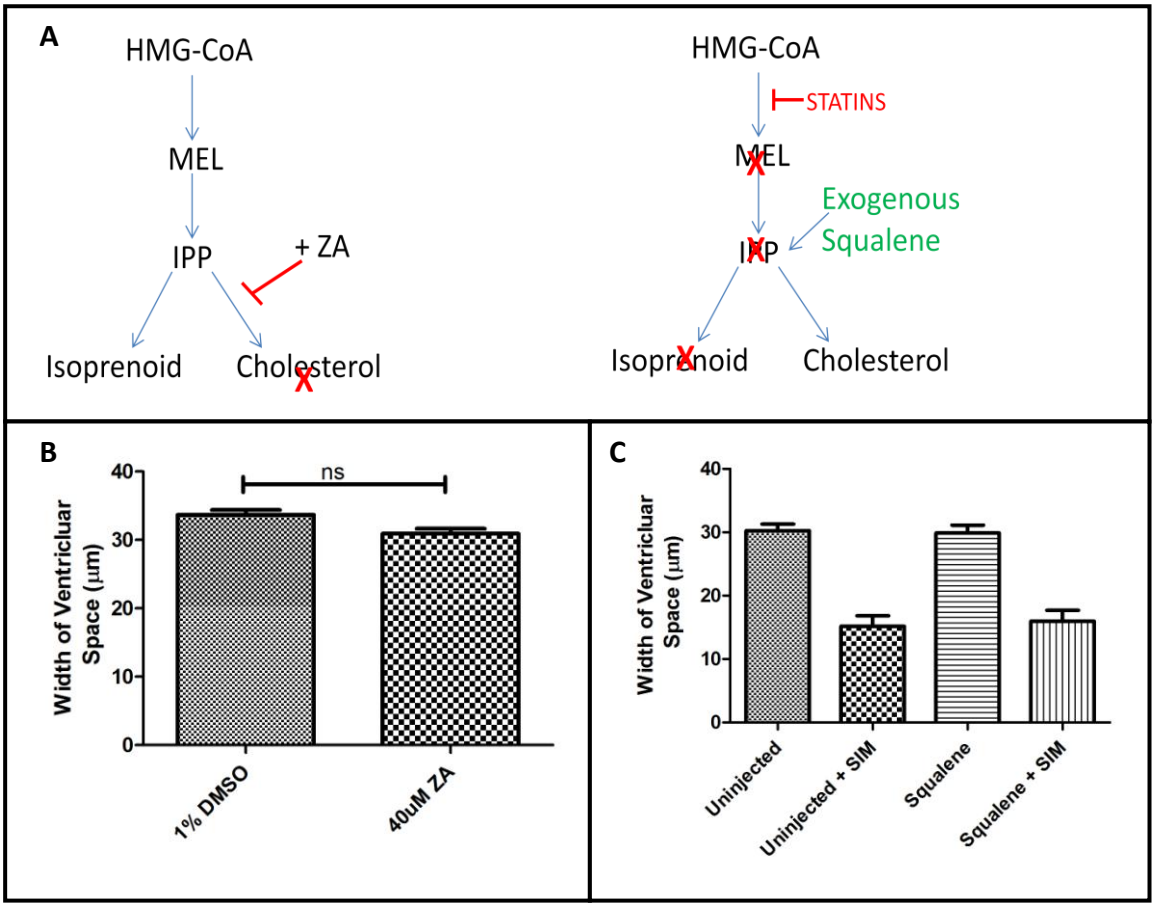

Figure 33 – Investigation of the cholesterol biosynthesis pathway.

Schematic representation of how zaragozic acid (ZA) and squalene treatment prior to statin treatment affects the HMGCoAR pathway (A). No significant difference in the width of the ventricular space between embryos treated with control vehicle (1% DMSO) and 40µM ZA (B). Squalene injections prior to statin treatment did not rescue statin-induced defects (C). Data represents mean distance ± SEM, n=10 in each treatment group. Statistical analysis used was t-test, $p > 0.05$.

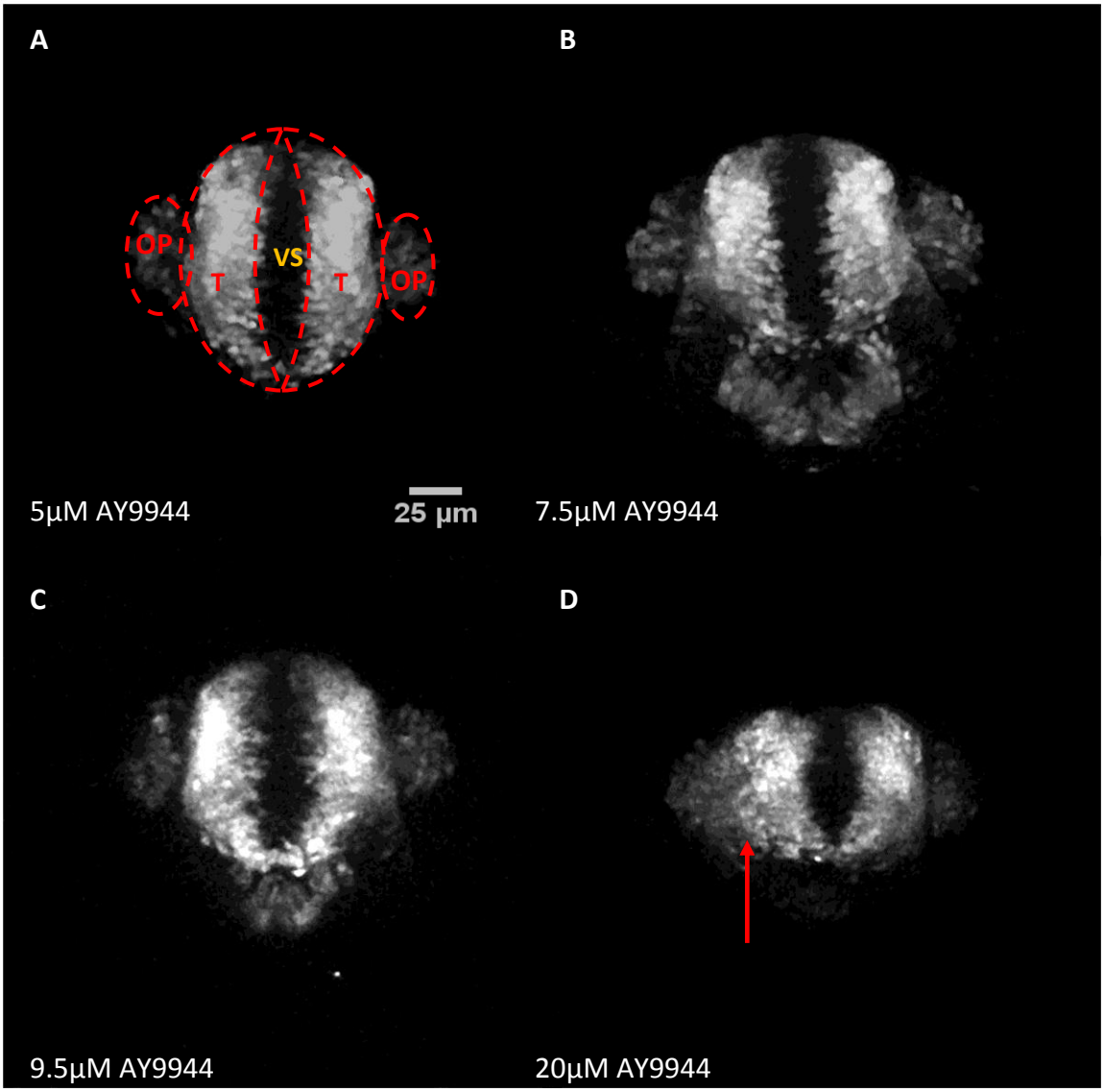

Figure 34 – Investigation of forebrain morphology upon AY9944 treatment.

Panels A-D displays maximum Z projections of confocal images of the frontal view of the forebrain upon varying doses of AY9944 treatment for 24hrs. No striking difference was observed in the telencephalon when embryos were treated with 5µM, 7.5µM, and 9.5µM (A-C). In comparison, the forebrain of embryos treated with 20µM appears to be smaller and displaying ectopic expression of HuC-positive cells outside of the regions of the olfactory placode and telencephalon (D) (red arrow). Red dash outlines the telencephalon (T) and the adjacent olfactory placode (OP)

4.6 Discussion

Through a combination of pharmacologic inhibition and metabolite rescue, this study demonstrates disruption in the HMGCoAR pathway results in a defective forebrain development. It is likely that inhibition of the HMGCoAR pathway disrupts signalling pathways which are instrumental in organising neuronal architecture in the forebrain. In keeping with this, HMGCoAR pathway is also important in other zebrafish developmental processes such as germ cell migration (Thorpe *et al.* 2004), myocardial cell migration (D'Amico *et al.* 2007), cranial vasculature (Eisa-Beygi *et al.* 2012), motor neuron migration (Mapp *et al.* 2011), and oligodendrocyte progenitor cells (Mathews *et al.* 2014).

Certain characteristics of the zebrafish provide an advantage for pharmacological analysis. Zebrafish are DMSO tolerant and readily absorb chemicals through their skin until 12-14 days post fertilisation, where they develop scales (Goldsmith 2004). Additionally, whole population of zebrafish embryos can be immersed in drug-containing solutions, ensuring equal administration.

Embryos treated with Simvastatin and Lovastatin at the beginning of the gastrulation period produced more severe somatic defects than embryos treated with Atorvastatin, a more hydrophobic statin (Figure 23). This has also been identified in other studies (Thorpe *et al.* 2004). One plausible explanation is that different statins have different partition co-efficient values determining the distribution within the body. As a hydrophobic drug, Atorvastain may partition in the yolk, thus limiting its availability within the embryo (Thorpe *et al.* 2004). Another plausible explanation may be that different statins are associated with different ranges of severity of muscle damage in the embryo, thus affecting phenotype. Upon statin treatment we identified ectopic HuC-positive cells amongst the ventricular surface and the boundary domains between the olfactory placode and telencephalon appeared disrupted (Figure 23 and Figure 25). In the forebrain, many neurons differentiate along boundaries, which are defined by the expression domains of various forebrain genes (Macdonald *et al.* 1994), suggesting an importance of boundary domain in telencephalon patterning. Using a novel method of quantifying the forebrain ventricular space, we show a decrease in the lumen between the telencephalic hemispheres upon statin treatment in a dose

dependent manner (Figure 26). During early brain development there is a correlation between the ventricular size and neuronal proliferation in that region, suggesting a reduction in ventricular surface may affects cell proliferation. Moreover, studies in mutants which display a defective cardiovascular system display smaller ventricles (Schier *et al.* 1996). Interestingly, inhibition of the HMGCoAR pathway leads to a phenotype which mimics cerebral cavernous malformation, resulting in cerebral haemorrhaging (Eisa-Beygi *et al.* 2013). It may be interesting to suggest a link between the HMGCoAR pathway, blood flow, and expansion of brain ventricles.

Mouse models that have expansion of dorsal telencephalic markers display defects in telencephalic structures (Martynoga *et al.* 2005). Zebrafish embryos deficient in foxg1, a regulator of telencephalic development, displays an expansion in emx3 expression (Danesin *et al.* 2009). Upon Atorvastatin treatment we identified increased expression of emx3, a homeobox gene which specifies neurons of a dorsal telencephalon fate (Viktorin *et al.* 2009), in the ventricular domain ventricular zone (Figure 27). We speculate that inhibition of HMGCoAR leads to inhibition of downstream genes which may affect pathways involved in boundary formation and/or neurogenesis.

One of the issues when using pharmacological methods is that it is difficult to assess specificity of a particular drug. To address whether the defects were due to specific inhibition of the enzymatic activity of HMGCoAR, we injected embryos with mevalonate, a direct product of HMGCoAR, prior to statin treatments. Mevalonate rescued the statin-induced morphological and telencephalon defects (Figure 28 - 29), suggesting the validity of our approach. We observed upon mevalonate injections alone, 47% of embryos displayed a mild defect (Figure 28). We suggest an accumulation of mevalonate may result in a slight toxic effect in embryos.

We demonstrate statin-induced defects were rescued by downstream prenylation precursors, farnesol and geranylgernaiol (Figure 30). We investigated the prenylation pathway further by inhibiting an enzyme involved in geranylgeranylation. Inhibition of geranylgeranyl transferase I (GGTase I) mimicked the statin-induced forebrain ventricular defects (Figure 32). Unfortunately, we were unable to test the phenotype upon inhibition of farnesyl transferase. Geranylgeranylation is an important pos-

translational modification for the Rho, Rab, and Rap family of GTPases (Rikitake *et al.* 2005). During development, the Rho family of GTPases have been implicated in the developing forebrain. Rac1, a member of the Rho family, is required to maintain proper proliferation and survival of neuronal progenitors in the forebrain (Leone *et al.* 2010). Rac1 deficiency in mouse embryos resulted in an abnormal survival and differentiation of telencephalic neuronal progenitors consequently leading to microcephaly (Chen *et al.* 2009). It is tempting to speculate that the inhibition of GGTase I inhibits downstream post-translational modification of a single and/or combination of the Rho family of GTPases, such as Rac1. The appearance of ectopic telencephalic HuC-positive cells when embryos are treated with HMGCoAR and GGTase I inhibitors may be explained by neural progenitors exiting the cell cycle at an increased rate, progenitors taking a misguided migratory route, or defects in cell polarisation, All of these mechanisms have been shown to be regulated by the Rho family of GTPases (Heasman *et al.* 2008).

We additionally investigated the cholesterol biosynthesis pathway. Upon squalene injections, to increase levels of cholesterol, and zaragozic acid treatment, to inhibit cholesterol production, we found no rescue or induction of telencephalon defects, respectively (Figure 33). To identify a positive control we attempted to replicate developmental malformations, such as partial cyclopia, observed when treating zebrafish embryos with an inhibitor of the 7-dehydrocholesterol reductase, AY9944 (Li *et al.* 2007). Unfortunately, we were unable to replicate this phenotypic assay in our experiments. Although we were unable to observe any partial cyclopia when embryos were treated 20µM of AY9944 for 24hrs, confocal images of the forebrain appeared to be smaller (Figure 34). Interestingly, Smith-Lemli-Opitz syndrome (SLOS) is caused by a deficit in 7-dehydrocholesterol reductase which is characterised by various developmental malformations such as, microcephaly, corpus callosum agenesis, and holoprosencephaly (Roux *et al.* 2000). In particular, holoprosencephly is a common developmental defect of the forebrain which arises due to a failure of the forebrain to cleave along its axis, thus consequently leading to defective patterning (Wallis *et al.* 1999). This suggests an importance of this the 7-dehydrocholesterol reductase enzyme activity during forebrain development. In chick models of SLOS, reducing cellular levels of cholesterol correlates with a decrease in sonic hedgehog (SHH)

signalling, a morphogen central to cell proliferation and differentiation (Cooper *et al.* 2003). Furthermore, developmental studies in mice have suggested a requirement for cholesterol modification of SHH to pattern the telencephalon (Huang *et al.* 2007).

4.7 Future Work

Our studies implicate the mevalonate pathway in telencephalon development. Additionally, we demonstrate that geranylgeranylation is required for proper telencephalon development and correct neuronal organisation. In future work, we would like to identify the downstream targets of the geranylgeranylation process. We speculate that Rac1, a member of the Rho family of GTPases, may be a target of geranylgeranylation and be involved in maintaining correct neuronal patterning in the developing forebrain. Other members of the Rho family of GTPases have also been implicated in neuronal processes, thus these genes can also be tested (Heasman *et al.* 2008). Furthermore we can investigate whether inhibition of HMGCoAR results in defective forebrain neurogenesis by examining proliferative patterns of neuronal progenitors using proliferating cell nuclear antigen, and whether progenitors are exiting the cell cycle early by using 5'bromo-2'-deoxyuridine (BrdU) (Mueller *et al.* 2002). We suggest that inhibition of HMGCoAR results in defective neurogenesis affecting the size of the forebrain ventricular space. It may be interesting to investigate whether statin treatment alters the size of other ventricular spaces, the midbrain and hindbrain.

Unfortunately we were unable to identify a suitable positive control to investigate the cholesterol biosynthesis pathway. Future work may involve employing assays which are sensitive to measuring cholesterol content in embryos such as the Amplex Red Cholesterol Assay Kit (Li et al 2007).

Overall we suggest the HMGCoAR pathway is required for correct forebrain development. Additionally, we demonstrate that the post-translational modification, gernanylgeranylation, is also required to normal neuronal patterning in the telencephalon.

4.8 Supplementary data

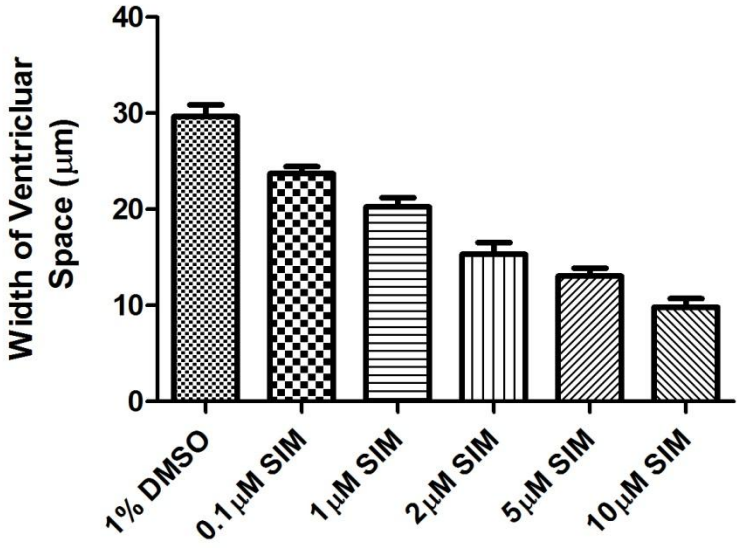

Figure 35 - Pharmacological inhibition of HMGCoAR pathway results in defective forebrain development.

Embryos exposed to varying concentration of SIM at 12hpf for 18 hrs. Embryos display a dose dependent decrease in the ventricular space. n=50 in each treatment group.

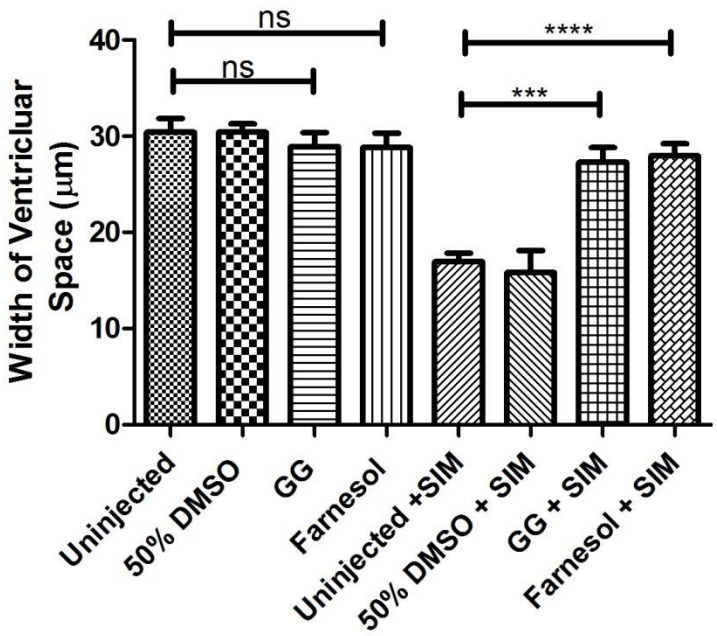

Figure 36 - The isoprenoid pathway plays a role in forebrain development

Width of ventricular space analysed in control and experimental groups, n=10 in each group*, p* > 0.05.

CHAPTER 5

ROLE OF FE65 PROTEINS IN NEURONAL DEVELOPMENT

5.1 Abstract

Amyloid precursor protein (APP) has a central role in Alzheimer's disease, but the physiological functions of the protein remains to be fully elucidated. A vast amount of literature has been focused on investigating altered Aβ production, a product derived from APP due to cleavage events. A second product, APP intracellular domain (AICD), generated simultaneously with Aβ can bind to adaptor proteins such as FE65. The FE65/AICD complex has been shown to be present in the nucleus. Additionally, this complex has been shown to participate in nuclear signalling events through the interaction of FE65 and a number of nuclear proteins such as, Tip60, a histone acetlytrasferase. Recently, it has been suggested that AICD fragments participate in p53-dependant pro-apoptotic pathways, and that p53 may be a target for the AICD/FE65/Tip60 complex. Mouse models have implicated FE65 in basement membrane assembly, neuronal migration, and patterning of the cortex, thus highlighting its importance in development. We therefore hypothesised that FE65 maintains integrity of the basement membrane in the zebrafish, and loss of function will disrupt neuronal development. We investigated the effect of FE65 knock down using morpholino antisense oligonucleotides targeted to block splicing and translation. We show that both FE65 splice and translation blocking morphants display defects in neuronal specification and axonal projection in the forebrain which can be rescued by knocking down p53, suggesting that p53 may be a downstream target of FE65 signalling.

5.2 Introduction

5.2.1 The FE65 family

The FE65 family of adaptor proteins compromises of FE65, FE65L1, FE65L2 located on chromosome 11, 4, and 5 in humans, respectively (Bressler *et al.* 1996; Blanco *et al.* 1998), (Tanahashi *et al.* 1999). Structurally these adaptor proteins all have 3 structural domains; one WW domain and two phosphotyrosine binding (PTB) domains (McLoughlin *et al.* 2008).

Tissue specificity of FE65 gene expression differs between the family members. FE65 is predominantly expressed in the brain, whereas FE65L1 and FE65L2 have ubiquitous expression (Duilio *et al.* 1998). Interestingly, FE65 is detected in the hippocampus of the mouse brain, a region which is affected by Alzheimer's disease (AD). Additionally, FE65 can exist as two isoforms; the full length transcript (p75) and the shorter transcript (p60) (Wang *et al.* 2004).

APP is a transmembrane protein which undergoes sequential cleavage to generate Aβ isoforms, the primary component identified in amyloid plaques in Alzheimer's disease. Amongst Aβ fragments, the cleavage process also generates the APP intracellular domain (AICD), which harbours a –YENPTY- motif, recognised by a variety of proteins. One family of proteins which recognise this motif is the FE65 adaptor proteins (Borg *et al.* 1996) and this interaction has been shown to stimulate nuclear (Cao *et al.* 2001). An important residue regulating the interaction between FE65 and AICD is thought to be Thr-668, located near the YENPTY motif (Ando *et al.* 2001). Mutant forms of the cytoplasmic tail of APP abolished binding with FE65 and results in nuclear localisation of FE65, suggesting that FE65 translocates to the cell surface where APP is expressed to form the FE65/AICD complex (Cao *et al.* 2001). There are many FE65-AICD complex-binding proteins complex (Figure 37). Some of the identified transcriptional targets of the AICD/FE65 pathway are BACE, TIP60, GSK3β, and APP. Thus regulating a variety of processes required in development, such as cell movement, cellular response to DNA damage, and nuclear transcription (von Rotz *et al.* 2004; Minopoli *et al.* 2007).

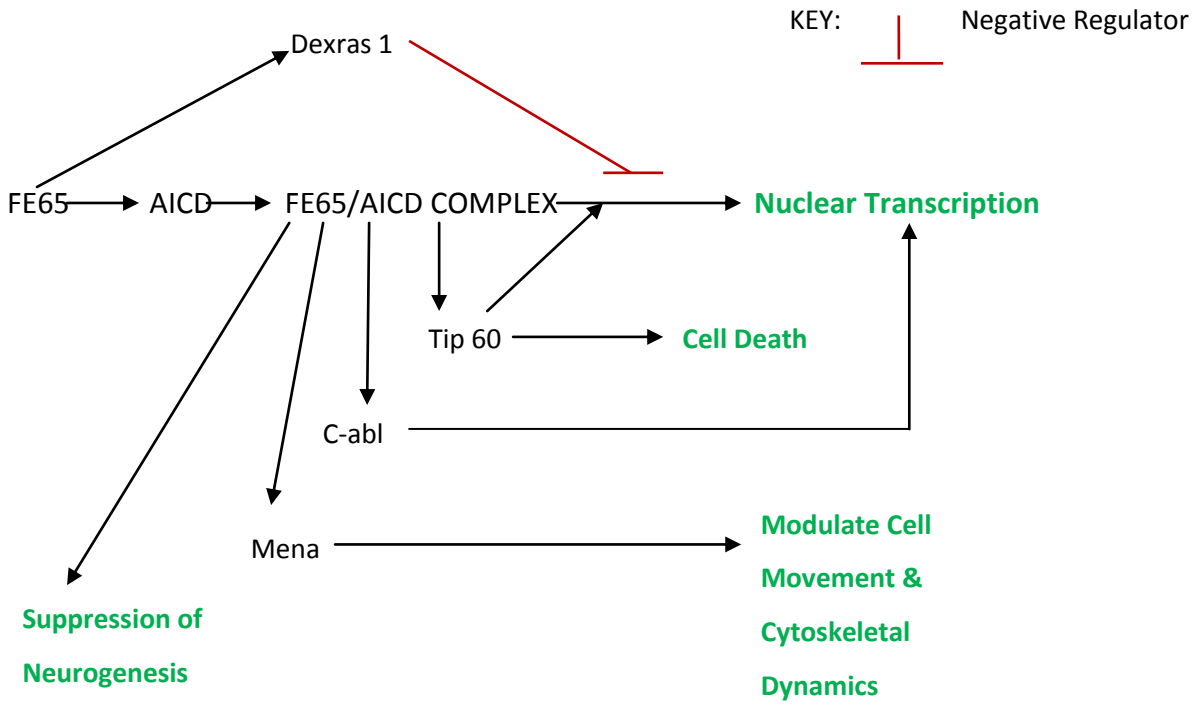

Figure 37 – A schematic representation of the FE65/AICD binding partners and the importance their pathways have on various cellular processes.

5.2.2 The role of FE65 in neuronal development

Many studies have focussed their attention on understanding the function of the APP binding partner, FE65. Immuflourescence have shown localisation of APP and FE65 in the actin-rich lamellipodia of growth cones and interaction within the nerve terminals (Sabo *et al.* 2001). Recently, it has been shown that FE65 colocalises and interacts with the small GTPase ADP ribosylation factor 6 (ARF6) in growth cones. The binding of FE65 with ARF6 induces Rac1, a downstream signalling factor known to play a role in actin dynamics (Cheung *et al.* 2014). These studies suggest an involvement of FE65 in dynamic processes such as neurite growth and synaptogenesis. A mouse model of an isoform-specific knockout of FE65, lacking the p75 isoform, display defects in learning and memory, processes dependent on the hippocampus (Wang *et al*. 2004). FE65 and FE65L1 double knockout mice display cortical heterotopias (Guenette *et al.* 2006), a phenotype resembling the triple APP knockout mice (Herms *et al.* 2004). The FE65

double mutant mice also display altered laminin organisation, disrupted axonal projections, and aberrant neuronal positioning. Studies have also revealed a role for FE65 in neurogenesis of gonadotrophin-releasing hormone-1 (GnRH-1). Analysis of GnRH-1 neurons showed a 25% increase during development in the absence of a functional WW domain. Further tracking of the GnRH-1 cell precursors showed cells had an extended timing for neurogenesis to occur in the developing nasal placode (Forni *et al.* 2011).

5.2.3 Studying Alzheimer's disease using the zebrafish embryo

As a result of gene duplication during evolution (Lee *et al.* 2007), the zebrafish harbours two APP genes (*appa* and *appb*). At 24hr post fertilisation, both genes are expressed in the telencephalon, regions of the diencephalon, and the trigeminal ganglia (Musa *et al.* 2001). There is approximately 70% amino acid identity between the human APP_{695} and the zebrafish *appa*. Studies have employed the zebrafish *appb* promoter to express GFP. This transgenic model can be further used to investigate mechanisms which regulate APP expression during development (Lee *et al*. 2007). Knockdown of appa and appb function in the zebrafish results in a defective convergent-extension, a phenotype displaying a shortened body axis and a short and curly tail. Migration of cells is a key mechanism to allow for elongation of anterior-posterior axis. These defects were rescued upon injections with human APP_{695}. These data suggest APP may have a role in cell migration during development, similar to the phenomenon observed in mouse models (Joshi *et al.* 2009). Knockdown of *appb* displayed defects in embryonic development which manifested in curly tails and atrophy in the midbrain. Additionally, *appb* morphants showed defective axonal projections of facial branchiomotor neurons and spinal motor neurons (Song *et al.* 2012). *Appb* morphants have additionally been shown to have a behavioural phenotype with an increased touch-induced activity. In the morphants spinal motor neurons display density changed in synapses at the neuromuscular junction (Abramsson *et al.* 2013). These data suggests a critical role of APPb in spinal motor neuron development.

Zebrafish orthologues of FE65 (ZfFE65, ZfFE65L1, and ZfFE65L2) have been identified to be expressed ubiquitously in the nervous system during development. As FE65 has been shown to play roles in neuronal development, we chose to utilise the zebrafish, as a powerful vertebrate model, to investigate the effects of FE65 knockdown in the zebrafish. Currently, there is no literature on the function of FE65 in the zebrafish animal model.

5.3 Optimisation of FE65 antisense morpholino oligonucleotide injections

Optimisation experiments were carried out for the FE65 translation blocking and splice blocking morpholinos (MO) (Table 14 and 15). Furthermore RT-PCR analysis was carried out on a range of splice morpholino doses (Figure 36). Doses of 0.5 pmol for the translation blocking morpholino, and 0.9 pmol for the splice blocking morpholino were chosen as these concentrations resulted in a consistent defective forebrain phenotype with a high survival rate (Table 15 and 16). Splice MOs were designed by GeneTools to cause mis-splicing of exon 7-8 in zebrafish *FE65*. By targeting the exon7intron7 boundary in the pre-mRNA, the most likely outcome would be an exon skip of exon 7. RT-PCR analysis (Figure38) suggests that the most abundant *FE65* mRNA splice variant is absent in embryos injected with 0.6 pmol and 0.9 pmol of the spliceMO. The absence of *FE65* in embryos treated with 0.6pmol and 0.9pmol splice MO is not due to an exon skip. An exon skip of exon 7 would produce a smaller sized product of 288bp which would be observed on the RT-PCR. Occasionally, cryptic splice sites can be activated which can lead to partial insertions or partial deletions. We considered that the absence of *FE65* may be due an activation of a cryptic splice site in the inton thus maybe leading to an intron inclusion. We designed primers within the intron, but unfortunately we did not find evidence for intron inclusion. The FE65 antibody has been previously been shown to have strong specificity in the mouse brain (Guenette *et al.* 2006). We attempted to validate the efficiency of the translation blocking MO by using the antibody for western blotting, but unfortunately we were unable to detect endogenous FE65 protein using zebrafish antibodies. It may be possible that specificity of the FE65 antibody may change when using the zebrafish as a model.

We carried out preliminary staining of HuC in embryos treated with 0.9 pmol and 0.6 pmol of the splice MO. Preliminary staining showed that there was a slightly more defective HuC patterning in the forebrain of embryos injected with 0.9pmol than embryos injected with 0.6pmol of the splice MO. Studies have suggested the use of morpholinos can be toxic in embryos, thus activating the p53 pathway (Robu *et al.* 2007). Embryos injected with 0.6 pmol of the control morpholino (COMO) were co-

injected with double the dose of the p53 morpholino (1.2 pmol) to confirm that embryos deficient in p53 were morphologically indistinguishable from uninjected embryos, thus confirming that knock down of p53 is not toxic. 0.5 pmol doses of the translation blocking morpholino were also co-injected with double the dose of COMO and p53 (1 pmol). 0.9 pmol doses of the splice morpholino were co-injected with the same amount of COMO and p53 (0.9 pmol), as optimising experiments with control morpholino (at 2.7 pmol) displayed non-specific, toxic effects.

We categorised phenotypes into three morphologies, normal, moderate, and necrotic (Figure 39A, 39B). A moderate phenotype defect was determined by overall body axis, somite development, and clear appearance of brain structures such as the cerebellum and the otic vesicle. Necrosis was determined by severe abnormality in development, resulting in a ball shaped embryo mass. At 30hpf, 100 embryos across 3 batches of injections were scored on the basis of their phenotype. Control treatments, embryos co-injected with p53 and COMO and uninjected embryos, result in a predominant normal phenotype as expected (Figure 39C, 39D). Upon co-injection of FE65sp/COMO and FE65atg/COMO we observed a high percentage of embryos with moderate phenotypic defect. Co-injection of splice MO with p53 morpholino embryos appeared to display a partial rescue of phenotypic defects, suggesting this defect is apoptosis dependent.

Table 15 – Optimisation FE65 translational blocking morpholino

Treatment	Number of embryos injected	Number of embryos that survived	Morphology
0.6pmol FE65atg + 1.2pmol Como	46	15	Severe necrosis in the brain and tail, CNS structures not visible. Developed only to mid-somite stage.
0.6pmol FE65atg + 1.2pmol p53	44	19	Severe necrosis in the embryo, tail not developed.
0.5pmol FE65atg + 1pmol Como	**54**	**44**	**Embryos display a flattened and underdeveloped brain. Cerebellum and otic vesicle structures were visible, reduced body axis of embryos.**
0.5pmol FE65atg + 1pmol p53	**64**	**50**	**Defective brain phenotype is rescued by suppression of p53 expression. Embryos appear to have normal brain phenotype. 27 embryos developed with curly tail.**
0.4pmol FE65atg + 0.8pmol Como	49	40	Similar phenotype to 0.5 pmol, flattened brain with reduced body axis.
0.4pmol FE65atg + 0.8pmol p53	53	46	Strong rescue of the defective brain phenotype
0.3pmol FE65atg + 0.6pmol Como	37	32	Mild phenotype, increased number of embryos which display normal phenotype
0.3pmol FE65atg + 0.6pmol p53	42	36	All embryos display normal phenotype

Table 16 – Optimisation of FE65 splice blocking morpholino

Treatment	Number of embryos injected	Number of embryos that survived	Morphology
0.1 FE65sp (7-8)	49	42	Embryos appear phenotypically normal, and brain morphology appears normal
0.3 FE65sp (7-8)	44	39	Normal phenotype, brain morphology appears to be normal, CNS structures clearly visible.
0.6 FE65sp (7-8)	42	35	20 embryos appear to have normal phenotype, 15 appear to have flattened, smaller brain
0.9 FE65sp (7-8)	**47**	**37**	**Consistent phenotype, all embryos have flattened, smaller brains. Embryos display reduced motility**

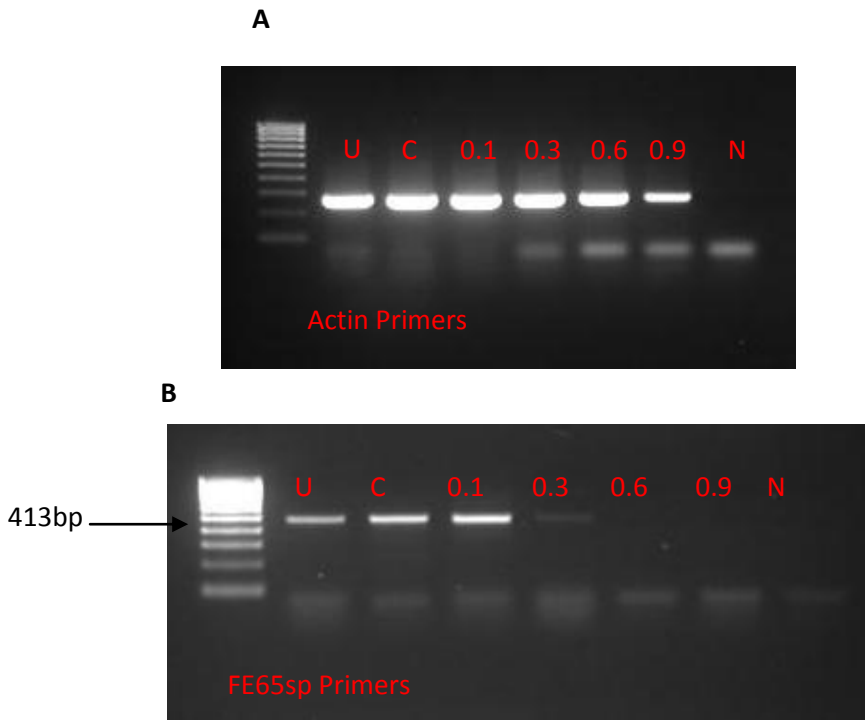

Figure 38 - Efficiency of the FE65 splice morpholino targeted for against exon 7-8.

Zebrafish embryos were injected with a range of FE65 splice morpholino doses and RT-PCR was carried out to assess the efficiency of the splice morpholino. Doses were tested using control actin primers (A) and FE65 splice primers (B). An expected band was observed in all samples when using the actin primers, except the sample with no template (N, which was expected). An expected product size of 413bp was evident in the uninjected, control, 0.1 pmol, and 0.3 pmol of the splice morpholino (B). At 0.3 pmol of the splice morpholino the intensity of the product band is significantly reduced. Furthermore, samples of the 0.6 pmol and 0.9 pmol have absent product bands, suggestive that FE65 mRNA is incorrectly processed. The expected band product of 213bp to show splicing at exon 7-8 was not observed at any dose. No product band was observed in the no template (N) control as expected.

Abbreviations : U- uninjected, C- Control doses (0.9 pmol of the splice MO and 0.9 of the p53 MO), 0.1 – 0.1 pmol of the splice MO, 0.3 – 0.3 pmol of the splice MO, 0.6 – 0.6 pmol of the splice MO, 0.9 – 0.9 pmol of the splice MO, and N – No cDNA template.

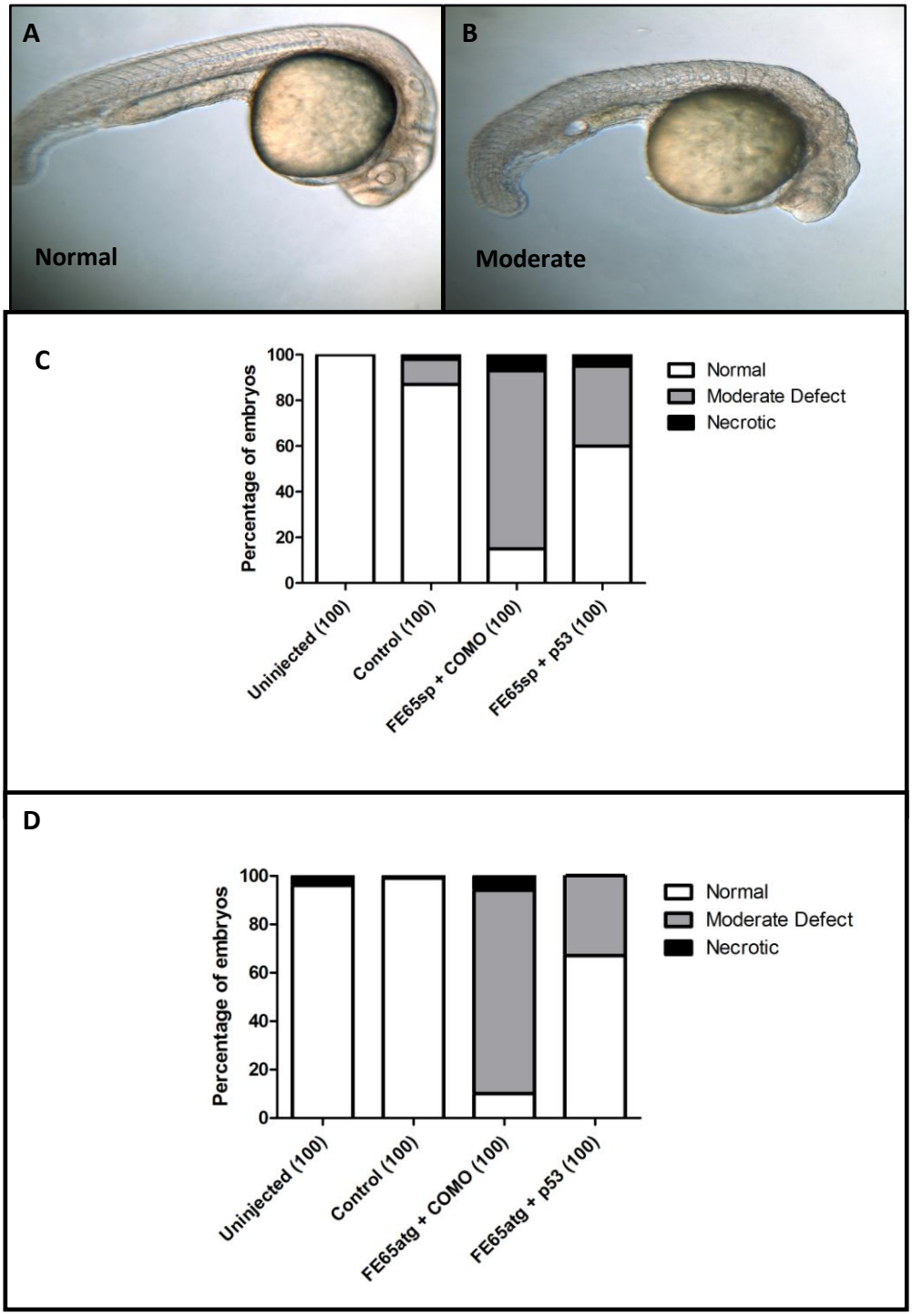

Figure 39 – Morpholino-mediated knockdown of FE65 results in a morphological defect in embryos at 30hpf

Representative brightfield images classifying normal and moderate phenotypes (A and B). FE65 splice and translation-blocking morpholinos show 78% and 84%, respectively, of embryos which display a moderate morphological defect (C and D). A partial phenotypic rescue can be observed with co-injection of p53. n=100 in each treatment group.

5.4 Morpholino mediated knockdown of FE65 leads to a defective production of post-mitotic neurons and axonal projections in the zebrafish forebrain.

In mouse studies, FE65 has been implicated in various neuronal processes in the developing cortex such as neuronal positioning, axonal branching, and maintaining the basement membrane (Guenette *et al.* 2006). We hypothesised that loss of FE65 function would disrupt integrity of the basement membrane and consequently affect neuronal development. This prompted an investigation of whether loss of FE65 function in the zebrafish embryo affected specification of differentiated neurons. Analysis of HuC expressing cells was carried out by immunohistochemistry using an anti-HuC antibody in wild-type, control, and morphant embryos. The percentage of embryos displaying defective staining of HuC-positive cells in the telencephalon and tail at 24hpf, 30hpf, and 36hpf upon injection treatments are documentated (Tables 17 and 18). At 30hpf, 100 embryos/ 4 batches of injections were scored on their neuronal patterning in the telencephalon and tail. Upon FE65 knockdown there is a significant increase of percentage of embryos which have defective neuronal patterning in the forebrain. Fe65 knockdown using splice or translation blocking morpholino result in 85% and 78%, respectively, of embryos with defective telencephalon patterning compared to control treatments. Consistently, the percentage of embryos with gross morphological defects is significantly increased when FE65 is knocked down compared with control batches. Neuronal patterning of the forebrain at 24hpf and 36hpf were also characterised. The data suggests that embryos at 24hpf and 36hpf show a similar trend to the 30hpf embryos; that there is an increase in the percentage of embryos with a defective neuronal population in the telencephalon when FE65 is knocked down (at 24hpf n=28, 94% for translation blocking morphants, at 36hpf n=20, 100% for translation blocking morphants, at 36hpf n=50, 96% for splice blocking morphants, compared with embryos co-injected with COMO/p53 and uninjected embryos.

In uninjected and COMO/p53 co-injected embryos there is a prominent HuC expression in the dorsal and ventral telencephalon, and in the olfactory placodes, which lie adjacent to the telencephalon (Figure 40A, B and Figure 41A, B)). In some

embryos post-mitotic neurons can also be observed towards the diencephalon, which are thought to project the diencephalic dorsoventral tracts (Chitnis *et al.* 1990). Upon *FE65* knockdown the boundary between the telencephalon and olfactory placode is lost at 30hpf (Figure 40D, Figure 41D). One can observe anterior telecephalic neurons present in the correct location, but the remaining neuronal cells which form the telencephalon appear to be absent. Both splice and translation blocking morphants display mislocalised ventral ectopic cells, suggesting a role for Fe65 in post-mitotic neuronal migration. The anterior view of the forebrain of the translation blocking morphant displays ectopic HuC-positive cells localised within the ventricular space (Figure 41D). This defective HuC patterninig is also evident at 36hpf in morpahnts (Figure 42A, B). Further staining of these sections with specific markers is required to determine whether the ectopic cells observed are telencephalic or of an olfactory fate. Individual ectopic neuronal cells in the telencephalon were counted using the compound microscope at 36hpf in embryos injected with *FE65* splice blocking MO (Figure 42C). In each batch, ectopic cells were counted in 10 individual embryos and the mean number upon different treamtments was taken. Co-injection of embryos with 0.9 pmol of the FE65 splice blocking morpholino/COMO resulted in a significant increase of individual ectopic cells (n=10, m=20.3), compared with the uninjected (n=10, mean=2.1) and embryos injected with COMO/p53 (n=10, mean=1.8). Interestingly co-injecting embryos with *FE65* translation blocking morpholino and p53 dramatically decreased the number of neuronal cells which can be counted (n=10, mean=2.4). We were unable to quantify the total neuronal number in the telencephalon upon different treatments, as neuronal density was far too great to count individual nuclei under the compound microscope. Utilising a GFP-HuC transgenic line may be able to overcome this problem as neuronal cells migrating to their destination can be quantified under the confocal microscope. In both translation and splice blocking morphants, embryos display a defective production of post-mitotic neuronal cells and aberrant localisation neural cells, consistent with the hypothesis that FE65 may have a role in basement membrane assembly. Further experiments will elucidate whether the mechanism underlying the defective neuronal specification observed is due to ectopic neuronal proliferation, abnormal neurogenesis, or cell death.

FE65/FE65L1 null mouse model show abnormal axonal trajectories in the cortex (Guenette *et al.* 2006), thus we further analysed axonal projections in *FE65* morphants. Using fluorescent immunohistochemistry we stained control and FE65 splice morphants with antibodies against acetylated tubulin. Control embryos appear to have normal projections of the olfactory nerve (Figure 43). Upon FE65 morpholino injection, morphants display defects in the axonal projections of the olfactory nerve (Figure 41D), suggesting that FE65 may function in maintaining axonal projections in the zebrafish embryo. In keeping with this, *FE65* morphants show defective HuC-positive patterning in the olfactory placode. We suggest a plausible role of FE65 in olfactory development.

In comparison to knockdown of FE65 alone, suppression of p53 and FE65 together resulted in a dramatic decrease of embryos with defective neuronal patterning in the (Table 16 and 17) Furthermore, there was a partial rescue of neuronal patterning cells in the forebrain when expression of p53 and FE65 are suppressed at 30hpf and 36hpf (Figure 40, Figure 41, amd Figure 42). With this, the acetylated tubulin staining pattern of the olfactory nerve also appears to be rescued (Figure 43). Taken together, these results suggest that FE65 and p53 may function in a common molecular pathway. Importantly, the p53 rescue is observed at all time points with both the translation and splice blocking morpholinos, suggesting this may be a specific effect, rather than a non-specific effect of morpholinos. Further mRNA rescue experiments would have to be performed to elucidate conclusive results.

Table 17 – Quantification of defective phenotype and post-mitotic neuronal expression in embryos using the FE65 splice blocking MO

Age	Treatment	n	Defective neuronal population in the telencephalon	Phenotype
30hpf	Uninjected	100	0%	100% normal
	0.9 pmol COMO +0.9 pmol p53	100	11%	87% normal, 11% moderate 2% necrotic
	0.9 pmol FE65sp + 0.9 pmol COMO	100	85%	15% normal, 78% moderate, 7% necrotic
	0.9 pmol FE65sp + 0.9 pmol p53	100	30%	60% normal, 35% moderate, 5% necrotic
36hpf	Uninjected	50	0%	100% normal
	0.9 pmol COMO + 0.9 pmol p53	50	4%	100% normal,
	0.9 pmol FE65sp + 0.9 pmol COMO	50	96%	4% normal, 96% moderate
	0.9 pmol FE65sp +0.9 pmol p53	50	16%	78% normal 22% moderate

Table 18 – Quantification of defective phenotype and post-mitotic neuronal expression in embryos using the FE65 translation blocking MO

Age	Treatment	n	Defective neuronal population in the telencephalon	Phenotype
24hpf	Uninjected	38	0%	100% normal
	0.6 pmol COMO +1.2 pmol p53	24	17%	83% normal 17% moderate
	0.5 pmol FE65atg + 1 pmol COMO	28	94%	6% normal 94% moderate
	0.5 pmol FE65atg + 1 pmol p53	25	16%	68% normal, 32% moderate
30hpf	Uninjected	100	0%	100% normal 4% necrotic
	0.6 pmol COMO + 1.2 pmol p53	100	6%	99% normal 1% moderate
	0.5 pmol FE65atg + 1 pmol COMO	100	78%	10% normal, 84% moderate, 6% necrotic
	0.5 pmol FE65atg +1 pmol p53	100	38%	67% normal 38% moderate 5% necrotic
36hpf	Uninjected	35	3%	97% normal 3% moderate
	0.6 pmol COMO + 1.2 pmol p53	20	0%	100% normal

0.5 pmol FE65atg + 1 pmol COMO	20	100%	85% moderate 15% abnormal
0.5 pmol FE65atg + 1 pmol p53	38	0%	100% normal

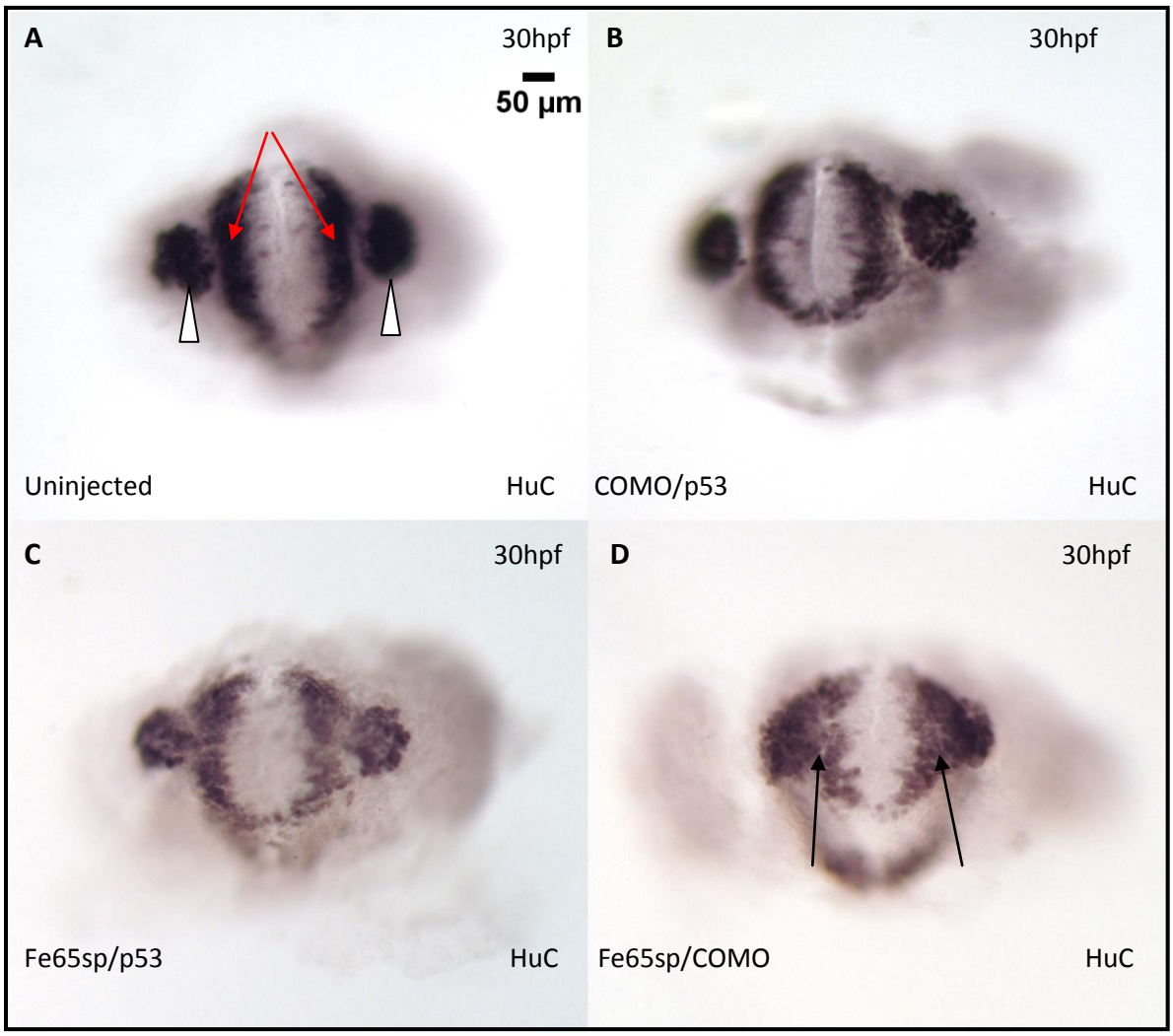

Figure 40 –Splice morpholino (MO)-mediated knockdown of FE65 results in defective patterninig of post-mitotic neurons at 30hpf

Images are of frontal views of the telencephalon stained using an anti-HuC antibody. Uninjected embryos (A) and control embryos (COMO/p53) (B) display a normal post-mitotic neuronal patterning in the telencephalon (red arrow) and olfactory placodes (white arrowhead). Boundary between the olfactory placode and telencephalon is lost in *FE65* morphants (D) (black arrow). Upon co-injection of splice MO and p53 a parital rescue of neuronal patterning can be observed in the forebrain (C).

Abbreviations: FE65sp – FE65 splice blocking MO, FE65atg – FE65 translation blocking MO

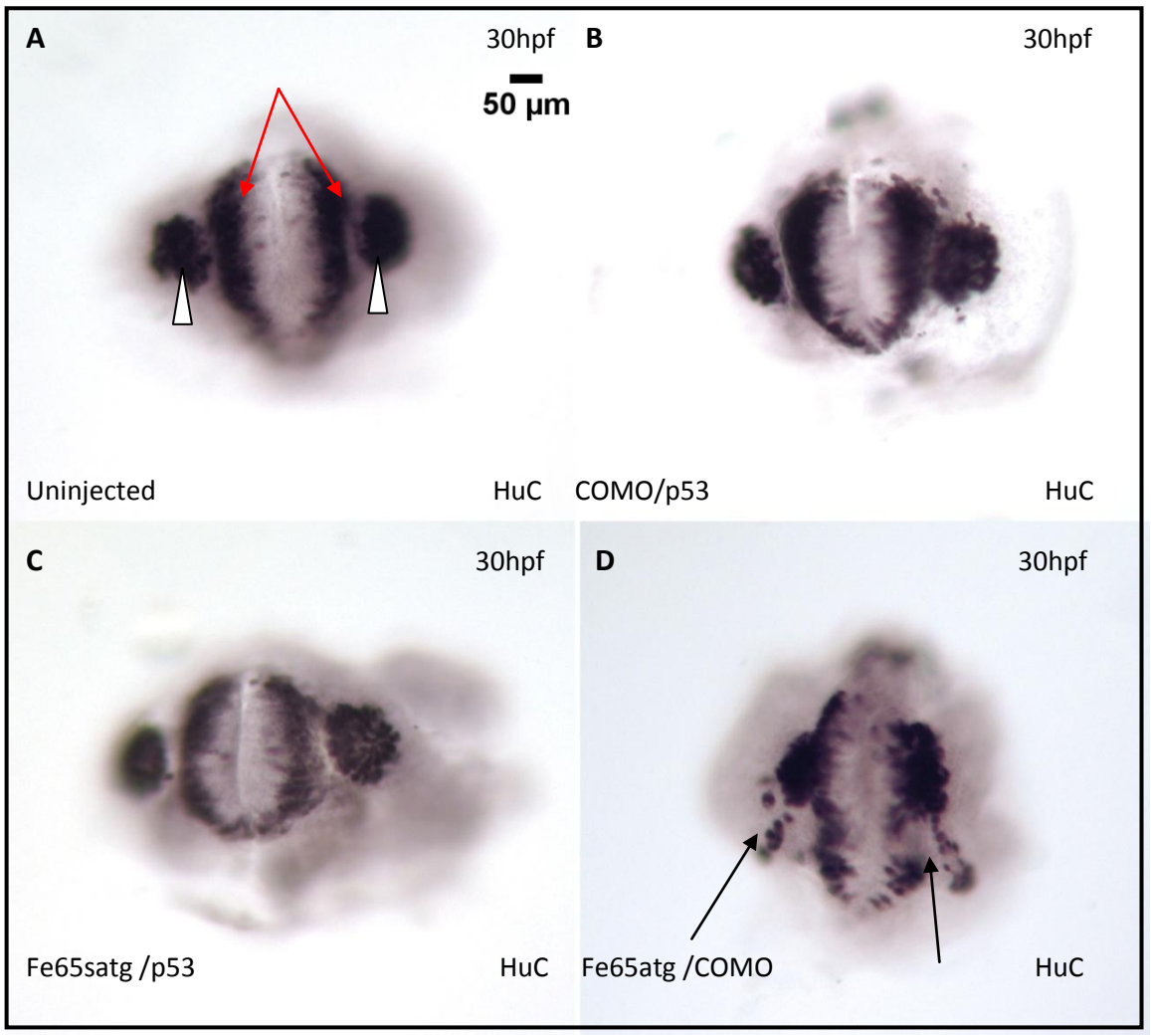

Figure 41 –Translation blocking morpholino (MO)-mediated knockdown of FE65 results in defective patterning of post-mitotic neurons.

Images are of frontal views of the telencephalon stained using an anti-HuC antibody. Uninjected embryos (A) and control embryos (COMO/p53) (B) display a normal post-mitotic neuronal patterning in the telencephalon (red arrow) and olfactory placodes (white arrowhead). Boundary between the olfactory placode and telencephalon is lost in *FE65* morphants and ectopic HuC-positive cells are localised ventrally (D) (black arrows). Upon co-injection of splice MO and p53 a rescue of neuronal patterning can be observed in the forebrain (C).

Abbreviations: FE65sp – FE65 splice blocking MO, FE65atg – FE65 translation blocking MO

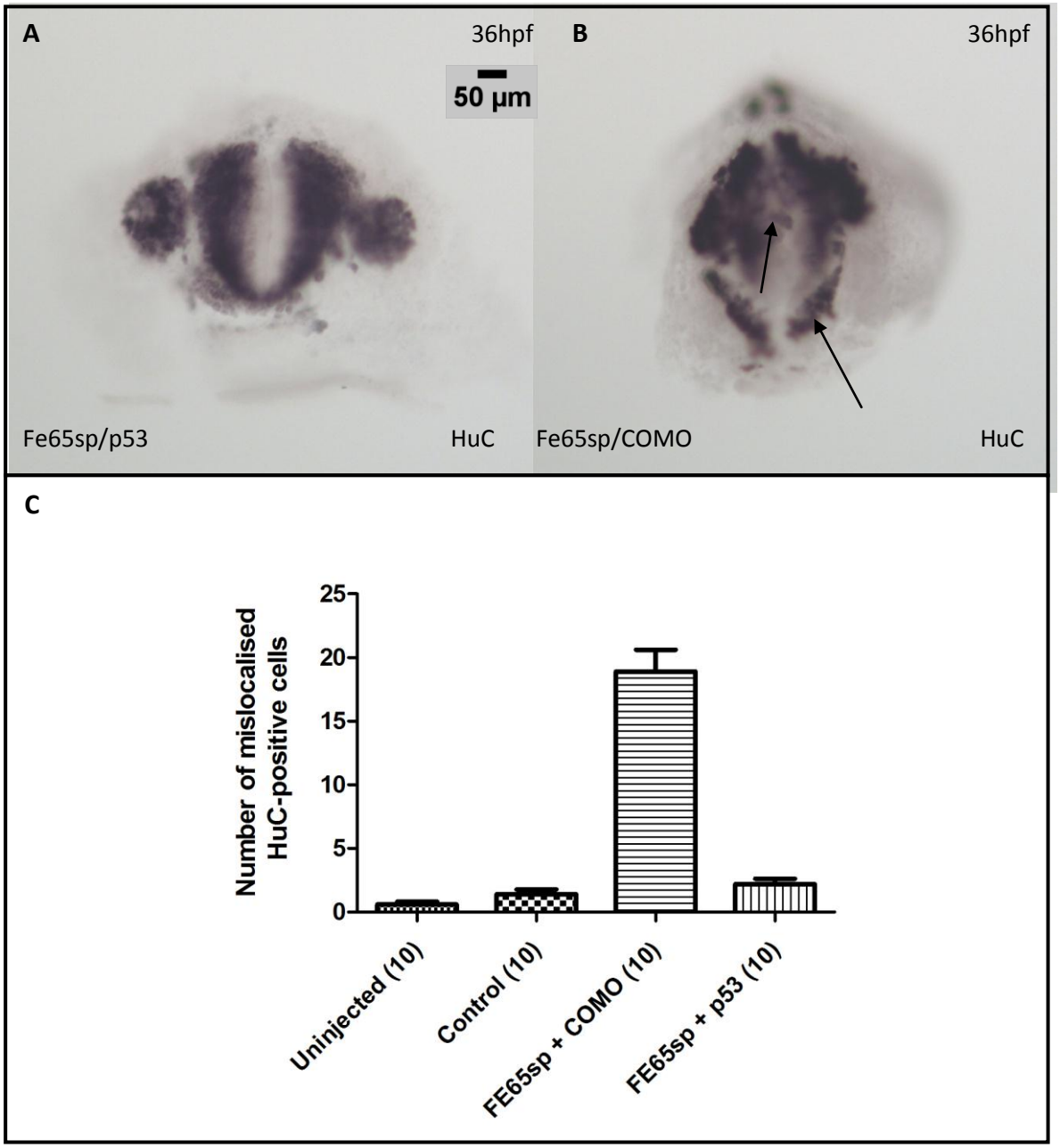

Figure 42 –Splice blocking morpholino (MO)-mediated knockdown of FE65 results in defective patterning of post-mitotic neurons at 36hpf.

Images are of frontal views of the telencephalon stained using an anti-HuC antibody (A and B). FE65 knockdown mediated by the splice MO drastically changes forebrain patternining with the appearance of mislocalised HuC-positive cells ventrally and within the ventricular surface (B, black arrows). Image C displays a graph representing the number of ectopic neurons in treatment groups at 36hpf. There is an increase in ectopic HuC-positive cells in *FE65* morphants, which appears rescued when p53 gene is knocked down. Values are given as mean cell count ± standard error of mean (S.E.M), n=10 in each treatment group, $p > 0.05$.

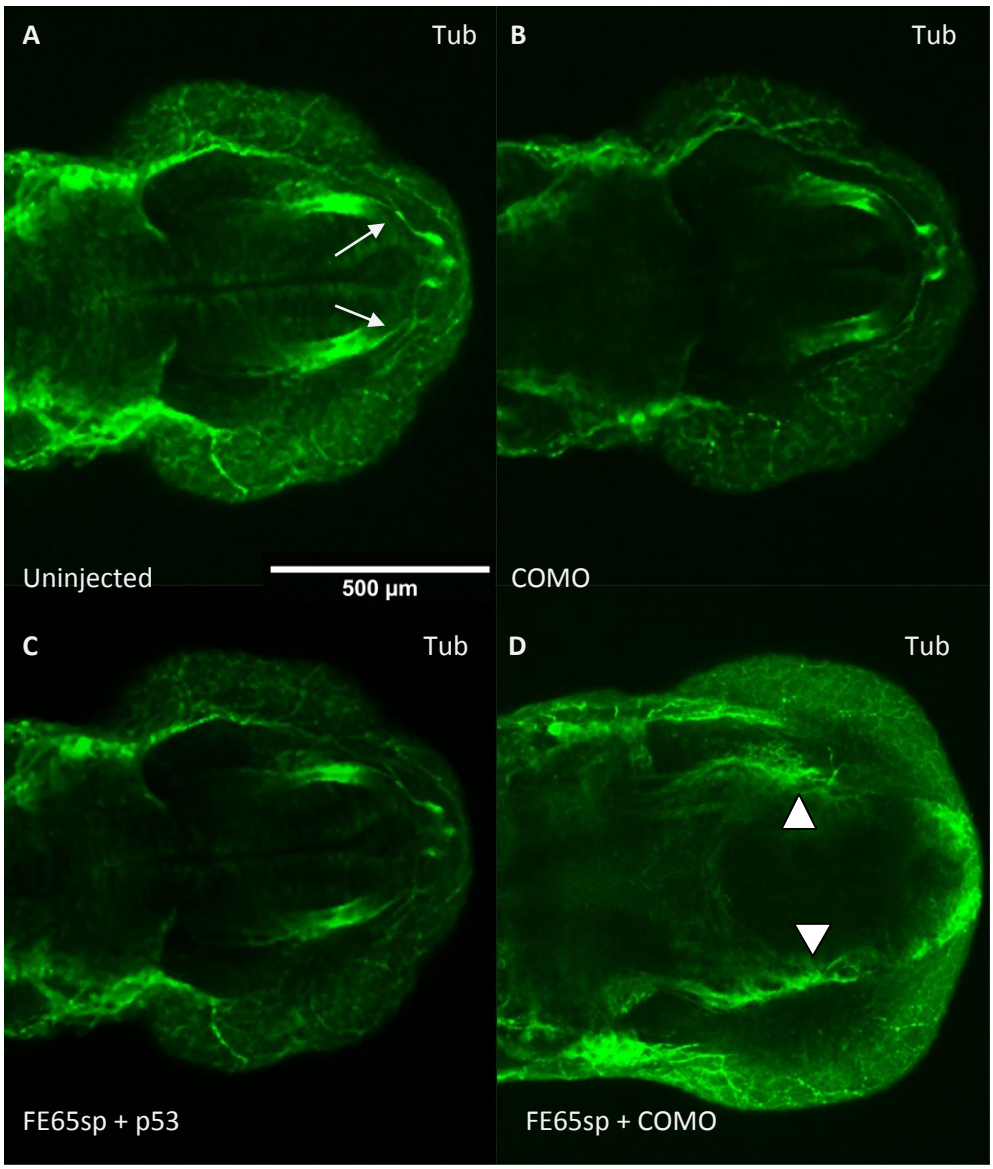

Figure 43 – Morpholino-mediated knockdown of FE65 results in defective axonal projections at 36hpf.

Images represent a maximum z projection stack of embryos immunostained with anti-acetylated α tubulin at 36hpf. Anti-acetylated α tubulin staining of the brain in control treated embryos showed normal axonal projection of the olfactory nerve (ofn) (white arrow) in the forebrain (A - C). Knockdown of FE65 using splice MO causes scaffolding defects in the ofn (D, white arrowhead).

5.5 Discussion

The main pathogenic event in Alzheimer's disease is the deposition of Aβ peptide in the brain. The APP protein undergoes intricate cleavage events by secretases to produce Aβ, and it is believed that altered processing events result in an upregulation of Aβ production (Van Vickle *et al.* 2007). A second product of the APP processing event is the AICD, which is simultaneously generated with Aβ. This processing event is highly similar to the cleavage of the notch signalling protein which releases the NICD (Struhl *et al.* 1999), which has been implicated in playing a role in nuclear signalling events (Buoso *et al.*). One hypothesis is that AICD fragments, like NICD fragments, participate in nuclear signalling events. The AICD has been shown to interact with various proteins, in particular the FE65 family (Borg *et al.* 1996). The AICD/FE65 complex has been further shown to interact with nuclear proteins such as Tip60 (Cao *et al.* 2001), c-abl (Perkinton *et al.* 2004), and mena (Sabo *et al.* 2001) to aid signalling events. In mouse models, FE65 has been shown to play a role in maintaining the basement membrane, axonal projections, and neuronal migration (Guenette *et al.* 2006). Additionally, it has been suggested that FE65/AICD/Mena participate in cell migration events (Sabo *et al.* 2001), suggesting an important role for FE65 in mammalian brain development. We hypothesised that a loss of FE65 function would result in an abnormal brain development in the zebrafish embryo.

In the mouse cortex FE65 is detected primarily in the hippocampus and the thalamus (Kesavapany *et al.* 2002). In the zebrafish embryo, FE65 expression can be identified in post mitotic neurons by 48hpf. Early FE65 expression can be detected during somitogenesis (14hpf -18hpf), suggesting a role in neuronal specification (Mahmood Q, MSc thesis, 2007). FE65 proteins have been suggested to play roles in CNS development such as projection of neurites and neuronal migration (Guenette *et al.* 2006). We investigated the effects of FE65 knockdown on neuronal specification in the telencephalon. At 30hpf neuronal loss can be observed in the FE65 translation and splice blocking morphants, as they display a reduced neuronal population as well as ectopic neurons, suggesting a role for FE65 in maintaining correct telencephalic patterning. Interestingly, the defective forebrain patternining observed in *FE65* morphants resemble the phenotype observed in laminin 1β mutants, which strengthens our belief that FE65 plays a role in basement membrane intergrity. In

keeping with this FE65 double knockout mice laminin expression was significantly reduced (Guenette *et al.* 2006), suggesting there may be a functional link between FE65 and laminin signalling. FE65 interacts with APP and Mena to form a complex which regulates cell movement (Sabo *et al.* 2001). We show ectopic HuC positive cells ventrally located in the forebrain of *FE65* morphants. Another possible explanation to the occurrence of ectopic cells may be due to defects in cell movement.

Mice deficient in the p75 FE65 isoform display impaired nuclear signalling which consequently result in learning and memory deficits (Cool *et al.* 2010). Our zebrafish model displays abnormalities in the development of forebrain structures. One can hypothesise that neuroanatomical abnormalities may lead to impaired nuclear signalling, thus consequently leading to and learning and memory deficits. The olfactory nerve originates in the olfactory placode and projects to the dorsal telencephalon (Wilson *et al.* 1990). Upon knocking down of FE65 we observed a defect in the development of the olfactory placode and axonal projections of the olfactory nerve in embryos at 36hpf, suggesting that FE65 may be involved in a process which regulates olfactory development. Interestingly, knockdown FE65 mouse models displayed abnormal neurogenesis of gonadotrophin-releasing hormone-1 (GnRH-1) neurons which originate in the developing olfactory placode (Forni *et al*. 2011), suggesting a link between FE65 and the developing olfactory placode. Abnormal axonal trajectories were also identified in the cortex of FE65/FE65L1 double knockout mice (Guenette *et al.* 2006).

Our results display a rescue of this neuronal deficit when expression of p53 is suppressed by co-injection of morpholinos targeting p53 and FE65. Previously it has been suggested that morpholinos can induce off-target effects, such as activating the apoptotic pathway, resulting in non-specific cell death (Robu *et al.* 2007). Our results display a p53-dependant neuronal rescue with both FE65 translation and splice blocking morpholinos, which are targeted to different sequence regions of the FE65 gene. The fact that two different morpholinos give the same telencephalic phenotype, suggests that this is a specific effect, and that rescue by p53 morpholino reflects a biological function of FE65 rather than identical non-specific toxic effects of the FE65 morpholinos. Interestingly, brain extracts exposed to non-lethal doses of hydrogen peroxide from mice deficient in FE65 displayed higher levels of p53, suggesting that

loss of function of FE65 increases cells sensitivity to DNA damaging agents (Minopoli *et al.* 2007). It has also been shown that FE65 and p53 co-localise in the nuclei of cells and that FE65 stabilises p53 (Nakaya *et al.* 2009) suggesting that FE65 may be involved in the regulation of p53 upon induced DNA damage in the cell. It may also be possible for p53 pathways to crosstalk with other pathways, such as the FE65 signalling pathway.

5.6 Future Work

To validate the translation blocking FE65 morphant we need to do a FE65 RNA rescue experiment. The splice blocking morphant can be utilised for further staining experiments to look at neuronal proliferative patterns and apoptosis. We can also investigate whether double knockdown of APP and FE65 in embryos will lead to further morphological and/or neuronal deficits.

It would be interesting to identify whether neuronal defects observed in *FE65* morphants are replicated in a zebrafish *FE65* mutant line. One approach to creating a mutant strain is the use of zinc finger nucleases (ZFNs) which can be engineered to recognise FE65 sequences. Injection of these nucleases can lead to mutagenic lesions at the target site in the germ line (Meng *et al.* 2008). Another recent approach is the use of transcription activator-like nucleases (TALENS), which can be engineered to induce double strand DNA breaks at target site. Repair of these lesions can lead to mutations at the target loci. Studies have shown TALEN technology can induce mutations in the zebrafish genome with high efficiency (Sander *et al.* 2011; Dahlem *et al.* 2012). Generation of a FE65 mutant line would give rise to the possibility to cross with a transgenic line, such as Tg:HuC, which labels post-mitotic neurons. To understand which pathways are regulated by FE65 signalling, mutant and sibling embryos could be used for microarray analysis. This would give a gene expression profile of downstream target genes, which could be investigated further.

CHAPTER 6

DISCUSSION

The construction of brain architecture and its complex neuronal circuitry are coordinated processes. Timely production and correct migration of neurons from proliferative regions are essential for cortical development. The neurons which form the mammalian cortex originate in the cortical ventricular zone and migrate to the cortical plate. The earliest born neurons which migrate are destined for the deepest cortical layers, whereas the neurons which are born later form the outer cortical layers, resulting in the typical inside-out patterninig (Verotti et al 2010). Cortical development involves a set of complex events which includes cell proliferation, migration and differentiation. Disruption in any of these processes can lead to cortical malformations (Pang *et al.* 2008). This thesis investigated different aspects of neuronal migration during development using the zebrafish embryo as a model. In this discussion I summarise how our work coincides with the current literature and how it advances knowledge on neuronal migration.

6.1 The Importance of the Basement Membrane

The basement membrane is a structure which surrounds the brain and blood vessels throughout the CNS, and is essential for migration of neurons from proliferative areas and cortical patterning. It is composed of collagen IV, nidogen, perlecan, agrin, collagen XVIII, and members of the laminin family (Timpl *et al.* 1996). Laminins interact with cell surface receptors to regulate a variety of cellular process, such as morphogenesis, influencing intracellular signalling pathways, and cell proliferation and growth. Many studies have identified the importance of the laminin family in basement membrane integrity during cortical development. In humans, mutations in LAMC3 have been associated with malformations of occipital cortical development (Barak *et al.* 2011). Infants with LAMA2 deficiency display lesions in the cerebral white matter and develop bioccipital polymicrogyria, a neuronal migration disorder (Tsao *et al.* 1998). Targeted deletion of the nidogen binding site of laminin γ1 caused an unstable formation of the basement membrane leading to aberrant migration of Cajal-Retzus cells and cortical dysplasia (Halfter *et al*. 2002). Consistent with this, mice deficient in both laminin β2 and γ3 isoforms exhibit hallmarks of cobblestone lissencephaly. These mice display a disruption in lamination, aberrant migration of Cajal-Retzus cells, and altered glial cell morphology (Radner *et al*. 2012). These studies

identify a role for laminins in neuronal migration and cortical development. Mutant zebrafish embryos defective in laminin β1 and γ1 display defects in two ocular basement membranes, manifesting as lens dysplasias (Lee *et al.* 2007). In this thesis I show that zebrafish laminin β1 mutants display defective patterning of postmitotic neurons in the zebrafish telencephalon and olfactory placodes, resulting in dysplasia. Mutants displayed an altered expression of *emx3*, *dlx3*, and *gabra1,* markers of dorsal telencephalon cells, olfactory placode precursor cells, and GABA receptor 1A, respectively. During development neuronal migration and cortical patterning is regulated by reelin (D'archangelo *et al.* 1995). Disruption of the basement membranes interferes with the secretion of reelin, thus resulting in defects in neuronal migration (Franco *et al.* 2011). Consistent with this, mutations in reelin have been associated with lissencephaly, a neuronal migration disorder (Suarez-Vega *et al.* 2013). We show that laminin β1 mutants display decreased expression of reelin in the forebrain and hindbrain during development. Laminin β1 mutation also results in the appearance of ectopic motor neurons, a defect phenocopied by laminin α1 mutants (Sittaramane *et al.* 2009), suggesting a functional link between laminin α1 and β1. The laminin β1 chain is ubiquitously expressed in the basement membrane zones of the developing fetal brain, further implying the importance of laminin β1 during brain development (Roediger *et al.* 2010). Additionally, we identify a decrease in the size of the forebrain ventricular space in laminin β1 mutants compared with siblings, suggesting a role in ventricle morphogenesis. Interestingly, laminin has also been identified to have a role in the formation of the midbrain-hindbrain boundary in zebrafish (Gutzman *et al.* 2008). We suggest forebrain patterning in the zebrafish is dependent on the integrity of the basement membrane. Disruptions in the integrity of the basement membrane may result in dysplasia and disrupted morphogenesis of the forebrain. One possible experiment to confirm this hypothesis would be to track individual labelled neurons by time lapse microscopy.

We also investigated the role of FE65 in forebrain development. FE65 proteins are a family (FE65, FE65L1, and FE65L2) of scaffolding proteins which bind to the APP intracellular domain (AICD) of APP (Turner *et al.* 2004). Previous studies have suggested a role of FE65 in neuronal development and basement membrane integrity. FE65/FE65L1 double knockouts mice displayed cortical dysplasia during development.

Staining of adult mice brains from *FE65* double knockout revealed defective neuronal patterning in the cortical plate, mislocalisation of reelin-positive cells, and disruption in the pial basement membrane, pathologies all of which resemble cobblestone Lissencephaly (Guenette *et al.* 2006). This phenotype also resembles the triple APP knockout mice (Herms *et al.* 2004), supporting the known functional link between FE65 and APP. In the zebrafish embryo, *Fe65* expression can be detected from 14hpf-18hpf (Mahmood *et al.* 2007). We show knockdown of *Fe65* in the zebrafish embryo leads to a defective patterning of HuC-positive cells in the forebrain, a phenotype resembling laminin 1β, suggesting that a loss of FE65 function may interfere with basement membrane integrity. FE65 interacts with APP and Mena to form a complex which regulates cell movement (Sabo *et al*. 2001). We show ectopic HuC positive cells ventrally located in the forebrain of *FE65* morphants. It is plausible that localisation of ectopic cells may be due to a defect in cell movement. FE65 may also be critical for the development of the olfactory placode. We observed that a loss of *FE65* function leads to defects in olfactory placode development and olfactory nerve projection. Consistent with this, neurogenesis of gonadotrophin releasing hormone-1, neurons which originate in the olfactory placode, is disrupted in FE65 null mice. Recently, FE65 has been shown to regulate neurite outgrowth by binding to a GTPase ADP-ribosylation factor 6 (ARF6) and activating downstream signalling of Rac1 (Cheung *et al.* 2014), highlighting its importance in neuronal development. Further work needs to be done to elucidate whether FE65 dysfunction has a role in Alzheimer's disease (Minopoli *et al.* 2012), but the evidence accumulated as of yet suggests a vital role for FE65 in development, in particular brain development. One approach to understanding the role of FE65 is to create mutant zebrafish *FE65* strain. One technique to generate zebrafish mutant stain is by using zinc finger nucleases (ZFNs) which can be engineered to recognise FE65 sequences. Injection of these nucleases can lead to mutagenic lesions at the target site in the germ line (Meng *et al.* 2008). Another recent approach is the use of transcription activator-like nucleases (TALENS), which can be engineered to induce double strand DNA breaks at target site. Repair of these lesions can lead to mutations at the target loci. Studies have shown TALEN technology can induce mutations in the zebrafish genome with high efficiency (Sander *et al.* 2011; Dahlem *et al.* 2012).

The basement membrane is important for orchestrating neuronal development. In both models I demonstrated abnormal development of the telencephalon and phenotypes resembling those which resemble phenotypes observed in cortical dysplasias.

6.2 Cobblestone Lissencephaly

Cobblestone (COB) lissencephaly (type II Lissencephaly), is a brain malformation characterised by cortical dysplasia and dysmyelination due to an over-migration of neurons through the basement membrane into the subarachnoid space. This aberrant migration causes a bumpy appearance on the surface of the brain. COB lissencephaly can be identified in three syndromes; Walker-Warburg syndrome, Muscle-Eye-Brain disease, and Fukuyama congenital muscular dystrophy, all of which are associated with ocular and muscular deficits (Meyer *et al.* 2007; Pang *et al.* 2013). Laminin β1 mutant zebrafish display reduced a forebrain ventricular space, defective patterning of post-mitotic neurons in the forebrain, reduced reelin expression in the forebrain and hindbrain, and ectopic motor neurons, all of which resemble features of COB lissencephaly. Recently, mutations in *LAMB1* were detected in two families with COB with less apparent muscular and ocular abnormalities. Patients displayed cortical gyral and white matter abnormalities, and brainstem and cerebellar hyperplasia (Radmanesh *et al*. 2013). This strengthens our belief that the defects we observed in zebrafish laminin β1 mutants are the same pathology observed in COB lissencephaly.

One characteristic of COB Lissencephaly is defects in eye development. The Zebrafish laminin β1 mutants display optic nerve disorganisation, thus displaying defects in eye development (Lee *et al.* 2007; Beihlmaier *et al.* 2007), whilst human patients display minor optic atrophy than typically found. A consanguineous Turkish transmitted a mutation localised on exon 17 which is predicted to cause mis-splicing of exon 16 to exon 17, thus also leading to a frameshift in affected offspring (Radmanesh *et al.* 2013). Whole exome sequencing of LAMB1 in a consanguineous Eygyptian family revealed a mutation located on chromosome 22, which encodes a laminin epidermal-growth-factor (EGF)-like domain, in affected offspring (Radmanesh *et al.* 2013). This mutation was a result from a frameshift and a premature stop codon. Interestingly, we show the best pathogenic mutation in the gup^{tj229a} is a frameshift/truncation in

precisely the same exon, exon 22. We investigated the mutation by sequencing cDNA from phenotypic embryos, and comparing with data from unaffected siblings and wild type controls. The best candidate for the mutation occurs in the region of a splice acceptor site, and results in the use of a cryptic splice site in exon 22. This in turn leads to an inclusion of 34bp of intronic sequence, resulting in a frameshift and the creation of a premature stop codon. This would result in a non-functional allele that is either subject to nonsense mediated decay or generates a truncated protein that lacks part of the Laminin LE domain and the C-terminal region of the protein. The zebrafish mutation gup^{m189} results in a premature stop codon also the laminin-type EGF-like domains (Parsons *et al.* 2002). Although similar pathogenic mutations are identified in the humans, and the zebrafish gup^{tj229a} and gup^{m189}, the effect on optic atrophy may differ in humans compared with the zebrafish animal model.

One of the DNA changes in this intronic region in gup^{tj229a} includes a polymorphic (GT)n microsatellite repeat. On the basis of our analysis we predict that the TC>AA mutation at -11 and -12 positions relative to the splice acceptor site is most likely to be pathogenic. This disrupts the only polypyrimidine tract in the region, a sequence known to regulate splicing (Reed *et al.* 1985). The reason for the use of the alternative, cryptic, splice site is more puzzling. In the mutant allele the (GT)n tract is interrupted by the insertion of AAGTTG, and AG/TT becomes the novel splice acceptor site.

Perhaps the only way to more fully understand the underlying cryptic splicing events would be to create an artificial splice cassette in a reporter gene construct to investigate the effects of the (GT)n and various mutations within the intron upon splicing. Since this falls outside the main goals of the PhD project relating to cell migration during development, we decided to shift our focus to the effects of the mutation rather than its specific mechanism of action at the level of transcription and splicing.

We propose the zebrafish laminin β1 mutants can be used in further studies as a model for COB lissencephly. Patients with COB lissencphaly display clinical aspects of generalised epilepsy from an early age (Verotti *et al.* 2010). Previous studies have indicated an altered expression of GABA receptor subunits in animal models of

epilepsy. We show an altered pattern of *gabra1* subunit in the forebrain of zebrafish mutant embryos. The zebrafish laminin 1 mutants may be a good model to investigate whether there is any alteration in other neurotransmitter receptors or proteins important for neurotransmission. Further studies could investigate which downstream signalling pathways lead to the defects observed in the forebrain and hindbrain of zebrafish laminin 1β mutants.

6.3 The Mevalonate Pathway

Hydroxymethylglutaryl co-enzyme A reductase (HMGCoAR) is the rate limiting enzyme converting hydroxymethygluatry co-enzyme A (HMGCoA) into mevalonate, an essential product in cholesterol and isoprenoid biosynthesis. Isoprenoids are short-chain lipid molecules produced by two processes of prenylation, farnesylation and geranylgeranylation. Isoprenoid biosynthesis generates farnesyl pyrophosphate and geranylgeranyl pyrophosphate, which are required for post-translational modification of proteins harbouring a –CaaX-motif. Invertebrate and vertebrates express HMGCoAR transcripts during embryogenesis (Aspbury *et al.* 1998; Santos *et al.* 2004), suggesting this signaling pathway is conserved during development.

Recently, studies have highlighted the importance of prenylation process in neuronal migration during development. Lamin B is an important protein which provides structural support for the nucleus. Knock-in mice expressing a mutant form of *lamin B* that is unable to be farnesylated, resulted in defects in neuronal patterning in the cerebral cortex. During neuronal migration, farnesylated lamin B is required to retain the nuclear chromatin within the nuclear lamina. In mutant *lamin B* mice, migrating neurons displayed nuclear abnormality and the nuclear lamina was pulled free from the chromatin (Jung *et al.* 2013). Using pharmacological inhibition of HMGCoAR we show that patterning in the forebrain of the zebrafish embryo is disrupted, resulting in ectopic HuC-positive cells and a smaller ventricular space. Consistently, facial branchiomotor neurons (FBMNs) migration defects are observed when pharmacologically inhibiting HMGCoAR. Mutation in the motif required for the farnesylation of *prickle 1b* phenocopies the FBMN migration defects. Furthemore, it is suggested that nuclear localisation of *prickle 1b* influences FBMN migration (Mapp *et*

al. 2011). Mutation in HMGCoA synthase 1, an enzyme which catalyses acetyl CoA to form HMGCoA, causes oligodendrocyte progenitor cells to migrate past their target axons (Mathew *et al.* 2014). The prenylation process targets certain proteins which containing –CaaX- motifs. Prenyl lipd groups are attached to proteins which in turn facilitates the proteins association to target membranes (Nguyen *et al.* 2010). It is possible that inhibition of prenylation may affect proteins, such as lamin B1 or prickle 1B, leading to an inability to attach to target membranes, thus disrupting their functions within the nucleus of the cell and resulting in migration defects within the zebrafish forebrain (Figure 40). Interestingly, knockdown of lamin B receptor results in defects in cell migration in the zebrafish embryo, suggesting that lamin B is important for development (Schild-Prufert *et al.* 2006).

The ventricular space (VS) forms between the telencephalon and diecephalon. The outfolding of the neuroepithelium appears at 18hpf followed by inflation of the VS. This inflation leads to the formation of the anterior intraencephalic sulcus (AIS). Between 24hpf and 48hpf, proliferative cells are located in the medial and posterior ventricular walls of the telencephalon. One of the key morphogenetic events in telecephalon development is the expansaion of the telencephalic domains resulting in the ventricular surface covering the upper surface of the telencephalon by day 5 hours post-fertilisation (5hpf) (Folgueira *et al.* 2012). Inhibition of HMGCoAR and metabolites required for prenylation results in a decreased ventricular space, suggesting inhibition of this pathway may affect morphogenesis of the telencephalon. One possible explanation may be that inhibition of isoprenylation affects the function of proteins required for cell proliferation, such as Rac1 GTPase (see below), in the medial and posterior ventricular walls, resulting in a defective neuronal proliferation in the forebrain, thus affecting the expansion of the telencephalic domains and disrupting the expansion of the ventricular space.

The Rho GTPase superfamily are intracellular proteins which cycle between active GTP-bound state and inactive GDP-bound state and are required by various cellular processes such as, cell cycle progression, vesicle trafficking, apoptosis, and transcription (Chen et al 2009). These GTPases undergo post-translational modification where they require the attachment of gernaylgernayl pyrophosphate (GGPP), thus being targets for the prenylation process (Afshoredel *et al.* 2013). Since

GTPases have been shown to have various roles in forebrain development, we also suggest that inhibition of HMGCoAR may disrupt the prenylation of certain GTPases, thus leading to a defective telencephalon morphogenesis. Rac1 GTPase has been implicated in maintaining cell proliferation (Chen et al 2007). Interestingly, deletion of *rac1* in the mouse telencephalon epithelium impairs cell cycle exit of proliferating progenitors, post-mitotic differentiation, resulting in a smaller forebrain which resembles the microcephaly phenotype (Chen *et al.* 2009). Additionally, cell cycle exit of interneuron progenitors is disrupted upon *rac1* deletion, leading to migratory defects (Vidaki *et al.* 2012). Mutations in LIS1, a gene associated with the neuronal migration disorder, Lissencephaly, leads to a downregulation of rac1 (Kohlmanskikh *et al.* 2003). These studies highlight the importance of Rac1 in the developing forebrain, thus it is possible by inhibiting its function may induce developmental defects in the forebrain. We would like to investigate whether inhibiting prenylation of Rac1 results in migratory defects in the developing zebrafish forebrain. Another avenue to explore is whether statin treatment alters the development of the midbrain or hindbrain, or the midbrain hindbrain constriction. This could be investigated by injecting Texas Red-dextran into ventricles of immesrsing embryos in biodipy, thus highlighting the ventricle space (Lowery *et al.* 2005).

Our data suggest that the isoprenoid pathway is required in telencephalon development. We propose a model whereby inhibiting enzymes involved in attachment of prenyl group to target proteins, disrupts their function and therefore consequently disrupting telencephalon development and ventricular space expansion. We hypothesise that these proteins could be proteins involved in cell movement, such as lamin or prickle 1b, and/or proteins involved in regulating progenitor proliferation and maintaining neuronal differentiation, such as Rac1 GTPase (Figure 44)

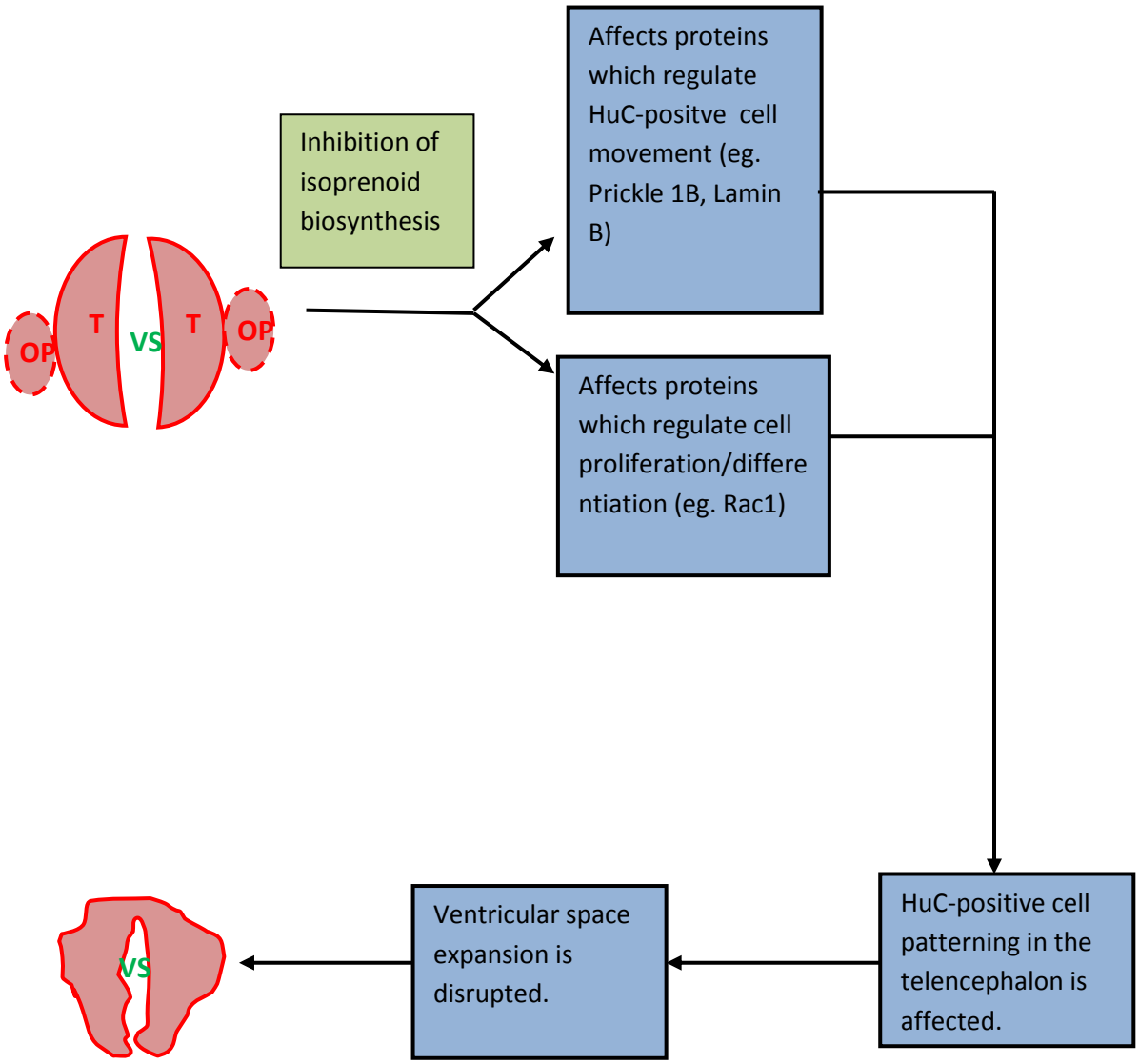

Figure 44 – A proposed model to demonstrate the morphological changes of the zebrafish forebrain upon inhibiting isoprenoid biosynthesis. Diagrams are of a transverse view through the forebrain.

6.4 Effects of Statins in Adulthood and Development

Primarily statins have been prescribed to patients for lowering cholesterol, thus preventing cardiovascular disease (Zhou *et al.* 2014). Statins predominantly lower levels of low density lipoprotein (LDL) cholesterol in the blood circulation by reducing its production in the liver and by removing it from circulation (Wierzbicki *et al.* 2013). Recently, much attention has been focused on statin treatment in neurological disorders due to their ability to cross the blood brain barrier. Administration of atorvastatin in a mouse model of stroke resulted in angiogenesis, neurogenesis, and synaptogenesis (Chen *et al.* 2005). In the adult hippocampus statins have been identified to enhance Wnt signalling, thus promoting neuronal specification from adult progenitor cells (Robin *et al.* 2013). The use of statins has also been investigated as a potential therapy for AD. During APP metabolism isoprenoids have been shown to regulate activities of α, β, and γ secretases. Isoprenoids and prenylated proteins have also suggested in being important in neuroinflammation, gliosis, and tau phosphorylation, all of which are contributors to AD pathology (Silva *et al.* 2013). Animal models of Alzheimer's disease treated with statins show a decrease in inflammation (Zhang *et al.* 2013), oxidative stress (Butterfield *et al.* 2011), senile plaques (Kurata *et al.* 2012), and an improvement in learning and memory (Ling et al 2006). Consistent with this, haplodeficiancy in farnesyl transferase, an enzyme important for farnesylation, reduced Aβ deposition and rescued cognitive function in the APP/PS1 double transgenic mouse model (Cheng *et al.* 2013). Many studies have focused their attention on the modulation of the mevalonate pathway by statins. Recently, it has been proposed that statins may also modulate the heme oxygenase-1/biliverdin reductase-A (HO-1/BVR-A). One argument proposed is that the HO-1/BVR-A system serves as a neuroprotective mechanism counteracting the oxidative stress observed in AD (Barone *et al.* 2014). Atorvastatin treatments in a canine model of AD showed an increased expression of heam oxygensae- 1, which was associated with a decrease in markers of oxidative stress (Barone *et al.* 2014), thus supporting a novel mechanism for the action of statins in AD.

Interestingly, the use of statins has been shown to be beneficial in adults in relation to neurological and neurodegenerative disorders. We and other groups have consistently shown that statin treatment during development results in aberrant migratory effects

in the CNS. One possibility why this difference occurs may be that the mevalonate pathway plays a different role during development and adulthood. In keeping with this, fetal exposure to pravastatin increases the availability of nitrogen oxide, and consequently results in acute hypoxia (Kane *et al.* 2012). During CNS development most, if not all, neurons undergo neuronal migration. In the mammalian adult brain there are only restricted regions, like the hippocampus and cerebellum, where neuronal migration occurs (Ghashghaei *et al.* 2007). This difference observed in the neuronal migration may potentially be another reason why statin treatment is different in development versus adulthood.

Due to the difference in how statins function within the adult and embryo, another potential avenue to explore may be the role of statins and HO-1/BVR-A system in development, in particular identifying if this system has a role in neuronal development. Additionally we could also investigate whether the mevalonate pathway affects the zebrafish adult brain and identify whether isoprenoids are important in postnatal brain. One technique to investigate whether inhibition of HMGCoAR results in defective forebrain neurogenesis is by examining proliferative patterns of neuronal progenitors using proliferating cell nuclear antigen and whether progenitors are exiting the cell cycle early by using 5'bromo-2'-deoxyuridine (BrdU) (Mueller *et al.* 2002).

CHAPTER 7

BIBLIOGRAPHY

Abramsson, A., P. Kettunen, et al. (2013). "The zebrafish amyloid precursor protein-b is required for motor neuron guidance and synapse formation." Dev Biol **381**(2): 377-388.

Akimenko, M. A., M. Ekker, et al. (1994). "Combinatorial expression of three zebrafish genes related to distal-less: part of a homeobox gene code for the head." J Neurosci **14**(6): 3475-3486.

Alberts, P., R. Rudge, et al. (2006). "Cdc42 and actin control polarized expression of TI-VAMP vesicles to neuronal growth cones and their fusion with the plasma membrane." Mol Biol Cell **17**(3): 1194-1203.

Alcantara, S., E. Pozas, et al. (2006). "BDNF-modulated spatial organization of Cajal-Retzius and GABAergic neurons in the marginal zone plays a role in the development of cortical organization." Cereb Cortex **16**(4): 487-499.

Anderson, S. A., M. Qiu, et al. (1997). "Mutations of the homeobox genes Dlx-1 and Dlx-2 disrupt the striatal subventricular zone and differentiation of late born striatal neurons." Neuron **19**(1): 27-37.

Ando, K., K. I. Iijima, et al. (2001). "Phosphorylation-dependent regulation of the interaction of amyloid precursor protein with Fe65 affects the production of beta-amyloid." J Biol Chem **276**(43): 40353-40361.

Angevine, J. B., Jr. and R. L. Sidman (1961). "Autoradiographic study of cell migration during histogenesis of cerebral cortex in the mouse." Nature **192**: 766-768.

Anton, E. S., M. A. Marchionni, et al. (1997). "Role of GGF/neuregulin signaling in interactions between migrating neurons and radial glia in the developing cerebral cortex." Development **124**(18): 3501-3510.

Arber, S. (2012). "Motor circuits in action: specification, connectivity, and function." Neuron **74**(6): 975-989.

Aspbury, R. A., M. C. Prescott, et al. (1998). "Isoprenylation of polypeptides in the nematode Caenorhabditis elegans." Biochim Biophys Acta **1392**(2-3): 265-275.

Barak, T., K. Y. Kwan, et al. (2011). "Recessive LAMC3 mutations cause malformations of occipital cortical development." Nat Genet **43**(6): 590-594.

Barone, E., F. Di Domenico, et al. (2014). "The Janus face of the heme oxygenase/biliverdin reductase system in Alzheimer disease: it's time for reconciliation." Neurobiol Dis **62**: 144-159.

Barth, K. A. and S. W. Wilson (1995). "Expression of zebrafish nk2.2 is influenced by sonic hedgehog/vertebrate hedgehog-1 and demarcates a zone of neuronal differentiation in the embryonic forebrain." Development **121**(6): 1755-1768.

Battaglia, C., U. Mayer, et al. (1992). "Basement-membrane heparan sulfate proteoglycan binds to laminin by its heparan sulfate chains and to nidogen by sites in the protein core." Eur J Biochem **208**(2): 359-366.

Baye, L. M. and B. A. Link (2007). "Interkinetic nuclear migration and the selection of neurogenic cell divisions during vertebrate retinogenesis." J Neurosci **27**(38): 10143-10152.

Bedard, A. and A. Parent (2004). "Evidence of newly generated neurons in the human olfactory bulb." Brain Res Dev Brain Res **151**(1-2): 159-168.

Behar, T. N., M. M. Dugich-Djordjevic, et al. (1997). "Neurotrophins stimulate chemotaxis of embryonic cortical neurons." Eur J Neurosci **9**(12): 2561-2570.

Bellion, A., J. P. Baudoin, et al. (2005). "Nucleokinesis in tangentially migrating neurons comprises two alternating phases: forward migration of the Golgi/centrosome associated with centrosome splitting and myosin contraction at the rear." J Neurosci **25**(24): 5691-5699.

Benito-Gonzalez, A. and F. J. Alvarez (2012). "Renshaw cells and Ia inhibitory interneurons are generated at different times from p1 progenitors and differentiate shortly after exiting the cell cycle." J Neurosci **32**(4): 1156-1170.

Biehlmaier, O., Y. Makhankov, et al. (2007). "Impaired retinal differentiation and maintenance in zebrafish laminin mutants." Invest Ophthalmol Vis Sci **48**(6): 2887-2894.

Blanco, G., N. G. Irving, et al. (1998). "Mapping of the human and murine X11-like genes (APBA2 and apba2), the murine Fe65 gene (Apbb1), and the human Fe65-like gene (APBB2): genes encoding phosphotyrosine-binding domain proteins that interact with the Alzheimer's disease amyloid precursor protein." Mamm Genome **9**(6): 473-475.

Bonner, J. and T. P. O'Connor (2001). "The permissive cue laminin is essential for growth cone turning in vivo." J Neurosci **21**(24): 9782-9791.

Borg, J. P., J. Ooi, et al. (1996). "The phosphotyrosine interaction domains of X11 and FE65 bind to distinct sites on the YENPTY motif of amyloid precursor protein." Mol Cell Biol **16**(11): 6229-6241.

Bressler, S. L., M. D. Gray, et al. (1996). "cDNA cloning and chromosome mapping of the human Fe65 gene: interaction of the conserved cytoplasmic domains of the human beta-amyloid precursor protein and its homologues with the mouse Fe65 protein." Hum Mol Genet **5**(10): 1589-1598.

Bronner, M. E. (2012). "Formation and migration of neural crest cells in the vertebrate embryo." Histochem Cell Biol **138**(2): 179-186.

Bubier, J. A., T. J. Sproule, et al. (2010). "A mouse model of generalized non-Herlitz junctional epidermolysis bullosa." J Invest Dermatol **130**(7): 1819-1828.

Buchroithner, B., A. Klausegger, et al. (2004). "Analysis of the LAMB3 gene in a junctional epidermolysis bullosa patient reveals exonic splicing and allele-specific nonsense-mediated mRNA decay." Lab Invest **84**(10): 1279-1288.

Buoso, E., C. Lanni, et al. "beta-Amyloid precursor protein metabolism: focus on the functions and degradation of its intracellular domain." Pharmacol Res.

Butterfield, D. A., E. Barone, et al. (2011). "Cholesterol-independent neuroprotective and neurotoxic activities of statins: perspectives for statin use in Alzheimer disease and other age-related neurodegenerative disorders." Pharmacol Res **64**(3): 180-186.

Cao, P., J. Hanai, et al. (2009). "Statin-induced muscle damage and atrogin-1 induction is the result of a geranylgeranylation defect." FASEB J **23**(9): 2844-2854.

Cao, X. and T. C. Sudhof (2001). "A transcriptionally [correction of transcriptively] active complex of APP with Fe65 and histone acetyltransferase Tip60." Science **293**(5527): 115-120.

Casoni, F., B. I. Hutchins, et al. (2012). "SDF and GABA interact to regulate axophilic migration of GnRH neurons." J Cell Sci.

Castiglia, D., P. Posteraro, et al. (2001). "Novel mutations in the LAMC2 gene in non-Herlitz junctional epidermolysis bullosa: effects on laminin-5 assembly, secretion, and deposition." J Invest Dermatol **117**(3): 731-739.

Causeret, F., M. Hidalgo-Sanchez, et al. (2004). "Distinct roles of Rac1/Cdc42 and Rho/Rock for axon outgrowth and nucleokinesis of precerebellar neurons toward netrin 1." Development **131**(12): 2841-2852.

Cerezo-Guisado, M. I., A. Alvarez-Barrientos, et al. (2007). "c-Jun N-terminal protein kinase signalling pathway mediates lovastatin-induced rat brain neuroblast apoptosis." Biochim Biophys Acta **1771**(2): 164-176.

Chandrasekhar, A., C. B. Moens, et al. (1997). "Development of branchiomotor neurons in zebrafish." Development **124**(13): 2633-2644.

Chang, Y., P. Ostling, et al. (2006). "Role of heat-shock factor 2 in cerebral cortex formation and as a regulator of p35 expression." Genes Dev **20**(7): 836-847.

Chen, G., J. Sima, et al. (2008). "Semaphorin-3A guides radial migration of cortical neurons during development." Nat Neurosci **11**(1): 36-44.

Chen, J., C. Zhang, et al. (2005). "Atorvastatin induction of VEGF and BDNF promotes brain plasticity after stroke in mice." J Cereb Blood Flow Metab **25**(2): 281-290.

Chen, L., J. Melendez, et al. (2009). "Rac1 deficiency in the forebrain results in neural progenitor reduction and microcephaly." Dev Biol **325**(1): 162-170.

Chen, Z. L., V. Haegeli, et al. (2009). "Cortical deficiency of laminin gamma1 impairs the AKT/GSK-3beta signaling pathway and leads to defects in neurite outgrowth and neuronal migration." Dev Biol **327**(1): 158-168.

Cheng, S., D. Cao, et al. (2013). "Farnesyltransferase haplodeficiency reduces neuropathology and rescues cognitive function in a mouse model of Alzheimer disease." J Biol Chem **288**(50): 35952-35960.

Cheung, H. N., C. Dunbar, et al. (2014). "FE65 interacts with ADP-ribosylation factor 6 to promote neurite outgrowth." FASEB J **28**(1): 337-349.

Chitnis, A. B. and J. Y. Kuwada (1990). "Axonogenesis in the brain of zebrafish embryos." J Neurosci **10**(6): 1892-1905.

Chizhikov, V. V. and K. J. Millen (2005). "Roof plate-dependent patterning of the vertebrate dorsal central nervous system." Dev Biol **277**(2): 287-295.

Colognato, H. and P. D. Yurchenco (2000). "Form and function: the laminin family of heterotrimers." Dev Dyn **218**(2): 213-234.

Cook, M., P. Mani, et al. (2012). "Increased RhoA prenylation in the loechrig (loe) mutant leads to progressive neurodegeneration." PLoS One **7**(9): e44440.

Cool, B. H., G. Zitnik, et al. (2010). "Structural and functional characterization of a novel FE65 protein product up-regulated in cognitively impaired FE65 knockout mice." J Neurochem **112**(2): 410-419.

Cooper, M. K., C. A. Wassif, et al. (2003). "A defective response to Hedgehog signaling in disorders of cholesterol biosynthesis." Nat Genet **33**(4): 508-513.

Costa, C., B. Harding, et al. (2001). "Neuronal migration defects in the Dreher (Lmx1a) mutant mouse: role of disorders of the glial limiting membrane." Cereb Cortex **11**(6): 498-505.

Costagli, A., M. Kapsimali, et al. (2002). "Conserved and divergent patterns of Reelin expression in the zebrafish central nervous system." J Comp Neurol **450**(1): 73-93.

Crick, D. C., C. J. Waechter, et al. (1994). "Utilization of geranylgeraniol for protein isoprenylation in C6 glial cells." Biochem Biophys Res Commun **205**(1): 955-961.

D'Amico, L., I. C. Scott, et al. (2007). "A mutation in zebrafish hmgcr1b reveals a role for isoprenoids in vertebrate heart-tube formation." Curr Biol **17**(3): 252-259.

Dahlem, T. J., K. Hoshijima, et al. (2012). "Simple methods for generating and detecting locus-specific mutations induced with TALENs in the zebrafish genome." PLoS Genet **8**(8): e1002861.

Danesin, C., J. N. Peres, et al. (2009). "Integration of telencephalic Wnt and hedgehog signaling center activities by Foxg1." Dev Cell **16**(4): 576-587.

Deshpande, G., A. Godishala, et al. (2009). "Ggamma1, a downstream target for the hmgcr-isoprenoid biosynthetic pathway, is required for releasing the Hedgehog ligand and directing germ cell migration." PLoS Genet **5**(1): e1000333.

Devisme, L., C. Bouchet, et al. (2012). "Cobblestone lissencephaly: neuropathological subtypes and correlations with genes of dystroglycanopathies." Brain **135**(Pt 2): 469-482.

Ding, Q., P. S. Joshi, et al. (2012). "BARHL2 transcription factor regulates the ipsilateral/contralateral subtype divergence in postmitotic dI1 neurons of the developing spinal cord." Proc Natl Acad Sci U S A **109**(5): 1566-1571.

Duilio, A., R. Faraonio, et al. (1998). "Fe65L2: a new member of the Fe65 protein family interacting with the intracellular domain of the Alzheimer's beta-amyloid precursor protein." Biochem J **330 (Pt 1)**: 513-519.

Dun, X. P., T. Bandeira de Lima, et al. (2012). "Drebrin controls neuronal migration through the formation and alignment of the leading process." Mol Cell Neurosci **49**(3): 341-350.

Eckert, G. P., G. P. Hooff, et al. (2009). "Regulation of the brain isoprenoids farnesyl- and geranylgeranylpyrophosphate is altered in male Alzheimer patients." Neurobiol Dis **35**(2): 251-257.

Edison, R. J. and M. Muenke (2004). "Mechanistic and epidemiologic considerations in the evaluation of adverse birth outcomes following gestational exposure to statins." Am J Med Genet A **131**(3): 287-298.

Edwards, M. M., E. Mammadova-Bach, et al. (2010). "Mutations in Lama1 disrupt retinal vascular development and inner limiting membrane formation." J Biol Chem **285**(10): 7697-7711.

Eisa-Beygi, S., G. Hatch, et al. (2012). "The 3-hydroxy-3-methylglutaryl-CoA reductase (HMGCR) pathway regulates developmental cerebral-vascular stability via prenylation-dependent signalling pathway." Dev Biol.

Elsen, G. E., L. Y. Choi, et al. (2008). "Zic1 and Zic4 regulate zebrafish roof plate specification and hindbrain ventricle morphogenesis." Dev Biol **314**(2): 376-392.

Emsley, J. G., J. R. Menezes, et al. (2012). "Identification of radial glia-like cells in the adult mouse olfactory bulb." Exp Neurol **236**(2): 283-297.

Ermekova, K. S., N. Zambrano, et al. (1997). "The WW domain of neural protein FE65 interacts with proline-rich motifs in Mena, the mammalian homolog of Drosophila enabled." J Biol Chem **272**(52): 32869-32877.

Farnsworth, C. C., M. C. Seabra, et al. (1994). "Rab geranylgeranyl transferase catalyzes the geranylgeranylation of adjacent cysteines in the small GTPases Rab1A, Rab3A, and Rab5A." Proc Natl Acad Sci U S A **91**(25): 11963-11967.

Fiore, F., N. Zambrano, et al. (1995). "The regions of the Fe65 protein homologous to the phosphotyrosine interaction/phosphotyrosine binding domain of Shc bind the intracellular domain of the Alzheimer's amyloid precursor protein." J Biol Chem **270**(52): 30853-30856.

Folgueira, M., P. Bayley, et al. (2012). "Morphogenesis underlying the development of the everted teleost telencephalon." Neural Dev **7**: 32.

Forni, P. E., M. Fornaro, et al. (2011). "A role for FE65 in controlling GnRH-1 neurogenesis." J Neurosci **31**(2): 480-491.

Franco, S. J. and U. Muller (2011). "Extracellular matrix functions during neuronal migration and lamination in the mammalian central nervous system." Dev Neurobiol **71**(11): 889-900.

Frantz, C., K. M. Stewart, et al. (2010). "The extracellular matrix at a glance." J Cell Sci **123**(Pt 24): 4195-4200.

Frotscher, M., C. A. Haas, et al. (2003). "Reelin controls granule cell migration in the dentate gyrus by acting on the radial glial scaffold." Cereb Cortex **13**(6): 634-640.

Garvalov, B. K., K. C. Flynn, et al. (2007). "Cdc42 regulates cofilin during the establishment of neuronal polarity." J Neurosci **27**(48): 13117-13129.

Ghashghaei, H. T., C. Lai, et al. (2007). "Neuronal migration in the adult brain: are we there yet?" Nat Rev Neurosci **8**(2): 141-151.

Goldsmith, P. (2004). "Zebrafish as a pharmacological tool: the how, why and when." Curr Opin Pharmacol **4**(5): 504-512.

Goldstein, L. S. and Z. Yang (2000). "Microtubule-based transport systems in neurons: the roles of kinesins and dyneins." Annu Rev Neurosci **23**: 39-71.

Gopal, P. P., J. C. Simonet, et al. (2010). "Leading process branch instability in Lis1+/- nonradially migrating interneurons." Cereb Cortex **20**(6): 1497-1505.

Grant, P. K. and C. B. Moens (2010). "The neuroepithelial basement membrane serves as a boundary and a substrate for neuron migration in the zebrafish hindbrain." Neural Dev **5**: 9.

Graziadei, P. P. and A. G. Monti-Graziadei (1992). "The influence of the olfactory placode on the development of the telencephalon in Xenopus laevis." Neuroscience **46**(3): 617-629.

Guenette, S., Y. Chang, et al. (2006). "Essential roles for the FE65 amyloid precursor protein-interacting proteins in brain development." EMBO J **25**(2): 420-431.

Guo, J., Z. Yang, et al. (2006). "Nudel contributes to microtubule anchoring at the mother centriole and is involved in both dynein-dependent and -independent centrosomal protein assembly." Mol Biol Cell **17**(2): 680-689.

Gupta, A., K. Sanada, et al. (2003). "Layering defect in p35 deficiency is linked to improper neuronal-glial interaction in radial migration." Nat Neurosci **6**(12): 1284-1291.

Gupta, A., L. H. Tsai, et al. (2002). "Life is a journey: a genetic look at neocortical development." Nat Rev Genet **3**(5): 342-355.

Gupta, V. A., G. Kawahara, et al. (2012). "A Splice Site Mutation in Laminin-alpha2 Results in a Severe Muscular Dystrophy and Growth Abnormalities in Zebrafish." PLoS One **7**(8): e43794.

Gutzman, J. H., E. G. Graeden, et al. (2008). "Formation of the zebrafish midbrain-hindbrain boundary constriction requires laminin-dependent basal constriction." Mech Dev **125**(11-12): 974-983.

Hartmann, D., B. De Strooper, et al. (1999). "Presenilin-1 deficiency leads to loss of Cajal-Retzius neurons and cortical dysplasia similar to human type 2 lissencephaly." Curr Biol **9**(14): 719-727.

He, M., Z. H. Zhang, et al. (2010). "Leading tip drives soma translocation via forward F-actin flow during neuronal migration." J Neurosci **30**(32): 10885-10898.

Heasman, S. J. and A. J. Ridley (2008). "Mammalian Rho GTPases: new insights into their functions from in vivo studies." Nat Rev Mol Cell Biol **9**(9): 690-701.

Hoe, H. S., L. A. Magill, et al. (2006). "FE65 interaction with the ApoE receptor ApoEr2." J Biol Chem **281**(34): 24521-24530.

Hooff, G. P., W. G. Wood, et al. (2012). "Brain isoprenoids farnesyl pyrophosphate and geranylgeranyl pyrophosphate are increased in aged mice." Mol Neurobiol **46**(1): 179-185.

Huang, X., Y. Litingtung, et al. (2007). "Region-specific requirement for cholesterol modification of sonic hedgehog in patterning the telencephalon and spinal cord." Development **134**(11): 2095-2105.

Hutcheson, H. B., L. M. Olson, et al. (2004). "Examination of NRCAM, LRRN3, KIAA0716, and LAMB1 as autism candidate genes." BMC Med Genet **5**: 12.

Ichikawa-Tomikawa, N., J. Ogawa, et al. (2012). "Laminin alpha1 is essential for mouse cerebellar development." Matrix Biol **31**(1): 17-28.

Istvan, E. S. and J. Deisenhofer (2001). "Structural mechanism for statin inhibition of HMG-CoA reductase." Science **292**(5519): 1160-1164.

Jensen, L. T., T. H. Moller, et al. (2012). "A new role for laminins as modulators of protein toxicity in Caenorhabditis elegans." Aging Cell **11**(1): 82-92.

Joshi, P., J. O. Liang, et al. (2009). "Amyloid precursor protein is required for convergent-extension movements during Zebrafish development." Dev Biol **335**(1): 1-11.

Jung, H. J., C. Nobumori, et al. (2013). "Farnesylation of lamin B1 is important for retention of nuclear chromatin during neuronal migration." Proc Natl Acad Sci U S A **110**(21): E1923-1932.

Kakita, A., S. Hayashi, et al. (2002). "Bilateral periventricular nodular heterotopia due to filamin 1 gene mutation: widespread glomeruloid microvascular anomaly and dysplastic cytoarchitecture in the cerebral cortex." Acta Neuropathol **104**(6): 649-657.

Kameda, H., H. Hioki, et al. (2012). "Parvalbumin-producing cortical interneurons receive inhibitory inputs on proximal portions and cortical excitatory inputs on distal dendrites." Eur J Neurosci **35**(6): 838-854.

Kane, A. D., E. A. Herrera, et al. (2012). "Statin treatment depresses the fetal defence to acute hypoxia via increasing nitric oxide bioavailability." J Physiol **590**(Pt 2): 323-334.

Kappeler, C., Y. Saillour, et al. (2006). "Branching and nucleokinesis defects in migrating interneurons derived from doublecortin knockout mice." Hum Mol Genet **15**(9): 1387-1400.

Karlstrom, R. O., T. Trowe, et al. (1996). "Zebrafish mutations affecting retinotectal axon pathfinding." Development **123**: 427-438.

Kawaji, K., H. Umeshima, et al. (2004). "Dual phases of migration of cerebellar granule cells guided by axonal and dendritic leading processes." Mol Cell Neurosci **25**(2): 228-240.

Kesavapany, S., S. J. Banner, et al. (2002). "Expression of the Fe65 adapter protein in adult and developing mouse brain." Neuroscience **115**(3): 951-960.

Kim, C. H., E. Ueshima, et al. (1996). "Zebrafish elav/HuC homologue as a very early neuronal marker." Neurosci Lett **216**(2): 109-112.

Kim, H., J. Shin, et al. (2008). "Notch-regulated oligodendrocyte specification from radial glia in the spinal cord of zebrafish embryos." Dev Dyn **237**(8): 2081-2089.

Kim, H. G., B. Bhagavath, et al. (2008). "Clinical manifestations of impaired GnRH neuron development and function." Neurosignals **16**(2-3): 165-182.

Knoll, R., R. Postel, et al. (2007). "Laminin-alpha4 and integrin-linked kinase mutations cause human cardiomyopathy via simultaneous defects in cardiomyocytes and endothelial cells." Circulation **116**(5): 515-525.

Kornack, D. R. and P. Rakic (2001). "The generation, migration, and differentiation of olfactory neurons in the adult primate brain." Proc Natl Acad Sci U S A **98**(8): 4752-4757.

Kurahashi, H., M. Taniguchi, et al. (2005). "Basement membrane fragility underlies embryonic lethality in fukutin-null mice." Neurobiol Dis **19**(1-2): 208-217.

Kurata, T., H. Kawai, et al. (2012). "Statins have therapeutic potential for the treatment of Alzheimer's disease, likely via protection of the neurovascular unit in the AD brain." J Neurol Sci **322**(1-2): 59-63.

Lau, K. F., W. M. Chan, et al. (2008). "Dexras1 interacts with FE65 to regulate FE65-amyloid precursor protein-dependent transcription." J Biol Chem **283**(50): 34728-34737.

Lavdas, A. A., M. Grigoriou, et al. (1999). "The medial ganglionic eminence gives rise to a population of early neurons in the developing cerebral cortex." J Neurosci **19**(18): 7881-7888.

Lee, J. A. and G. J. Cole (2007). "Generation of transgenic zebrafish expressing green fluorescent protein under control of zebrafish amyloid precursor protein gene regulatory elements." Zebrafish **4**(4): 277-286.

Lee, S., J. Hjerling-Leffler, et al. (2010). "The largest group of superficial neocortical GABAergic interneurons expresses ionotropic serotonin receptors." J Neurosci **30**(50): 16796-16808.

Leone, D. P., K. Srinivasan, et al. (2010). "The rho GTPase Rac1 is required for proliferation and survival of progenitors in the developing forebrain." Dev Neurobiol **70**(9): 659-678.

Li, J., W. L. Lee, et al. (2005). "NudEL targets dynein to microtubule ends through LIS1." Nat Cell Biol **7**(7): 686-690.

Li, S., Z. Jin, et al. (2008). "GPR56 regulates pial basement membrane integrity and cortical lamination." J Neurosci **28**(22): 5817-5826.

Li, Y. X., H. T. Yang, et al. (2007). "Fetal alcohol exposure impairs Hedgehog cholesterol modification and signaling." Lab Invest **87**(3): 231-240.

Liao, J. K. and U. Laufs (2005). "Pleiotropic effects of statins." Annu Rev Pharmacol Toxicol **45**: 89-118.

Liapi, A., J. Pritchett, et al. (2008). "Stromal-derived factor 1 signalling regulates radial and tangential migration in the developing cerebral cortex." Dev Neurosci **30**(1-3): 117-131.

Lichtenthaler, H. K., J. Schwender, et al. (1997). "Biosynthesis of isoprenoids in higher plant chloroplasts proceeds via a mevalonate-independent pathway." FEBS Lett **400**(3): 271-274.

Liem, K. F., Jr., G. Tremml, et al. (1995). "Dorsal differentiation of neural plate cells induced by BMP-mediated signals from epidermal ectoderm." Cell **82**(6): 969-979.

Liesi, P. (1990). "Extracellular matrix and neuronal movement." Experientia **46**(9): 900-907.

Liu, J. S. (2011). "Molecular genetics of neuronal migration disorders." Curr Neurol Neurosci Rep **11**(2): 171-178.

Liu, X., L. Sun, et al. (2012). "Connexin 43 controls the multipolar phase of neuronal migration to the cerebral cortex." Proc Natl Acad Sci U S A **109**(21): 8280-8285.

Liu, Z., R. Steward, et al. (2000). "Drosophila Lis1 is required for neuroblast proliferation, dendritic elaboration and axonal transport." Nat Cell Biol **2**(11): 776-783.

Lois, C., J. M. Garcia-Verdugo, et al. (1996). "Chain migration of neuronal precursors." Science **271**(5251): 978-981.

Lowery, L. A., G. De Rienzo, et al. (2009). "Characterization and classification of zebrafish brain morphology mutants." Anat Rec (Hoboken) **292**(1): 94-106.

Lowery, L. A. and H. Sive (2005). "Initial formation of zebrafish brain ventricles occurs independently of circulation and requires the nagie oko and snakehead/atp1a1a.1 gene products." Development **132**(9): 2057-2067.

Lumsden, A. (1990). "The cellular basis of segmentation in the developing hindbrain." Trends Neurosci **13**(8): 329-335.

Machado, C. F., F. H. Beraldo, et al. (2012). "Disease-associated mutations in the prion protein impair laminin-induced process outgrowth and survival." J Biol Chem **287**(52): 43777-43788.

Malicki, J. (2004). "Cell fate decisions and patterning in the vertebrate retina: the importance of timing, asymmetry, polarity and waves." Curr Opin Neurobiol **14**(1): 15-21.

Malicki, J., S. C. Neuhauss, et al. (1996). "Mutations affecting development of the zebrafish retina." Development **123**: 263-273.

Mapp, O. M., G. S. Walsh, et al. (2011). "Zebrafish Prickle1b mediates facial branchiomotor neuron migration via a farnesylation-dependent nuclear activity." Development **138**(10): 2121-2132.

Marin, O. and J. L. Rubenstein (2003). "Cell migration in the forebrain." Annu Rev Neurosci **26**: 441-483.

Marins, M., A. L. Xavier, et al. (2009). "Gap junctions are involved in cell migration in the early postnatal subventricular zone." Dev Neurobiol **69**(11): 715-730.

Markham, J. A. and J. E. Vaughn (1991). "Migration patterns of sympathetic preganglionic neurons in embryonic rat spinal cord." J Neurobiol **22**(8): 811-822.

Marko, K., T. Kohidi, et al. (2011). "Isolation of radial glia-like neural stem cells from fetal and adult mouse forebrain via selective adhesion to a novel adhesive peptide-conjugate." PLoS One **6**(12): e28538.

Martini, F. J. and M. Valdeolmillos (2010). "Actomyosin contraction at the cell rear drives nuclear translocation in migrating cortical interneurons." J Neurosci **30**(25): 8660-8670.

Martini, F. J., M. Valiente, et al. (2009). "Biased selection of leading process branches mediates chemotaxis during tangential neuronal migration." Development **136**(1): 41-50.

Martynoga, B., H. Morrison, et al. (2005). "Foxg1 is required for specification of ventral telencephalon and region-specific regulation of dorsal telencephalic precursor proliferation and apoptosis." Dev Biol **283**(1): 113-127.

Mathews, E. S., D. J. Mawdsley, et al. (2014). "Mutation of 3-hydroxy-3-methylglutaryl CoA synthase I reveals requirements for isoprenoid and cholesterol synthesis in oligodendrocyte migration arrest, axon wrapping, and myelin gene expression." J Neurosci **34**(9): 3402-3412.

Mattila, P. K. and P. Lappalainen (2008). "Filopodia: molecular architecture and cellular functions." Nat Rev Mol Cell Biol **9**(6): 446-454.

Maurus, D. and W. A. Harris (2009). "Zic-associated holoprosencephaly: zebrafish Zic1 controls midline formation and forebrain patterning by regulating Nodal, Hedgehog, and retinoic acid signaling." Genes Dev **23**(12): 1461-1473.

Mayer, U., R. Nischt, et al. (1993). "A single EGF-like motif of laminin is responsible for high affinity nidogen binding." EMBO J **12**(5): 1879-1885.

McEvilly, R. J., M. O. de Diaz, et al. (2002). "Transcriptional regulation of cortical neuron migration by POU domain factors." Science **295**(5559): 1528-1532.

McLoughlin, D. M. and C. C. Miller (2008). "The FE65 proteins and Alzheimer's disease." J Neurosci Res **86**(4): 744-754.

McMahon, S. S. and K. W. McDermott (2002). "Morphology and differentiation of radial glia in the developing rat spinal cord." J Comp Neurol **454**(3): 263-271.

Meng, X., M. B. Noyes, et al. (2008). "Targeted gene inactivation in zebrafish using engineered zinc-finger nucleases." Nat Biotechnol **26**(6): 695-701.

Mesngon, M. T., C. Tarricone, et al. (2006). "Regulation of cytoplasmic dynein ATPase by Lis1." J Neurosci **26**(7): 2132-2139.

Meyer, K. D. and J. A. Morris (2009). "Disc1 regulates granule cell migration in the developing hippocampus." Hum Mol Genet **18**(17): 3286-3297.

Millen, K. J., J. H. Millonig, et al. (2004). "Roof plate and dorsal spinal cord dl1 interneuron development in the dreher mutant mouse." Dev Biol **270**(2): 382-392.

Miner, J. H. and C. Li (2000). "Defective glomerulogenesis in the absence of laminin alpha5 demonstrates a developmental role for the kidney glomerular basement membrane." Dev Biol **217**(2): 278-289.

Minopoli, G., M. Stante, et al. (2007). "Essential roles for Fe65, Alzheimer amyloid precursor-binding protein, in the cellular response to DNA damage." J Biol Chem **282**(2): 831-835.

Mione, M., D. Baldessari, et al. (2008). "How neuronal migration contributes to the morphogenesis of the CNS: insights from the zebrafish." Dev Neurosci **30**(1-3): 65-81.

Miyata, T., A. Kawaguchi, et al. (2001). "Asymmetric inheritance of radial glial fibers by cortical neurons." Neuron **31**(5): 727-741.

Miziorko, H. M. (2011). "Enzymes of the mevalonate pathway of isoprenoid biosynthesis." Arch Biochem Biophys **505**(2): 131-143.

Moosajee, M., K. Gregory-Evans, et al. (2008). "Translational bypass of nonsense mutations in zebrafish rep1, pax2.1 and lamb1 highlights a viable therapeutic option for untreatable genetic eye disease." Hum Mol Genet **17**(24): 3987-4000.

Mueller, T. and M. F. Wullimann (2002). "BrdU-, neuroD (nrd)- and Hu-studies reveal unusual non-ventricular neurogenesis in the postembryonic zebrafish forebrain." Mech Dev **117**(1-2): 123-135.

Mulligan, T., H. Blaser, et al. (2010). "Prenylation-deficient G protein gamma subunits disrupt GPCR signaling in the zebrafish." Cell Signal **22**(2): 221-233.

Mulligan, T. and S. A. Farber (2011). "Central and C-terminal domains of heterotrimeric G protein gamma subunits differentially influence the signaling necessary for primordial germ cell migration." Cell Signal **23**(10): 1617-1624.

Musa, A., H. Lehrach, et al. (2001). "Distinct expression patterns of two zebrafish homologues of the human APP gene during embryonic development." Dev Genes Evol **211**(11): 563-567.

Nadarajah, B., P. Alifragis, et al. (2003). "Neuronal migration in the developing cerebral cortex: observations based on real-time imaging." Cereb Cortex **13**(6): 607-611.

Nakaya, T., T. Kawai, et al. (2009). "Metabolic stabilization of p53 by FE65 in the nuclear matrix of osmotically stressed cells." Febs J **276**(21): 6364-6374.

Nguyen, N. M., D. G. Kelley, et al. (2005). "Epithelial laminin alpha5 is necessary for distal epithelial cell maturation, VEGF production, and alveolization in the developing murine lung." Dev Biol **282**(1): 111-125.

Nguyen, U. T., R. S. Goody, et al. (2010). "Understanding and exploiting protein prenyltransferases." Chembiochem **11**(9): 1194-1201.

Nishimura, T., K. Kato, et al. (2004). "Role of the PAR-3-KIF3 complex in the establishment of neuronal polarity." Nat Cell Biol **6**(4): 328-334.

Noctor, S. C., A. C. Flint, et al. (2002). "Dividing precursor cells of the embryonic cortical ventricular zone have morphological and molecular characteristics of radial glia." J Neurosci **22**(8): 3161-3173.

Norden, C., S. Young, et al. (2009). "Actomyosin is the main driver of interkinetic nuclear migration in the retina." Cell **138**(6): 1195-1208.

Noviello, C., P. Vito, et al. (2003). "Autosomal recessive hypercholesterolemia protein interacts with and regulates the cell surface level of Alzheimer's amyloid beta precursor protein." J Biol Chem **278**(34): 31843-31847.

O'Rourke, N. A., D. P. Sullivan, et al. (1995). "Tangential migration of neurons in the developing cerebral cortex." Development **121**(7): 2165-2176.

Oegema, R., A. Maat-Kievit, et al. (2012). "Asymmetric polymicrogyria and periventricular nodular heterotopia due to mutation in ARX." Am J Med Genet A **158A**(6): 1472-1476.

Ohshima, T., M. Ogawa, et al. (2002). "Cyclin-dependent kinase 5/p35 contributes synergistically with Reelin/Dab1 to the positioning of facial branchiomotor and inferior olive neurons in the developing mouse hindbrain." J Neurosci **22**(10): 4036-4044.

Ono, K., T. Shokunbi, et al. (1997). "Filopodia and growth cones in the vertically migrating granule cells of the postnatal mouse cerebellum." Exp Brain Res **117**(1): 17-29.

Palmesino, E., D. L. Rousso, et al. (2010). "Foxp1 and lhx1 coordinate motor neuron migration with axon trajectory choice by gating Reelin signalling." PLoS Biol **8**(8): e1000446.

Pang, T., R. Atefy, et al. (2008). "Malformations of cortical development." Neurologist **14**(3): 181-191.

Parsons, M. J., S. M. Pollard, et al. (2002). "Zebrafish mutants identify an essential role for laminins in notochord formation." Development **129**(13): 3137-3146.

Patton, B. L., B. Wang, et al. (2008). "A single point mutation in the LN domain of LAMA2 causes muscular dystrophy and peripheral amyelination." J Cell Sci **121**(Pt 10): 1593-1604.

Paulus, J. D. and M. C. Halloran (2006). "Zebrafish bashful/laminin-alpha 1 mutants exhibit multiple axon guidance defects." Dev Dyn **235**(1): 213-224.

Pencea, V. and M. B. Luskin (2003). "Prenatal development of the rodent rostral migratory stream." J Comp Neurol **463**(4): 402-418.

Peretto, P., C. Giachino, et al. (2005). "Chain formation and glial tube assembly in the shift from neonatal to adult subventricular zone of the rodent forebrain." J Comp Neurol **487**(4): 407-427.

Perkinton, M. S., C. L. Standen, et al. (2004). "The c-Abl tyrosine kinase phosphorylates the Fe65 adaptor protein to stimulate Fe65/amyloid precursor protein nuclear signaling." J Biol Chem **279**(21): 22084-22091.

Placzek, M., T. M. Jessell, et al. (1993). "Induction of floor plate differentiation by contact-dependent, homeogenetic signals." Development **117**(1): 205-218.

Pramatarova, A., K. Chen, et al. (2008). "A genetic interaction between the APP and Dab1 genes influences brain development." Mol Cell Neurosci **37**(1): 178-186.

Puehringer, D., N. Orel, et al. (2013). "EGF transactivation of Trk receptors regulates the migration of newborn cortical neurons." Nat Neurosci **16**(4): 407-415.

Qin, S. and C. L. Zhang (2012). "Role of kruppel-like factor 4 in neurogenesis and radial neuronal migration in the developing cerebral cortex." Mol Cell Biol **32**(21): 4297-4305.

Radakovits, R., C. S. Barros, et al. (2009). "Regulation of radial glial survival by signals from the meninges." J Neurosci **29**(24): 7694-7705.

Radmanesh, F., A. O. Caglayan, et al. (2013). "Mutations in LAMB1 cause cobblestone brain malformation without muscular or ocular abnormalities." Am J Hum Genet **92**(3): 468-474.

Radner, S., C. Banos, et al. (2013). "beta2 and gamma3 laminins are critical cortical basement membrane components: ablation of Lamb2 and Lamc3 genes disrupts cortical lamination and produces dysplasia." Dev Neurobiol **73**(3): 209-229.

Rakic, P. (1971). "Neuron-glia relationship during granule cell migration in developing cerebellar cortex. A Golgi and electronmicroscopic study in Macacus Rhesus." J Comp Neurol **141**(3): 283-312.

Rakic, P., E. Knyihar-Csillik, et al. (1996). "Polarity of microtubule assemblies during neuronal cell migration." Proc Natl Acad Sci U S A **93**(17): 9218-9222.

Rathod, R., S. Havlicek, et al. (2012). "Laminin induced local axonal translation of beta-actin mRNA is impaired in SMN-deficient motoneurons." Histochem Cell Biol **138**(5): 737-748.

Rikitake, Y. and J. K. Liao (2005). "Rho GTPases, statins, and nitric oxide." Circ Res **97**(12): 1232-1235.

Roberts, P. J., N. Mitin, et al. (2008). "Rho Family GTPase modification and dependence on CAAX motif-signaled posttranslational modification." J Biol Chem **283**(37): 25150-25163.

Robu, M. E., J. D. Larson, et al. (2007). "p53 activation by knockdown technologies." PLoS Genet **3**(5): e78.

Roediger, M., N. Miosge, et al. (2010). "Tissue distribution of the laminin beta1 and beta2 chain during embryonic and fetal human development." J Mol Histol **41**(2-3): 177-184.

Roux, C., C. Wolf, et al. (2000). "Role of cholesterol in embryonic development." Am J Clin Nutr **71**(5 Suppl): 1270S-1279S.

Rozario, T. and D. W. DeSimone (2010). "The extracellular matrix in development and morphogenesis: a dynamic view." Dev Biol **341**(1): 126-140.

Rubenstein, J. L., S. Martinez, et al. (1994). "The embryonic vertebrate forebrain: the prosomeric model." Science **266**(5185): 578-580.

Sabo, S. L., A. F. Ikin, et al. (2001). "The Alzheimer amyloid precursor protein (APP) and FE65, an APP-binding protein, regulate cell movement." J Cell Biol **153**(7): 1403-1414.

Sander, J. D., J. R. Yeh, et al. (2011). "Engineering zinc finger nucleases for targeted mutagenesis of zebrafish." Methods Cell Biol **104**: 51-58.

Santos, A. C. and R. Lehmann (2004). "Isoprenoids control germ cell migration downstream of HMGCoA reductase." Dev Cell **6**(2): 283-293.

Sasaki, S., A. Shionoya, et al. (2000). "A LIS1/NUDEL/cytoplasmic dynein heavy chain complex in the developing and adult nervous system." Neuron **28**(3): 681-696.

Saueressig, H., J. Burrill, et al. (1999). "Engrailed-1 and netrin-1 regulate axon pathfinding by association interneurons that project to motor neurons." Development **126**(19): 4201-4212.

Schaar, B. T. and S. K. McConnell (2005). "Cytoskeletal coordination during neuronal migration." Proc Natl Acad Sci U S A **102**(38): 13652-13657.

Schier, A. F., S. C. Neuhauss, et al. (1996). "Mutations affecting the development of the embryonic zebrafish brain." Development **123**: 165-178.

Schild-Prufert, K., M. Giegerich, et al. (2006). "Structural and functional characterization of the zebrafish lamin B receptor." Eur J Cell Biol **85**(8): 813-824.

Seo, S. and B. Leitch (2014). "Altered thalamic GABAA-receptor subunit expression in the stargazer mouse model of absence epilepsy." Epilepsia **55**(2): 224-232.

Shu, T., R. Ayala, et al. (2004). "Ndel1 operates in a common pathway with LIS1 and cytoplasmic dynein to regulate cortical neuronal positioning." Neuron **44**(2): 263-277.

Siegenthaler, J. A. and S. J. Pleasure (2011). "We have got you 'covered': how the meninges control brain development." Curr Opin Genet Dev **21**(3): 249-255.

Silva, T., J. Teixeira, et al. (2013). "Alzheimer's disease, cholesterol, and statins: the junctions of important metabolic pathways." Angew Chem Int Ed Engl **52**(4): 1110-1121.

Sittaramane, V., A. Sawant, et al. (2009). "The cell adhesion molecule Tag1, transmembrane protein Stbm/Vangl2, and Lamininalpha1 exhibit genetic interactions during migration of facial branchiomotor neurons in zebrafish." Dev Biol **325**(2): 363-373.

Smyth, N., H. S. Vatansever, et al. (1999). "Absence of basement membranes after targeting the LAMC1 gene results in embryonic lethality due to failure of endoderm differentiation." J Cell Biol **144**(1): 151-160.

Sohal, A. P., T. Montgomery, et al. (2012). "TUBA1A mutation-associated lissencephaly: case report and review of the literature." Pediatr Neurol **46**(2): 127-131.

Solecki, D. J., N. Trivedi, et al. (2009). "Myosin II motors and F-actin dynamics drive the coordinated movement of the centrosome and soma during CNS glial-guided neuronal migration." Neuron **63**(1): 63-80.

Song, P. and S. W. Pimplikar (2012). "Knockdown of amyloid precursor protein in zebrafish causes defects in motor axon outgrowth." PLoS One **7**(4): e34209.

Staquicini, F. I., E. Dias-Neto, et al. (2009). "Discovery of a functional protein complex of netrin-4, laminin gamma1 chain, and integrin alpha6beta1 in mouse neural stem cells." Proc Natl Acad Sci U S A **106**(8): 2903-2908.

Starr, C. J., J. A. Kappler, et al. (2004). "Mutation of the zebrafish choroideremia gene encoding Rab escort protein 1 devastates hair cells." Proc Natl Acad Sci U S A **101**(8): 2572-2577.

Stipursky, J., D. Francis, et al. (2012). "Activation of MAPK/PI3K/SMAD pathways by TGF-beta(1) controls differentiation of radial glia into astrocytes in vitro." Dev Neurosci **34**(1): 68-81.

Struhl, G. and I. Greenwald (1999). "Presenilin is required for activity and nuclear access of Notch in Drosophila." Nature **398**(6727): 522-525.

Suarez-Vega, A., B. Gutierrez-Gil, et al. (2013). "Identification of a 31-bp deletion in the RELN gene causing lissencephaly with cerebellar hypoplasia in sheep." PLoS One **8**(11): e81072.

Sun, W., H. Kim, et al. (2010). "Control of neuronal migration through rostral migration stream in mice." Anat Cell Biol **43**(4): 269-279.

Sun, Y. M., M. Cooper, et al. (2008). "Rest-mediated regulation of extracellular matrix is crucial for neural development." PLoS One **3**(11): e3656.

Sussel, L., O. Marin, et al. (1999). "Loss of Nkx2.1 homeobox gene function results in a ventral to dorsal molecular respecification within the basal telencephalon: evidence for a transformation of the pallidum into the striatum." Development **126**(15): 3359-3370.

Sztal, T., S. Berger, et al. (2011). "Characterization of the laminin gene family and evolution in zebrafish." Dev Dyn **240**(2): 422-431.

Tabata, H. and K. Nakajima (2003). "Multipolar migration: the third mode of radial neuronal migration in the developing cerebral cortex." J Neurosci **23**(31): 9996-10001.

Tamayev, R., D. Zhou, et al. (2009). "The interactome of the amyloid beta precursor protein family members is shaped by phosphorylation of their intracellular domains." Mol Neurodegener **4**: 28.

Tanahashi, H. and T. Tabira (1999). "Molecular cloning of human Fe65L2 and its interaction with the Alzheimer's beta-amyloid precursor protein." Neurosci Lett **261**(3): 143-146.

Tanaka, D. H. and K. Nakajima (2012). "Migratory pathways of GABAergic interneurons when they enter the neocortex." Eur J Neurosci **35**(11): 1655-1660.

Tanaka, T., F. F. Serneo, et al. (2004). "Lis1 and doublecortin function with dynein to mediate coupling of the nucleus to the centrosome in neuronal migration." J Cell Biol **165**(5): 709-721.

Tanaka, T., I. Tatsuno, et al. (2000). "Geranylgeranyl-pyrophosphate, an isoprenoid of mevalonate cascade, is a critical compound for rat primary cultured cortical neurons to protect the cell death induced by 3-hydroxy-3-methylglutaryl-CoA reductase inhibition." J Neurosci **20**(8): 2852-2859.

Tarr, P. E., R. Roncarati, et al. (2002). "Tyrosine phosphorylation of the beta-amyloid precursor protein cytoplasmic tail promotes interaction with Shc." J Biol Chem **277**(19): 16798-16804.

Taru, H., K. Iijima, et al. (2002). "Interaction of Alzheimer's beta -amyloid precursor family proteins with scaffold proteins of the JNK signaling cascade." J Biol Chem **277**(22): 20070-20078.

Terashima, T., Y. Kishimoto, et al. (1993). "Musculotopic organization of the facial nucleus of the reeler mutant mouse." Brain Res **617**(1): 1-9.

Thorpe, J. L., M. Doitsidou, et al. (2004). "Germ cell migration in zebrafish is dependent on HMGCoA reductase activity and prenylation." Dev Cell **6**(2): 295-302.

Timmer, J. R., C. Wang, et al. (2002). "BMP signaling patterns the dorsal and intermediate neural tube via regulation of homeobox and helix-loop-helix transcription factors." Development **129**(10): 2459-2472.

Timpl, R. (1989). "Structure and biological activity of basement membrane proteins." Eur J Biochem **180**(3): 487-502.

Trommsdorff, M., J. P. Borg, et al. (1998). "Interaction of cytosolic adaptor proteins with neuronal apolipoprotein E receptors and the amyloid precursor protein." J Biol Chem **273**(50): 33556-33560.

Tryggvason, K. (1993). "The laminin family." Curr Opin Cell Biol **5**(5): 877-882.

Tsai, J. W., K. H. Bremner, et al. (2007). "Dual subcellular roles for LIS1 and dynein in radial neuronal migration in live brain tissue." Nat Neurosci **10**(8): 970-979.

Tsao, C. Y., J. R. Mendell, et al. (1998). "Congenital muscular dystrophy with complete laminin-alpha2-deficiency, cortical dysplasia, and cerebral white-matter changes in children." J Child Neurol **13**(6): 253-256.

Urano, Y., I. Hayashi, et al. (2005). "Association of active gamma-secretase complex with lipid rafts." J Lipid Res **46**(5): 904-912.

Valiente, M. and F. J. Martini (2009). "Migration of cortical interneurons relies on branched leading process dynamics." Cell Adh Migr **3**(3): 278-280.

Van Vickle, G. D., C. L. Esh, et al. (2007). "TgCRND8 amyloid precursor protein transgenic mice exhibit an altered gamma-secretase processing and an aggressive, additive amyloid pathology subject to immunotherapeutic modulation." Biochemistry **46**(36): 10317-10327.

Vidaki, M., S. Tivodar, et al. (2012). "Rac1-dependent cell cycle exit of MGE precursors and GABAergic interneuron migration to the cortex." Cereb Cortex **22**(3): 680-692.

Vigliano, P., P. Dassi, et al. (2009). "LAMA2 stop-codon mutation: merosin-deficient congenital muscular dystrophy with occipital polymicrogyria, epilepsy and psychomotor regression." Eur J Paediatr Neurol **13**(1): 72-76.

Viktorin, G., C. Chiuchitu, et al. (2009). "Emx3 is required for the differentiation of dorsal telencephalic neurons." Dev Dyn **238**(8): 1984-1998.

von Rotz, R. C., B. M. Kohli, et al. (2004). "The APP intracellular domain forms nuclear multiprotein complexes and regulates the transcription of its own precursor." J Cell Sci **117**(Pt 19): 4435-4448.

Vranova, E., D. Coman, et al. (2012). "Structure and dynamics of the isoprenoid pathway network." Mol Plant **5**(2): 318-333.

Wallis, D. E. and M. Muenke (1999). "Molecular mechanisms of holoprosencephaly." Mol Genet Metab **68**(2): 126-138.

Wang, B., Q. Hu, et al. (2004). "Isoform-specific knockout of FE65 leads to impaired learning and memory." J Neurosci Res **75**(1): 12-24.

Webb, A. E., J. Sanderford, et al. (2007). "Laminin alpha5 is essential for the formation of the zebrafish fins." Dev Biol **311**(2): 369-382.

Whitman, M. C., W. Fan, et al. (2009). "Blood vessels form a migratory scaffold in the rostral migratory stream." J Comp Neurol **516**(2): 94-104.

Wichterle, H., D. H. Turnbull, et al. (2001). "In utero fate mapping reveals distinct migratory pathways and fates of neurons born in the mammalian basal forebrain." Development **128**(19): 3759-3771.

Wierzbicki, A. S., A. Viljoen, et al. (2013). "New therapies to reduce low-density lipoprotein cholesterol." Curr Opin Cardiol **28**(4): 452-457.

Willem, M., N. Miosge, et al. (2002). "Specific ablation of the nidogen-binding site in the laminin gamma1 chain interferes with kidney and lung development." Development **129**(11): 2711-2722.

Wilson, D. A., K. M. Guthrie, et al. (1990). "Modification of olfactory bulb synaptic inhibition by early unilateral olfactory deprivation." Neurosci Lett **116**(3): 250-256.

Wilson, P. M., R. H. Fryer, et al. (2010). "Astn2, a novel member of the astrotactin gene family, regulates the trafficking of ASTN1 during glial-guided neuronal migration." J Neurosci **30**(25): 8529-8540.

Wingate, R. J. and M. E. Hatten (1999). "The role of the rhombic lip in avian cerebellum development." Development **126**(20): 4395-4404.

Woo, K. and S. E. Fraser (1995). "Order and coherence in the fate map of the zebrafish nervous system." Development **121**(8): 2595-2609.

Wray, S. (2010). "From nose to brain: development of gonadotrophin-releasing hormone-1 neurones." J Neuroendocrinol **22**(7): 743-753.

Xiang, H., H. X. Chen, et al. (2006). "Reduced excitatory drive in interneurons in an animal model of cortical dysplasia." J Neurophysiol **96**(2): 569-578.

Youn, Y. H., T. Pramparo, et al. (2009). "Distinct dose-dependent cortical neuronal migration and neurite extension defects in Lis1 and Ndel1 mutant mice." J Neurosci **29**(49): 15520-15530.

Young-Pearse, T. L., S. Suth, et al. (2010). "Biochemical and functional interaction of disrupted-in-schizophrenia 1 and amyloid precursor protein regulates neuronal migration during mammalian cortical development." J Neurosci **30**(31): 10431-10440.

Zambrano, N., P. Bruni, et al. (2001). "The beta-amyloid precursor protein APP is tyrosine-phosphorylated in cells expressing a constitutively active form of the Abl protoncogene." J Biol Chem **276**(23): 19787-19792.

Zambrano, N., G. Minopoli, et al. (1998). "The Fe65 adaptor protein interacts through its PID1 domain with the transcription factor CP2/LSF/LBP1." J Biol Chem **273**(32): 20128-20133.

Zhang, X., K. Lei, et al. (2009). "SUN1/2 and Syne/Nesprin-1/2 complexes connect centrosome to the nucleus during neurogenesis and neuronal migration in mice." Neuron **64**(2): 173-187.

Zhang, Y. Y., Y. C. Fan, et al. (2013). "Atorvastatin attenuates the production of IL-1beta, IL-6, and TNF-alpha in the hippocampus of an amyloid beta1-42-induced rat model of Alzheimer's disease." Clin Interv Aging **8**: 103-110.

Zhou, Y. T., L. S. Yu, et al. (2014). "Pharmacokinetic drug-drug interactions between 1,4-dihydropyridine calcium channel blockers and statins: factors determining interaction strength and relevant clinical risk management." Ther Clin Risk Manag **10**: 17-26.

Zupanc, G. K., R. F. Sirbulescu, et al. (2012). "Radial glia in the cerebellum of adult teleost fish: implications for the guidance of migrating new neurons." Neuroscience **210**: 416-430.